

The Potential of Pulsed Low Intensity Ultrasound to stimulate Chondrocytes in a 3D Model System

Vaughan, Natalie Marlene

The copyright of this thesis rests with the author and no quotation from it or information derived from it may be published without the prior written consent of the author

For additional information about this publication click this link.

<http://qmro.qmul.ac.uk/jspui/handle/123456789/1790>

Information about this research object was correct at the time of download; we occasionally make corrections to records, please therefore check the published record when citing. For more information contact scholarlycommunications@qmul.ac.uk

**The Potential of Pulsed Low Intensity
Ultrasound to stimulate Chondrocytes in a
3D Model System**

Natalie Marlene Vaughan

2009

Confined to the Library

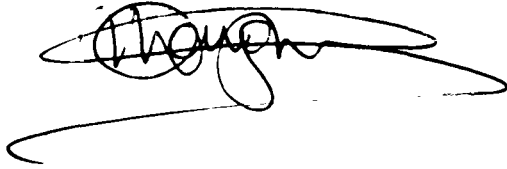
School of Engineering and Materials Science



This thesis is presented as part of the requirements for the degree of Doctor of
Philosophy

DECLARATION

I hereby declare that all the work carried out and presented in this thesis is original and my own.

A handwritten signature in black ink, appearing to read 'Natalie Marlene Vaughan', with a long horizontal flourish extending to the right.

Natalie Marlene Vaughan

ACKNOWLEDGEMENTS

I would like to thank all those who helped me down the long and arduous path towards the completion of this thesis. I got there eventually!

My heartfelt thanks go to my supervisors Professor Dan Bader and Dr Martin Knight for their guidance, support, encouragement, boundless patience and occasional (but necessary!) boot up the backside.

This work was funded by the Engineering and Physical Sciences Research Council and Smith and Nephew, Inc., York. Particular thanks go to Dr Robin Chivers from Smith and Nephew Inc. for his assistance and time.

Thanks to Dr Tina Chowdhury and Chris Mole for their guidance and assistance in the undertaking of experimental work in the Cell and Tissue Engineering Lab. Thanks also to Danny Neighbour, Vincent Ford and Michael Collins for their technical support in the creation and alteration of experimental system components. Thanks to Dr Katie Smith for her assistance in printing my thesis.

To the members of the Room 205 Crew (Mile End Massive!): Drs Davidson Ateh, Joshua Eniwumide, Stephen Mellon, and my girls Drs Judy Norton and Oto-ola Akanji. Thank you for keeping me sane! Without you guys my time at QMUL wouldn't have been half as fun! I have mad love for all of you. Oto, I have to thank you especially for all your help and support – you're the best!

Thanks to my friends outside QMUL who provided me with much needed respite: Amanda, Bridget, Christiana, Kate, Kechi, Mark, Sylvanie and Tess.

Thanks to my Dad, Mummies Norton and Akanji, Iris, and my family overseas for keeping me in their thoughts and prayers.

Last but not least, to those who've had to put up with my slobbish zombie-like behaviour at home – my mum and sister. My sincerest thanks go to my Mummy, who is an enduring tower of strength. Where would I be without you to take care of my nutritional requirements? I love you very much. Cheryl, I promise I'll take you out now, as I no longer have an excuse! ☺

ABSTRACT

Pulsed low intensity ultrasound (PLIUS) is used clinically to accelerate fracture healing, although the mode of action is unclear. However studies suggest that PLIUS may stimulate endochondral ossification and consequently PLIUS may also be beneficial for cartilage regeneration, either *in vivo* or as part of a tissue engineered approach. Previous studies using chondrocytes cultured in monolayer have suggested that PLIUS may stimulate glycosaminoglycan (GAG) synthesis, and that calcium signalling is implicated in this process. Therefore the present studies set out to investigate the influence of PLIUS on bovine articular chondrocytes in monolayer and agarose culture. This required the design of a bioreactor system which enabled cell-agarose constructs to be subjected to PLIUS, as well as a microscope-mounted test rig enabling confocal visualisation of intracellular calcium dynamics.

A PLIUS system and signalling characteristics were provided by Smith and Nephew, Inc. (York, UK). Chondrocytes in agarose demonstrated a reduction in cell viability associated with PLIUS above a spatial averaged time averaged (SATA) intensity of 200mW/cm^2 , presumably associated with transducer heating. In subsequent studies, 30 and 100mW/cm^2 were applied to monolayer and agarose cultures for up to 20 days, and biosynthesis was examined by assessment of GAG synthesis and cell proliferation using biochemical and radio-labelling protocols. Intracellular calcium signalling was investigated as a possible mechanotransduction pathway, using confocal microscopy and the calcium indicator Fluo-4.

In monolayer culture PLIUS did not stimulate total GAG content or cell proliferation at either 30 or 100mW/cm^2 . In agarose cultures, PLIUS had no effect on total GAG content at 30mW/cm^2 . At 100mW/cm^2 PLIUS induced a very small increase in total GAG content but there was no detectable effect on the rate of GAG synthesis in either model system at either 30 or 100mW/cm^2 . There were no PLIUS associated changes in the levels of intracellular calcium signaling in either monolayer or agarose cultures. Preliminary studies using Fluorescent Recovery after Photobleaching (FRAP) showed that PLIUS at 30mW/cm^2 increased diffusion of 70kDa FITC-dextran, although this clearly had no effect on GAG synthesis or cell proliferation.

These studies indicate that PLIUS-induced fracture healing, or any potential use of PLIUS for cartilage repair, is unlikely to involve direct stimulation of proteoglycan synthesis or cell proliferation. Indeed the proposed use of PLIUS in cartilage tissue engineering is more limited than previously suggested.

CONTENTS

DECLARATION	ii
ACKNOWLEDGEMENTS	iii
ABSTRACT	iv
CONTENTS	v
LIST OF FIGURES	xi
LIST OF TABLES	xvii
1 COMPOSITION AND STRUCTURE OF ARTICULAR CARTILAGE	
1.1 Introduction to cartilage and articular cartilage	2
1.2 Extracellular matrix	4
1.2.1 Tissue fluid	5
1.2.2 Collagens	5
1.2.2.1 Collagen structure	5
1.2.2.2 Cartilage-specific collagens	8
1.2.3 Proteoglycans	9
1.2.4 Non-collagenous proteins and glycoproteins	12
1.3 Chondrocytes	13
1.3.1 Chondrocyte development	13
1.3.2 Chondrocyte organelles and synthesis of extracellular matrix components	14
1.3.3 Chondrocyte metabolism	15
1.4 Articular cartilage zones and matrix regions	16
1.5 Loading of articular cartilage	20
1.6 Articular cartilage pathology	22
1.6.1 Trauma and injury	22
1.6.2 Ageing	23
1.6.3 Disease	24
1.7 Repair strategies	25

2	RESPONSE OF ARTICULAR CARTILAGE TO MECHANICAL STIMULI	
2.1	Introduction to mechanotransduction in cartilage	29
2.2	<i>In vivo</i> studies	29
2.3	<i>In vitro</i> studies	30
2.3.1	Cartilage explants	30
2.3.2	Monolayer cultures	31
2.3.3	Three-dimensional cultures	31
2.4	Mechanotransduction signaling pathways	33
2.4.1	Tissue and cellular level	33
2.4.1.1	Hydrostatic pressure	33
2.4.1.2	Matrix deformation	35
2.4.1.3	Cellular deformation	37
2.4.1.4	Specific pathways associated with 3D scaffolds	38
2.4.2	Intracellular level	38
2.4.2.1	Cytoskeleton	38
2.4.2.2	Nucleus deformation	40
2.4.2.3	Calcium signalling and associated pathways	40
2.5	Ultrasound	43
2.5.1	Physics of ultrasound	43
2.5.2	Temporal and spatial characteristics of continuous wave and pulsed wave ultrasound	45
2.5.3	Amplitude and intensity	47
2.5.4	Attenuation	49
2.5.5	Standing wave production	49
2.5.6	Medical applications of ultrasound	50
2.5.7	Safety considerations for use of ultrasound	52
2.5.8	Biophysical effects of ultrasound in clinical applications	52
2.5.8.1	Thermal effects	52
2.5.8.2	Non-thermal effects	53
2.5.9	Therapeutic pulsed low intensity ultrasound for bone repair	55
2.5.10	Use of low intensity ultrasound for cartilage regeneration	57
2.6	Aims and Objectives	60

3	DEVELOPMENT OF MODEL SYSTEM FOR INVESTIGATING EFFECT OF PULSED LOW-INTENSITY ULTRASOUND	
3.1	Introduction	63
3.2	Cell culture methods	64
3.2.1	Cell-seeded agarose model	64
3.2.2	Preparation of culture medium and other solutions	64
3.2.3	Isolation of bovine articular chondrocytes	65
3.2.4	Preparation of chondrocyte-agarose constructs	67
3.3	Ultrasound apparatus	67
3.4	Pulsed low intensity ultrasound (PLIUS) signal	69
3.5	Attenuation of PLIUS	71
3.5.1	Spatial variation in PLIUS intensity	71
3.5.2	Standing wave investigation	73
3.6	Design and development of microscope mounted ultrasound rig	74
3.6.1	Rig design	74
3.6.2	Preparation of 3D chondrocyte-agarose constructs for use in the microscope mounted test rig	79
3.6.3	Optimisation of microscope mounted test rig – prevention of specimen drift	79
3.7	3D model system for matrix synthesis experiments	82
3.8	Standard protocols for biochemical analysis	82
3.8.1	Digest of chondrocyte-seeded agarose constructs	82
3.8.2	DMB assay for total sGAG content in constructs	82
3.8.3	DMB assay for sGAG content in medium	83
3.8.4	Fluorimetric assay of DNA	84
3.8.5	Cell viability determination	85
3.9	PLIUS intensity and temporal changes in sulphated GAG content	86
3.9.1	Method	86
3.9.2	Statistical analysis	87
3.9.3	Results	87
3.9.4	Discussion	90
3.10	Conclusion	96

4	STIMULATION OF PROTEOGLYCAN SYNTHESIS BY PULSED LOW INTENSITY ULTRASOUND IN A 3D AGAROSE SYSTEM	
4.1	Introduction	98
4.2	Materials and methods	99
4.2.1	Preparation of chondrocyte-agarose constructs	99
4.2.2	PLIUS regime	99
4.2.3	Temporal changes in sGAG and DNA content	99
4.2.4	Incorporation of SO ₄ into sGAGs	100
4.2.5	Incorporation of [³ H]thymidine into DNA	101
4.2.6	Statistical analysis	102
4.3	Results	102
4.3.1	Total sGAG content	103
4.3.1.1	The effect of a SATA intensity of 30mW/cm ²	103
4.3.1.2	The effect of a SATA intensity of 100mW/cm ²	109
4.3.2	Total DNA content	113
4.3.3	Cell activity	116
4.3.4	SO ₄ incorporation	117
4.3.5	[³ H]thymidine incorporation	120
4.4	Discussion	124
5	STIMULATION OF PROTEOGLYCAN SYNTHESIS BY PULSED LOW INTENSITY ULTRASOUND IN A MONOLAYER SYSTEM	
5.1	Introduction	131
5.2	Materials and methods	132
5.2.1	Preparation of chondrocyte monolayer culture	132
5.2.2	PLIUS regime	132
5.2.3	Temporal changes in sGAG and DNA content	132
5.2.4	Statistical analysis	133
5.3	Results	133
5.3.1	Total sGAG content	133
5.3.1.1	30mW/cm ² studies	133
5.3.1.2	100mW/cm ² studies	135

5.3.2	Total DNA content	135
5.3.3	Cell activity	138
5.3.4	SO ₄ incorporation	138
5.3.5	[³ H]thymidine incorporation	140
5.4	Discussion	141
6	CALCIUM SIGNALLING IN PULSED LOW INTENSITY ULTRASOUND-STIMULATED CHONDROCYTES	
6.1	Introduction	146
6.2	Materials and methods	147
6.2.1	Preparation of bicarbonate-free chondrocyte medium	147
6.2.2	Preparation of 3D chondrocyte-agarose constructs	147
6.2.3	Preparation of chondrocyte monolayer culture	147
6.2.4	Fluo-4 labelling of constructs and monolayers	148
6.2.5	Application of PLIUS to chondrocytes	149
6.2.6	Ultrasound regime	150
6.2.7	Confocal system and experimental parameters for calcium signalling	150
6.2.8	Cell selection and identification of calcium transients	151
6.2.9	Statistical analysis	152
6.2.10	Summary of experimental test procedures	153
6.3	Results	154
6.3.1	Effect of PLIUS on calcium signalling in chondrocytes in 3D culture	154
6.3.2	Effect of PLIUS on calcium signalling in chondrocytes cultured in monolayer	157
6.3.3	Influence of PLIUS intensity on calcium signalling in chondrocytes in 3D culture	160
6.3.4	Influence of PLIUS intensity on calcium signalling in chondrocytes cultured in monolayer	164
6.4	Discussion	169

7	DISCUSSION AND FUTURE WORK	
7.1	Introduction	174
7.2	Rationale for methodology	175
7.2.1	PLIUS regime	175
7.2.2	Rig and system design for PLIUS transmission	175
7.2.3	Cell source	177
7.2.4	Cell model systems	177
7.2.5	Cell seeding densities	178
7.3	PLIUS-induced mechanotransduction	179
7.3.1	Variability issues	179
7.3.2	Effect of PLIUS intensity	181
7.3.3	Comparison of monolayer and 3D culture	183
7.3.4	Influence of PLIUS on chondrocyte biosynthesis	185
7.3.5	PLIUS-induced diffusion in agarose culture	190
	7.3.5.1 Materials and methods	191
	7.3.5.2 Results	191
	7.3.5.3 Discussion	194
7.3.6	Use of PLIUS in bone and cartilage repair strategies	194
7.4	Future work	195
7.4.1	Further investigation of the 100mW/cm ² signal	195
7.4.2	Influence of PLIUS on other ECM molecules	196
7.4.3	Other intracellular mechanotransduction events	196
7.4.4	Alteration of the model system and PLIUS signal	197
7.5	Final summary	198
	APPENDIX 1: Microscope images taken to accompany 30mW/cm² monolayer study in Chapter 5	200
	APPENDIX 2: Microscope images taken to accompany 100mW/cm² monolayer study in Chapter 5	201
	REFERENCES	202
	CONFERENCES AND PRESENTATIONS	236

LIST OF FIGURES

Figure 1.1	<i>Schematic of a synovial joint.</i>	3
Figure 1.2	<i>Portion of collagen molecule, showing three α-chains coiled to form a triple helix.</i>	6
Figure 1.3	<i>Schematic showing collagen synthesis, secretion and assembly.</i>	7
Figure 1.4	<i>A schematic of the aggrecan molecule and its binding to hyaluronan.</i>	10
Figure 1.5	<i>Schematic of an aggregating proteoglycan molecule (aggrecan).</i>	11
Figure 1.6	<i>Schematic of a typical chondrocyte with its major organelles.</i>	14
Figure 1.7	<i>Schematic representation of the different zones and regions of articular cartilage.</i>	18
Figure 1.8	<i>Viscoelastic response of articular cartilage to the application (t_1) and removal (t_2) of a compressive load.</i>	22
Figure 2.1	<i>Schematic illustrating tissue level mechanotransduction events experienced by chondrocytes on tissue loading.</i>	34
Figure 2.2	<i>Schematic illustrating the basic elements of calcium signalling.</i>	42
Figure 2.3	<i>A) Production of sound by a transducer causing B) regions of compression and C) rarefaction of molecules of a medium, resulting in a sound wave of wavelength λ.</i>	44
Figure 2.4	<i>Schematic diagram showing A) continuous and B) pulsed waves of ultrasound.</i>	45
Figure 2.5	<i>Schematic diagram showing reflection and transmission or refraction of ultrasound at a A) perpendicular and B) non-perpendicular boundary.</i>	46
Figure 2.6	<i>A) Constant and B) non-constant amplitude pulses.</i>	48
Figure 2.7	<i>Attenuation, the reduction in amplitude and intensity of ultrasound as it travels through a medium.</i>	49
Figure 2.8	<i>Schematic plot of temperature versus time at a point in a tissue exposed to continuous ultrasound.</i>	53
Figure 3.1	<i>Photographic sequence showing the key stages in the opening of a bovine metacarpophalangeal joint (A, B) and extraction of</i>	66

	<i>articular cartilage from the proximal joint surfaces (C).</i>	
Figure 3.2	<i>The ultrasonic signal employed for the experimental work undertaken in this thesis.</i>	68
Figure 3.3	<i>Ultrasound apparatus employed for cell stimulation.</i>	69
Figure 3.4	<i>LED indicator placed on transducer with coupling gel.</i>	69
Figure 3.5	<i>The temporal voltage profiles showing input (A and B) and output ultrasound signals (C and D) emitted from the PLIUS transducer at a SATA intensity of 30mW/cm².</i>	70
Figure 3.6	<i>A) Spatial profile of ultrasonic intensity for a typical transducer emitting a 30mW/cm² signal, showing the variation in intensity over its face with increased distance from the source and B) corresponding plot of SATA intensity versus distance from the centre of the transducer.</i>	72
Figure 3.7	<i>Graphical representation of standing waves occurring in water placed in the well of a six well plate stimulated with PLIUS, based on observation of vibration in water.</i>	74
Figure 3.8	<i>Chamber component of microscope rig.</i>	76
Figure 3.9	<i>Photograph of the temperature control unit (Intracel, U.K.) attached to the base plate of the confocal rig.</i>	76
Figure 3.10	<i>A) Diagram of a cross-section through the lid component of the rig and B) Photo of plan view of lid component of rig.</i>	77
Figure 3.11	<i>Schematic of confocal rig setup.</i>	78
Figure 3.12	<i>Photograph of a 5mm diameter x 5mm height chondrocyte-agarose construct on a coverslip.</i>	79
Figure 3.13	<i>Construct mould/insert for the confocal rig.</i>	80
Figure 3.14	<i>Perspex inserts positioned in mould for casting of cell-agarose suspension in inserts.</i>	80
Figure 3.15	<i>Photograph of construct insert, containing a cell-agarose construct, in the chamber of the confocal rig.</i>	81
Figure 3.16	<i>Schematic of well plate showing location of 6mm diameter cores removed from cell-agarose gels.</i>	81
Figure 3.17	<i>A typical standard curve obtained from chondroitin sulphate standards.</i>	83
Figure 3.18	<i>A typical standard curve obtained from Hoechst 33258 standards.</i>	85

Figure 3.19	<i>Effect of pulsed low intensity ultrasound (PLIUS) on total sGAG content in agarose-chondrocyte constructs.</i>	87
Figure 3.20	<i>Effect of pulsed low intensity ultrasound (PLIUS) on total DNA content in agarose-chondrocyte constructs.</i>	89
Figure 3.21	<i>Cell viability in agarose-chondrocyte constructs at 9 days of culture.</i>	89
Figure 3.22	<i>Graphical representation of temperature rise (after 10 seconds) with increasing depth of water placed in the well of a six well plate being stimulated with PLIUS.</i>	94
Figure 4.1	<i>Effect of pulsed low intensity ultrasound (PLIUS) on total sGAG content in agarose-chondrocyte constructs undertaken from three separate isolations (0504, 1204 and 0305).</i>	105
Figure 4.2	<i>Effect of pulsed low intensity ultrasound (PLIUS) on total sGAG released into the medium from agarose-chondrocyte constructs from three separate isolations (0504, 1204 and 0305).</i>	106
Figure 4.3	<i>Effect of pulsed low intensity ultrasound (PLIUS) on total sGAG content in agarose-chondrocyte constructs and sGAG released into the medium undertaken from three separate isolations (0504, 1204 and 0305).</i>	108
Figure 4.4	<i>Effect of pulsed low intensity ultrasound (PLIUS) on total sGAG content in agarose-chondrocyte constructs undertaken from two separate isolations (0805 and 1105).</i>	110
Figure 4.5	<i>Effect of pulsed low intensity ultrasound (PLIUS) on total sGAG released into the medium for agarose-chondrocyte constructs from two separate isolations (0805 and 1105).</i>	111
Figure 4.6	<i>Effect of pulsed low intensity ultrasound (PLIUS) on total sGAG content in agarose-chondrocyte constructs and sGAG released into the medium undertaken from two separate isolations (0805 and 1105).</i>	112
Figure 4.7	<i>Effect of pulsed low intensity ultrasound (PLIUS) on total DNA content in agarose-chondrocyte constructs undertaken from three separate isolations (0504, 1204 and 0305).</i>	114
Figure 4.8	<i>Effect of pulsed low intensity ultrasound (PLIUS) on total DNA content in agarose-chondrocyte constructs undertaken</i>	115

	<i>from two separate isolations (0805 and 1105).</i>	
Figure 4.9	<i>Effect of pulsed low intensity ultrasound (PLIUS) on the rate of $^{35}\text{SO}_4$ incorporation in agarose-chondrocyte constructs undertaken from two separate isolations (1204 and 0305).</i>	118
Figure 4.10	<i>Effect of pulsed low intensity ultrasound (PLIUS) on the rate of $^{35}\text{SO}_4$ incorporation in agarose-chondrocyte constructs undertaken from two separate isolations (0805 and 1105).</i>	120
Figure 4.11	<i>Effect of pulsed low intensity ultrasound (PLIUS) on the rate of [^3H]thymidine incorporation in agarose-chondrocyte constructs undertaken from two separate isolations (1204 and 0305).</i>	121
Figure 4.12	<i>Effect of pulsed low intensity ultrasound (PLIUS) on the rate of [^3H]thymidine incorporation in agarose-chondrocyte constructs undertaken from two separate isolations (0805 and 1105).</i>	123
Figure 4.13	<i>Cell viability at day 16 in agarose-chondrocyte constructs exposed to $30\text{mW}/\text{cm}^2$ PLIUS every 24 hours from day 1 to day 16.</i>	128
Figure 5.1	<i>Effect of pulsed low intensity ultrasound (PLIUS) on total sGAG content in chondrocyte monolayer culture undertaken from two separate isolations (isolations 0206 and 0306).</i>	134
Figure 5.2	<i>Effect of pulsed low intensity ultrasound (PLIUS) on total sGAG content in chondrocyte monolayer culture undertaken from two separate isolations (isolations 0905 and 1205).</i>	136
Figure 5.3	<i>Effect of pulsed low intensity ultrasound (PLIUS) on total DNA content in chondrocyte monolayer culture undertaken from four separate isolations and at two PLIUS SATA intensities.</i>	137
Figure 5.4	<i>Effect of pulsed low intensity ultrasound (PLIUS) on the rate of SO_4 incorporation in chondrocytes in monolayer, undertaken from four separate isolations and at two PLIUS SATA intensities.</i>	139
Figure 5.5	<i>Effect of pulsed low intensity ultrasound (PLIUS) on the rate of [^3H]thymidine incorporation in chondrocytes in monolayer, undertaken from four separate isolations and at</i>	140

	<i>two PLIUS SATA intensities.</i>	
Figure 5.6	<i>Sulphate incorporation data obtained by Parvizi and colleagues (1999).</i>	143
Figure 6.1	<i>Fluorescence emission spectra of Fluo-4 in solution with free Ca^{2+} concentrations as labelled.</i>	149
Figure 6.2	<i>Glass-bottomed dish (MaTtek Corp., USA) and adapted transducer for application of ultrasound to dish contents.</i>	150
Figure 6.3	<i>Schematic diagram showing the nature of the increasing PLIUS intensity applied to chondrocytes cultured in monolayer and in 3D-agarose constructs over the 20-minute period for calcium signalling experiments investigating the influence of PLIUS intensity.</i>	151
Figure 6.4	<i>Selection of cells for calcium signalling analysis.</i>	152
Figure 6.5	<i>Two typical greyscale plots, A from a chondrocyte in 3D agarose culture, where the cell underwent three $[Ca^{2+}]_i$ transients, and B from a chondrocyte in monolayer, where the cell underwent two $[Ca^{2+}]_i$ transients.</i>	152
Figure 6.6	<i>Summary of experimental procedures with relevant sections.</i>	153
Figure 6.7	<i>Cumulative number of chondrocytes in agarose constructs exhibiting a $[Ca^{2+}]_i$ transient over the 10 minute experimental period.</i>	154
Figure 6.8	<i>Number of $[Ca^{2+}]_i$ transients elicited by chondrocytes in agarose culture at 5 and 10 minutes (Figures A and B respectively), divided into cells eliciting between 1-3 transients, and those eliciting 4 or more transients.</i>	155
Figure 6.9	<i>Temporal profile of $[Ca^{2+}]_i$ signalling exhibited by chondrocytes in agarose culture over the 600 second imaging period, divided into two minute intervals.</i>	156
Figure 6.10	<i>Cumulative number of chondrocytes in monolayer exhibiting a $[Ca^{2+}]_i$ transient over the 10 minute experimental period.</i>	157
Figure 6.11	<i>Number of $[Ca^{2+}]_i$ transients elicited by chondrocytes in monolayer culture at 5 and 10 minutes (Figures A and B respectively), divided into cells eliciting between 1-3 transients, and those eliciting 4 or more transients.</i>	158
Figure 6.12	<i>Temporal profile of $[Ca^{2+}]_i$ signalling exhibited by</i>	159

	<i>chondrocytes in monolayer culture over the 600 second imaging period, divided into two minute intervals.</i>	
Figure 6.13	<i>Cumulative number of chondrocytes in 3D agarose constructs exhibiting a $[Ca^{2+}]_i$ transient over the 20 minute experimental period.</i>	160
Figure 6.14	<i>Number of transients elicited by chondrocytes in 3D agarose constructs over a 20 minute period, divided into cells eliciting between 1-3 transients, and those eliciting 4 or more transients.</i>	162
Figure 6.15	<i>Temporal profile of $[Ca^{2+}]_i$ signalling over the 1200 second imaging period, split into 2 minute intervals.</i>	163
Figure 6.16	<i>Cumulative number of chondrocytes in monolayer culture exhibiting a $[Ca^{2+}]_i$ transient over the 20 minute experimental period.</i>	165
Figure 6.17	<i>Number of transients elicited by chondrocytes cultured in monolayer over a 20 minute period, divided into cells eliciting between 1-3 transients, and those eliciting 4 or more transients.</i>	166
Figure 6.18	<i>Temporal profile of $[Ca^{2+}]_i$ signalling over the 1200 second imaging period, split into 2 minute intervals.</i>	168
Figure 7.1	<i>Possible pathways by which pulsed low intensity ultrasound (PLIUS) affects matrix biosynthesis in cultured chondrocytes.</i>	189
Figure 7.2	<i>Representative FRAP analysis for 70kDa FITC-dextran showing A) confocal time series over the approximate 30 second post bleach period and B) the resulting normalized FRAP curve.</i>	192
Figure 7.3	<i>Effect of PLIUS on diffusion quantified using FRAP.</i>	193

LIST OF TABLES

Table 1.1	<i>The three cartilage types.</i>	2
Table 1.2	<i>Proportional ranges of the major components of articular cartilage, as provided by various authors.</i>	4
Table 1.3	<i>Collagen types in mammalian adult articular cartilage.</i>	8
Table 1.4	<i>The non-collagenous matrix proteins of articular cartilage.</i>	12
Table 1.5	<i>Various therapeutic interventions for cartilage repair and replacement.</i>	27
Table 2.1	<i>Measured attenuation coefficients for biological tissues.</i>	50
Table 2.2	<i>Clinical applications of ultrasound.</i>	51
Table 2.3	<i>Animal models employing low intensity pulsed ultrasound for bone repair.</i>	56
Table 2.4	<i>Studies investigating the effect of pulsed low intensity ultrasound (PLIUS) on cartilage biosynthesis.</i>	58
Table 3.1	<i>Additives for standard chondrocyte medium.</i>	65
Table 3.2	<i>Effect of pulsed low intensity ultrasound (PLIUS) on normalised sGAG content in agarose-chondrocyte constructs.</i>	88
Table 3.3	<i>Mean values of approximate cell number and amount of sGAG synthesised by each chondrocyte in agarose-chondrocyte constructs.</i>	89
Table 4.1	<i>Details of buffers and reagents used for alcian blue assay for the measurement of SO_4 incorporation.</i>	101
Table 4.2	<i>Summary of results investigating the effect of PLIUS on elaboration of total sGAG content in chondrocyte-agarose constructs exposed to once or twice daily $30mW/cm^2$ PLIUS, as determined by total sGAG content.</i>	104
Table 4.3	<i>Effect of pulsed low intensity ultrasound (PLIUS) on the ratio values of sGAG content released in the medium when compared to total sGAG content (construct + medium).</i>	107
Table 4.4	<i>Summary of results investigating the effect of PLIUS on elaboration of sGAG in chondrocyte-agarose constructs exposed to once daily $100mW/cm^2$ PLIUS, as determined by total sGAG content.</i>	110

Table 4.5	<i>Effect of pulsed low intensity ultrasound (PLIUS) on the ratio values of sGAG content released in the medium when compared to total sGAG content (construct + medium).</i>	112
Table 4.6	<i>Summary of results investigating the effect of PLIUS on cell proliferation in chondrocyte-agarose constructs exposed to once or twice daily 30mW/cm² or 100mW/cm² PLIUS, as determined by total DNA content.</i>	116
Table 4.7	<i>Mean amount of sGAG per cell in chondrocyte/agarose construct. Constructs exposed to once or twice daily 30mW/cm² or 100mW/cm² PLIUS (n=6-7).</i>	117
Table 4.8	<i>Summary of results investigating the effect of PLIUS on sGAG production in chondrocyte-agarose constructs exposed to once or twice daily 30mW/cm² and 100mW/cm² PLIUS, as determined by rate of ³⁵SO₄ incorporation.</i>	119
Table 4.9	<i>Summary of results investigating the effect of PLIUS on cell proliferation in chondrocyte-agarose constructs exposed to once or twice daily 30mW/cm² or 100mW/cm² PLIUS, as determined by [³H]thymidine incorporation.</i>	122
Table 5.1	<i>Effect of PLIUS at 30mW/cm² on the ratio values of sGAG content released in the medium when compared to total sGAG content (monolayer + medium).</i>	134
Table 5.2	<i>Effect of PLIUS at 100mW/cm² on the ratio values of sGAG content released in the medium when compared to total sGAG content (monolayer + medium).</i>	136
Table 5.3	<i>Mean amount of sGAG per cell in chondrocytes cultured in monolayer.</i>	138
Table 6.1	<i>Summary of results illustrating signalling behaviour for all experimental conditions in terms of percentage [Ca²⁺]_i transients.</i>	171
Table 7.1	<i>The influence of pulsed low intensity ultrasound (PLIUS) on the metabolic behaviour of chondrocytes.</i>	186

Chapter 1

Composition and Structure of Articular Cartilage

1.1	Introduction to cartilage and articular cartilage	2
1.2	Extracellular matrix	4
1.2.1	Tissue fluid	5
1.2.2	Collagens	5
1.2.2.1	Collagen structure	5
1.2.2.2	Cartilage-specific collagens	8
1.2.3	Proteoglycans	9
1.2.4	Non-collagenous proteins and glycoproteins	12
1.3	Chondrocytes	13
1.3.1	Chondrocyte development	13
1.3.2	Chondrocyte organelles and synthesis of extracellular matrix components	14
1.3.3	Chondrocyte metabolism	15
1.4	Articular cartilage zones and matrix regions	16
1.5	Loading of articular cartilage	20
1.6	Articular cartilage pathology	22
1.6.1	Trauma and injury	22
1.6.2	Ageing	23
1.6.3	Disease	24
1.7	Repair strategies	25

1.1 Introduction to Cartilage and Articular Cartilage

Cartilage is a specialized connective tissue that provides support, protects underlying subchondral bone and forms structural models for many developing bones (Shier *et al.*, 1999). Cartilage consists of cells called *chondrocytes*, and an extracellular matrix consisting of proteins, fibres and tissue fluid. The chondrocytes are responsible for the synthesis and secretion of matrix molecules (Junqueira *et al.*, 1998; Poole *et al.* 2001).

There are three types of cartilage which can be differentiated by the nature and amount of fibre contained within the matrix, namely hyaline cartilage, fibrocartilage and elastic cartilage, as detailed in Table 1.1. Hyaline cartilage is the most common type of cartilage found in the body, and forms the focus of the present thesis.

TABLE 1.1: *The three cartilage types.*

Cartilage type	Characteristics and Function	Location
Hyaline	Contains fine collagenous fibres in its matrix. Provides support and flexibility.	Embryonic skeleton Articular cartilage Costal cartilage Respiratory system (nose, larynx, trachea, bronchi) Epiphyseal plate
Fibrocartilage	Contains many large bundles of collagenous fibres. Gradually merges with neighbouring dense fibrous tissue or hyaline cartilage. Tough and resilient, acts as 'shock absorber'.	Symphysis pubis Intervertebral disks Menisci of Knee Attachment of certain ligaments to cartilaginous surface of bones Lining of tendon grooves
Elastic	Contains dense network of elastic fibres. Provides flexibility and lightweight support.	External ear Eustachian (auditory) tubes Parts of larynx Epiglottis

(Based on Van Wynsberg *et al.*, 1995; Junqueira *et al.*, 1998; Kessel *et al.*, 1998; Shier *et al.*, 1999).

Articular cartilage is the hyaline cartilage covering the subchondral bone ends in a synovial joint, as illustrated in Figure 1.1. In its healthy state it provides an almost frictionless gliding and load-bearing surface that is essential to normal joint function (Buckwalter and Hunziker, 1999; Poole *et al.*, 2001). By deforming, articular cartilage

distributes joint loads and, as a result, reduces the peak stresses to which the subchondral bone is exposed (Bader and Lee, 2000).

Cartilage lacks lymphatic vessels, nerves and blood vessels and contains only one cell type. The chondrocytes in articular cartilage are sustained by the diffusion of nutrients, such as glucose and oxygen, from the surrounding synovial fluid, a process facilitated by joint loading (Huber *et al.*, 2000; Hall, 1998).

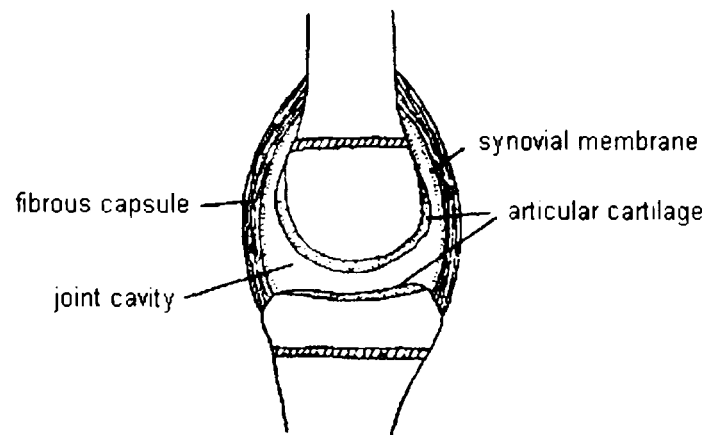


FIGURE 1.1: Schematic of a synovial joint. Articular cartilage covers the subchondral bone. The bones are separated by the joint cavity and connected by a fibrous capsule, which is lined by a synovial membrane that secretes synovial fluid. (Adapted from Benjamin, 1999).

Articular cartilage exhibits a complex and highly ordered structure, maintained by the interaction between the chondrocytes and the extracellular matrix. It varies in thickness, cell density, matrix composition and mechanical properties within the same joint, between joints and with different species (Hunziker, 1992). For humans, articular cartilage thickness in major load bearing joints is generally between 1.5-3.5mm thick (Bader and Lee, 2000), although this value is exceeded on the underside of the patellar surface in the knee joint.

Articular cartilage in its adult form has a low level of metabolic activity when compared to other tissues, such as muscle or bone, and appears less responsive to changes in loading or injury. However, it has excellent durability as exemplified by its ability to both retain its physical properties to a large degree when subjected to stress, and, in many cases, provide normal joint function for 80 years or more (Buckwalter and Mankin, 1998).

1.2 Extracellular Matrix

The extracellular matrix consists of tissue fluid and a framework of macromolecules, namely collagens, proteoglycans, glycoproteins and non-collagenous proteins. Collagen forms a fibrillar network that provides the capacity to withstand tensile and shear forces (Kempson, 1979). The collagen meshwork contains a non-fibrous 'filler' substance principally composed of proteoglycans and non-collagenous proteins (Meachim and Stockwell, 1979). The interaction of tissue fluid with the macromolecular framework gives cartilage its stiffness, resilience and ability to participate in joint lubrication (Buckwalter and Mankin, 1998).

The approximate percentage of the components of articular cartilage are summarized in Table 1.2, in both dry and wet weight forms.

TABLE 1.2: Proportional ranges of the major components of articular cartilage, as provided by various authors.

Component	% wet weight	% dry weight
Tissue Fluid	65-80 (<i>Muir, 1979; Hall, 1998; Bader and Lee, 2000</i>) 68-85 (<i>Mow and Ratcliffe, 1997</i>) 60-78 (<i>Kessel, 1998</i>)	N/A
Collagen	↑	20-30 (<i>Muir, 1979</i>) 15-30 (<i>Hall, 1998</i>) 15-20 (<i>Bader and Lee, 2000</i>) ~50 (<i>Muir, 1979</i>) 68-85 (<i>Mow and Ratcliffe, 1997</i>) ~60 (<i>Buckwalter and Hunziker, 1999</i>)
Proteoglycan	↓	5-10 (<i>Mow and Ratcliffe, 1997</i>) 3-10 (<i>Hall, 1998</i>) 3-15 (<i>Bader and Lee, 2000</i>) 20-40 (<i>Buckwalter and Hunziker, 1999</i>) 25-35 (<i>Buckwalter and Hunziker, 1999</i>)
Non-collagenous proteins and glycoproteins	↓	1 (<i>Bader and Lee, 2000</i>) 15-20 (<i>Buckwalter and Hunziker, 1999</i>)

1.2.1 Tissue Fluid

Water makes up the majority of the wet weight of articular cartilage (Table 1.2). The highest content is found adjacent to the articular surface, with a decrease towards the subchondral bone (Maroudas, 1979). Tissue fluid contains gases, small proteins, metabolites, and a high concentration of mobile cations that balance the negatively charged proteoglycans (Buckwalter and Hunziker, 1999), including calcium, sodium and hydrogen ions (Bader and Lee, 2000).

The volume, concentration, and behaviour of the water within the tissue depend on its interaction with the structural macromolecules. Approximately 30% of water is strongly associated with the collagenous network (Mow and Ratcliffe, 1997; Bader and Lee, 2000). The remaining bound water is associated with the hydrophilic proteoglycans (Kessel, 1998). Only a small proportion of the total water in cartilage is intracellular (Bader and Lee, 2000).

The water associated with the proteoglycans is freely exchangeable during joint loading and unloading. The movement of water is important for joint lubrication and also chondrocyte nutrition and viability, as these cells rely on diffusion of nutrients through the matrix due to the absence of a vascular supply (Bader and Lee, 2000; Buckwalter and Hunziker, 1999). The interstitial fluid also permits the removal of metabolic by-products (Hall, 1998).

1.2.2 Collagens

Collagen is the most abundant protein in the body, and is the major structural macromolecule in connective tissues (Van der Rest and Garrone, 1991). To date, 29 forms of collagen have been identified, made up of more than 30 different gene products (Veit *et al.*, 2006; Söderhäll *et al.*, 2007). Each collagen type has individual characteristics enabling them to perform specific functions in various tissues.

1.2.2.1 Collagen Structure

The common structural feature shared by all collagens is a triple helix region within the molecule. This triple helix is composed of three polypeptide chains folded in a rope-like coil formation. Each chain is known as an alpha chain (α -chain), characterised by repeated sequences of three amino acids, glycine-X-Y, where approximately 10-12% of each of the X and Y residues are proline and hydroxyproline respectively, their

distribution allowing an orderly arrangement of interchain hydrogen bonds that stabilize the helix (Thomas *et al.*, 1994). Each α -chain contains approximately 1000 amino acid residues (Bader and Lee, 2000). Glycine is the smallest amino acid and occupies the crowded interior of the triple helix (Muir, 1995). Its repetition as every third amino acid is paramount for the correct folding of the three α -chains into the helical formation (Culav *et al.*, 1999), as indicated in Figure 1.2.

Specific collagen types are formed by a variety of α -chains in various combinations. In some collagens all the α -chains are identical, whereas, in others two α -chains may be identical or, in some cases, all the α -chains are different.

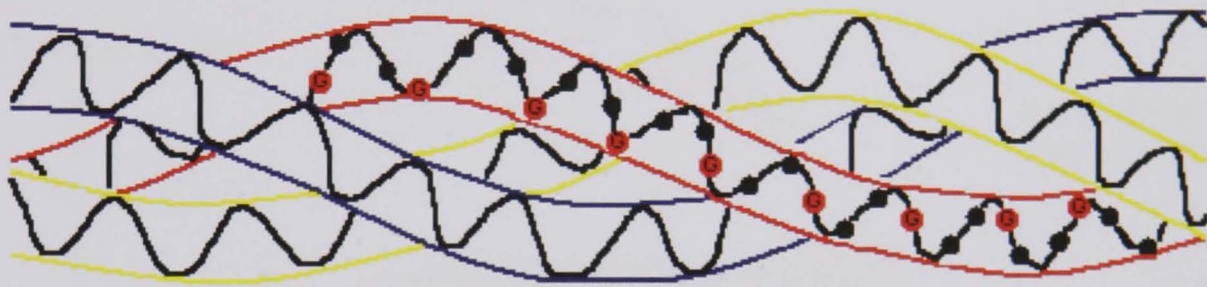


FIGURE 1.2: Portion of collagen molecule, showing three α -chains coiled to form a triple helix. Within each chain the amino acids are also arranged in a helix, with Glycine (G) facing the centre of the triple helix, as shown in the red chain. The other amino acids are represented by the dots. Adapted from Culav *et al.*, 1999.

The prominent feature of most collagens is their ability to resist tensile loads. They usually demonstrate up to 10-15% elongation under tension. This is, in part, due to the straightening of the fibres packed in the three-dimensional arrays as opposed to the actual elongation of individual fibres. The intermolecular bonds between the α -chains of adjacent molecules impart stiffness and strength to the helical complex, which further resists tension (Culav *et al.*, 1999).

The α -chains of the major collagens are synthesized with extended extremities. The terminal ends of the collagen molecule are non-helical in nature, and are important for collagen fibril formation and for alternative functions, such as interaction with other extracellular components. After formation of the triple helix, the newly formed collagen, termed procollagen, is delivered by the chondrocyte into the extracellular space, where a high proportion of the non-helical ends are removed enzymatically. This results in a shortened molecule approximately 1.5nm in diameter and 300nm long,

termed tropocollagen (Buehler, 2006). Five molecules of tropocollagen can cross-link to form pentameric fibrils, characterized by a distinct banding structure when viewed under an electron microscope (Culav *et al.*, 1999). The formation of the cross-links requires some overlap between adjacent molecules, and the fibrils demonstrate a 64nm periodicity (Bader and Lee, 2000; Junqueira *et al.*, 1998). These fibrils can aggregate to form fibres and bundles of fibres, as shown schematically in Figure 1.3.

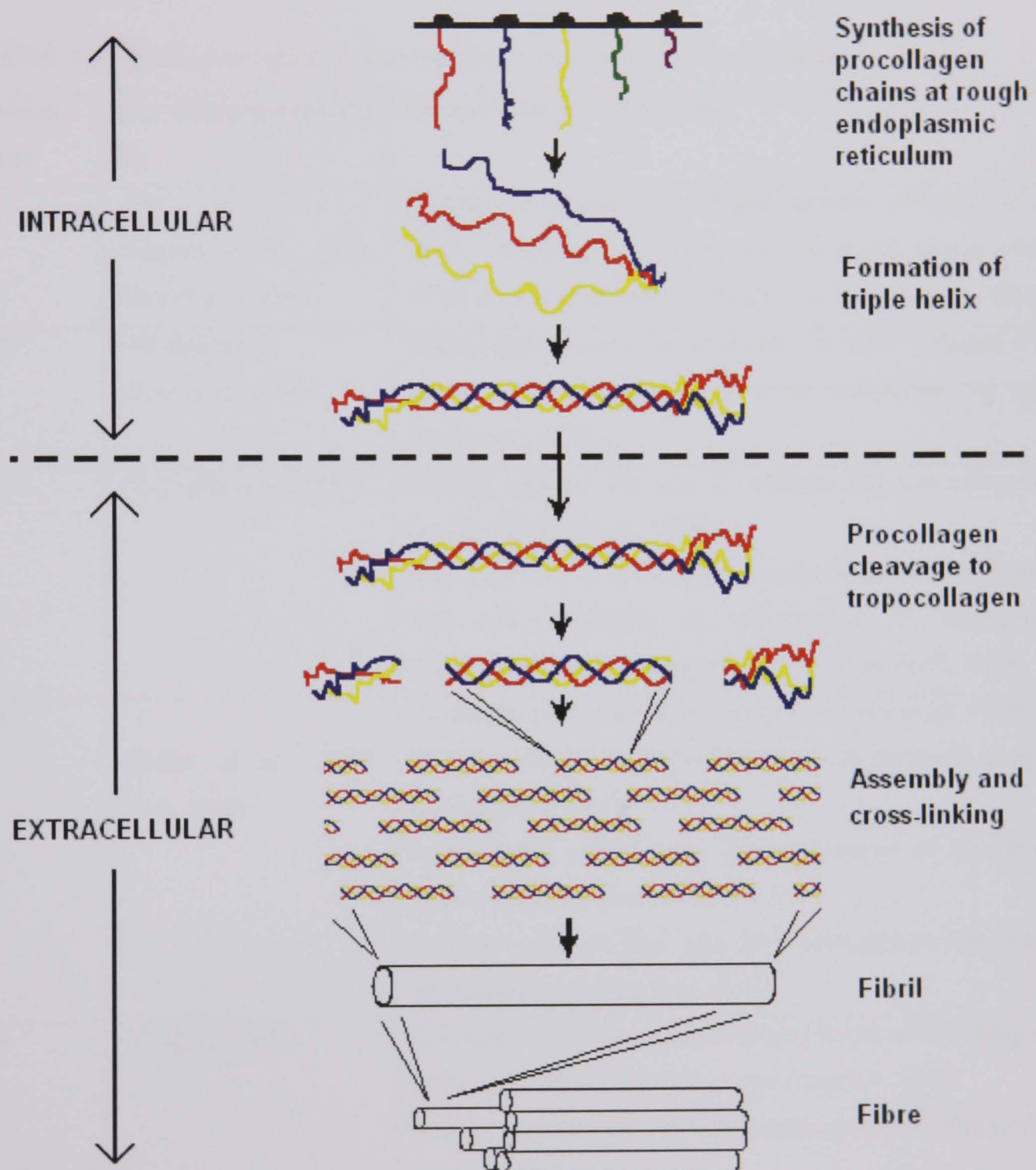


FIGURE 1.3: Schematic showing collagen synthesis, secretion and assembly. Adapted from Culav *et al.*, 1999

1.2.2.2 Cartilage-specific Collagens

The fibrous network of articular cartilage is composed primarily of polymerized collagen type II molecules that form a hetero-fibril with types IX and XI (Huber *et al.*, 2000, Eyre *et al.*, 2006). Type II collagen is found in tissues with high proteoglycan and water content, suggesting specific properties that enable an ordered relationship with proteoglycans that create and maintain a highly hydrated matrix (Buckwalter *et al.*, 1987a). Table 1.3 presents a summary of the different articular cartilage collagens.

TABLE 1.3: Collagen types in mammalian adult articular cartilage.

Collagen Type	Dry weight percentage %	Characteristics and function
II	>90 (Duance <i>et al.</i> , 1999; Eyre <i>et al.</i> , 2006)	Primary component of collagen network (Duance <i>et al.</i> , 1999). Composed of three identical $\alpha_1(\text{II})$ chains (Muir, 1979). Forms endoskeleton of cartilage (Huber <i>et al.</i> , 2000).
III	>10 (human) (Eyre <i>et al.</i> , 2006)	Copolymerised molecule, covalently linked to collagen II (in human tissue). Possible role in tissue remodelling and repair (Eyre <i>et al.</i> , 2006).
VI	<2 (Pullig <i>et al.</i> , 1999)	Binding capacity for type II collagen and non-collagenous proteins (Pullig <i>et al.</i> , 1999). Important role in pericellular matrix organization (Section 1.4) and anchoring of chondrocyte in surrounding extracellular matrix (Pullig <i>et al.</i> , 1999; Eyre <i>et al.</i> , 2006).
IX	~1 (Huber <i>et al.</i> , 2000; Eyre, 2002)	Covalently fibril-associated collagen (Duance <i>et al.</i> , 1999). Bonds to superficial layers of collagen II fibrils (Buckwalter and Hunziker, 1999). Considered a proteoglycan due to presence of chondroitin sulphate chain (Duance <i>et al.</i> , 1999). Mediator of fibril-fibril and fibril-proteoglycan interactions (Buckwalter and Hunziker, 1999).
XI	~3 (Eyre, 2002)	Covalently fibril-associated collagen; forms part of interior of collagen II fibrils (Buckwalter and Hunziker, 1999). Acts as template to constrain lateral growth of hetero-fibril (Eyre, 2002).
XII/XIV	Not specified	Non-covalently fibril-associated collagens. Also classed as proteoglycans; possible interaction with other fibril-binding proteins (Eyre, 2002).
XIII	Not specified	Transmembrane (Eyre <i>et al.</i> , 2006).
X	Not specified	Found in hypertrophic cartilage in calcified region only (Buckwalter and Hunziker, 1999).

The arrangement and alignment of the collagen fibres reflect the mechanical stresses acting on articular cartilage (Culav *et al.*, 1999). Both the diameter and orientation of fibres vary with depth below the articular surface (Bader and Lee, 2000) as described in section 1.4. Additionally, under pathological conditions and in ageing, the collagen composition of cartilage is subject to change, with evidence of collagen type I and an increase in levels of collagen XI (Duance *et al.*, 1999; Pullig *et al.*, 1999).

1.2.3 Proteoglycans

Proteoglycans are molecules characterized by a core protein covalently attached to one or more glycosaminoglycan (GAG) chains (Huber *et al.*, 2000). GAG chains are composed of repeating disaccharide units, comprising two amino sugars, n-acetyl hexosamine and either hexuronic acid or hexose (Bader and Lee, 2000). Each disaccharide unit has at least one negatively charged carboxylate or sulphate group, so the GAGs can form long strings of negative charges that repel each other and attract water molecules and cations (Buckwalter *et al.*, 1987a). The core proteins are usually specific to each of the proteoglycan types and can vary considerably in size. The four GAGs found in articular cartilage are chondroitin sulphates 4 and 6, keratan sulphate and hyaluronan. Hyaluronan, present in relatively small amounts in articular cartilage, is an uncharacteristic GAG in that it is not attached to a protein core, is non-sulphated, and is not found as a component of a proteoglycan monomer (Culav *et al.*, 1999).

The most common proteoglycan, accounting for approximately 90% of total proteoglycan mass in articular cartilage, is the large aggregating macromolecule termed *aggrecan* (Huber *et al.*, 2000). This is shown schematically in Figure 1.4. Aggrecan is composed of a core protein filament 200-400nm in length with multiple bonded chondroitin sulphate and keratan sulphate chains, approximately 100 chains of the former and 30 of the latter GAG (Mow and Ratcliffe, 1997; Muir, 1995). The GAGs contribute approximately 95% to the molecule, with the remainder composed of protein. As the GAG chains contain a high number of negative charges, adjacent chains repel each other and extend from the core protein like the bristles of a bottle-brush, maintaining aggrecan in an expanded form in solution (Buckwalter *et al.*, 1987a; Culav *et al.*, 1999).

As seen in Figure 1.4, the protein core filament has three globular domains and two extended domains, termed G1, G2, G3 and E1 and E2, respectively (Hardingham *et al.*,

1992). The G1 domain is at the amino-terminal end of the molecule, and acts as the binding site for hyaluronan, the interaction of which is stabilized by a glycoprotein, known as the link protein, which has structural homology to the G1 domain (Bader and Lee, 2000, Culav *et al.*, 1999).

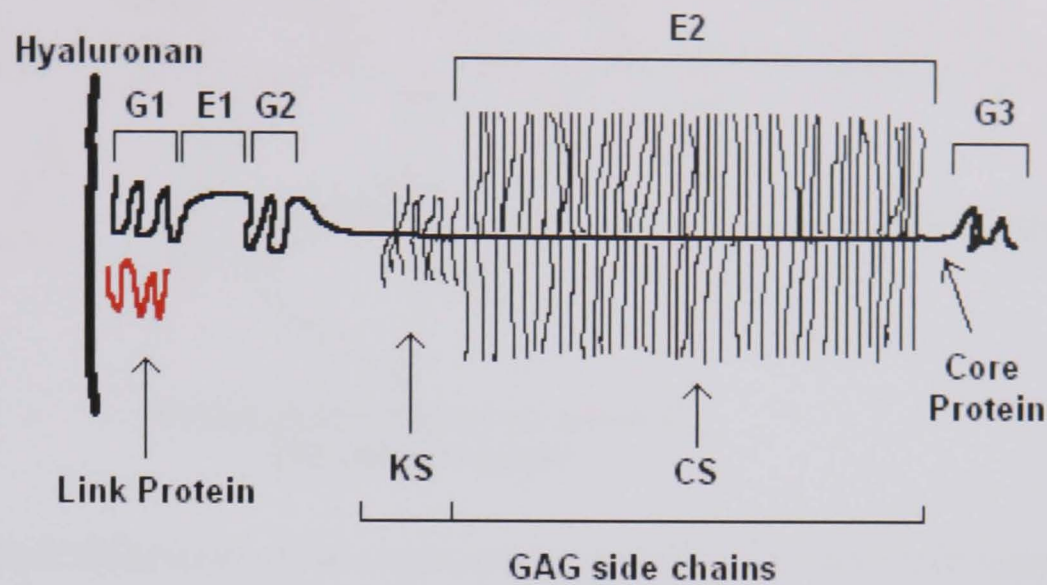


FIGURE 1.4: A schematic of the aggrecan molecule and its binding to hyaluronan. The protein core has three globular domains (G1, G2, G3) with other regions containing the keratan sulphate (KS) and chondroitin sulphate (CS) molecules. Adapted from Hardingham *et al.*, 1992.

Many aggrecan molecules can bind to a single hyaluronan to form multimolecular aggregates, as shown in Figure 1.5. The hyaluronan backbone can range in length from several hundred to several thousand nanometres, and form aggregates of between 300 and 800 associated aggrecan molecules (Poole *et al.*, 1982; Hardingham *et al.*, 1992; Buckwalter and Hunziker, 1999).

Aggrecan contributes to the compressive stiffness of cartilage due to the hydration of the large numbers of chondroitin sulphate and keratan sulphate chains occupying the core protein. These GAGs create a high charge density inducing an osmotic swelling pressure that attracts water into the matrix. Molecular swelling is resisted by the collagen network, which is under constant tension even in unloaded cartilage (Muir, 1995). This mechanism, in conjunction with the bonding of negatively charged GAG chains to regions of positive charge on collagen fibrils, limits proteoglycan expansion to between 10-20% of their swelling capacity (Mow and Ratcliffe, 1997; Culav *et al.*, 1999; Hall, 1998; Poole *et al.*, 2001).

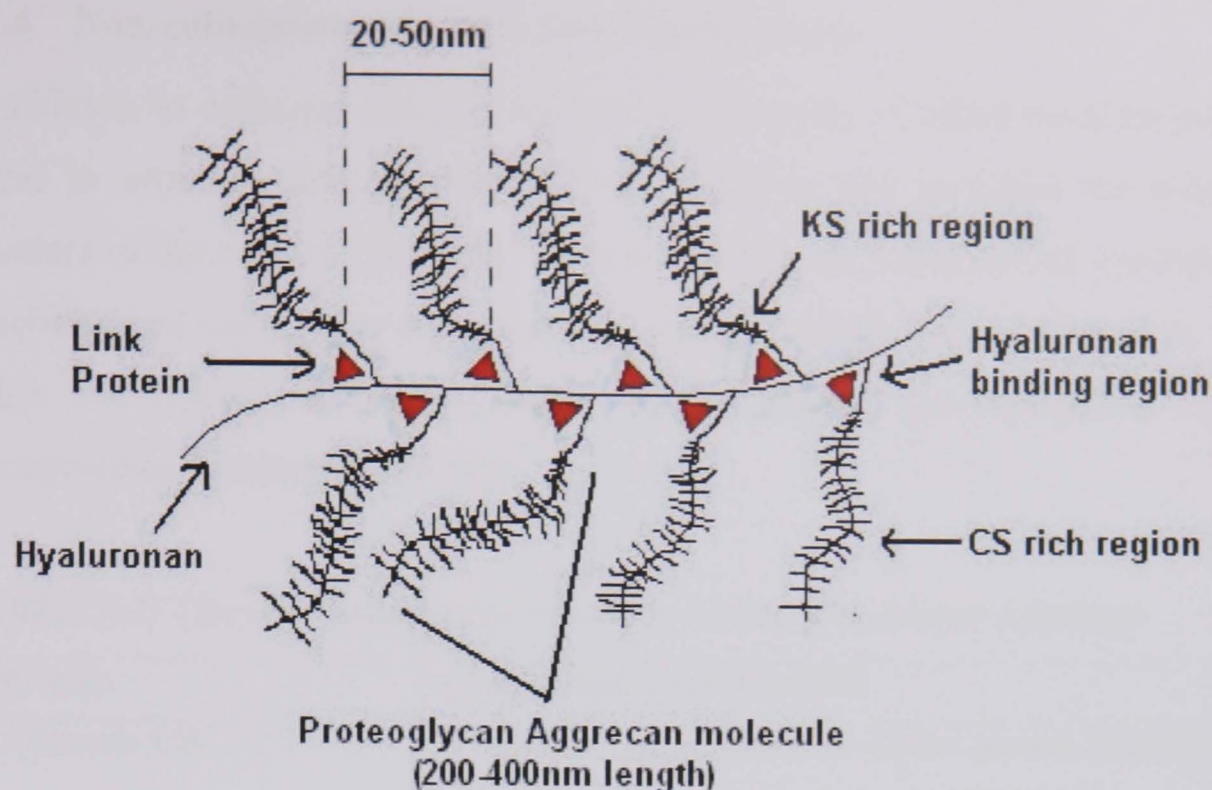


FIGURE 1.5: Schematic of an aggregating proteoglycan molecule (aggrecan). This is composed of keratan sulphate (KS) and chondroitin sulphate (CS) covalently bound to a hyaluronan protein core molecule at regular intervals of 20-50nm via a link protein. Adapted from figure by Mow and Ratcliffe, 1997.

There is a small percentage (<10%) of large non-aggregating proteoglycans found in articular cartilage, which may represent degraded aggrecans (Huber *et al.*, 2000). Loss of the larger aggregating proteoglycans appears to be one of the earliest changes associated with osteoarthritis, immobilization of the joint and ultimate joint degeneration. There is also an associated loss of large aggregates with age, which may be influenced by a reduction in proteoglycan synthesis by chondrocytes and/or an increase in proteoglycan degradation (Buckwalter and Mankin, 1998).

A number of smaller, non-aggregating proteoglycans are found in articular cartilage. These proteoglycans are leucine-rich and include decorin, biglycan and fibromodulin, which account for approximately 3% of total proteoglycan mass (Huber *et al.*, 2000). Decorin contains one GAG chain, biglycan contains two, and fibromodulin has up to four GAG chains (Poole *et al.*, 2001). These molecules interact with collagen and are thought to play a role in organizing and stabilizing the type II collagen network (Mow and Ratcliffe, 1997). Chondroadherin (CD44), a multi-functional cell surface receptor, has one GAG chain and is the chondrocyte receptor for hyaluronan, anchoring this molecule to the cell surface (Taylor and Gallo, 2006; Poole *et al.*, 2001).

1.2.4 Non-collagenous proteins and Glycoproteins

In addition to collagen and proteoglycans, a number of other macromolecules can be found in articular cartilage that help to organize and maintain the macromolecular structure of the matrix. Generally, these molecules are composed of a protein with a few attached monosaccharides and oligosaccharides (Buckwalter and Hunziker, 1999).

Table 1.4 below summarises some of the known non-collagenous proteins and glycoproteins in articular cartilage.

TABLE 1.4: *The non-collagenous matrix proteins of articular cartilage*

Protein	Characteristics and Function
Anchorin CII	Collagen-binding chondrocyte surface protein. Mediates binding of type II collagen to chondrocytes (<i>Heinegård and Pimentel, 1992; Huber et al., 2000</i>).
Cartilage Oligomeric Protein (COMP)	An acidic protein appearing only in cartilage (<i>Buckwalter and Hunziker, 1999</i>). Role in binding type II collagen to chondrocytes. Possible role in repair process and matrix assembly (<i>Huber et al., 2000; Poole et al., 2001</i>).
Chondronectin	A glycoprotein that binds to collagen type II and GAGs, mediating adhesion between chondrocytes and extracellular matrix (<i>Junqueira et al., 1998</i>).
Fibronectin Tenascin	Glycoproteins with important role in cell attachment to matrix components (<i>Heinegård and Pimentel, 1992; Culav et al., 1999</i>). May also play a part in the tissue response to inflammatory arthritis and osteoarthritis (<i>Buckwalter and Hunziker, 1999</i>).
Link Protein	Stabilizes matrix proteoglycan aggregates (<i>Hardingham, 1979; Heinegård and Pimentel, 1992; Culav et al., 1999</i>).
Lubricin	A glycoprotein synthesized and localized in the superficial zone (see Section 1.4) of articular cartilage. Roles in cytoprotection, lubrication and matrix binding (<i>Jones et al., 2007</i>). Also known as superficial zone protein (SZP), or Proteoglycan-4 (PRG4) due to the fact that it has the potential for GAG attachment (<i>Poole et al., 2001; Rees et al., 2002</i>).

1.3 Chondrocytes

Chondrocytes are the sole cell type existing in articular cartilage. These specialised cells produce and maintain the extracellular matrix components that provide articular cartilage with the mechanical and physical properties necessary for load bearing and joint locomotion.

The chondrocytes contribute between 1% and 10% of the volume of mammalian articular cartilage (Stockwell and Meachim, 1979). Under histological examination, the chondrocytes are contained in spaces in the matrix, called *lacunae*, although these features are not evident in living cartilage. Chondrocytes vary in size, shape, distribution and metabolic activity according to their distance from the articular surface.

1.3.1 Chondrocyte Development

Chondrocytes are derived from the mesenchyme, namely embryonic connective tissue. In the foetus, mesenchymal cells differentiate by retracting their extensions and multiplying rapidly to form mesenchymal condensations, or chondroblasts, exhibiting a ribosome-rich basophilic cytoplasm. The chondroblasts then begin the synthesis, packaging and exporting of large amounts of extracellular matrix causing the cells to separate from each other, at which stage the cells are now classed as chondrocytes. Cartilage can grow from within via a process called interstitial growth, where chondrocytes multiply via mitosis and these new cells go on to produce further matrix. This only occurs during the early stages of cartilage formation as a way of increasing tissue mass (Junqueira *et al.*, 1998; Kessel, 1998).

After growth has ceased there is no detectable cell division in healthy adult articular cartilage (Buckwalter and Mankin, 1998). However, chondrocytes retain the ability to replicate, particularly noted following damage to the collagenous network, such as in cases of osteoarthritis (Muir, 1995).

It is notable that the cellularity of cartilage changes greatly with the stage of development. In the embryonic limb before bone is formed, the volume ratio of cells to matrix is approximately 1:3. As the limb grows matrix volume increases, such that in the superficial articular cartilage zone where single cells tend to occur, the ratio is 1:50 (Hall, 1998).

1.3.2 Chondrocyte Organelles and Synthesis of Extracellular Matrix Components

Chondrocytes are eukaryotic cells, characterised by a plasma membrane, a membrane-bound nucleus and organelles, as shown in Figure 1.6. The predominant organelles found in the cytoplasm of the synthetically active chondrocyte are the rough endoplasmic reticulum (rER) and the Golgi apparatus, both of which are involved in the production and secretion of extracellular matrix molecules. The rER synthesises the core proteins and link proteins of the proteoglycans, type II collagen chains, and oligosaccharides. These products are secreted and transferred to the Golgi apparatus via membrane-bound vesicles. Synthesis of procollagen and polysaccharides occur in the Golgi apparatus, where they are then packaged for transport out of the cell, approximately 3-6 hours after synthesis has occurred (Kessel, 1998). Hyaluronan is synthesized at the plasma membrane (Knudson, 1993). Secretory products are removed from the cell via exocytosis. Both proteoglycan aggregates and tropocollagen molecules are formed in the extracellular matrix.

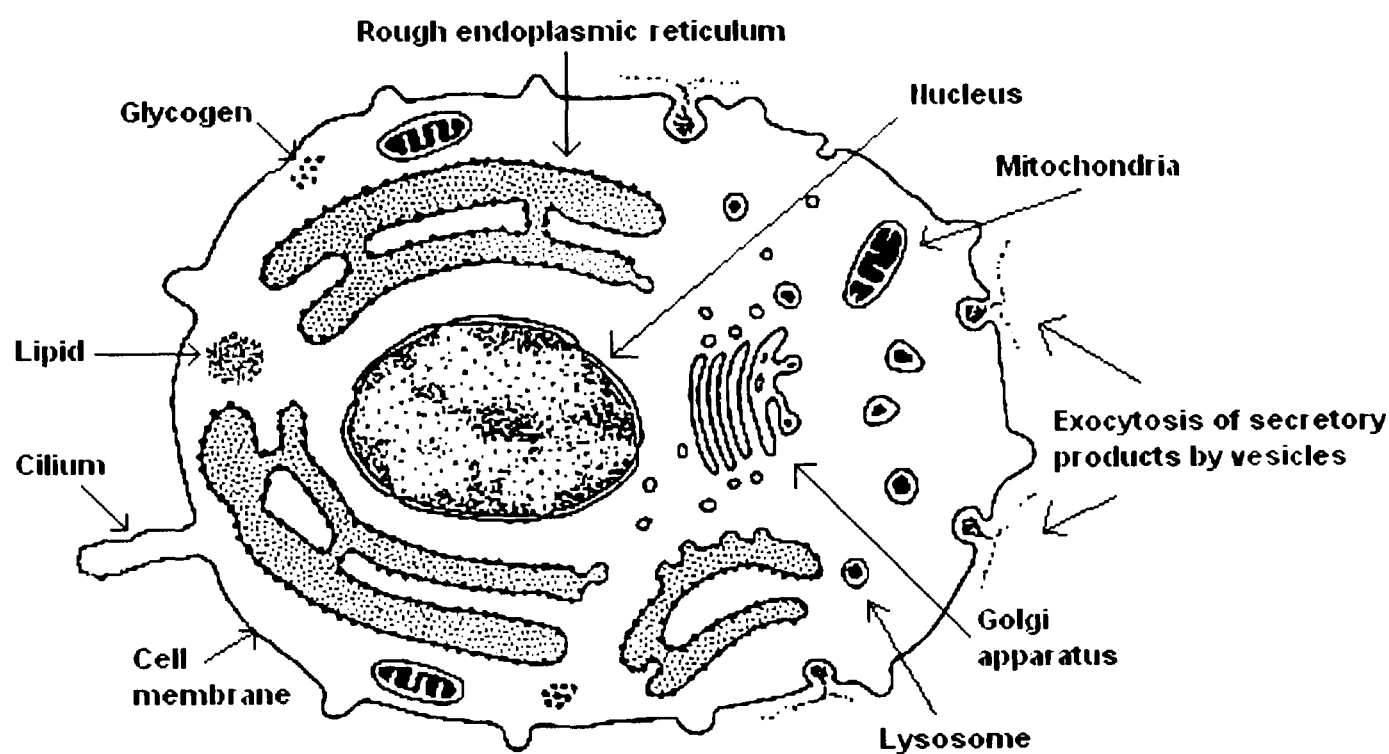


FIGURE 1.6: Schematic of a typical chondrocyte with its major organelles. Adapted from Kessel, 1998.

Other organelles of note (Figure 1.6) are the lysosomes, a type of vacuole present in the Golgi apparatus involved in intracellular digestion of waste material as well as the turnover of extracellular matrix via endocytosis, and the mitochondria, the organelles responsible for converting oxygen and nutrients into adenosine triphosphate (ATP) via glycolysis (Stockwell, 1978; Heywood *et al.*, 2004). ATP is an essential energy source for biochemical reactions. Mitochondria are numerous in the chondrocytes of immature

cartilage but are more scarce and smaller in adult chondrocytes, reflecting the low respiratory activity in adult tissue (Stockwell, 1978, Terkeltaub *et al.*, 2002).

Lipid and glycogen deposits are present in the cytoplasm, as well as the filamentous structures of the cytoskeleton, which can be extensive in some chondrocytes (Horton, 1993). The cytoskeleton is composed of actin microfilaments, tubulin microfilaments and vimentin intermediate filaments, each with a diameter in the order of nanometres. These structures act to give the cell its shape and provide a basis for cell movement. Other functions of the cytoskeleton in chondrocytes may include cell-matrix interactions, cell signaling, intracytoplasmic transport, control of secretion/endocytosis, control of chondrocyte phenotype, and in mechanotransduction (Durrant *et al.*, 1999; Langelier *et al.*, 2000).

The plasma membranes of chondrocytes are generally scalloped with many processes containing microfilaments that extend into the matrix. Small invaginations called caveolae are also prominent on the cell surface, which are involved in cell signaling and endocytosis and exocytosis (Horton, 1993; Durrant *et al.*, 1999; Schwab *et al.*, 1999). Additionally, most articular chondrocytes have a single cilium that may be involved in regulation of matrix turnover (McGlashan *et al.*, 2006).

1.3.3 Chondrocyte Metabolism

Cartilage is an avascular tissue, which means that chondrocytes have no blood supply that can provide nutrition. The main pathway by which articular cartilage receives vital nutrients is through diffusion from the surrounding synovial fluid to the extracellular matrix during normal joint loading. Diffusion distances are therefore greater than with vascular tissues (Stockwell and Meachim, 1979), resulting in a low concentration of oxygen available to the cells of between 10% at the articular surface to under 1% in the deep zones (Goldring, 2006). However, chondrocytes are able to exist under very low oxygen tensions compared to other cell types, metabolising glucose primarily by glycolysis to produce lactate via anaerobic respiration, which is preferentially maintained even under low aerobic conditions (Stefanovic-Racic *et al.*, 1994).

Maintenance of cartilage tissue occurs via continued interactions between the chondrocyte and its extracellular matrix. Chondrocyte metabolism occurs via enzymatic reactions controlling activities, such as respiration and glycolysis, and the synthesis,

remodelling and degradation of extracellular matrix molecules (Mow and Ratcliffe, 1997).

Degradation and repair of extracellular matrix involve proteases, enzymes that hydrolytically degrade proteins into peptides or amino acids. Cathepsins, a class of lysosomal proteases, and metalloproteinases, which are secreted by the cell, are two classes of proteases that can degrade both proteoglycan and collagen (Tyler *et al.*, 1992; Werb, 1992). Proteolytic components are released into the pericellular matrix and partially digest matrix molecules, before the breakdown products are taken into the cell by pinocytosis or phagocytosis and digestion completed within the lysosome (Stockwell and Meachim, 1979). Protease expression has been shown to increase with age and pathological changes (Goldring, 2006).

Metabolic rates are influenced by changes in their mechanical and physiochemical environment. The main directors of metabolism are the *cytokines*, chemical messenger proteins that are synthesized by chondrocytes and released into the matrix. Cytokines may bind to cell surface receptors to stimulate both catabolic and anabolic effects (Huber *et al.*, 2000). Examples of anabolic cytokines include transforming growth factor β (TGF- β), insulin-like growth factor-1 (IGF-1), and interleukin-4 (IL-4), that have stimulatory effects on matrix synthesis and can antagonize the action of some catabolic cytokines (Tyler *et al.*, 1992; Mow and Ratcliffe, 1997; Chowdhury *et al.*, 2006). Cytokines involved in catabolic processes include interleukin-1 β (IL-1 β) and tumour necrosis factor- α (TNF- α), which both predominate in the osteoarthritic disease process (Goldring, 2006).

1.4 Articular Cartilage Zones and Matrix Regions

Due to the structural differences in articular cartilage with depth, four layers or zones can be identified within the tissue. From the articular surface to the subchondral bone, there exists the superficial zone, the middle or transitional zone, the deep or radial zone and the zone of calcified cartilage (Figure 1.7). Although distinct in features, the superficial, middle and deep zones merge into each other and have no clear boundaries. However, the calcified zone is separated from the radial zone by a weakly basophilic line of mineral deposits, termed the *tidemark* (Hunziker, 1992). Depending on species and joint location, the superficial zone constitutes between 5-20% of articular cartilage

depth, the middle zone and deep zones between 30-60%, and the calcified zone between 5-10% (Meachim and Stockwell, 1979; Poole *et al.*, 1982; Mow and Ratcliffe, 1997).

Each articular cartilage zone can be identified by distinct differences in the amounts and orientation of the different components (Figure 1.7). The chondrocytes are rounded or polygonal in all regions of the cartilage, except for the superficial zone where they are flattened or discoid (Archer and Francis-West, 2003). The collagen fibrils and filaments are organized into a tight network extending throughout the cartilage, which vary in diameter from approximately 20nm in the superficial zone to 70-120nm in the deep zone (Buckwalter and Hunziker, 1999; Poole *et al.*, 2001). The proteoglycan content increases with increasing depth from the articular surface (Hall, 1998).

The superficial zone is itself divided into two layers, an acellular layer and a deeper cellular layer. The former layer, 2-3 μ m in depth, is termed the *lamina splendens*, which consists of fine randomly arranged 2-20nm diameter collagen fibrils associated with abundant proteoglycan, which are most likely collagen-associated biglycan, decorin, and lubricin (Buckwalter and Hunziker, 1999; Poole *et al.*, 2001). In the subjacent cellular layer, the discoid chondrocytes, 8-15 μ m in diameter, exist either singularly or in pairs, have their major axes parallel to the articular surface and secrete collagen fibrils arranged around the cells in the same orientation (Hall, 1998). The fibrils are organised in closely packed sheet-like layers, the fibrillar orientations varying both in each layer and between layers (Bader and Lee, 2000). There is very little hyaluronan present, which suggests low amounts of proteoglycan aggregates compared to deeper zones. This layer of the superficial zone is the most cellular region of cartilage, representing one third of the total number (Stockwell and Meachim, 1979). Additionally, this region also contains the highest concentration of collagen, decorin and biglycan, as well as the only region to contain lubricin, also known as superficial zone protein (Hall, 1998; Poole *et al.*, 2001). The superficial zone exhibits the highest tensile properties found in articular cartilage, which is important in order to resist the shear forces generated during joint loading (Hall, 1998; Buckwalter *et al.*, 1987a).

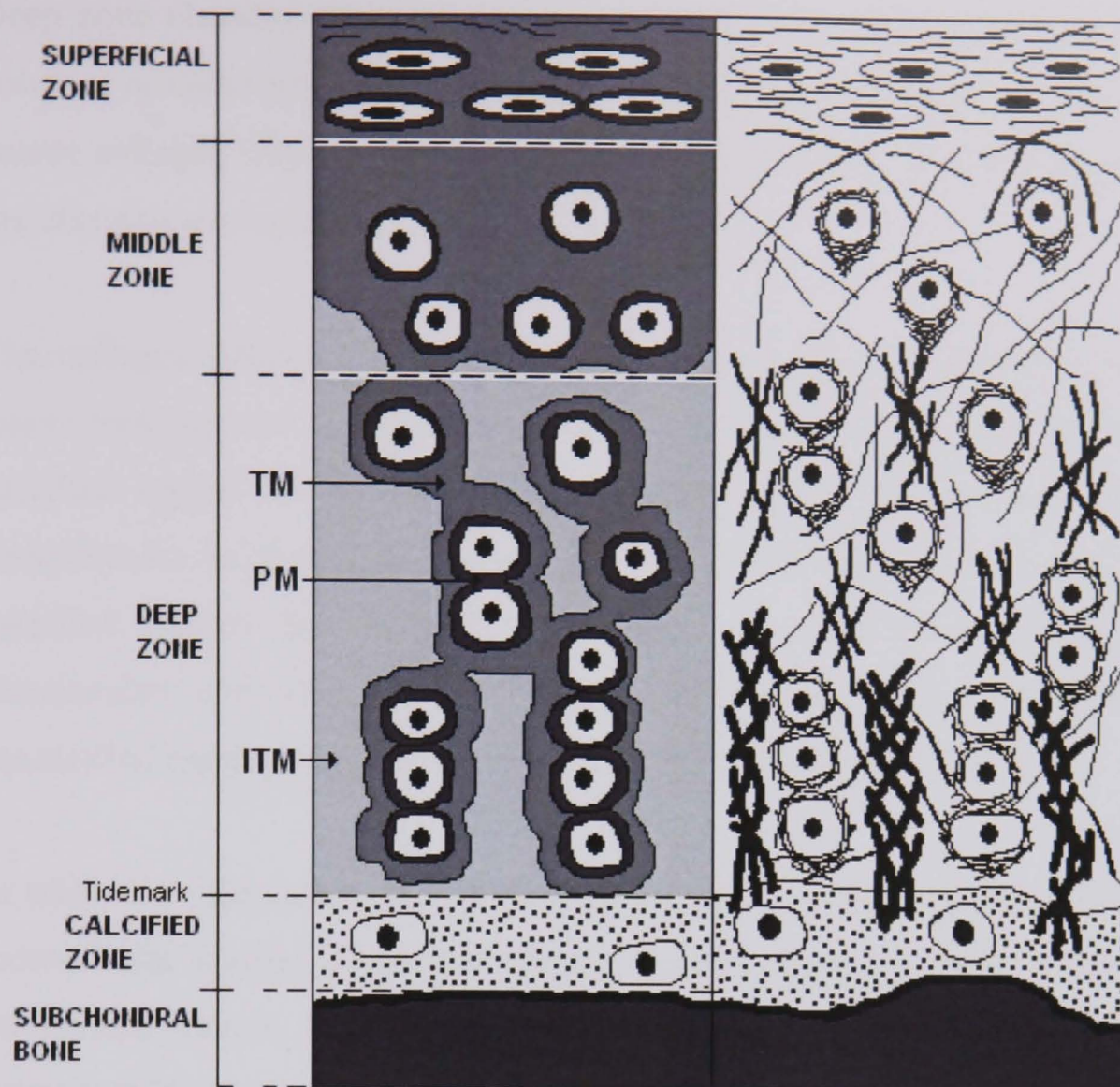


FIGURE 1.7: Schematic representation of the different zones and regions of articular cartilage. Matrix distribution around the chondrocytes (PM=pericellular matrix, TM=territorial matrix, ITM=interterritorial matrix) and collagen fibre orientation, showing the presence of chondrons in the middle and deep zones, are shown. Based on Poole *et al.*, 2001, and Buckwalter and Hunziker, 1999.

In the middle zone chondrocytes are spheroidal in shape, 10 μm or more in diameter. Deeper in this zone cells appear in groups of two or more, with numerous well-developed rER and Golgi apparatus for matrix synthesis, in contrast to those in the superficial layer (Stockwell and Meachim, 1979). Collagen fibrils, which are larger with diameters of between 30-70nm, are more widely spaced than in the superficial zone. These fibres are arranged randomly, although a degree of orientation is evident due to the presence of cross-linking between neighbouring fibril segments, where there is a folding over of radial fibre bundles to lie in the plane of the articular surface (Eyre *et al.*, 2006).

Deep zone chondrocytes are similar to those in the middle zone, but are arranged in columns oriented perpendicular to the articular surface (Hunziker, 1992). The relatively coarse collagen fibres occur in bundles perpendicular to the surface, passing between the chondrocyte columns (Culav *et al.*, 1999).

The collagen fibres from the deep zone project into the calcified zone of cartilage, where they may act to physically couple the cartilage to the subchondral bone. In this calcified region, collagen fibrils are radially aligned (Bader and Lee, 2000). The chondrocytes in this region are large and hypertrophic, surrounded by an entirely calcified matrix that suggests they have an extremely low metabolic activity (Buckwalter and Mankin, 1998). The calcified layer acts as a transition between uncalcified cartilage and the subchondral bone (Poole *et al.*, 2001).

In addition to the zonal variation seen in articular cartilage, there is also variation in the extracellular matrix within the zones. Indeed, there are three distinct regions, the pericellular matrix, the territorial matrix and the interterritorial matrix, these regions being roughly concentric around the chondrocytes in the matrix, as shown in Figure 1.7. The pericellular region, approximately 2 μ m wide, contains selective molecules, such as type VI collagen and the proteoglycans, decorin and aggrecan (Poole *et al.*, 2001). There is little or no fibrillar collagen present in this region (Buckwalter and Hunziker, 1999). However, in all regions excluding the superficial zone, a fine fibrillar basket, involving collagens II, VI, IX and XI from the surrounding territorial region, is formed around the chondrocyte and its pericellular region. This has been termed the pericellular basket or capsule, which forms a distinct boundary between the territorial and pericellular regions (Poole, 1997; Eyre *et al.*, 2006). Collectively, the chondrocyte, pericellular matrix and capsule have been termed the chondron (Poole *et al.*, 1987), a unit which is believed to provide mechanical protection of chondrocytes during cartilage deformation (Culav *et al.*, 1999, Knight *et al.*, 2001). Cytoplasmic extensions from the chondrocytes project out through the pericellular matrix into the surrounding territorial matrix, which can surround both individual cells and, in some locations, pairs or clusters of cells and their pericellular matrices (Buckwalter and Mankin, 1998).

The interterritorial matrix is the region most remote from the chondrocytes, and constitutes the majority of the volume of mature articular cartilage (Figure 1.7). The interterritorial region is most distinct in the deep zone due to the highly organized

proteoglycan-collagen lattice, not apparent in the other matrix regions. Proteoglycan concentration is highest in the interterritorial regions of the deep zone where the proteoglycans are in aggregate form (Poole *et al.*, 1982; Bader and Lee, 2000).

1.5 Loading of articular cartilage

During normal walking, the forces applied to the articular surface of the major load bearing joints of the human lower limb, such as the hip and knee, can vary from almost zero to several times body weight at a frequency of approximately 1Hz (Morrison, 1970). During more strenuous activities, however, load values can be in excess of fifteen times body weight. In addition, the area of contact at the joint surface varies in a complex manner, both spatially across the joint surface and temporally during the gait cycle. Under physiological conditions articular cartilage will be exposed to contact stresses of the order of 5-10MPa (Kempson, 1979). The stiffness of healthy articular cartilage is designed to enable the reduction of contact stresses placed on both itself and the underlying bone. The associated maximum strains have been estimated to be of the order of 15-30% in human load bearing cartilage (Broom and Myers, 1980; Guilak *et al.*, 1995). This deformation increases the effective area over which the physiological loads are distributed.

The physicochemical interaction between the various components of the extracellular matrix is responsible for the mechanical properties of healthy articular cartilage (Bader and Lee, 2000). Proteoglycans are able to interact with the surrounding tissue fluid by means of their negatively charged glycosaminoglycan chains that repel each other and bind matrix water and mobile cations (Buckwalter *et al.*, 1987a). Proteoglycans are only partially hydrated in cartilage tissue, and therefore exert a constant pressure to expand. This swelling pressure, which is known as the Donnan osmotic effect, is caused by the increase in total inorganic ion concentration associated with the proteoglycans, which increases the osmolarity in the tissue. The swelling pressure in unloaded cartilage is approximately 0.35MPa (Maroudas, 1979). The collagen fibril network resists the osmotic pressure. In unloaded cartilage, an equilibrium exists between the swelling pressure (P_{swelling}) on the interstitial fluid and the hydrostatic pressure due to tensile forces established in the collagen network (P_{collagen}), such that

$$P_{\text{collagen}} = P_{\text{swelling}}$$

Equation 1.1

If a sudden compressive force is applied to the cartilage surface, there is a rapid deformation of the bulk extracellular matrix with minimal volume change. This deformation is, for the most part, elastic and instantaneously recoverable (Armstrong *et al.*, 1984). If the external compressive force is sustained (P_{applied}), it causes an increase in hydrostatic pressure, altering the equilibrium and establishing a net pressure differential (ΔP):

$$\Delta P = P_{\text{applied}} + P_{\text{collagen}} - P_{\text{swelling}} \quad \text{Equation 1.2}$$

This causes fluid flow away from the loaded tissue area and further deformation of the tissue. The removal of fluid increases the proteoglycan concentration within the tissue, which increases the osmotic swelling pressure (P_{swelling}). From equation 1.2, there is a resulting decrease in the pressure differential, which reduces the fluid expulsion and therefore also reduces the effective deformation rate. If the compressive load remains constant, the rate of fluid flow away from the loaded area decreases over time until it tends to zero and a new equilibrium is established, where there is no pressure differential ($\Delta P = 0$):

$$P_{\text{swelling}} - P_{\text{collagen}} = P_{\text{applied}} \quad \text{Equation 1.3}$$

The time-dependent behaviour exhibited by articular cartilage when exposed to a static compressive force is termed creep, and is characteristic of viscoelastic materials (Figure 1.8). The time taken to reach equilibrium is inversely proportional to the square of the cartilage thickness. For relatively thick human cartilage up to 4mm it can take up to 16 hours for the tissue to reach equilibrium (Kempson 1979). During this time up to 70% of the total water content may be exuded from the tissue.

On sudden release of the applied force, the cartilage recoils almost instantaneously, to a limited extent, before gradually recovering to its original thickness (Figure 1.8). This response is also time-dependent, as water is re-imbibed into the cartilage matrix until the original unloaded equilibrium is reached. Cyclic loading produces similar time-dependent behaviour. However, the extent of recovery after each cycle is dependent on the form and frequency of the loading pattern (Bader and Lee, 2000).

The ability of cartilage to resist compression is governed by the bulk compressive stiffness of the tissue, the Donnan osmotic swelling pressure and the resistance to fluid movement. Therefore, in order for articular cartilage to fulfil its functional role as a load bearing material, it is essential that the mechanical integrity of the tissue is maintained.

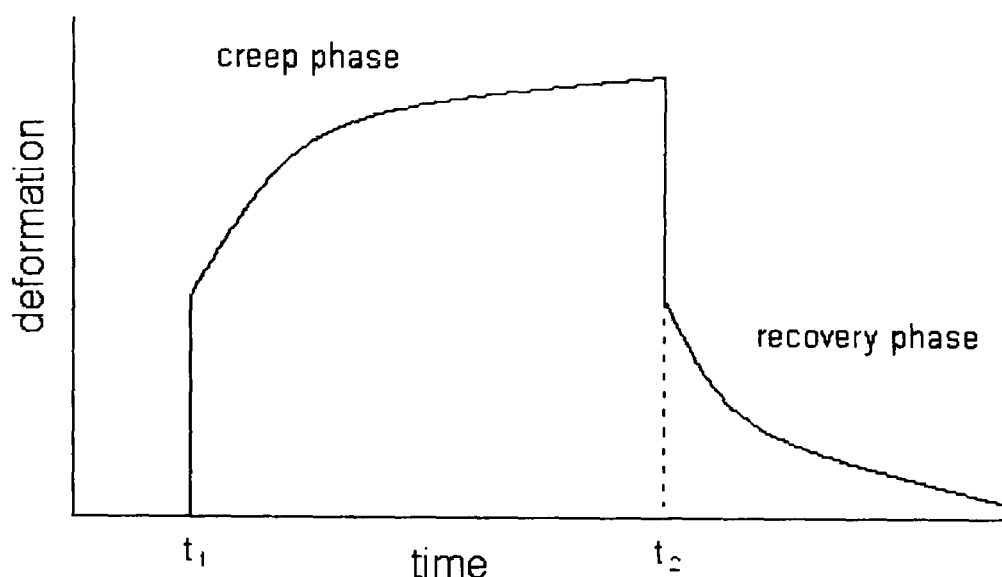


FIGURE 1.8: Viscoelastic response of articular cartilage to the application (t_1) and removal (t_2) of a compressive load.

1.6 Articular Cartilage Pathology

Over an average life-span of 75 years in the developed world, cartilage is susceptible to injuries and diseases that cause changes in chondrocyte metabolism and, as a consequence, have a direct effect on the function of articular cartilage. These will be examined in the following sub-sections.

1.6.1 Trauma and Injury

Over-loading of the major joints, occurring, for example, during high-impact activity, can cause blunt trauma, penetrating injuries and frictional abrasions to articular cartilage (Buckwalter *et al.*, 1987b). These can, in turn, lead to mechanical disruptions of both cells and matrix, with loss of matrix macromolecules from the framework and, in more severe cases, associated localised cell injury or death. In cases of minor injury, the synthetic response of the chondrocytes in producing new matrix is critical in order for cartilage to re-establish normal composition and function.

The response of cartilage to injury is dependent on the depth of the defect into the tissue. Partial thickness lesions are unable to heal spontaneously due to the absence of a blood supply. These lesions are analogous to the fissures seen during the early stages of

osteoarthritis (Hunziker, 1999). Chondrocytes near the lesion may proliferate and synthesise new matrix, but there is no associated migration to the site of injury, and thus the defect is not adequately filled. However, these lesions seldom progress through the tissue depth (Buckwalter *et al.*, 1987b).

Full depth lesions penetrating the subchondral bone elicit a typical inflammatory response resulting in the formation of fibrocartilage, which only has a partial resemblance to hyaline cartilage. Indeed, fibrocartilage does not provide a suitable bearing surface or adequate mechanical function, and degeneration of this tissue is evident within six to twelve months. This process is associated with a significant decrease in proteoglycan content and an extensive fibrillation of the remaining repair tissue (Buckwalter *et al.*, 1987b).

1.6.2 Ageing

The synthetic functions of chondrocytes have been shown to change with age. In particular, cells produce smaller and more variable proteoglycans, and exhibit a reduced sensitivity to the anabolic and catabolic regulatory cytokines that regulate turnover. Chondrocytes in aged tissues are therefore less able to maintain and repair tissue following injury (Buckwalter and Hunziker, 1999).

Superficial fibrillation is commonly seen in weight-bearing articular cartilage from middle age, although in the vast majority of cases this is a non-progressive and asymptomatic form of the condition (Buckwalter and Hunziker, 1999). Fatigue failure of the collagen network leads to a decrease in the tensile properties of cartilage with age from as early as the third decade of life (Kempson, 1982 and 1991). Collagen fibrils become more widely spaced and larger in diameter and are less able to withstand the osmotic swelling pressure of the proteoglycans, leading to localized tissue swelling (Huber *et al.*, 2000). Additionally, there may be an increase in cross-linking of collagen via non-enzymatic glycation reactions (Buckwalter and Hunziker, 1999).

Proteoglycan aggregate composition is altered with age, with a decrease in the number and size of chondroitin sulphate chains and an increase in the number and size of keratan sulphate chains (Hardingham and Bayliss, 1990). Proteolytic changes to aggrecan monomers, hyaluronan chains and core and link proteins result in a reduction in both the size and nature of the aggregated proteoglycans. An increase in hyaluronan

concentration reported in aged tissue is due to either an increased synthesis and/or accumulation of degraded molecules (Buckwalter and Hunziker, 1999). Changes to the collagen/proteoglycan network cause a reduction in water content and softening of the tissue, thereby reducing its deformation capabilities and resulting in acceleration of degenerative processes and cartilage destruction (Huber *et al.*, 2000).

1.6.3 Disease

Arthritis is a generic term encompassing a group of conditions causing pain, stiffness and inflammation of the joints. These disorders can be isolated to a single joint, or be polyarticular in nature (Beris *et al.*, 2005). The factors affecting the onset of arthritis in a patient can be hereditary in origin, or can be due to ageing, trauma or inflammation. Such factors can sometimes be related (Goldring, 2006). The two most well-known forms of arthritis are rheumatoid arthritis and osteoarthritis.

Rheumatoid arthritis is a chronic systemic autoimmune disorder where the immune system attacks the synovium in the joint capsule, causing inflammation with increased presence of proteases and catabolic cytokines that disintegrate cartilage and the underlying bone (Ritchlin, 2004). This disease affects both the major load-bearing joints as well as the more peripheral smaller joints in the hands and feet.

Osteoarthritis is the most common form of arthritis, and is caused by wear and tear of the articular surface. Although the incidence of osteoarthritis increases with age, it is not caused by ageing *per se*, but rather, the changes to the tissue that occur with ageing increase the risk of degeneration (Bader and Lee, 2000). Primary osteoarthritis is characterized by late onset in an otherwise healthy tissue, whereas secondary osteoarthritis has an earlier onset and is induced by other factors such as disease or joint trauma (Goldring, 2006). There has been an increase in the number of young people who develop the disease due to traumatic changes, such as those sustained during sporting and other high-risk activities, often involving joint structures such as the anterior cruciate ligament and the meniscus in the knee.

The earliest stage of osteoarthritis involves fraying of the superficial layer collagen, termed fibrillation. The cartilage then develops vertical fissures, with an associated disruption/loss of proteoglycan and an increase in water (Buckwalter *et al.*, 1987b; Buckwalter and Mow, 1992). Chondrocytes proliferate by forming clusters to synthesise

new matrix; however, an increase in degradative enzymes means that catabolism predominates, leading to further tissue breakdown (Huber *et al.*, 2000). Breakdown products can cause inflammation in the synovial space as the cells lining the joint attempt to remove them. Osteoarthritic lesions progress both in width and depth down to the subchondral bone, with associated thinning of cartilage, cell death, fibrocartilage formation and bony out-growth on the joint surface, the latter known as spurs or osteophytes (Hunziker, 2001; Buckwalter *et al.*, 1987b; Huber *et al.*, 2000). The resulting bone-on-bone contact during joint motion and loading is the cause of both pain and debilitation. Various pharmacological therapies can be used to reduce symptoms, primarily pain, but none have proved significantly effective at modifying or reversing the disease process (Goldring, 2006).

1.7 Repair strategies

The limited repair capacity of articular cartilage has spawned a number of surgical methods that have been used to alleviate the symptoms of osteoarthritis and restore function to the joint by stimulating repair, replicating cartilage function, or regenerating/replacing cartilage tissue. Some of the common repair strategies are summarised in Table 1.5.

In addition to these well-established methods, scientists have increasingly examined the potential of a tissue engineering solution for cartilage repair. This strategy involves the development of a functional hyaline cartilage that can integrate with existing host tissue, thus reducing/eliminating the pathological changes occurring during both natural and surgical repair processes. This tissue engineering approach typically involves the *in vitro* culture of chondrogenic cells that are then implanted into the defect site. Cell-types investigated include autologous chondrocytes and mesenchymal stem cells (Brittberg *et al.*, 2001; Raghunath *et al.*, 2005). Cells can be manipulated during the culture process genetically, chemically and mechanically within a controlled bioreactor environment to influence cell metabolism. There are three general strategies for producing new tissue, which may be used alone or in combination (Fauza, 2003):

1. *Isolated cell suspensions*: The most common technique involves autologous chondrocyte implantation (ACI), where a biopsy of healthy cartilage is removed from a non-loading bearing area. The biopsy is enzymatically digested to isolate chondrocytes, which are cultured *in vitro* and re-implanted

into the defect site, which is traditionally covered with a periosteal flap. Use of ACI in clinical practice has given satisfactory results, particularly over the short- and mid- terms, although for larger/deeper and irregular shaped defects ACI has been used in combination with bone grafts (Beris *et al.*, 2005).

2. *Tissue-inducing substances*: Anabolic factors have been employed to promote chondrogenic differentiation and matrix reconstitution (Weisser *et al.*, 2001). These may be introduced *ex-vivo* before implantation, or incorporated into injectible/implantable carriers at the defect site (Goldring, 2006). Such morphogens include TGF- β , insulin-like growth factor, basic fibroblast growth factor (bFGF), and bone morphogenic proteins (BMPs) (Raghunath *et al.*, 2005, Fujisato *et al.*, 1996; Goldring, 2006).
3. *Cells placed on/within matrix*: Cells are attached to biocompatible scaffold materials made of either naturally occurring substances or synthetic polymers or ceramics, which act to guide tissue organization and growth (Fauza, 2003). Porous scaffolds have applications for repair of larger cartilage defects, and have the advantage of allowing chondrocytes to maintain their differentiated phenotype and function as they are cultured in a 3D environment (Raghunath *et al.*, 2005, Temenoff and Mikos, 2001). Scaffolds can be protein-based (e.g. fibrin, collagen), carbohydrate-based (e.g. polyglycolic and polylactic acid, hyaluronan, alginate, agarose), made of artificial materials (e.g. carbon fibres, hydroxyapatite), or a combination of these (Hunziker, 2001).

Scaffolds need to have sufficient porosity for tissue ingrowth as well as adequate mechanical integrity to withstand both the implantation procedure and the mechanical forces experienced at the joint surface post-implantation. Additionally, scaffolds should promote integration of regenerated tissue with native tissue (Frenkel and Di Cesare, 2004). Unfortunately, many of the above scaffolds do not have long-term functionality, in terms of biocompatibility and mechanical properties, to be used successfully in humans.

Although much progress has been made in combating cartilage pathology, more research is required in order to produce a fully functional cartilage repair tissue with the necessary longevity to prevent repeated clinical intervention.

TABLE 1.5: Various therapeutic interventions for cartilage repair and replacement.

Intervention	Rationale	Disadvantages
Lavage (joint irrigation) Shaving/Debridement (Hunziker, 2001)	Removal of degradation products from synovial space. 'Smoothing' articular surface.	Only short term pain relief. Cell apoptosis and necrosis. Continued degeneration of tissue.
Abrasion Chondroplasty Pridie Drilling Microfracture (Hunziker, 2001)	Instigate inflammatory response and cartilage formation.	Repair tissue is fibrocartilage not hyaline cartilage. Eventual fibrillation and breakdown.
Osteotomy (Hunziker, 2001)	Realignment/correction of deformed joint structure and biomechanics.	Can precipitate slow onset of progressive osteoarthritis.
Perichondrial/periosteal grafts (Beris <i>et al.</i> , 2005)	Transplantation into full depth cartilage defects due to presence of chondrocyte precursor cells in cambial layer of the tissue.	No long term stability of repair tissue or restoration of hyaline cartilage layer. Problems with graft attachment and calcification.
Osteochondral transplantation or 'mosaicplasty' (Beris <i>et al.</i> , 2005; Görtz and Bugbee, 2006)	Full depth osteochondral plugs to replace lost tissue. Allografts used for large defects, autologous grafts for smaller defects.	Chondrocyte death during graft harvesting. Problems with matching geometry of graft(s) with that of defect. Absence of lateral mechanical support.
Total Joint Replacement (Huo <i>et al.</i> , 2007; Buechel, 2004)	Removal of diseased joint surfaces and replacement with functional biomaterial 'ball and socket' components	Finite implantation life of up to 20 years (hip/knee), with decreased life-spans for subsequent revision replacement implants. Inflammation caused by wear particles, leading to loosening of implant and bone resorption. Risk of dislocation /infection /DVT. Not recommended for young active individuals.

Chapter 2

Response of Articular Cartilage to Mechanical Stimuli

2.1	Introduction to mechanotransduction in cartilage	29
2.2	<i>In vivo</i> studies	29
2.3	<i>In vitro</i> studies	30
2.3.1	Cartilage explants	30
2.3.2	Monolayer cultures	31
2.3.3	Three-dimensional cultures	31
2.4	Mechanotransduction signaling pathways	33
2.4.1	Tissue and cellular level	33
2.4.1.1	Hydrostatic pressure	33
2.4.1.2	Matrix deformation	35
2.4.1.3	Cellular deformation	37
2.4.1.4	Specific pathways associated with 3D scaffolds	38
2.4.2	Intracellular level	38
2.4.2.1	Cytoskeleton	38
2.4.2.2	Nucleus deformation	40
2.4.2.3	Calcium signalling and associated pathways	40
2.5	Ultrasound	43
2.5.1	Physics of ultrasound	43
2.5.2	Temporal and spatial characteristics of continuous wave and pulsed wave ultrasound	45
2.5.3	Amplitude and intensity	47
2.5.4	Attenuation	49
2.5.5	Standing wave production	49
2.5.6	Medical applications of ultrasound	50
2.5.7	Safety considerations for use of ultrasound	52
2.5.8	Biophysical effects of ultrasound in clinical applications	52
2.5.8.1	Thermal effects	52
2.5.8.2	Non-thermal effects	53
2.5.9	Therapeutic pulsed low intensity ultrasound for bone repair	55
2.5.10	Use of low intensity ultrasound for cartilage regeneration	57
2.6	Aims and Objectives	60

2.1 Introduction to mechanotransduction in cartilage

The structure and composition of articular cartilage can alter in response to the forces it experiences during physical activity. It is the cellular component of articular cartilage, the chondrocytes, which maintain this structure and function. The loading of articular cartilage acts to stimulate the chondrocytes, which respond by altering their synthesis and catabolism of matrix molecules to maintain the cartilage integrity (Tammi *et al.*, 1987; Urban, 1994). In normal joints, load-bearing areas are thicker, exhibit a higher proteoglycan content and are mechanically stronger than non-load-bearing regions of the same joint (Buckwalter and Mow, 1992, Slowman and Brandt, 1986). They also contain larger chondrocytes with a greater volume of intracellular organelles (Eggli *et al.*, 1988). In order to further understand the effects of mechanical loading on chondrocyte metabolism, the following sections will describe *in vivo* and *in vitro* research into cartilage loading and the associated mechanotransduction signalling pathways.

2.2 *In vivo* studies

Various studies examining the effects of immobilization using animal models show that proteoglycan content in articular cartilage is altered by changes in load bearing of a joint. Load is deemed to be the significant factor in the maintenance of cartilage rather than joint motion. As an example, the absence of weight bearing in a canine model where a distal portion of the limb is amputated was shown to lead to cartilage atrophy, even when joint motion was permitted (Palmoski *et al.*, 1980).

LeRoux and colleagues (2001), using a canine model, found that cast immobilization of the knee significantly reduced proteoglycan concentration and shear modulus in tibial cartilage after four weeks. However, Richardson and colleagues (1993), in a similar experiment using an equine model, found no significant decrease in rates of proteoglycan synthesis after 30 days of immobilization. Clearly, the effects of joint immobilization are dependent on the experimental period, the nature of the immobilization, and the species and age of animals used (Tammi *et al.*, 1987).

Although some of these alterations can be reversed to an extent by reloading of the joint, full restoration of articular cartilage proteoglycan levels was not seen in a canine knee model after a 50 week remobilization period, following on from 11 weeks of immobilization (Jortikka *et al.*, 1997). Furthermore, in skeletally immature joints,

immobilization may affect development of articular cartilage in such a way that very slow recovery or permanent alterations are induced (Kiviranta *et al.*, 1994).

Controlled exercise has the opposite effect to immobilization. For example, chondrocytes were shown to be enlarged after exercise in rabbits (Paukkonen *et al.*, 1985), and non-strenuous exercise in beagles produced increased cartilage thickness, proteoglycan content and matrix stiffness (Kiviranta *et al.*, 1988). By contrast, excessive and prolonged loading of the joint can damage otherwise healthy cartilage. Animal models of osteoarthritis can be mechanically induced by introducing joint instability or altering the load across the joint, with load changes affecting both chondrocyte metabolism and cartilage structure (Muir and Carney, 1987).

2.3 *In vitro* studies

In vitro studies investigating the effect of load on cartilage have involved the use of explants, isolated chondrocytes and chondrocytes seeded in 3D scaffolds. These will be discussed in separate sub-sections.

2.3.1 Cartilage explants

Cartilage explants can be maintained *in vitro* in a stable and controlled environment (Sah *et al.*, 1992; Dumont *et al.*, 1999). Static compression of explants causes an inhibition of glycosaminoglycan synthesis, as assessed by reduced radiolabelled sulphate incorporation, in proportion to the applied stress (Sah *et al.*, 1992; Guilak *et al.*, 1994; Buschmann *et al.*, 1996; Li *et al.*, 2001). Furthermore, under static compression, deposition of proteoglycan matrix around individual chondrocytes appeared to be directionally dependent, forming perpendicular to the axis of compression (Quinn *et al.*, 1998). These effects were reported to be dependent on such factors as the length of the loading period. As an example, Bachrach and colleagues (1995) found that a compressive load of 0.1MPa applied for 10 minutes stimulated proteoglycan synthesis, whereas the same load applied for 20 hours suppressed synthesis. The authors suggested that the effects during the former period were predominantly due to pressure, and the latter effects due to cell strain as fluid is exuded from the system.

Dynamic loading of cartilage explants produces alterations in proteoglycan synthesis and other metabolic effects dependent on factors, such as the amplitude and frequency

of loading (Sah *et al.*, 1989; Li *et al.*, 2001). Buschmann *et al.* (1999) using loading regimes of both 0.01 Hz and 0.1 Hz showed significantly increased GAG synthesis compared to control explants. The lower frequency yielded a homogeneous spatial GAG distribution, whereas at the higher frequency increased GAG was observed to occur at the periphery of the explants. The authors suggested these findings were due to enhanced interstitial fluid velocities at explant peripheries, supporting the idea that load-induced fluid flow triggers the up-regulation of aggrecan synthesis.

It is important to note that when using explants to investigate chondrocyte behaviour, the presence of a charged extracellular matrix leads to the coupling of both mechanical and physicochemical effects, which may have implications when examining isolated signaling pathways (Bader and Lee, 2000).

2.3.2 Monolayer cultures

Isolated chondrocytes can be successfully grown as primary monolayer cultures. Such cultures, however, are not particularly suitable for studying the effects of isolated mechanical stimuli on cell metabolism, due to the difficulty in applying physiological strains. Moreover, cells cultured in monolayer do not generally maintain the chondrocytic phenotype. In particular, at low seeding densities under 10^4 cells/cm², cells spread out and attach to the substrate producing an elongated and flattened morphology. This fibroblastic phenotype is characterised by a transition to the production of both type I collagen and non-aggregating proteoglycans (Lee *et al.*, 2003). Experiments using high-density monolayers have investigated the effect of hydrostatic pressure (Parkkinen *et al.*, 1993; Smith *et al.*, 1996), tensile strain (De Witt *et al.*, 1984; Wright *et al.*, 1997), and flow-induced shear (Smith *et al.*, 1995, 2000) on chondrocyte metabolism. Such studies have generally demonstrated an up-regulation of aggrecan and collagen II in response to these forms of mechanical loading.

2.3.3 Three-dimensional cultures

The advantage of using chondrocytes seeded into scaffolds producing three-dimensional cultures is that chondrocytes are able to adopt a spherical morphology and thus maintain chondrocyte phenotype. The majority of model systems which have been investigated employ natural hydrogels, such as alginate and agarose.

Alginate is a negatively charged linear polysaccharide derived from sea algae, made of block copolymers of 1-4 linked β -D-mannuronic acid (M) and α -L-guluronic acid (G) (LeRoux *et al.*, 1999). In the presence of calcium or other divalent cations, alginate polymerises to form a non-toxic hydrogel. Alginate has similar structural and chemical properties to GAGs, in which chondrocytes maintain phenotype for long periods (van Osch *et al.*, 1998). Accordingly, alginate gel has been widely proposed as a suitable scaffold material for tissue engineered cartilage repair (Fragonas *et al.*, 2000; Rowley *et al.*, 1999; Drury *et al.*; 2004). Indeed, chondrocytes encapsulated in alginate gel have been shown to synthesise matrix consisting of aggrecan, decorin and collagen types II, IX and XI (Hauselman *et al.*, 1992; Petit *et al.*, 1992). Gross compression of chondrocyte-alginate constructs causes cell and nucleus deformation provided that the modulus of the gel is greater than that of the cell ($E_{\text{cell}} \approx 0.5\text{-}4\text{kPa}$) (Knight *et al.*, 2002). However, the most commonly utilized 3D culture system for chondrocytes involves agarose, a polysaccharide polymer material extracted from seaweed. Due to the presence of a large number of hydroxyl groups, agarose is hydrophilic, forming an uncharged gel. Chondrocytes seeded in agarose gel maintain their phenotype in long-term culture as demonstrated in 2% agarose, with production of cartilage matrix for up to 70 days in culture (Buschmann *et al.*, 1992) and cytoskeletal organization similar to that seen *in situ* (Idowu *et al.*, 2000). Newly synthesized macromolecules become trapped and accumulate pericellularly, forming a matrix that is of greater physiological relevance in terms of quantity, composition and structure than that produced in monolayer culture systems (Quinn *et al.*, 2002).

Gross compression of the chondrocyte-agarose system permits the investigation of cell deformation in cartilage mechanotransduction in the absence of other events associated with compression of a charged extracellular matrix (Freeman *et al.*, 1994, Knight *et al.*, 1998a; Mauck *et al.*, 2000). Additionally, temporal changes to chondrocyte deformation due to matrix elaboration can also be investigated (Buschmann *et al.*, 1995; Knight *et al.*, 1998b and 2006a, Lee *et al.*, 2000a).

Investigation in the host lab on 3D agarose constructs revealed a reduction in GAG synthesis and cell proliferation under 15% static compression for 48 hours compared to controls (Lee and Bader, 1997). By contrast, dynamic compression at 15% strain was shown to be frequency dependent. For example, a 0.3 Hz frequency caused inhibition of GAG synthesis similar to that seen with static compression, whereas at 1Hz the

synthesis was stimulated. At 3Hz, GAG synthesis returned to control levels, suggesting the possibility of a ‘window’ of frequencies whereby effective fluid flow was initiated to produce a stimulatory response. Further temporal modeling over 48 hours using the 1Hz frequency yielded the maximal GAG synthesis after at least 12 hours continuous compression, whereas cell proliferation was maximal after 1.5 hours of continuous compression followed by 46.5 hours of unloaded recovery (Chowdhury *et al.*, 2003). Clearly, these studies show that it is possible to regulate loading in such a way as to selectively stimulate metabolic activity of chondrocytes in 3D constructs.

2.4 Mechanotransduction signalling pathways

From the *in vivo* and *in vitro* studies described in Sections 2.2-2.3, it is clear that chondrocytes sense changes in their mechanical environment and respond by altering their metabolic pathways. The sequence of events and pathways by which chondrocytes respond to mechanical loading is termed mechanotransduction. A variety of effects are produced by mechanical compression of cartilage that may be involved in these processes, although many are still poorly understood. Mechanotransduction events can be separated into two levels; namely, the tissue and cellular level and the intracellular level.

2.4.1 Tissue and Cellular Level

The interplay between tissue level mechanotransduction events is summarized schematically in Figure 2.1.

2.4.1.1 Hydrostatic Pressure

The osmotic pressure differences present in articular cartilage, termed the Donnan osmotic swelling pressure (Section 1.5), generates a hydrostatic pressure even in unloaded tissue. During joint loading, articular cartilage is subject to hydrostatic pressure changes before deformation and subsequent events (Weightman and Kempson, 1979). Hydrostatic pressure in human articular cartilage varies from a resting pressure of 0.2 MPa to 4-5 MPa during walking, and to as high as 20 MPa during more vigorous activity (Urban *et al.*, 1994; Weightman and Kempson., 1979).

In vitro studies using explants (Urban and Hall 1992), monolayer (Ikenoue *et al.*, 2003) and 3D culture (Mizuno *et al.*, 2002, Toyoda *et al.*, 2003) have shown that both static and dynamic hydrostatic pressure in the range of 1-15 MPa produces a change in

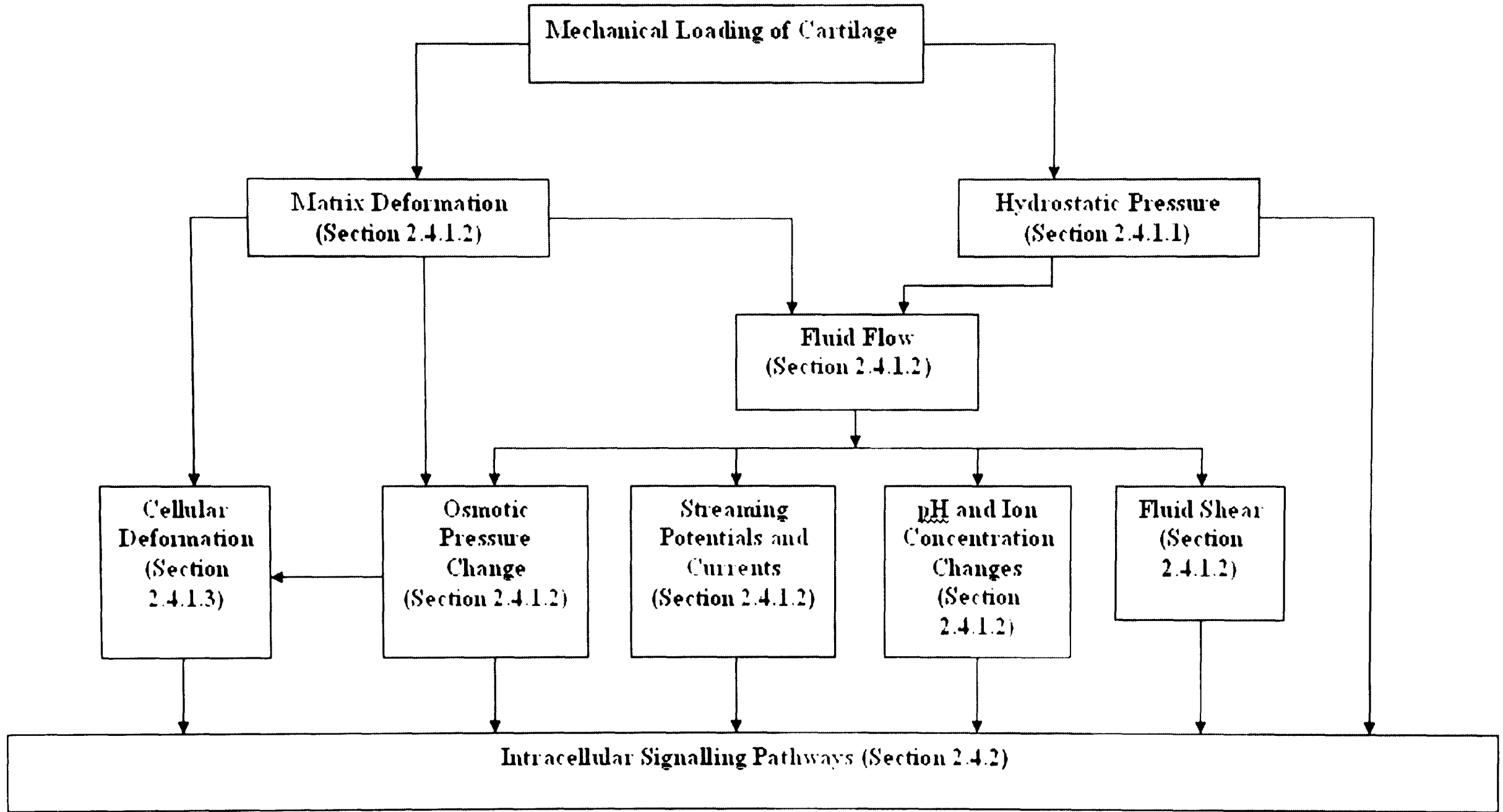


FIGURE 2.1: Schematic illustrating tissue level mechanotransduction events experienced by chondrocytes on tissue loading.

chondrocyte metabolism, particularly related to GAG synthesis. However, the nature of the response appears to be highly dependent on the time and magnitude of the hydrostatic pressure. Pressures between 5 and 10 MPa generally stimulated synthesis, while lower pressures had either a minimal effect or inhibited synthesis.

Hydrostatic pressure, in isolation from other factors, does not cause significant cell or matrix deformation or induce interstitial fluid flow (Guilak *et al.*, 1997; Myers *et al.*, 2007). The mechanisms by which hydrostatic pressures may affect cartilage behaviour are unclear, but suggestions include changes to the transmembrane potential (Wright *et al.*, 1992) and membrane transport activity (Hall, 1999; Browning *et al.*, 2004), affecting intracellular concentrations of ions such as Ca^{2+} and K^+ . Stretch-activated channels have also been proposed (Mizuno *et al.*, 2002), although this seems unlikely given that the level of cell deformation is probably minimal. However, some cell deformation may occur due to the pressure differential across the cell membrane. Hydrostatic pressure changes have been shown to alter cytoskeletal polymerization and organization, shown in chondrocytes seeded in monolayer (Parkinen *et al.*, 1993) and agarose (Knight *et al.*, 2006a). It has been recently proposed that these alterations could initiate changes in matrix synthesis by activating pathways involving the release and/or activation of cytoskeletal proteins (Myers *et al.*, 2007).

2.4.1.2 Matrix Deformation

Compression of articular cartilage causes deformation of the cellular matrix, resulting in a variety of effects which may have a part to play in mechanotransduction.

Interstitial Fluid Flow: The generation of spatial gradients in hydrostatic pressure, and subsequent matrix deformation, causes the flow of interstitial fluid, resulting in mass transport and fluid redistribution. Fluid flow may alter chondrocyte metabolism directly aiding nutrient delivery and accelerating the transport of macromolecules and other solutes into the cell (Yellowley *et al.*, 1999) as has been suggested in bone (Jacobs *et al.*, 1998; Donahue *et al.*, 2003). However, other authors do not believe this plays a major role in cartilage mechanotransduction (Hung *et al.* 1996a, Ferguson *et al.*, 2004). *In vitro* studies have demonstrated that fluid flow may alter chondrocyte metabolism by directly exerting shear stresses on the membrane of chondrocytes and other cell types, activating calcium signalling (Helmlinger *et al.*, 1996; Hung *et al.*, 1996b) and mitogen-activated protein kinase (MAPK) signalling (Ishida *et al.*, 1997; Hung *et al.*, 2000),

leading to stimulation of proteoglycan synthesis (Buschmann *et al.*, 1999, Eifler *et al.* 2006).

Osmotic Pressure: Cartilage loading leads to changes in extracellular osmolarity due to expulsion of water and proteoglycan-associated counter ions from the tissue. This will result in an increased proteoglycan concentration and movement of fluid and ions back into the tissue in an attempt to restore osmotic equilibrium (Urban, 1994). Matrix synthesis is significantly influenced by osmolarity outside the cell, suggesting that the coupling of mechanical and physicochemical environments may be important as a process of signal transduction associated with applied loads (Guilak *et al.*, 1997). Chondrocyte culture in defined media produced maximal proteoglycan synthesis at osmolarities of 250-450 mOsmole, which is similar to that seen *in situ* (Urban and Hall, 1992). Addition of hypotonic and hypertonic medium to chondrocytes in monolayer and agarose (Hung *et al.*, 2003) and explants (Schneiderman *et al.*, 1986) caused an increase and reduction in sulphated proteoglycan synthesis, respectively. Responses may be mediated directly by osmotically-gated ion channels such as TRPV4, which activate intracellular signalling cascades, or indirectly through the control of cell volume (Hall *et al.*, 1996; Browning *et al.*, 2004; Clark *et al.*, 2008).

Streaming potentials and currents: Deformation of cartilage induces a separation of charge between mobile counter ions and the negatively charged GAGs, producing an electrical field parallel to fluid flow (Légaré *et al.*, 2002). Streaming potentials may modulate matrix metabolism (for review see Sander and Nauman, 2003). *In vivo* and *in vitro* studies have reported modulation of aggrecan synthesis after the application of an electric current (Brighton *et al.*; 1976 and 2006). Electrical streaming potentials arising from mechanical loading may activate voltage-gated ion channels with associated alterations in membrane potential (Sugimoto *et al.*, 1996; Wilson *et al.*, 2004).

pH and ion concentration: The pH of the extracellular matrix in unloaded articular cartilage is estimated to be approximately 6.9 and is clearly influenced by the concentration of ions (Maroudas, 1979). Static compression produces an expulsion of interstitial fluid and an increased concentration of fixed negative charges from the proteoglycans, attracting protons into the extracellular matrix and therefore reducing the pH (Sah *et al.*, 1992; Wilkins and Hall, 1995). Previous reports have demonstrated that a reduction in extracellular pH causes a decrease in matrix synthesis by chondrocytes

(Gray *et al.*, 1988, Boustany *et al.*, 1995). It has been suggested that variation in extracellular pH affects intracellular pH in chondrocytes ($[pH_i]$) via transport mechanisms, such as the Na^+/H^+ exchanger systems, altering intracellular ion concentration (Hall *et al.*, 1996). The resulting changes in $[pH_i]$ may cause other cellular events including alterations in intracellular Ca^{2+} concentration ($[Ca^{2+}]_i$) which ultimately trigger downstream changes in cell metabolism (Gray *et al.*, 1988).

2.4.1.3 Cellular Deformation

Various studies have shown that physiological levels of mechanical stress and strain cause changes in chondrocyte shape and volume. Compression of explants results in a reduction in cell dimension parallel to the axis of compression with minimal lateral expansion associated with the Poisson ratio for articular cartilage (Quinn *et al.*, 1998; Buschmann *et al.*, 1996). Guilak and colleagues (1995) found a decrease in volume for chondrocytes contained in explants subjected to physiological static compressive strain of 15%. This effect may be due to compression-induced osmotic changes (Szafranski *et al.*, 2004) or the prevention of lateral expansion. By contrast, Lee and colleagues (2000a) observed no changes in the volume of chondrocytes compressed in 3D agarose constructs strained to 25%. This difference may reflect the uncharged nature of agarose compared to the extracellular matrix cartilage, or the unconfined nature of loading. The extent of cell deformation is dependent on the presence and deformation of the surrounding extracellular matrix (Knight *et al.*, 1998b).

Mechanotransduction events associated with changes in cell shape and volume have been reported to involve activation of stretch-sensitive membrane channels and transmembrane receptor molecules, which may influence intracellular calcium concentrations and cytoskeletal organization (Guilak *et al.*, 1999; Roberts *et al.*, 2001; Sachs *et al.*, 1991; Szafranski *et al.*, 2004). Recent work has implicated a purinergic pathway involving the release of ATP in modulating downstream calcium signalling caused by cyclic compression of chondrocytes in agarose (Pinguann-Murphy *et al.*, 2006). Additionally, chondrocyte primary cilia have been highlighted as mechanosensors that can trigger intracellular events downstream from cartilage compression (Poole *et al.*, 2002; Whitfield, 2008).

2.4.1.4 Specific Pathways associated with 3D Scaffolds

The events described in the previous sections and the manner in which cells sense and respond to them will differ based on the nature of the physical environment of the cell. The various scaffolds used to culture cells in 3D culture (see Section 2.3.3) provide a very different environment to that seen *in vivo*.

The charged, fluid-filled extracellular matrix of chondrocytes in cartilage tissue *in situ* gives rise to coupled chemical and electrical phenomena during loading. These pathways will not be seen in cell-seeded scaffolds prior to the synthesis of extracellular matrix. Even then, the relative stiffness of the extracellular matrix compared to the scaffold material may prevent matrix deformation until a confluent matrix has been elaborated. However, the absence of matrix enables investigation of specific pathways in isolation from other factors present *in vivo*. For this reason, the 3D agarose model system has been used to investigate the role of cell deformation in isolation from factors associated with compression of a charged extracellular matrix.

It is important to note that many of the biophysical events occurring in the body occur in combination and therefore *in vitro* results can only provide part of the picture on cartilage tissue mechanotransduction.

2.4.2 Intracellular Level

Load-induced changes to the extracellular environment are communicated to the chondrocyte, triggering an intracellular response. A selection of these events is discussed in the following sub-sections.

2.4.2.1 Cytoskeleton

The cytoskeleton is deemed to play an important role in sensing the mechanical stresses applied to chondrocytes in cartilage. The three cytoskeletal components form a framework that provide structure and shape to the cell. Actin microfilaments, vimentin intermediate filaments and tubulin microtubules form a link between the plasma membrane and the nucleus and are believed to be involved in mechanotransduction processes incorporating stretch-activated ion channels, integrin receptors, and distortion of intracellular organelles (Janmey *et al.*, 1998; Millward-Sadler and Salter, 2004; Wang *et al.*, 1993 and 2001; Knight *et al.*, 2006b).

A number of studies have investigated the effects of mechanical stimuli on the organization of the cytoskeleton of the chondrocyte. Actin microfilaments are most concentrated in the periphery of the cell, and are responsible for resisting tension and maintaining cellular shape (Glogauer *et al.*, 1997), and participating in cell-cell or cell-matrix interactions. Application of osmotic pressure (Erickson *et al.*, 2003, Chao *et al.*, 2006) and hydrostatic pressure (Parkkinen *et al.*, 1995) to monolayer culture, and mechanical compression and hydrostatic pressure in cell-seeded agarose constructs (Knight *et al.*, 2006b; Campbell *et al.*, 2007a) have all resulted in altered actin organization. Actin polymerization occurs via actin binding proteins, some of which are sensitive to intracellular calcium changes. Recent studies in agarose demonstrated mechanically induced changes in cofilin gene expression, an actin-associated protein responsible for actin depolymerisation (Campbell *et al.*, 2007a).

Microtubules are involved in cytoplasmic transport (Langelier *et al.*, 2000) and the organization and distribution of organelles and other cytoskeletal elements within the cytoplasm. Specifically, they have been implicated in Golgi apparatus organization (Parkkinen *et al.*, 1993). Destabilisation of microtubules in primary bovine chondrocytes led to down-regulation of hydrostatic pressure-induced proteoglycan synthesis, suggesting that microtubules modulate pressure changes and subsequent biosynthesis at the Golgi apparatus.

Vimentin intermediate filaments are closely associated with the microtubule network, together forming a link between the plasma membrane and the nucleus (Idowu *et al.*, 2000). Both cytoskeletal components are co-localised with the mitochondria, and they may have a role in potential mechanotransduction processes associated with mitochondrial deformation (Knight *et al.*, 2006a). Indeed, intermediate filaments specifically are thought to directly transmit cell deformation from the plasma membrane to the nucleus (Janmey, 1998). They are also thought to contribute to the maintenance of chondrocytic phenotype (Blain *et al.*, 2006). Changes to this network may play a role in the early stages of the osteoarthritic process (Benjamin *et al.*, 1995).

Cytoskeletal organization varies with depth in native tissue, with a directly proportional relationship between the extent of immunofluorescent staining and the level of loading experienced by tissue regions (Langelier *et al.*, 2000). This suggests that a more dense

cytoskeleton may be present in response to greater levels of cell deformation or hydrostatic pressure, in order to provide enhanced structural integrity to the cells.

Furthermore, temporal changes in cytoskeletal organization in 3D agarose cultures may be directly associated with elaboration of pericellular matrix and formation of integrin-matrix attachments, with changes in the mechanotransduction pathways (Lee *et al.*, 2000a).

2.4.2.2 Nucleus deformation

Deformation of chondrocytes in explants by application of mechanical strain causes an associated change to the cell nucleus, with a reduction in nuclear height and volume (Guilak, 1995). Similar behaviour was seen in chondrocytes cultured in agarose (Buschmann *et al.*, 1996; Lee *et al.*, 2000a) and alginate (Knight *et al.*, 2002). Nucleus deformation may cause alterations in gene transcription and other cell activity, possibly involving nucleopore distortion (Pavalko *et al.*, 2003).

2.4.2.3 Calcium Signalling and associated pathways

Calcium (Ca^{2+}) is a ubiquitous second messenger involved in many cellular processes, such as secretion and proliferation. In resting cells, intracellular Ca^{2+} concentration ($[\text{Ca}^{2+}]_i$) is maintained at approximately 10-100nM, but can rise to several micromolar on stimulation (Berridge *et al.*, 2000). $[\text{Ca}^{2+}]_i$ is initially elevated in a discrete area of the cell, giving rise to a local Ca^{2+} response, before diffusion or regenerative mechanisms spread $[\text{Ca}^{2+}]_i$ across the cell, causing a global response (Bootman *et al.*, 2001). These global $[\text{Ca}^{2+}]_i$ signals can occur as a single *transient* or regular repetitive transients, termed *oscillations*. The generation of these $[\text{Ca}^{2+}]_i$ signals requires the release of sequestered Ca^{2+} from intracellular stores and/or an influx from the extracellular space. Mechanisms that increase $[\text{Ca}^{2+}]_i$ need to be balanced by mechanisms that remove $[\text{Ca}^{2+}]_i$, due to the potential toxic effects of sustained high $[\text{Ca}^{2+}]_i$ concentrations. This complex system can be simplified by division into four parts (Berridge *et al.*, 2000; Bootman *et al.*, 2001) (Figure 2.2):

- **Ca^{2+} mobilizing signals:** Stimuli act via various cell-surface receptors and trigger events that lead to the influx of Ca^{2+} into the cytoplasm from intracellular or extracellular stores. For example, the binding of ligands to G protein-linked receptors (GPLR) and tyrosine kinase receptors (TRK) generate signals such as inositol-1,4,5-triphosphate (IP_3) that then bind to its specific receptor at the

endoplasmic reticulum (ER) to release Ca^{2+} . Other signals, for example cell deformation, can trigger direct Ca^{2+} influx from extracellular sources.

- **ON Mechanisms:** Mobilizing signals activate ON mechanisms that feed Ca^{2+} into the cytoplasm. In the release of $[\text{Ca}^{2+}]_i$, Ca^{2+} is the principle activator of these channels in process termed *Ca²⁺ induced Ca²⁺ release* (CICR). Influx of extracellular Ca^{2+} is controlled via various plasma membrane Ca^{2+} channels:
 - *Voltage-operated (VOCC):* activated by membrane depolarization
 - *Receptor-operated (ROCC):* activated by binding of agonist e.g. ATP to extracellular domain of channel
 - *Mechanically-activated (MACC):* respond to cell deformation
 - *Store-operated (SOCC):* activated in response to depletion of $[\text{Ca}^{2+}]_i$.
- **Activation of Ca^{2+} -sensitive processes:** Ca^{2+} -sensitive processes translate Ca^{2+} signal into cellular response, regulated by two main types of Ca^{2+} binding proteins; *buffers* that bind to cytosolic Ca^{2+} and shape the amplitude and duration of Ca^{2+} signals, and *sensors* that respond to Ca^{2+} by activating diverse processes.
- **OFF mechanisms:** These regulatory mechanisms act to remove cytoplasmic Ca^{2+} and restore a cell rest state:
 - Plasma membrane Ca^{2+} -ATPase (PCMA) pumps and $\text{Na}^+/\text{Ca}^{2+}$ exchangers remove Ca^{2+} to extracellular space
 - Sarco-endoplasmic reticulum ATPase (SERCA) pumps return $[\text{Ca}^{2+}]_i$ to internal stores
 - The mitochondria sequester Ca^{2+} during the development of a signal (via a uniporter) and gradually release it during the recovery phase. Once a cell is in its rest state, mitochondrial $\text{Na}^+/\text{Ca}^{2+}$ exchangers release stored Ca^{2+} back into the cytoplasm to be returned to the ER or removed from the cell entirely. Calcium can also leave the mitochondrion via a permeability transition pore (PTP).

Chondrocytes have been shown to exhibit mechanosensitive $[\text{Ca}^{2+}]_i$ signaling activated by a variety of mechanical stimuli including micropipette aspiration (Guilak *et al.*, 1999; Kono *et al.*, 2006; Ohashi *et al.*, 2006), fluid flow (D'Andrea *et al.*, 2000; Edlich *et al.*, 2004), hydrostatic pressure (Mizuno, 2005), osmotic change (Erickson *et al.*, 2001 and 2003) and uniaxial compression of cell-seeded agarose constructs (Roberts *et al.*, 2001; Pingguan-Murphy *et al.*, 2005 and 2006).

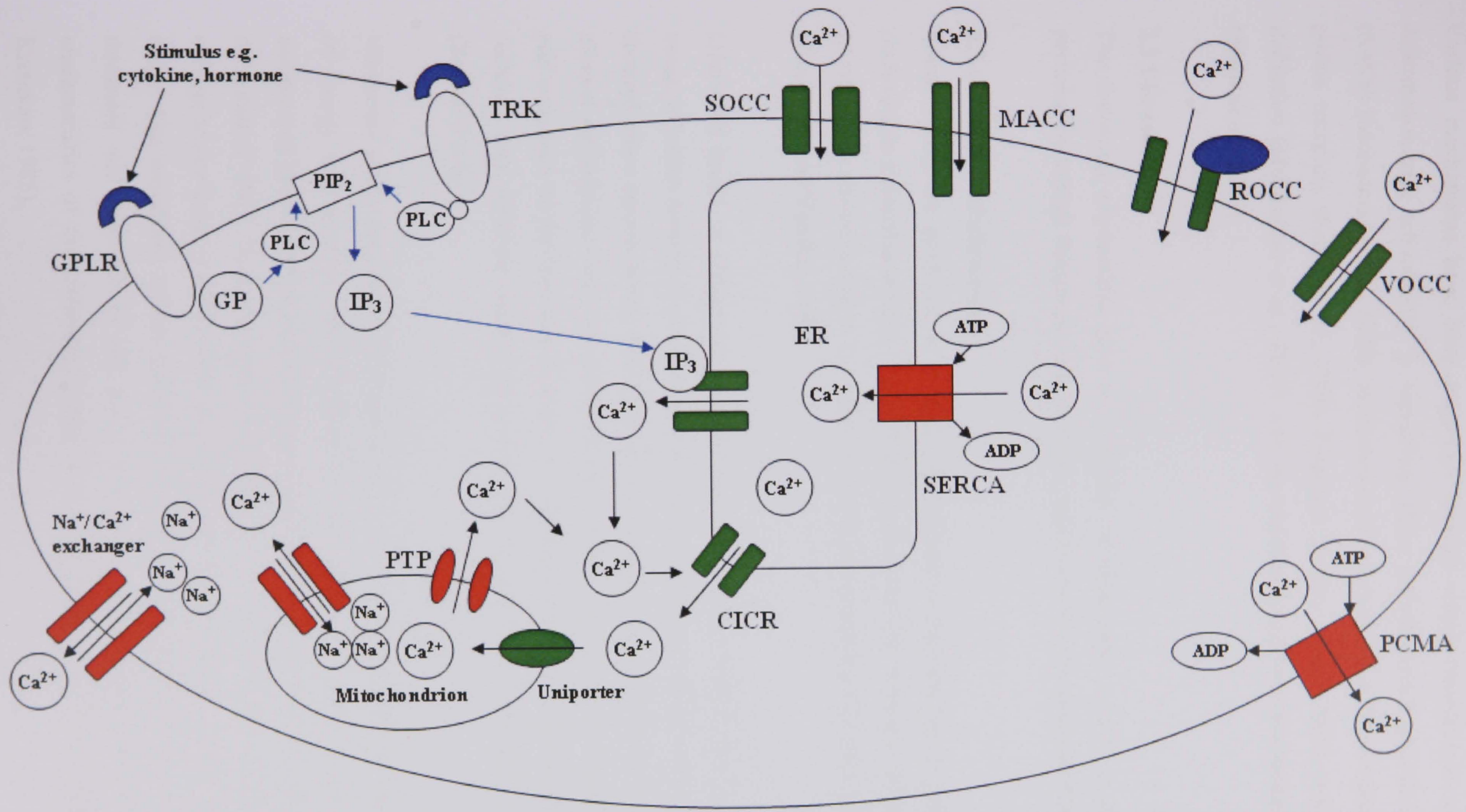


FIGURE 2.2: Simple schematic representation of some of the mechanisms involved in calcium signalling as described in Section 2.4.2.3. Blue denotes Ca^{2+} mobilizing signals, green ON mechanisms and red OFF mechanisms. PLC = phospholipase C, PIP_2 = phosphatidylinositol bisphosphate, ATP = adenosine-5'-triphosphate, ADP = adenosine diphosphate. Other abbreviations can be found in Section 2.4.2.3.

Various mechanisms have been suggested through which chondrocyte mechanical deformation may activate $[Ca^{2+}]_i$ signalling. These include stretch-activated channels (SACs) (Mobasher *et al.*, 2002), mechanosensitive release of ATP and activation of purine receptors (Kono *et al.*, 2006; Pinguan-Murphy *et al.*, 2006), primary cilia deflection (McGlashan *et al.*, 2006), and the mechanosensitive osmochannel, TRPV4 (Clark *et al.*, 2008).

2.5 Ultrasound

The following sub-sections give an overview of ultrasound, a form of mechanical perturbation at high frequencies that has been used in one form to stimulate tissue.

2.5.1 Physics of ultrasound

Sound waves are produced as a result of mechanical disturbances or perturbations occurring in a material medium. These disturbances cause the molecules of the medium to vibrate, as shown in Figure 2.3. This is an essential property of acoustic propagation (Grandolfo and Vecchia, 1987).

Ultrasonic sound, or ultrasound, exists at frequencies above 20kHz, that is, above the range of human hearing. It exhibits a shorter wavelength than audible sound, and can be focused into a narrow beam, which has made it possible to use ultrasound in a range of clinical applications (Farr and Allisy-Roberts, 1998). Ultrasound undergoes reflection and refraction at the interface between two different media. It is these reflections or 'echoes' from different tissues that produce the images seen in diagnostic ultrasound (Section 2.5.6).

Ultrasonic waves are produced by transducers, which are devices that convert one type of energy into another. These transducers are commonly made of flat disks of compressed polycrystalline lead zirconate titanate (PZT) or the polymer, polyvinylidene difluoride (PVDF). These materials are piezoelectric i.e. when deformed they develop a voltage across them, or conversely, they expand or contract when a voltage is applied to them. The movement of the faces of the disk is proportional to the voltage. The thickness and diameter of the disks determine the operating frequency and the characteristics of the ultrasound beam, respectively (Farr and Allisy-Roberts, 1998, Kremkau, 1985).

Ultrasound can be either continuous wave or pulsed wave in nature (Figure 2.3). For continuous ultrasound production, an alternating current (AC) of appropriate frequency is applied to the transducer, resulting in continuous expansion and contraction of the transducer. This produces successive compressions and rarefactions in the material through which the ultrasound wave is passing (Figure 2.3). The wave produced is of the same frequency as the applied voltage.

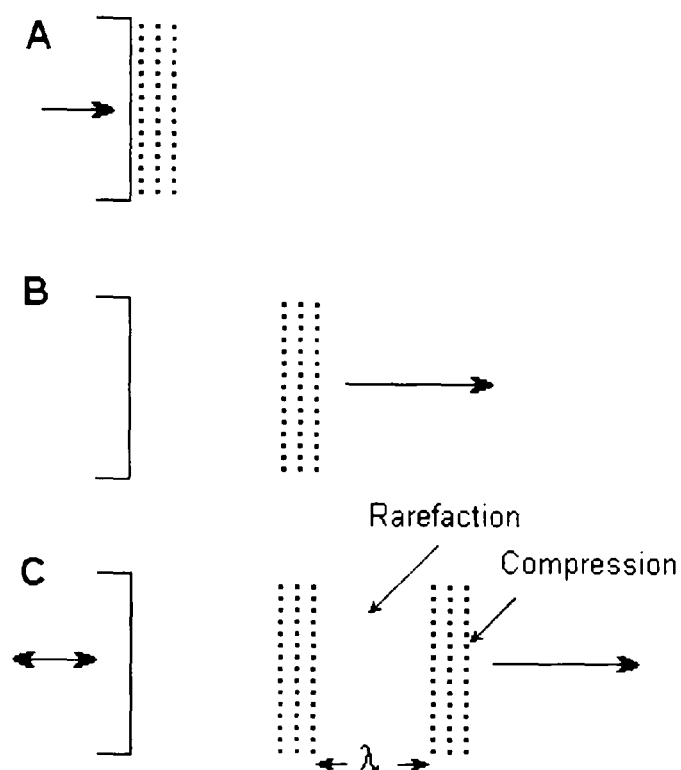


FIGURE 2.3: A) Production of sound by a transducer causing B) regions of compression and C) rarefaction of molecules of a medium, resulting in a sound wave of wavelength λ (adapted from Farr and Allisy-Roberts, 1998).

With pulsed wave ultrasound, either AC or direct current (DC) is used. To generate the pulses, short bursts consisting of a few cycles of alternating voltage are repeatedly applied to the transducer. With DC applications, a very short electrical voltage impulse, of a fraction of a microsecond duration, is applied to the transducer. This results in a few cycles of ultrasound produced by the transducer.

Transducers used only for continuous ultrasound production are air-backed i.e. have air behind the rear face of the transducer inside the transducer assembly. For the production of short ultrasound pulses, a damping material is required to be placed directly behind its rear face. The higher the damping effect, the shorter the pulses produced. However, damping decreases the efficiency of the transducer (Kremkau, 1985).

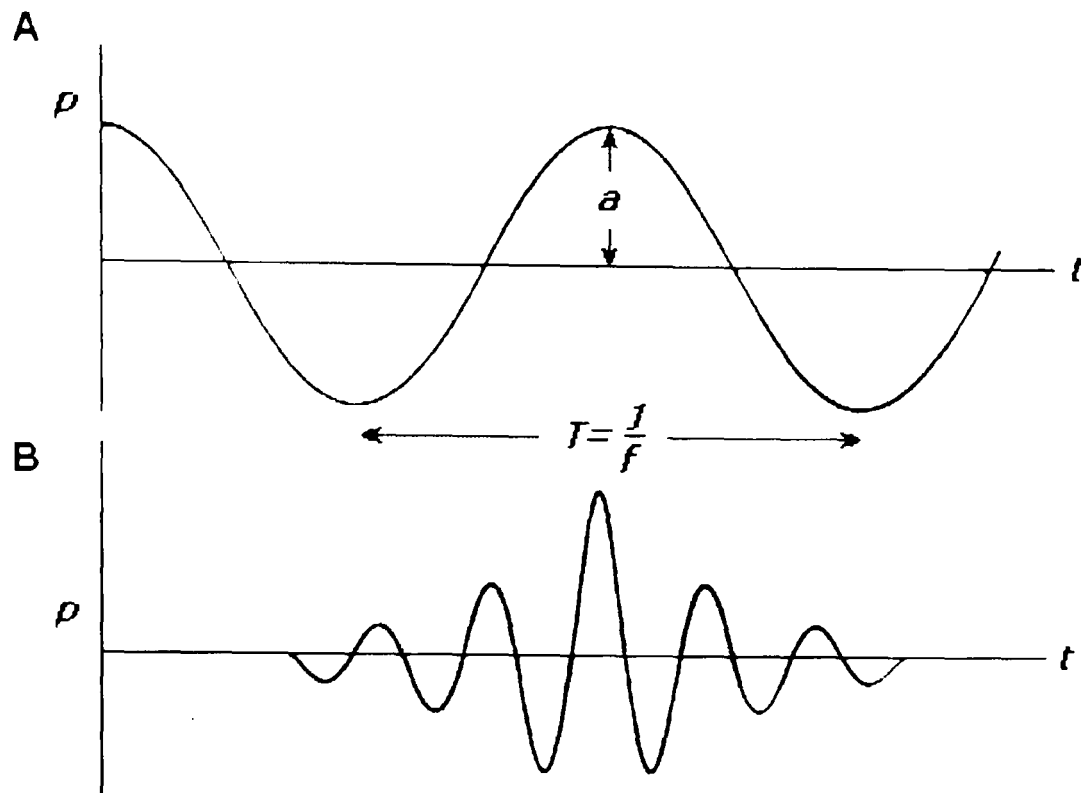


FIGURE 2.4: Schematic diagram showing A) continuous and B) pulsed waves of ultrasound (p =pressure, a =amplitude, t =time, T =period of wave, f =frequency).

2.5.2 Temporal and Spatial Characteristics of Continuous Wave and Pulsed Wave Ultrasound

The *period* of a continuous wave is the time required for one cycle to occur, and is inversely proportional to the frequency, f , measured in Hertz (Hz), namely:

$$T=1/f \quad \text{Equation 2.1}$$

The *propagation speed* is the speed at which ultrasound travels through a medium, and is determined by the density and compressibility, related to the mechanical stiffness, of the medium. Frequency, wavelength and propagation speed are related by the equation:

$$c=f\lambda \quad \text{Equation 2.2}$$

where λ is the wavelength, and c is the propagation speed. Propagation speeds in soft tissues, cells suspensions and liquid media are commonly of the order of 1500ms^{-1} .

Impedance, a second parameter determined by the medium, is defined by the product of the density of the medium and the propagation speed:

$$Z=c\rho \quad \text{Equation 2.3}$$

where Z is the acoustic impedance and ρ is the density.

Acoustic impedance is important with reference to the reflection of ultrasound at the boundary between two materials. When ultrasound encounters a boundary a portion of the wave is reflected and the remainder is transmitted into the new material medium.

In the case where the incident ultrasound is perpendicular to the boundary, the *intensity reflection coefficient* (IRC) represents the fraction of energy or intensity reflected, and is related to the acoustic impedances of the two mediums as follows:

$$IRC = \left[\frac{(Z_2 - Z_1)}{(Z_2 + Z_1)} \right]^2 \quad \text{Equation 2.4}$$

where Z_1 and Z_2 are the acoustic impedances of materials 1 and 2 respectively, as shown in Figure 2.5A.

The fraction of ultrasound transmitted into the second medium is called the *intensity transmission coefficient* (ITC). When incident ultrasound is not perpendicular to the boundary, as illustrated in Figure 2.5B, the IRC and ITC are dependent on the incident angle and the relative impedances. Refraction is the change in direction of the transmitted ultrasound as it crosses a boundary, and is caused by the different propagation speeds on either side of the boundary.

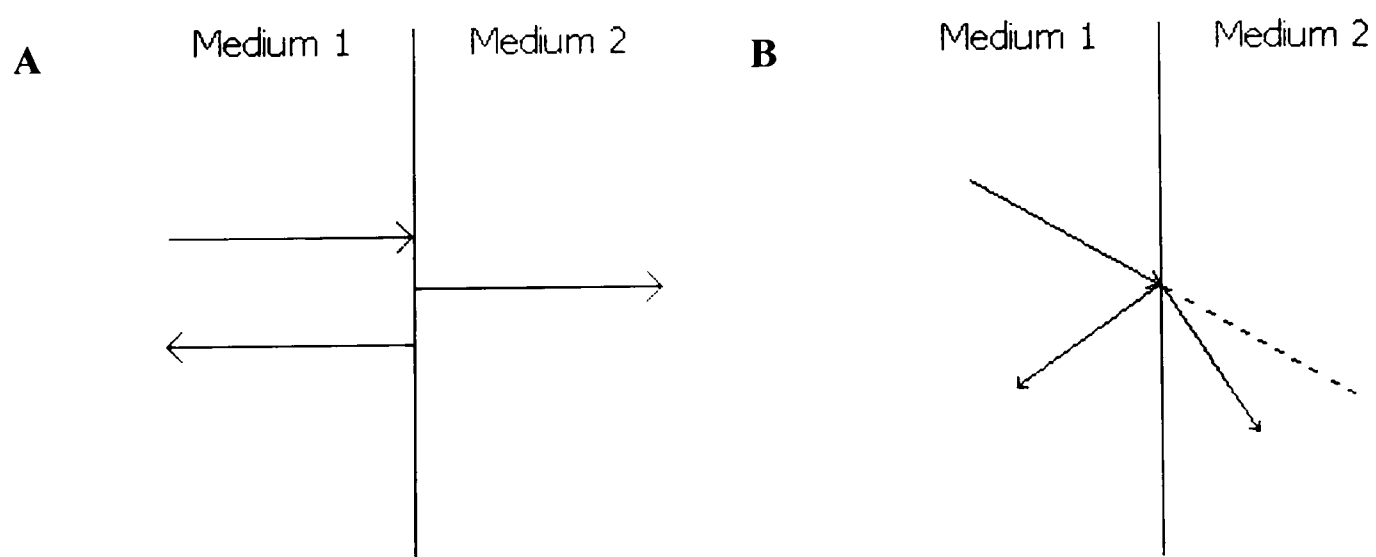


FIGURE 2.5: Schematic diagram showing reflection and transmission or refraction of ultrasound at a A) perpendicular and B) non-perpendicular boundary (Kremkau, 1985).

A further set of parameters relate specifically to pulsed ultrasound.

- The *pulse repetition frequency* (PRF) is the number of pulses occurring per second, which, in typical ultrasound scanning equipment, is approximately 1000s^{-1} . The inverse of PRF is the *pulse repetition period* (PRP).
- The *pulse duration* (PD) is the length of time required for a pulse to occur, and is equal to the product of the period and the number of cycles (n) in the pulse:

$$PD = nT = n/f \quad \text{Equation 2.5}$$

- The duty cycle, or duty factor is the fraction of time that pulsed ultrasound is active. It is determined by the pulse duration and pulse repetition period:

$$DF = PD/PRP = PD \times PRF = nT \times PRF \quad \text{Equation 2.6}$$

2.5.3 Amplitude and Intensity

The amplitude of a wave is the maximum deviation from the normal value for an acoustic variable occurring during a cycle. Variables include pressure, displacement and particle velocity, each of which can be used to describe continuous wave or pulsed wave ultrasound.

- The *acoustic power* (P) of an ultrasound beam is the rate of passage of energy through the cross-section of the beam, and is measured in watts (W).
- The *intensity* of the beam (I) is the acoustic power passing through an the area of the cross-section, A , and is also related to amplitude, Where p is pressure and z is impedance:

$$I = P/A = p^2/2z \quad \text{Equation 2.7}$$

As power and intensity are non-uniform through the beam and will, in the case of pulsed ultrasound, vary with time, then several intensities must be defined:

- The *spatial-average temporal-average* (SATA) intensity is the value calculated when the total power in the ultrasound beam is divided by the beam area and averaged over the pulsed repetition period (for pulsed ultrasound). When evaluated at the transducer face this is called I_t .
- The *spatial-peak temporal-average* (SPTA) intensity is the maximum value of intensity occurring in the beam averaged over the pulse repetition period (for pulsed ultrasound) in the beam.
- The *spatial-average temporal-peak* (SATP) intensity is the maximum value occurring in time of the spatially averaged intensity. For pulses of constant amplitude, as illustrated in Figure 2.6A, the SATP intensity is represented by the spatial average of the intensity during a pulse, and is equal to the SATA intensity divided by the duty factor. The *spatial-average pulse-average* (SAPA) intensity is the spatially averaged intensity averaged also over the pulse duration for pulses of non-constant amplitude (Figure 2.6B).
- A distinction between temporal peak (TP) and pulse average (PA) values is required because very short pulses, as well as the longer pulses which are traditionally used in physical therapy, are usually not of constant amplitude. For constant-amplitude pulses, TP and PA are equivalent. For pulses of non-constant amplitude (Figure 2.6B) the *spatial-peak pulse-average* (SPPA) intensity is the maximum intensity in the beam averaged over the pulse duration.
- The *maximum intensity* (I_m) is the maximum value within the beam occurring in space. Typical values for scanning equipment range from $<1 \text{ mW/cm}^2$ to 300 mW/cm^2 .

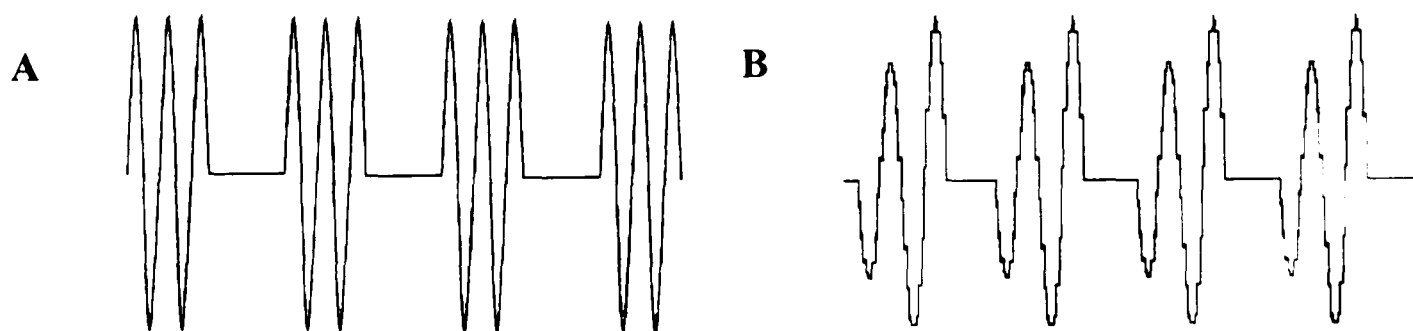


FIGURE 2.6: A) Constant and B) non-constant amplitude pulses.

2.5.4 Attenuation

Attenuation of ultrasound as it travels through a medium reduces both the amplitude and intensity, as illustrated in Figure 2.7. Attenuation is caused by:

- scattering of sound in a heterogeneous media
- reflection at interfaces in the media
- conversion of sound energy to heat, termed *absorption*.

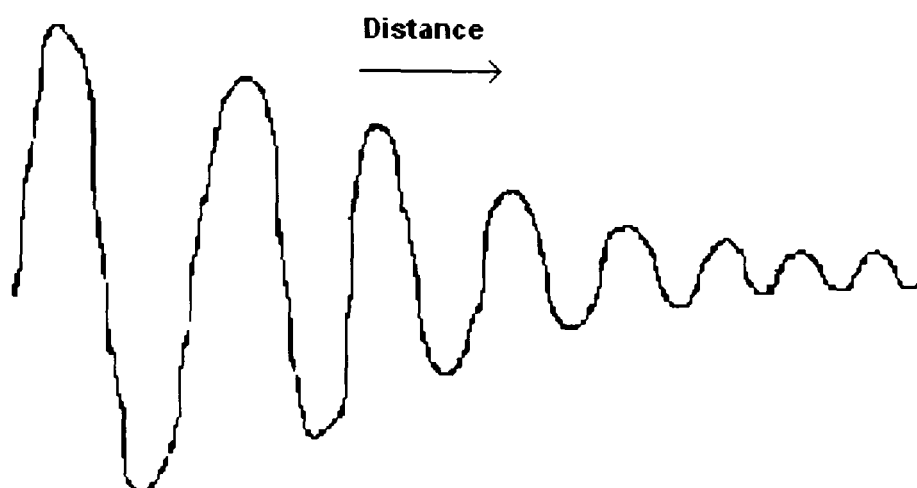


FIGURE 2.7: *Attenuation, the reduction in amplitude and intensity of ultrasound as it travels through a medium (adapted from Kremkau, 1985).*

The *attenuation coefficient* (α) is commonly measured in decibels (dB) per centimetre. In soft tissues the attenuation in dBcm^{-1} is approximately equal to half the ultrasound frequency in megahertz. In a liquid medium, attenuation is generally proportional to the squared frequency. Table 2.1 gives the measured attenuation coefficients for a variety of biological materials for a frequency of 1 MHz.

2.5.5 Standing wave production

Standing or *stationary wave* patterns are the result of reflection and interference of two or more acoustic waves of identical frequency, whereby reflected waves interact with incident waves. All standing wave patterns consist of *nodes* and *antinodes*. Nodes are points of no resultant displacement caused by the destructive interference of the two waves. Antinodes result from the constructive interference of the two waves and thus undergo maximum displacement from the rest position. Under these conditions the resultant wave appears to vibrate in regions of the medium and it is not apparent that these vibrations in fact caused by travelling waves, hence the term standing wave. Nodes and antinodes occur typically every $\lambda/2$. In practice, energy losses mean that a perfect reflection and a pure standing wave are never achieved.

TABLE 2.1: Measured attenuation coefficients for biological tissues.

Tissue	Attenuation Coefficient α (dBcm ⁻¹ MHz ⁻¹)	Model	Source
Bone	20		Bushong, 1999; Dowsett <i>et al.</i> , 1998
	3.6±0.2	Human thigh	Jiřík <i>et al.</i> , 2004
	43.3-47.5	Rabbit supraspinatus tendon insertion	Sano <i>et al.</i> , 2006
Blood	0.18		Bushong, 1999
	0.2		Dowsett <i>et al.</i> , 1998
Brain	0.85		Bushong, 1991
	0.9		Dowsett <i>et al.</i> , 1998
Fat	0.63		Bushong, 1991
	0.6		Dowsett <i>et al.</i> , 1998
	0.3±0.0	Human thigh	Jiřík <i>et al.</i> , 2004
Muscle (normal to fibrous)	1.8-3.3		Dowsett <i>et al.</i> , 1998
	1.2±0.1	Human thigh	Jiřík <i>et al.</i> , 2004
Tendon	22.25-30.65	Rabbit supraspinatus tendon insertion	Sano <i>et al.</i> , 2006
Articular cartilage	9.2-14.7	Superficial bovine AC	Agemura <i>et al.</i> , 1990
	~2.57	Full thickness bovine patella AC	Nieminen <i>et al.</i> , 2004
Non-mineralised fibrocartilage	1.25-9.65	Rabbit supraspinatus tendon insertion	Sano <i>et al.</i> , 2006
Mineralised fibrocartilage	43.3-47.5	Rabbit supraspinatus tendon insertion	Sano <i>et al.</i> , 2006
Liver	0.94		Bushong, 1999
	0.7		Jiřík <i>et al.</i> , 2004
Kidney	1.0		Bushong, 1999
Lung	41		Bushong, 1999
Water	0.002		Dowsett <i>et al.</i> , 1998
Air	12		Dowsett <i>et al.</i> , 1998

2.5.6 Medical Applications of Ultrasound

Ultrasound applications in medicine can be divided into three major categories, namely, surgical, diagnostic, and therapeutic, each distinguished by their applied intensity level. The majority of these applications employ ultrasound at frequencies between 0.5 and 15MHz as stated by the National Council on Radiation Protection and Measurement (NCRP) (Report No. 71, Operational Radiation Safety Training, 1983, cited by Benwell and Bly, 1987). Table 2.2 outlines a range of their typical applications.

TABLE 2.2: *Clinical applications of ultrasound.*

US Type	Applications	SATA Intensity
Surgical	<p>Focused beam ultrasound ablation via mechanical hyperthermia: High intensity ultrasound wave causes compression, refraction and particle movement resulting in kinetic energy and heat production (Williams <i>et al.</i>, 2004). Used to treat:</p> <ul style="list-style-type: none"> • Meniere's disease, an inner ear disorder leading to vertigo (James 1963). • Hepatocellular carcinoma, osteosarcoma, breast cancer (Wu <i>et al.</i>, 2004). Prostate cancer (Chaussy and Thuroff, 2003). • Neurosurgery (Fry and Johnson, 1978; Clement 2004). • Preclinical stage for cardiac surgery (Williams <i>et al.</i>, 2004). <p>Breakdown of unwanted tissue:</p> <ul style="list-style-type: none"> • <i>Phacoemulsification and aspiration for cataract removal</i> (Kelman, 1967). Vibrating probe (20-40 kHz) used to break up cataract and vacuum up fragments. • <i>ESWL (extracorporeal shock wave lithotripsy)</i>. Focused pulsed ultrasound to break up kidney stones (Addonizio <i>et al.</i>, 1984; Chaussy <i>et al.</i>, 1984). 	<p>$\geq 10\text{W}/\text{cm}^2$ (Benwell and Bly, 1985)</p> <p>$25\text{W}/\text{cm}^2$ (James, 1963)</p>
Diagnostic	<p>Non-invasive imaging of vital organs, foetal development, peripheral blood flow, metabolic bone diseases, evaluation of fracture callus healing (Kaufman and Einhorn, 1993; Moed <i>et al.</i>, 1998). Typical frequencies used:</p> <ul style="list-style-type: none"> • 3.5-5 MHz – general purpose abdominal scanning including heart, liver and uterus. • 5-10 MHz – Superficial tissues such as thyroid, carotid, breast, testis. Also used for infants. • 10-15 MHz – the eye. Increasing frequency improves image resolution but decreases penetration depth of ultrasound (Farr and Allisy-Roberts, 1998). <p>Biomechanical measurement of fracture healing (Cunningham <i>et al.</i>, 1990).</p>	<p>$100\text{mW}/\text{cm}^2$, $10\text{mW}/\text{cm}^2$, $40\text{mW}/\text{cm}^2$, and $10\text{mW}/\text{cm}^2$ for A mode, manual scan B mode, M mode and Foetal Doppler scans respectively (Repacholi, 1987).</p>
Therapeutic	<p>Pain relief, decreases soft tissue stiffness and accelerates healing (Dyson and Suckling, 1978). High intensities used to decrease joint stiffness, reduce pain and muscle spasms and improve mobility where heating is desired effect. Frequencies of 0.2-20 MHz employed according to depth of tissue (ter Harr, 2007). Low intensities used for stimulation of cells in absence of thermal effects. Applications in wound and bone healing, sports therapy (Rubin <i>et al.</i>, 2001; Warden, 2003).</p>	<p>$<3\text{W}/\text{cm}^2$ (Duck <i>et al.</i>, 2007)</p>

2.5.7 Safety considerations for use of ultrasound

Ultrasound parameters are strictly monitored in order to limit unwanted effects for specific clinical applications. Whereas high intensity ultrasound is used particularly for its heating effect on tissue, lower intensity ultrasound applications involving diagnostic imaging should not produce any effects that could compromise cell and tissue function. Safety aspects of ultrasound are detailed in reviews by Duck (2007) and O'Brien (2007). In brief, government regulatory bodies are guided by international standards, most noticeably those published by the International Electro-technical Commission (IEC). The current IEC guidelines (IEC 60601-2-37, 2001, cited by Duck, 2007) state that the temperature rise of an ultrasonic transducer surface should not increase above 10°C or 6°C during external and internal use respectively, with a maximum surface temperature of 43°C. Additionally, manufacturers of diagnostic ultrasound equipment employing a SATA intensity of $>100 \text{ mW/cm}^2$ need to provide detailed output information (IEC 61157, 1992, cited by Duck, 2007). The US Food and Drug Administration have set SPTA intensity limits to 720 mW/cm^2 and 50 mW/cm^2 for non-ophthalmic and ophthalmic imaging, respectively (FDA 510k, 1997, cited by Duck, 2007).

2.5.8 Biophysical effects of ultrasound in clinical applications

The biological effects of ultrasound can be separated into non-thermal and thermal effects, which are discussed in the following sub-sections.

2.5.8.1 Thermal effects

For many of the therapeutic and surgical applications of ultrasound the mechanism is provided by heat (Table 2.2). Ultrasound is desirable compared to other methods in that heat can be generated within the tissue rather than at its surface. Additionally, the spatial distribution of heat can be controlled by focusing of the ultrasound beam.

The attenuation of an ultrasound beam in body tissues and water result in an increase in local temperature. Quantitative estimates for ultrasonic heating at any location can be made by calculating the local rate of heat production in calories per cubic centimetre of exposed tissue per second ($\text{cal/cm}^2 \text{ s}$) using the following equation:

$$\text{Heating rate} = 0.055\alpha I$$

Equation 2.8

where α is the absorption coefficient (dB/cm) and I is the local time-averaged intensity (W/cm^2).

With time, the rate of temperature decreases as heat is transported to cooler tissue (Figure 2.8). Transport occurs via blood flow in the form of perfusion and/or convection and conduction (Nyborg, 1985).

The final temperature rise and the 50% 'rise time', defined as the time taken to reach 50% of the final temperature rise, are dependent on a number of factors (NCRP, 1983, cited by Benwell and Bly, 1987). For an unfocused continuous beam the final temperature rise increases with increasing intensity, absorption coefficient and beam diameter. The rise time increases with increasing beam diameter only (Nyborg, 1985).

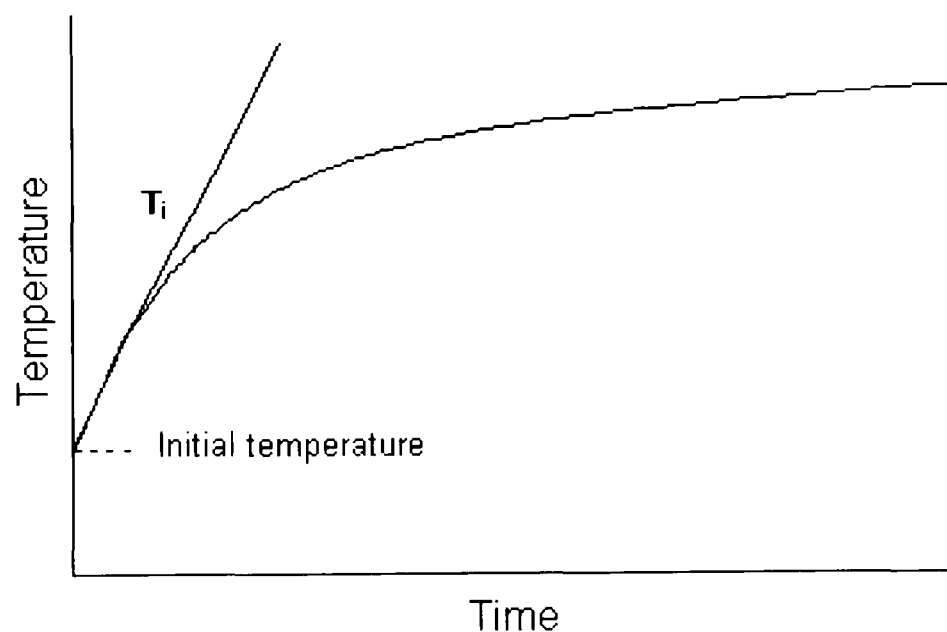


FIGURE 2.8: Schematic plot of temperature versus time at a point in a tissue exposed to continuous ultrasound. The initial rate of temperature rise T_i is constant but subsequently reduced as heat is dissipated such that the tissue temperature tends towards an equilibrium value.

2.5.8.2 Non-thermal effects

The use of ultrasound in applications employing non-thermally induced therapeutic effects may indeed cause some local heating. However, the World Federation for Ultrasound in Medicine and Biology (WFUMB) in a comprehensive report published in 1998 stated that "a diagnostic exposure that produces a maximum temperature rise of no more than 1.5°C above normal physiological levels (37°C) may be used clinically without reservation" and is hence considered as 'non-thermal' (Barnett *et al.*, 2000).

The non-thermal effects of ultrasound have been attributed to a combination of *cavitation* and *acoustic streaming*. Cavitation refers to the formation, growth and pulsation of gas or vapour-filled voids found in a liquid or liquid-like material (Dyson and Suckling, 1978). Tiny bubbles are formed at locations termed nucleation sites. However, the exact nature and source of these sites are not well understood in a complex medium such as biological tissues (O'Brien, 2007). Bubbles, at a micron or sub-micron level, remain stabilized against diffusion in pores, channels and cracks. At sufficient ultrasound pressures, these gaseous bodies may exert mechanical stresses on surrounding cells or other structures or may generate chemical activity (Nyborg, 1985).

Two types of cavitation can be distinguished:

- *Stable cavitation*, in which the gas bubbles oscillate in a regular fashion for many acoustic cycles
- *Transient or inertial cavitation*, where bubbles are formed at the low pressure part of the ultrasonic cycle, resulting in rapid growth and collapse within the wave period. This releases a large amount of energy in a region of only a few microns, which causes irreparable cell damage (Dyson, 1985). However, transient cavitation occurs at very high intensities and is not thought to be induced in therapeutic or diagnostic applications (Baker *et al.*, 2001; O'Brien, 2007). In high intensity applications, the risk of transient cavitation can be minimized by use of higher frequencies (Dyson, 1985).

Acoustic streaming relates to the movement of fluid in an ultrasonic pressure field. Streaming can be divided into *bulk streaming* and *microstreaming*, the former referring to movement of fluid in a single direction, and the latter forming as eddies of flow adjacent to an oscillating source (Baker *et al.*, 2001). Connective tissue fibres and plasma membranes of immobile cells act as barriers to the ultrasonic field, which causes high velocity gradients to develop (Dyson, 1985). Microstreaming, which is more significant at the cellular and intracellular levels, can only occur in association with cavitation *in vivo* (Nyborg, 1985; Baker *et al.*, 2001).

At its most basic level, enhanced fluid movement can increase nutrient delivery and waste removal associated with cells. However, acoustic streaming exposes boundaries, such as cell membranes, to hydrodynamic shear stress, which, as described in Section 2.4.1.2, may itself represent a mechanotransduction mechanism. Proposed effects of combined cavitation and microstreaming include increased passage of sodium and

calcium ions, which may lead to increased synthesis of protein, as observed in fibroblast cultures (Dyson and Suckling, 1978; Dinno *et al.*, 1989).

2.5.9 Therapeutic pulsed low-intensity ultrasound for bone repair

The first clinical use of ultrasound followed the discovery by Corradi and Cozzolino in 1953 that continuous ultrasound could stimulate the formation of bone callus in rabbit radial fractures and proved safe for use with humans (Rubin *et al.*, 2001). However subsequent research focused on the effects of pulsed low intensity ultrasound and, in 1983, Dyson and Brookes published data from a study of bilateral fibular fractures in rats showing that pulsed ultrasound (1.5 MHz or 3.0 MHz US frequency, pulsed 200 μ s on: 800 μ s off i.e. 20% duty cycle, SATP intensity 500 mW/cm²), applied for 5 minutes four times a week, accelerated fracture healing compared to no stimulation therapy. In addition, these authors noted that treatment was most effective at a frequency of 1.5 MHz rather than 3.0 MHz and during the early stages of healing. Other researchers extrapolated these studies to the clinical setting and found that using a lower intensity of 30mW/cm² and exposure time of 20 minutes a day, healed 70% of twenty-six bone non-unions (Xavier and Duarte, 1983, cited by Rubin *et al.*, 2001). More recent animal models and one *in-vitro* model are presented in Table 2.3. It can be seen that the majority of studies indicate that PLIUS has a positive therapeutic effect on bone healing. In particular, it influences the process of fracture healing and mineralisation in animal models. Furthermore, bone healing is sensitive to specific characteristics of the ultrasound signal. It can also be seen that the most commonly used ultrasonic signal has a SATA intensity of 30 mW/cm² of carrier frequency 1.5 MHz with a 200 μ s pulse burst repeating at 1.0 kHz (e.g. Uglow *et al.*, 2003). These ultrasonic parameters have been employed in various fracture healing clinical models (Cook *et al.*, 1997; Heckman *et al.*, 1994 and 1997; Kristiansen *et al.*, 1997; Busse *et al.*, 2002; Rubin *et al.*; 2001), and the apparatus is now commercially available as the Exogen Sonic Accelerated Fracture Healing System (SAFHS). Although this system has been used in the USA, to date, it has not gained worldwide acceptance as a therapeutic enhancement of bone healing.

These studies, although highlighting the apparent benefit of using ultrasound for bone healing, do not provide insight into the biological mechanisms that facilitate these processes. Stable cavitation and acoustic micro-streaming (Section 2.5.8.2) can alter cell membrane permeability. In healing fractures, these acoustic pressure waves are then

TABLE 2.3: Animal models employing pulsed low intensity ultrasound (PLIUS) for bone repair.

Author	Animal model	Ultrasound regimen	Results and Comments
Pilla <i>et al.</i> , 1990	Rabbit fibula osteotomy	1.5 MHz, duty cycle 20% SATA $30 \pm 5\text{mW/cm}^2$ 20 mins daily after POD1.	PLIUS-treated fibulas as strong as intact fibulas by POD 17, compared to POD28 for contralateral fibulas.
Wang <i>et al.</i> , 1994	Rat femoral shaft fracture	0.5 or 1.5 MHz Duty cycle 20% SATA $30 \pm 5\text{mW/cm}^2$ 15 mins daily up to POD 14.	Max US torque to failure > controls. Enhanced stiffness with 1.5MHz compared to 0.5MHz. SSD between 1.5MHz and controls ($p < 0.05$).
Yang <i>et al.</i> , 1996	Rat femoral shaft fracture	0.5 MHz, duty cycle 20% SATA 50 or 100mW/cm^2 Up to fifteen daily 15-min exposures between POD1-21.	Max US torque and torsional stiffness > controls. SSD at 50mW/cm^2 ($p < 0.05$). No SSD for DNA, collagen and calcium. Aggrecan gene exp enhanced at POD7 for 50mW/cm^2 ($p < 0.05$).
Jingushi <i>et al.</i> , 1998	Rat femoral fracture	Freq: 1.5 MHz SATA: $30 \pm 5\text{mW/cm}^2$ 100, 200 or $400\mu\text{s}$ repeating at 1.0 or 2.0 kHz	\uparrow bone mineral content and density. \uparrow peak torque and stiffness. \uparrow endochondral ossification. $200\mu\text{s}$ and 1.0kHz optimal parameters.
Eberson <i>et al.</i> , 2001	Rat femur distraction osteogenesis	1 MHz, duty cycle 20% SATA: 30mW/cm^2 20-mins daily from POD28. Sacrifice on POD63	\uparrow bone volume and trabecular bone pattern factors. No SSD in stiffness, bone mineral content or density.
Uglow <i>et al.</i> , 2003	Rabbit tibia distraction osteogenesis	Sonic Accelerated Fracture Healing System (SAFHS, Exogen): 1.5 MHz, duty cycle 20% SATA: 30mW/cm^2 20-mins daily up to 6 wks.	No SSD between US and controls for bone mineral content, cross sectional area, strength and bone volume fraction.
Carvalho and Cliquet, 2004	Rat osteopenic femoral bone	SAFHS parameters. 20 mins daily for 20 days.	No SSD in bone mineral content. Recent bone formation shown in PLIUS-treated femora only.
Erdoğan <i>et al.</i> , 2006	Rabbit mandibular osteotomy	SAFHS parameters. 20 mins daily for 20 days.	\uparrow mechanical properties of PLIUS-treated bone, assessed by 3-point bend test, histology and radiology.
Nolte <i>et al.</i> , 2001	<i>In-vitro</i> foetal murine metatarsal rudiments	SAFHS device and parameters. Once daily PLIUS D1-7 of culture.	Increased length of calcified diaphysis in PLIUS-treated rudiments ($p < 0.01$).

POD = post-operative day, SSD = statistically significant difference.

acting as high frequency micromechanical perturbations that may be a surrogate for the forces usually acting on bone during micromotion. Indeed, this direct mechanical effect of the ultrasound may produce the same cellular and intracellular changes seen with the compressive and cyclic loading of cells.

In-vitro studies have shown that PLIUS may influence calcium activity (Ryaby *et al.*, 1989), prostaglandin-E₂ (PGE₂) production (Kokubu *et al.*, 1999), platelet-derived growth factor release (Ito *et al.*, 2000), transforming growth factor (TGFβ1) (Li *et al.*, 2003), and promote the maturation of collagenous matrix as a scaffold for calcification (Saito *et al.*, 2004). Additionally, MAPK activity (Naruse *et al.*, 2003), G protein and extracellular signal-related kinase (ERK) activity (Chen *et al.*, 2003), and integrins and cytoskeletal reorganization (Yang *et al.*, 2005) have been implicated as possible transduction pathways.

These results generally demonstrate the ability of ultrasound to influence cell activity in bone cells. Of interest is the expression of genes involved in the inflammation and remodelling stages of fracture repair. As an example, Yang *et al.* (1996) showed an increase in aggrecan gene expression in a rat femur model (see Table 2.3). They proposed that earlier stimulation of extracellular matrix proteins may alter chondrocyte maturation and endochondral bone formation, thereby increasing the mechanical properties of the healing callus. The possible influence of PLIUS on chondrocyte behaviour was supported by further investigations undertaken by the group using cultured chondrocytes in monolayer, where upregulation of aggrecan gene expression and extracellular matrix protein synthesis were seen, using SATA intensities of 50 and 120mW/cm² (Wu *et al.*, 1996; Parvizi *et al.*, 1999). These authors also showed that calcium signalling mediated these mechanotransduction processes by release of [Ca²⁺]_i and influx of extracellular calcium (Parvizi *et al.*, 2002).

2.5.10 Use of low intensity ultrasound for cartilage regeneration

Following on from the chondrocyte work highlighted in Section 2.5.9, there has been growing interest in the possible use of PLIUS in the management of cartilage injury and disease. A number of studies are highlighted in Table 2.4.

In addition to these studies, the use of both pulsed and continuous LIUS has been investigated for its effect on mesenchymal stem cells (MSCs). Ebisawa and colleagues

TABLE 2.4: Studies investigating the effect of pulsed low intensity ultrasound (PLIUS) on cartilage biosynthesis using SAHFS parameters as described in Section 2.5.9 unless otherwise stated.

Author	Model	Ultrasound regimen	Results and Comments
Cook <i>et al.</i> , 2001	Rabbit patella osteochondral defects	Once daily 20/40 mins up to 52 wks	Histology demonstrated PLIUS ↑ cartilage repair. Beneficial effect of doubling dose.
Nishikori <i>et al.</i> , 2001	Cultured rabbit chondrocytes in Atellocollagen® gel	Once daily 20 mins for 3 weeks	PLIUS ↑ chondroitin sulphate synthesis. No SSD in cell proliferation or construct stiffness.
Zhang <i>et al.</i> , 2002	Chick embryo proximal and distal sterna (PS and DS) explants	Single 20 mins after 24 hr culture.	Immunohistochemical staining for Coll types II and X and aggrecan over 7 days. SSD for PLIUS-treated PS for all markers, and in DS except for Coll X.
Zhang <i>et al.</i> , 2003	Chick embryo DS chondrocytes in alginate bead culture.	Single 20 mins using 2 or 30 mW/cm ² after 24 hr culture.	↑ proliferation at 2mW/cm ² lost by day 7. 30 mW/cm ² ↓ cell proliferation. PLIUS ↑ Coll II but not aggrecan exp by day 7. 2mW/cm ² inhibited Coll X exp.
Duda <i>et al.</i> (2004)	BACs in copolymer scaffold nude mice model.	Once daily 20 mins after POD1 up to 12 weeks.	No effect of PLIUS based on indentation testing, histology for matrix formation, or gene exp for Coll types I and II, TGFβ.
Mukai <i>et al.</i> , 2005	Rat neonatal distal femur chondrocyte aggregates.	Once daily 20 mins from D5-D15.	PLIUS ↑ Coll type II and aggrecan mRNA, ↓ Coll X, ↑ DNA content, ↓ alkaline phosphatase, ↑ TGFβ.
Hsu <i>et al.</i> , 2006	Primary cultured HACs seeded in polyester scaffolds.	1MHz, 67mW/cm ² , 10 mins daily for up to 7 wks.	PLIUS ↑ cell proliferation and sGAG and collagen II content by 4 weeks which returned to control values by 6 weeks.
Kopakkala-Tani <i>et al.</i> , 2006	12-24 month femoral BACs in monolayer culture.	1 MHz, 580mW/cm ² 10 mins D9-13.	↑ sGAG synthesis. PLIUS did not induce heat shock protein 70, which was induced with equivalent direct heat.
Hsu <i>et al.</i> , 2007	Primary HAC monolayer	Single 20 mins after 24 hr culture.	PLIUS ↑ integrin exp with downstream PGE ₂ and COX-2 exp.

SSD = statistically significant difference. BAC = bovine articular chondrocytes. HAC = human articular chondrocytes. Exp = expression. COX-2 = cyclooxygenase.

(2004) found that daily 20 minute PLIUS (SAHFS parameters) enhanced TGF-β-mediated chondrogenic differentiation of human mesenchymal stem cell (hMSC) pellets, as assessed by aggrecan deposition. PLIUS in the absence of TGF-β had no effect. In contrast, Lee and co-workers (2006) found that continuous LIUS (1MHz, 200mW/cm²)

was able to induce chondrogenesis in rabbit MSCs (rMSCs) in the absence of TGF- β . Another study by Schumann and colleagues (2006) found that daily 20 minute stimulations in the first week of hMSC aggregate culture reduced proteoglycan and collagen gene expression, and had no effect on matrix content at day 21 of culture. In contrast, an increased 40 minute exposure enhanced these markers as well as matrix deposition in both aggregate and composite scaffold cultures.

Purported LIUS mechanotransduction pathways involved in the downstream metabolic response of chondrocytes include SACs and integrins, with downstream $[Ca^{2+}]_i$ and c-Jun N-terminal kinase (JNK) and ERK pathways (Choi et al., 2007; Parvizi *et al.*, 2002).

A recent study by Noriega and co-workers (2007), involved the use of continuous ultrasound at higher frequencies than previously seen. HAC-seeded chitosan scaffolds were treated with continuous ultrasound of 1.5, 5.0 or 8.5 MHz (estimated intensity 30mW/cm²) twice in a 24 hour period and then left in culture for 10 days before analysis. The application time of the ultrasound varied between frequencies so as to keep the number of ultrasonic cycles ($\sim 4.3 \times 10^6$) the same for all experimental groups. US-stimulated constructs were found to have enhanced aggrecan and collagen II gene expression that was directly proportional to frequency. US-stimulated constructs were also seen to have greater viability, and increased collagen content was seen for those stimulated at the two higher frequencies. Of note, cell morphology was also altered at these latter frequencies. The 5.0 MHz frequency was found to be optimal with regard to cell proliferation and collagen content, and the authors proposed that this frequency was in the region of chondrocyte resonance and therefore could provide appropriate strain levels to induce mechanotransduction effects.

From the above review of the literature, it is apparent that there may be a role for ultrasound in the repair of cartilage defects and tissue engineering. However, more research is required, using both 3D scaffold systems and *in vivo* animal models, to optimise the ultrasonic signal and determine the ultrasound-induced mechanotransduction processes that affect chondrocyte biosynthesis in order to clarify whether the use of ultrasound is advantageous in cartilage tissue engineering applications.

2.6 Aims and Objectives

As discussed in the previous sections, pulsed low intensity ultrasound (PLIUS) has been shown to enhance both fresh fractures and bony non-unions (Heckman *et al.*, 1997, Cook *et al.*, 1997, Kristiansen *et al.*, 1997), the process of which involves the stimulation of earlier expression of cartilage specific genes (Yang *et al.*, 1996) thereby altering chondrocyte maturation and endochondral bone formation. *In vitro* studies of rat chondrocytes in monolayer reported up-regulations of proliferation, collagen type II synthesis and aggrecan synthesis (Wu *et al.*, 1996; Parvizi *et al.*, 1999). Furthermore increased synthesis of aggrecan has also been reported in chondrocytes in 3D collagen gels (Nishikori *et al.*, 2001). One possibility is that PLIUS activates an intracellular calcium ($[Ca^{2+}]_i$) signalling pathway (Parvizi *et al.*, 2000), similar to that which mediates increased proteoglycan synthesis in chondrocytes subjected to more physiological mechanical loading in agarose (Pingguan-Murphy *et al.*, 2006; Chowdhury and Knight, 2006). However, the potential mechanotransduction processes by which pulsed low intensity ultrasound induce alterations in cellular metabolism is largely unknown.

The aims of this project are therefore to:

1. Examine the effects of PLIUS on glycosaminoglycan (GAG) matrix synthesis and cell proliferation, using the well-established in-vitro 3D cell-seeded agarose model system (Buschmann *et al.*, 1992 and 1995; Lee and Bader, 1995 and 1997).
2. Identify the influence of PLIUS on $[Ca^{2+}]_i$ signalling as a possible mechanotransduction pathway.

The following objectives will need to be undertaken in order to fulfil the above aims:

1. Design a system for applying PLIUS to chondrocytes cultured in agarose over a 20 day period.
2. Determine the influence of PLIUS on cell proliferation and synthesis of GAG in bovine chondrocytes cultured in 3D agarose constructs.
3. Repeat the PLIUS study undertaken by Parvizi and colleagues (1999) in bovine chondrocyte monolayer culture.

4. Design a rig that will enable microscope visualisation of $[Ca^{2+}]_i$ dynamics in cells subjected to PLIUS within monolayer cultures and 3D agarose constructs.
5. Examine the effect of PLIUS on Ca^{2+} signalling in chondrocytes in both 3D agarose and monolayer systems.
6. Examine the influence of PLIUS intensity, duration and frequency of PLIUS exposure on sGAG synthesis, cell proliferation and $[Ca^{2+}]_i$ signalling.

Chapter 3

Development of Model System for Investigating Effect of Pulsed Low-Intensity Ultrasound

3.1	Introduction	63
3.2	Cell culture methods	64
3.2.1	Cell-seeded agarose model	64
3.2.2	Preparation of culture medium and other solutions	64
3.2.3	Isolation of bovine articular chondrocytes	65
3.2.4	Preparation of chondrocyte-agarose constructs	67
3.3	Ultrasound apparatus	67
3.4	Pulsed low intensity ultrasound (PLIUS) signal	69
3.5	Attenuation of PLIUS	71
3.5.1	Spatial variation in PLIUS intensity	71
3.5.2	Standing wave investigation	73
3.6	Design and development of microscope mounted ultrasound rig	74
3.6.1	Rig design	74
3.6.2	Preparation of 3D chondrocyte-agarose constructs for use in the microscope mounted test rig	79
3.6.3	Optimisation of microscope mounted test rig – prevention of specimen drift	79
3.7	3D model system for matrix synthesis experiments	82
3.8	Standard protocols for biochemical analysis	82
3.8.1	Digest of chondrocyte-seeded agarose constructs	82
3.8.2	DMB assay for total sGAG content in constructs	82
3.8.3	DMB assay for sGAG content in medium	83
3.8.4	Fluorimetric assay of DNA	84
3.8.5	Cell viability determination	85
3.9	PLIUS intensity and temporal changes in sulphated GAG content	86
3.9.1	Method	86
3.9.2	Statistical analysis	87
3.9.3	Results	87
3.9.4	Discussion	90
3.10	Conclusion	96

3.1 Introduction

This chapter details the materials and methods employed in the subsequent experimental chapters, as well as a series of characterisation studies.

The cell-seeded agarose model systems used for the metabolic and calcium signalling experiments are described. To review briefly, chondrocytes are isolated from bovine metacarpal cartilage via enzymatic digestion and cultured in a 3D agarose construct. The procedures for preparing reagents necessary for cell culture and subsequent assays are also detailed.

The ultrasound apparatus is described. This applies pulsed low intensity ultrasound (PLIUS) to constructs maintained within a tissue cell-culture incubator.

A rig had to be designed for calcium signalling experiments that allowed PLIUS to be applied to 3D constructs, whilst mounted on the stage of an inverted confocal microscope to enable live cell imaging. Optimisation of both these ultrasound rigs is described.

A series of characterisation studies are described, examining the nature of the PLIUS signal, its spatial variation, standing wave generation, attenuation and heating effects. In addition, a range of biochemical assays are detailed, which will be subsequently used to quantify the effects of PLIUS on matrix synthesis and metabolism. This is followed by detail of a study examining the effect of PLIUS intensity on chondrocyte proliferation, sGAG synthesis and viability in 3D agarose constructs.

3.2 Cell culture methods

The following sub-sections detail the procedures utilised for preparation and culture of chondrocytes in agarose.

3.2.1 Cell-seeded agarose model

The cell-seeded agarose model has been characterised in a number of studies (Buschmann *et al.*, 1992; Lee and Bader, 1995). Chondrocytes seeded in agarose gels maintain their phenotype in long-term culture up to 70 days, forming a cartilaginous matrix, as opposed to chondrocytes in monolayer which de-differentiate with time in culture (Buschmann *et al.*, 1992; Quinn *et al.*, 2002). In addition, the relative stiffness of agarose compared to the cells per se enables application of controlled cell deformation through gross compression of the cell-agarose constructs (Lee *et al.*, 2000a). For these reasons, the cell-agarose model has been used widely in the host laboratory in a range of cell deformation and mechanotransduction studies (Lee and Bader, 1995; Knight *et al.*, 1998b; Idowu *et al.*, 2000; Roberts *et al.*, 2001; Chowdhury *et al.*, 2001; Bader *et al.*, 2002; Shelton *et al.*, 2003; Pinguan-Murphy *et al.* 2005; Heywood *et al.* 2006).

3.2.2 Preparation of culture medium and other solutions

Standard Chondrocyte Culture Medium: Dulbecco's Modified Eagles Medium (DMEM) (Sigma, UK) was used for culturing chondrocytes. A 500ml bottle of DMEM was supplemented with specific additives, as detailed in Table 3.1, and filtered using a 0.22µm pore cellulose acetate filter before being aliquoted and frozen until required. The resulting medium is referred to as DMEM + 16.1%FCS. The preparation of culture medium was undertaken in a sterile environment within a laminar flow hood.

Pronase: Pronase is a proteolytic enzyme commonly used in solution to degrade proteoglycan contained in the extracellular matrix of articular cartilage. In a laminar flow hood, powdered pronase type E (BDH Laboratory Supplies, UK) was dissolved in DMEM + 16.1% FCS at a concentration of 700 units.ml⁻¹, filtered using a 0.22 µm pore cellulose acetate filter and then frozen in aliquots of 10ml until needed.

Collagenase: Collagenase is an enzyme used to catalyse the hydrolysis of collagen. In a laminar flow hood, powdered collagenase Type XI (Sigma UK) was dissolved in

DMEM + 16.1% FCS at a concentration of 100 units.ml⁻¹, filtered using a 0.22µm pore cellulose acetate filter and then frozen in aliquots of 30ml until needed.

TABLE 3.1: Additives for standard chondrocyte medium.

Additive	Stock concentration	Amount added	Final Concentration	Function
Penicillin/ Streptomycin	5,000 units/ml 5 mg/ml	5ml	40 units/ml 0.04 µg/ml	Antibiotic
L-Glutamine	200mM	5ml	1.61mM	Energy Source
HEPES	1M	10ml	16.1mM	Buffer
L-ascorbic acid	N/A	0.075g	0.69µM	Physiological nutrient and free-radical scavenger
Foetal Calf Serum (FCS)	N/A	100ml	16.1%	Physiological nutrients e.g. growth factors

All reagents obtained from Sigma, UK.

3.2.3 Isolation of bovine articular chondrocytes

Articular chondrocytes were isolated from the cartilage removed from the metacarpal joints of steers aged 18-24 months, using well established procedures (Kuettnner *et al.*, 1982; Lee and Bader, 1995; Knight *et al.*, 1996). Bovine front feet, obtained from a local abattoir, were washed in warm water to remove dirt before being soaked in 70% (v/v) Industrial Methylated Spirit (IMS) for 10-15 minutes. Each foot was then transferred to a sterile laminar flow hood and sterile equipment used to extract the cartilage from the joint, as described below:

Cartilage Explant Extraction: Scalpels were used to remove the skin of the bovine foot and expose the underlying tissue (Figure 3.1a), so that the synovial joint could be disarticulated (Figure 3.1b). Full-depth articular cartilage was then removed from the proximal surface using a scalpel (Figure 3.1c) and placed in a petri dish filled with DMEM+16.1% FCS.

Isolation of chondrocytes: Once all the proximal cartilage had been removed from the articular surface, the DMEM+16.1% FCS was aspirated from the petri dish and the cartilage shavings were finely chopped up using two scalpel blades simultaneously. The cartilage pieces were transferred into a 60ml falcon tube, to which 10ml of pronase solution was added, and then placed onto a rolamixer for one hour at 37°C. The pronase solution was aspirated and 30ml of collagenase solution added to the tube, which was

placed on the rolamixer at 37°C for 12-16 hours. After this time period, the resulting cloudy mixture was passed through a cell sieve into a second falcon tube to remove any undigested cartilage. The cell suspension was spun in a centrifuge (2000rpm, 5 mins), the supernatant discarded and the cells washed with 10ml DMEM+16.1%FCS. The cell suspension was spun and washed for a further two times and finally suspended in 10ml of DMEM+16.1%FCS.

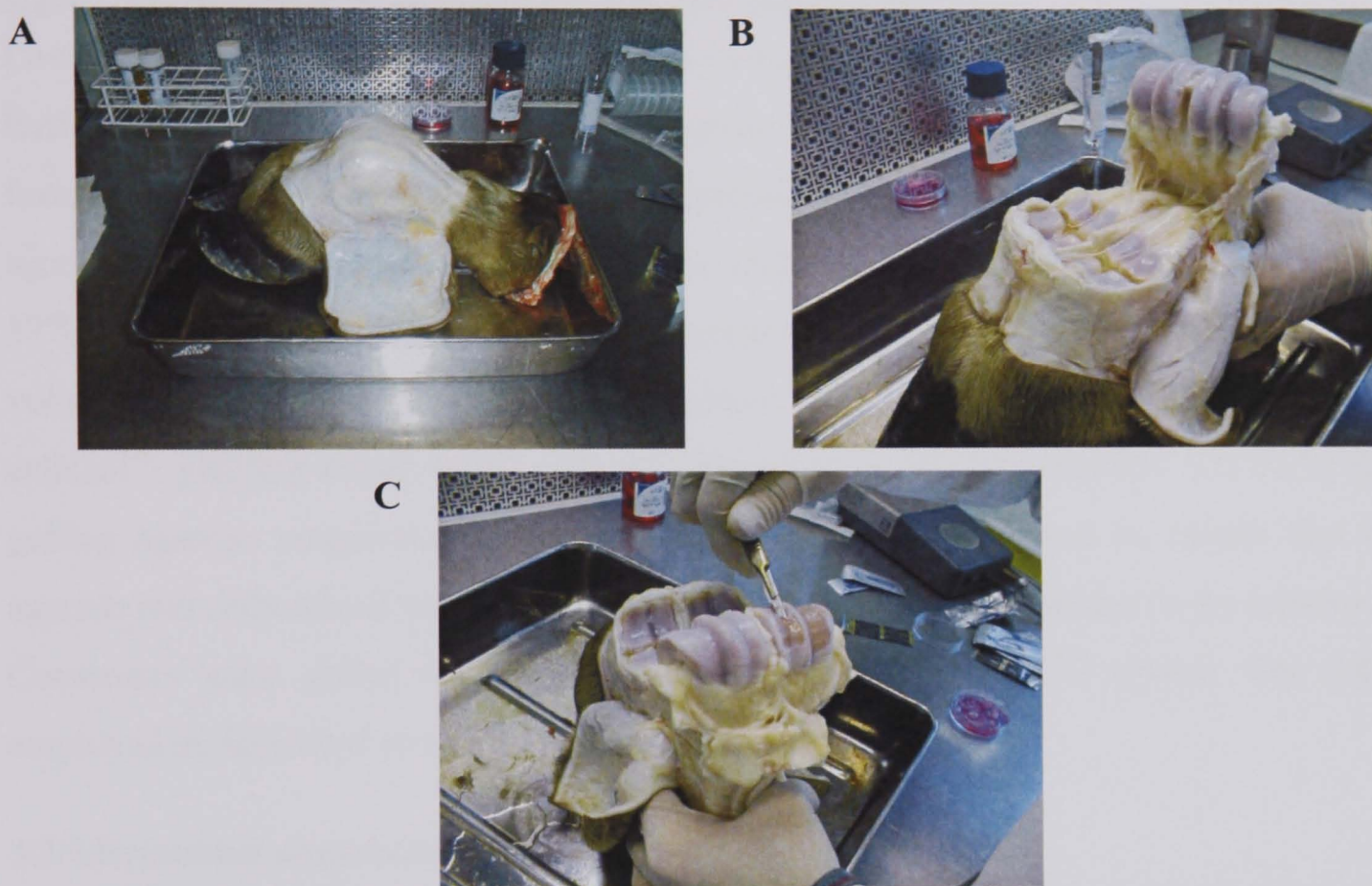


FIGURE 3.1: *Photographic sequence showing the key stages in the opening of a bovine metacarpal joint (A, B) and extraction of articular cartilage from the proximal joint surfaces (C).*

A small aliquot of cell suspension was removed and diluted 1:1 with trypan blue, a stain that stains non-viable cells blue whilst excluding viable cells. Once mixed the solution was applied to a haemocytometer and the cell number counted. Cell number was estimated using the following equation:

$$\text{Total cell number} = \frac{N \times 2 \times V_{total}}{V_h} \quad \text{Equation 3.1}$$

Where:

N = Number of cells within the grid of the haemocytometer

2 = dilution factor

V_{total} = Total volume of cell suspension (ml)

V_h = Volume of haemocytometer chamber (10^{-4} ml)

From this equation both chondrocyte yield and viability were calculated. The chondrocyte suspension was adjusted to the desired cell concentration by addition or removal of DMEM+16.1%FCS. Cell concentration was adjusted to 8×10^6 cells.ml⁻¹ for the matrix synthesis experiments (Chapters 4 and 5), and 20×10^6 cells.ml⁻¹ for experiments examining calcium signalling (Chapter 6).

3.2.4 Preparation of chondrocyte-agarose constructs

Low gelling agarose (Type VII, Sigma, UK) was employed for preparing the constructs. Earle's Balanced Salt Solution (EBSS, Sigma, UK) was added to agarose powder to form a 6% (w/v) solution of low gelling agarose. This was then autoclaved to melt the agarose and ensure sterility and mixing. The molten gel was then transferred to rollers at 37°C for 15 minutes to cool down to physiological temperatures, before adding an equal volume of cell suspension at a concentration of either 8×10^6 cells.ml⁻¹ or 20×10^6 cells.ml⁻¹, yielding either 4×10^6 cells.ml⁻¹ 3% (w/v) or 10×10^6 cells.ml⁻¹ 3% (w/v) low gelling agarose suspension. This was placed on the 37°C rollers to ensure that the agarose and cells mixed and there was minimal retention of air bubbles in the solution. Constructs were gelled differently depending on which PLIUS system was being employed as described in sections 3.6 and 3.7.

3.3 Ultrasound apparatus

The ultrasound equipment was provided by Smith and Nephew Inc. (York, UK). The ultrasonic signal exhibited a series of nominal characteristics, namely a Spatial Average and Temporal Average intensity (SATA) of 30mW/cm² of carrier frequency 1.5MHz with a 200µs pulse burst repeating every 1000µs (presented graphically in Figure 3.2).

The ultrasonic driver box (A in Figure 3.3) controls six transducers mounted in a frame made of Delrin® polyoxymethylene (B in Figure 3.3) specifically for use with a standard six-well plate (C in Figure 3.3). The duration of the ultrasound stimulation is controlled by a switch on the circuit board inside the driver box, equivalent to four prescribed settings of 10, 20, 30 and 40 minutes. However, unless stated otherwise, a twenty minute duration was routinely used to be equivalent to both the time used in previous studies and that used in the clinical setting (Cook *et al.*, 1997; Heckman *et al.*, 1994; Nishikori *et al.*, 2001; Zhang *et al.*, 2002).

The ultrasonic box has manual off and on controls. In order to automatically control how often the 20-minute ultrasound treatment was applied, a timer module designed by

a technician in the host department was incorporated into the system (labelled **D** in figure 3.3). The timer could be programmed to trigger the ultrasound signal after any time period ranging from seconds to hours.

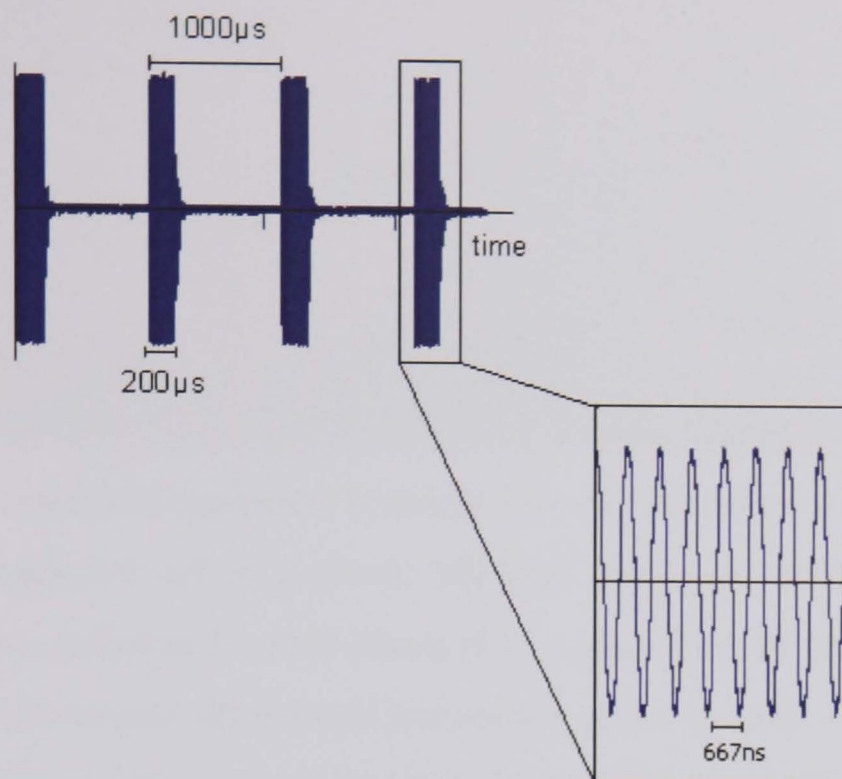


FIGURE 3.2: The ultrasonic signal employed for the experimental work undertaken in this thesis. A $200\mu\text{s}$ burst sine wave of frequency 1.5 MHz repeats every $1000\mu\text{s}$ (duty cycle 20%). The $200\mu\text{s}$ burst is composed of approximately 300 cycles, each of duration 667ns.

Coupling gel (Exogen, USA), a viscous gel placed between the ultrasonic transducer and culture plate wells, was used to minimise an air gap between surfaces, allowing transmission of ultrasound. Smith and Nephew also provided an LED indicator for each transducer to monitor its functional state of 'off' or 'on' (Figure 3.4).

In addition to the above equipment, a secondary ultrasonic driver box was available to vary the Spatial Average and Temporal Average (SATA) intensities of the pulsed ultrasound to six settings between 13 and $300\text{mW}/\text{cm}^2$. However, this system differed from the one described above, incorporating only three output ports, enabling only three transducers to be used at any one time, each providing three different intensities of ultrasound.

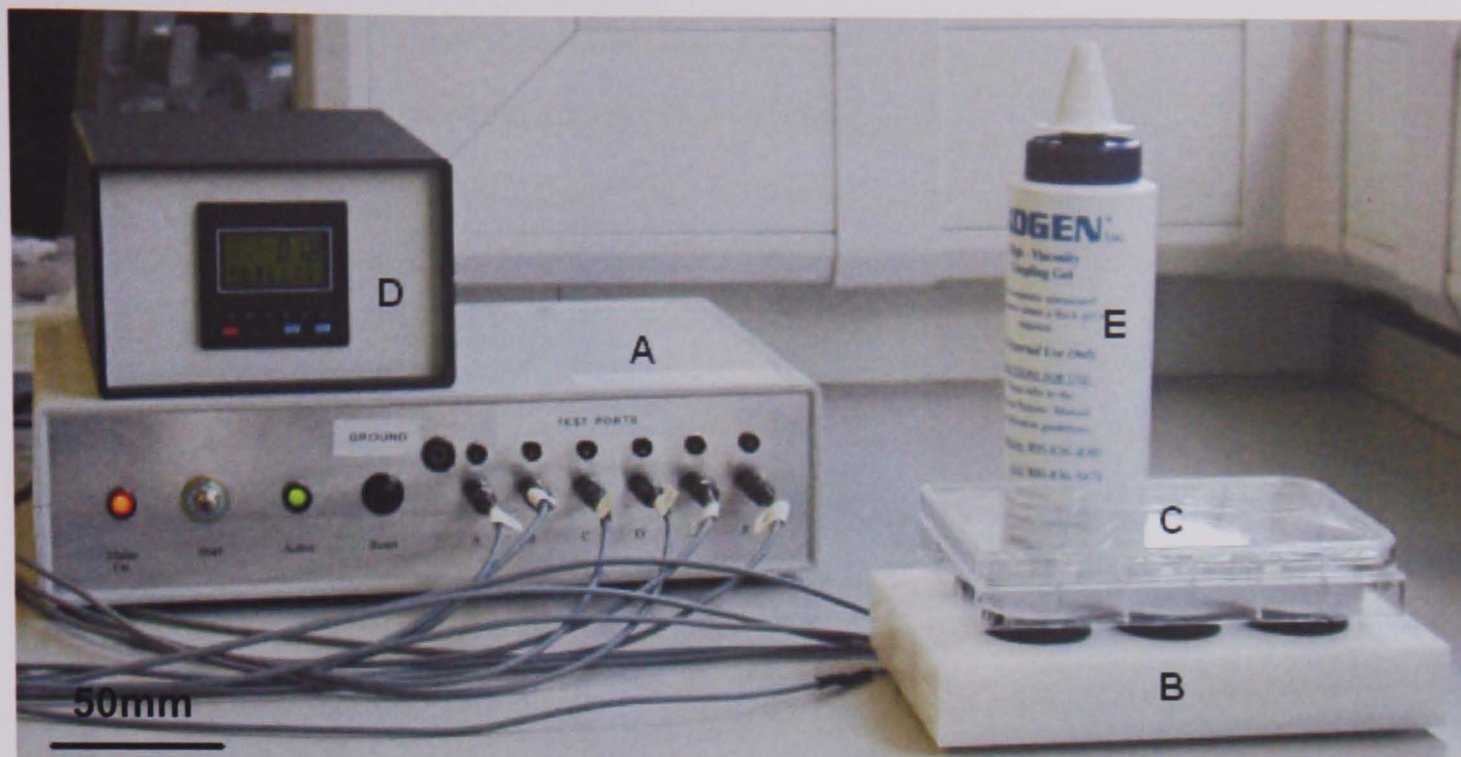


FIGURE 3.3: Ultrasound apparatus employed for cell stimulation. Ultrasonic box (A) controls six transducers set in a frame (B) that transmits PLIUS to chondrocyte-agarose constructs gelled in six well plates (C). A timer-box (D) is used to control the daily number of 20-minute ultrasound treatments given to cells. Coupling gel (E) is used to eliminate any ultrasonic attenuation between the transducers and wells. The transducers and six-well plate can be maintained within a humidified cell culture incubator.



FIGURE 3.4: LED indicator placed on transducer with coupling gel. The LED glowed yellow when PLIUS was transmitted.

3.4 Pulsed low intensity ultrasound (PLIUS) signal

As described in section 3.3, the ultrasonic signal emitted from the equipment provided by Smith and Nephew Inc. was pre-set in accordance with commonly used parameters. An oscilloscope (HAMEG 20MHz Storage, HM205-3) was used to visualise this ultrasonic signal, both as it was produced by the driver circuit (henceforth referred to as

the *input* signal) and when it left the transducer box and entered the biological system through the transducer (referred to as the *output* signal).

The typical US input and output signal were obtained, as illustrated in the form of temporal voltage profiles in Figure 3.5.

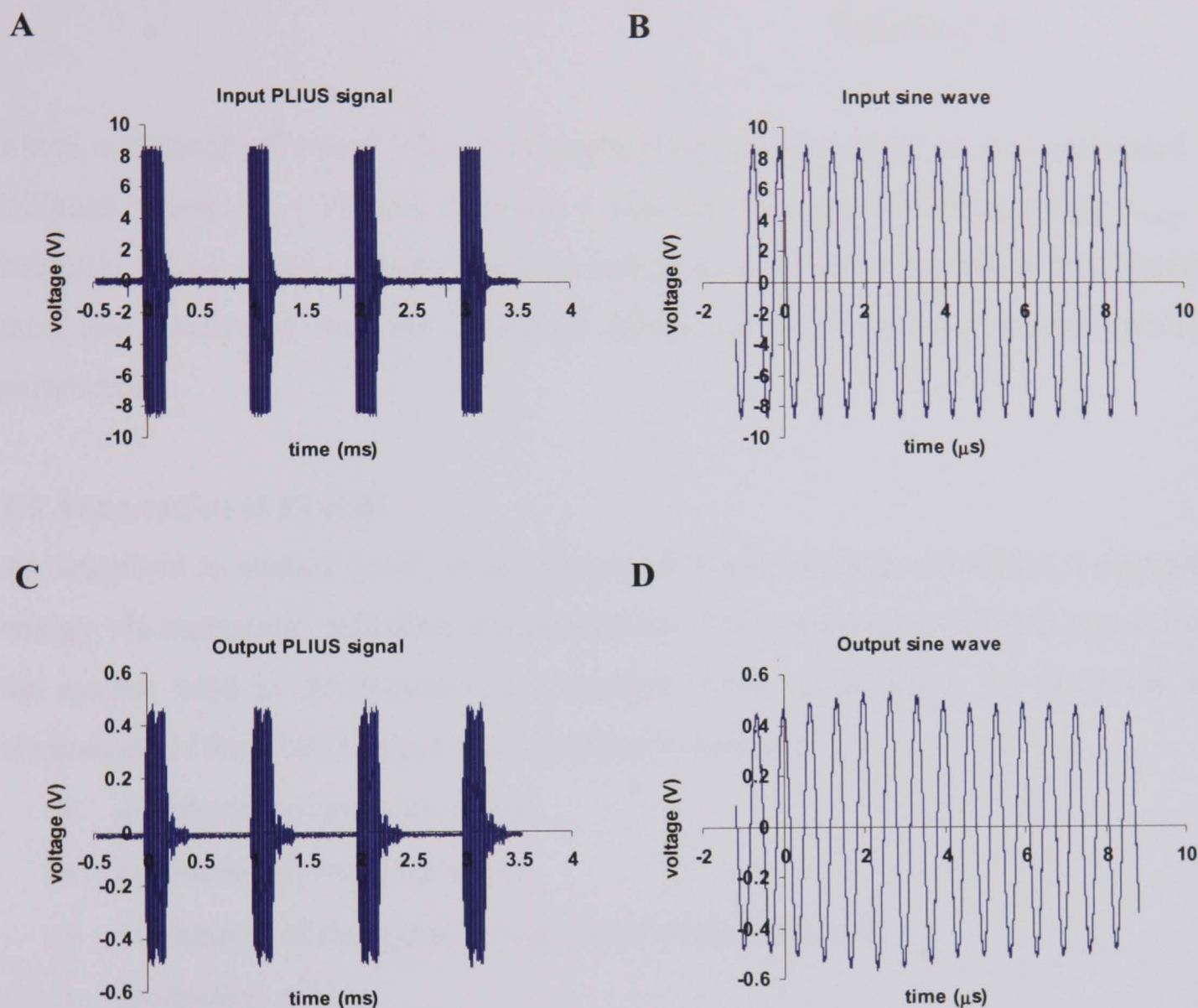


FIGURE 3.5: The temporal voltage profiles showing input (**A** and **B**) and output ultrasound signals (**C** and **D**) emitted from the PLIUS transducer at a SATA intensity of $30\text{mW}/\text{cm}^2$. **A** and **C** show the pulsed nature of the ultrasound, which has a 20% duty cycle. **B** and **D** show expanded sections of the ultrasound signal from which the frequency could be estimated at 1.5 MHz.

The reduction in voltage seen for the output profiles are a result of the resistance incurred in the transducer. The approximate wavelength of the ultrasound was obtained from the input and output sine waves. This value was estimated by counting the number of waves, to the nearest wavelength in an $8\mu\text{s}$ time period:

$$\begin{aligned} \text{Average time period } (t) &= \text{number of waves / time taken for waves} \\ &= 12 \text{ waves} / 8 \times 10^{-6} \text{ seconds} = 667 \text{ ns} \end{aligned}$$

As the time period of a wave is the inverse of its frequency (f), the wavelength (λ) in a specific medium was calculated using the formula:

$$\lambda = ct \quad \text{Equation 3.2}$$

where c = speed of sound. The wavelength of the ultrasound in air was calculated as 0.22mm, where $c_{air} = 330\text{m/s}$. In water, λ was calculated as 0.987mm, taking c_{water} as 1480m/s. These results corroborated the information provided by Smith and Nephew Inc., and confirmed that the ultrasonic equipment was operating within optimum parameters.

3.5 Attenuation of PLIUS

As described in section 2.5.4, when ultrasound travels through a medium it dissipates energy via scattering, reflection and absorption. The nature of the PLIUS signal from the system used in the present work required some investigation. In particular, the attenuation of the PLIUS signal was examined in terms of:

- distribution of pressure waves
- production of standing waves
- attenuation of the signal through the model system and
- production of heat.

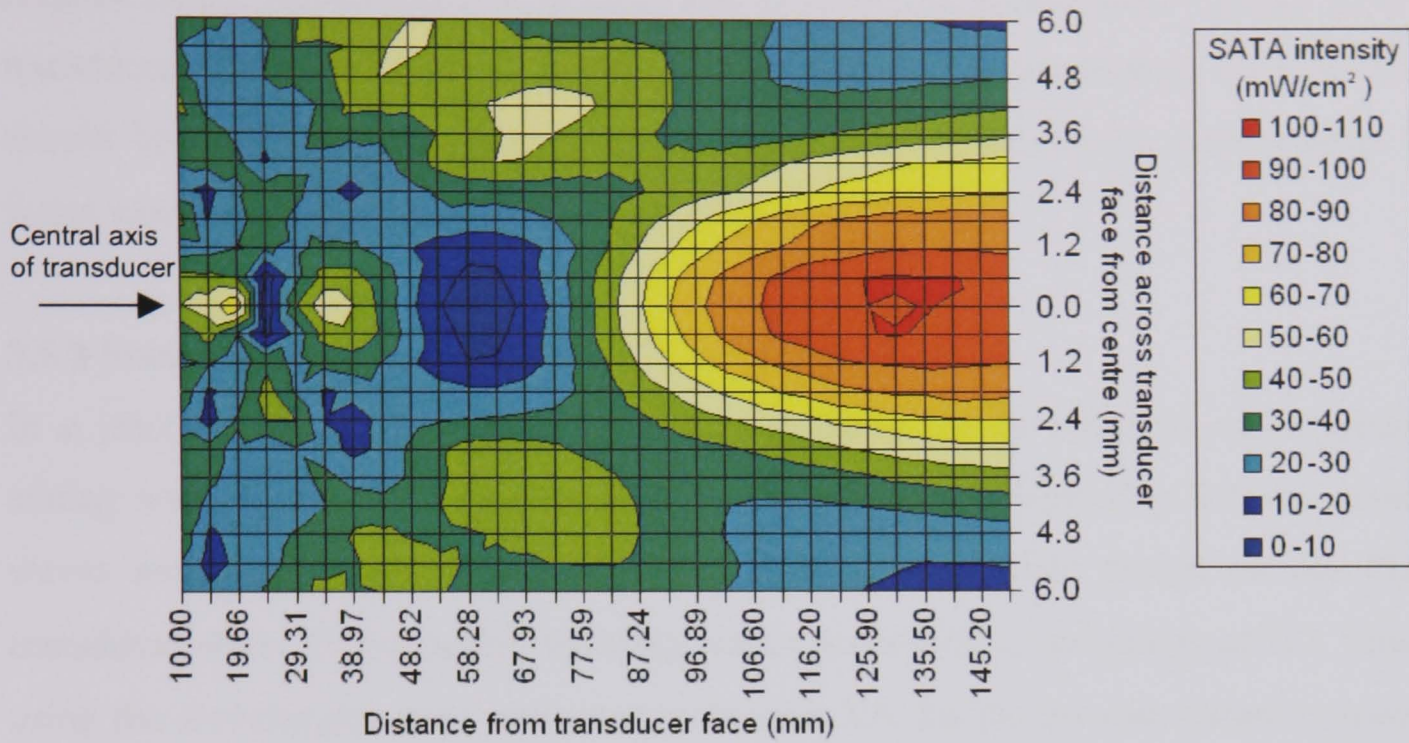
The latter two events, which were investigated solely by Smith and Nephew Inc., are discussed in Section 3.10.

3.5.1 Spatial variation in PLIUS intensity

Characterisation of the distribution of the ultrasonic signal with distance from the transducer surface is of particular importance when attempting to understand the possible mechanisms by which PLIUS produces a therapeutic effect. Colleagues at Smith and Nephew Research Centre (York, UK) undertook a study at Natural Physical Laboratories at Teddington. It involved a needle hydrophone to measure the SATA intensity across the central 12mm diameter face of an ultrasonic transducer in water emitting the 30mW/cm^2 signal. A spatial intensity profile was produced showing

variation in intensity both across the surface of the transducer, and with increasing distance from the transducer face (Figure 3.6).

A)



B)

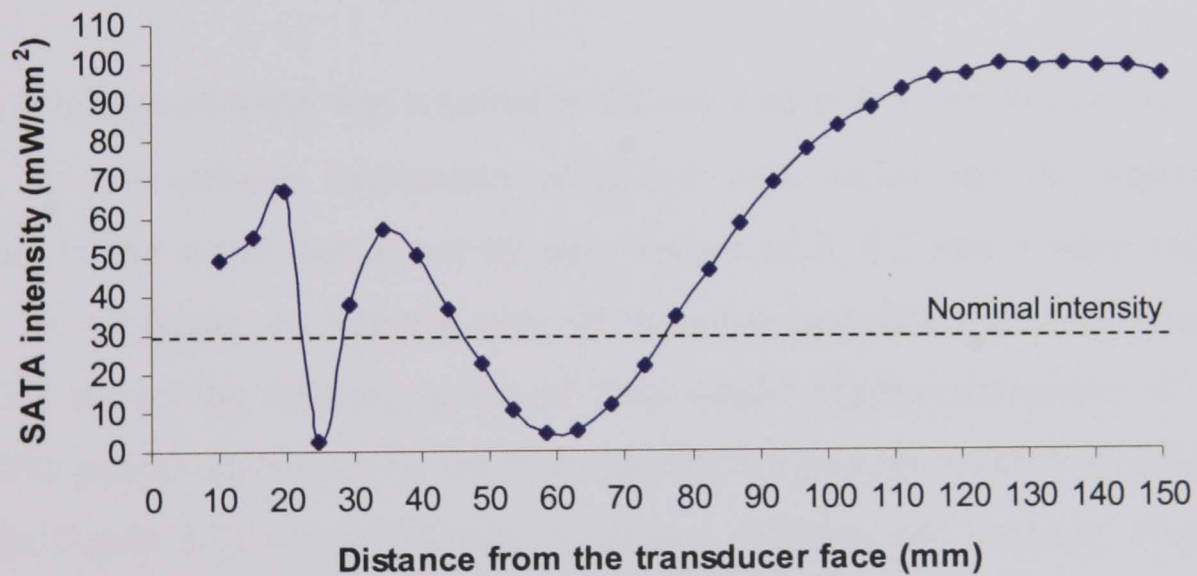


FIGURE 3.6: A) Spatial profile of ultrasonic intensity for a typical transducer emitting a $30\text{mW}/\text{cm}^2$ signal showing the variation in intensity over its face with increased distance from the source and B) corresponding plot of SATA intensity versus distance from the centre of the transducer. Image obtained from Smith and Nephew Inc., York, UK.

It can be seen from Figure 3.6 that there is a considerable variation in the intensity of the PLIUS signal with distance through water, particularly in the near field. It is evident that the PLIUS signal is not uniform over the transducer face at any distance. If the

profile from the centre of the transducer is examined (Figure 3.6B), at distances approximately 105mm from the transducer face the signal intensity exceeds $100\text{mW}/\text{cm}^2$, threefold greater than the nominal intensity. To achieve an intensity of $30\text{mW}/\text{cm}^2$, the distance from the centre of the transducer was approximately 78mm (Figure 3.6B). Additionally, it is clear that at distances greater than 120mm from the transducer, the intensity levels remain fairly constant at approximately $100\text{mW}/\text{cm}^2$. It should be noted however, that the attenuation characteristics of a system other than water would influence these intensity profiles.

3.5.2 Standing wave investigation

In a pilot investigation, it was noted that standing waves occurred while gradually adding water to a well exposed to PLIUS. Therefore the relationship between standing waves and fluid height was investigated in a six-well plate placed on the PLIUS transducer plate. Theoretically, standing waves occur with a periodicity of $\lambda/2$. Thus by using the wavelength value estimated in Section 3.4, for the present system to transmit ultrasound to water, standing waves would be predicted to occur at intervals of 0.493 mm.

A $2270\mu\text{l}$ volume of water was required to fill one well of a six-well plate to a height of 2.5mm. To this volume, increments of $22.7\mu\text{l}$ were added and the appearance of vibrations in the water was noted by eye. Values of 0, 0.5 and 1 were assigned to indicate no vibration, an isolated area of vibration and full vibration, respectively. Figure 3.7 shows the resulting graph of fluid height against appearance of standing waves. The periodicity values for the four standing waves (calculated from periods t_1 - t_4 , shown in Figure 3.7) were 0.525mm, 0.625mm, 0.55mm and 0.45mm, respectively. This provides a mean periodicity of $0.54\text{mm}\pm 0.07$, the range of which encompasses the theoretical value of 0.493mm.

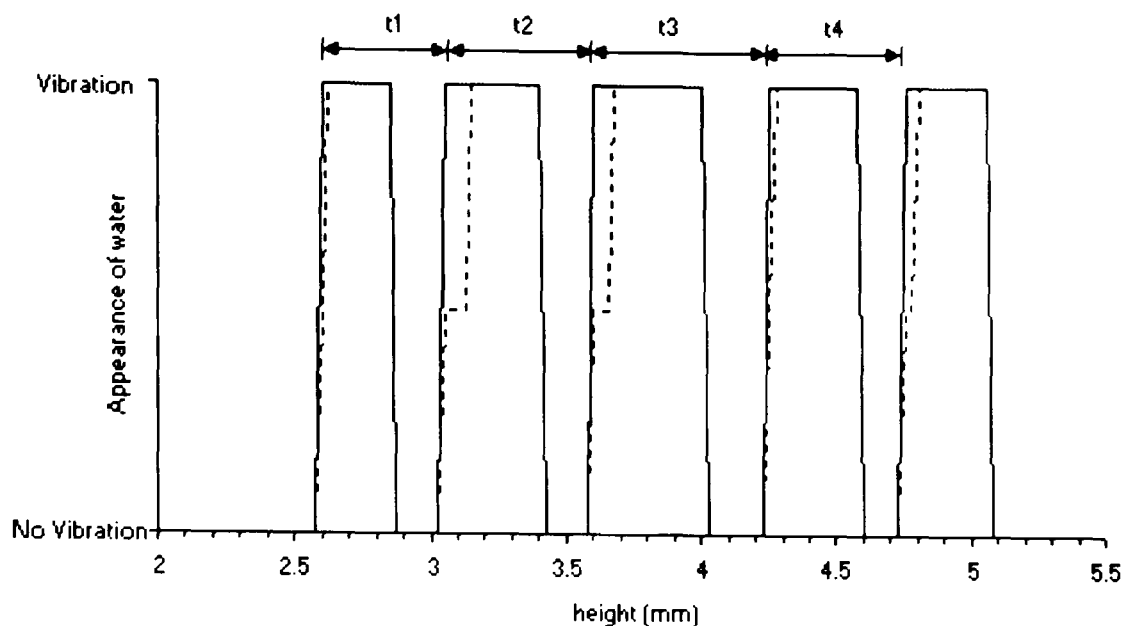


FIGURE 3.7: Graphical representation of standing waves occurring in water placed in the well of a six well plate stimulated with PLIUS, based on observation of vibration in water. The broken line represents the same dataset, but includes incidences where a small degree of vibration was apparent. The average standing wave periodicity of t_1 - t_4 was calculated as $0.54\text{mm} \pm 0.07$.

3.6 Design and development of microscope mounted ultrasound rig

The following sub-sections detail the design and development of a microscope mounted ultrasound rig necessary for the undertaking of calcium signalling experiments (Chapter 6) along with associated components.

3.6.1 Rig design

The aforementioned rig needed to fulfil the following design specifications:

- 1) The coupling of the ultrasonic transducer to the cell system should be accomplished with no intervening air gap
- 2) The cells should be imaged on the inverted stage of a confocal microscope
- 3) The cells should be maintained in a physiological environment, namely, hydration with culture medium maintained at 37°C .

As the rig needed to be mounted on an inverted microscope, then the ultrasonic transducer had to be positioned above the cell model system. The rig was therefore designed in two parts; a chamber which would be placed onto the stage of the microscope and a lid component, incorporating the transducer, which would be used to cover the chamber and enclose the cells. Figure 3.8, 3.9 and 3.10 illustrate the two components.

The stainless steel base-plate of the chamber component of the rig (Figure 3.8) formed a pre-existing component of a rig designed previously in the host laboratory (Knight, 1997), with dimensions to fit onto the stage of the confocal microscope. The gap in the base plate allowed for placement of a glass coverslip (22x40mm), which was sealed with silicon grease to make the chamber watertight. Attached to the underside of the base plate were two heater pads and a thermistor (1.25W, 50x25mm, 12V DC, RS Stock No.245-499). These components connected to a commercial temperature control unit (Intracel, Herts., UK, Figure 3.9) via the connection shown in Figure 3.8, enabling the chondrocyte medium to be maintained at 37°C in order to simulate physiological conditions.

The 70x70mm chamber component (Figure 3.8) was designed to contain the construct and be filled with the appropriate chondrocyte medium in order to both hydrate the construct and to ensure no air gap lay between the ultrasound transducer (contained in the lid of the rig, Figure 3.10) and the construct. This arrangement ensured that a continuous pathway for ultrasound transmission was maintained.

The lid component of the rig (Figure 3.10) incorporated an area where the transducer could be located. The base of this area was composed of the bottom of one well of a six-well plate, in order to more closely replicate the system used to stimulate cells for the metabolic studies (Section 3.3). Coupling medium was placed between the transducer and the base for continuity of ultrasound transmission to the chondrocytes. The lid component of the rig slotted into the chamber component of the rig, to provide a flush connection. Perspex spacers were used to create space within the chamber for the 3D constructs/monolayer, as seen schematically in Figure 3.11. Once the rig was set up with construct in place, the chamber could be filled with medium via the channel in the lid (Figures 3.10 and 3.11) and maintained at 37°C by the temperature control unit (Figure 3.9).

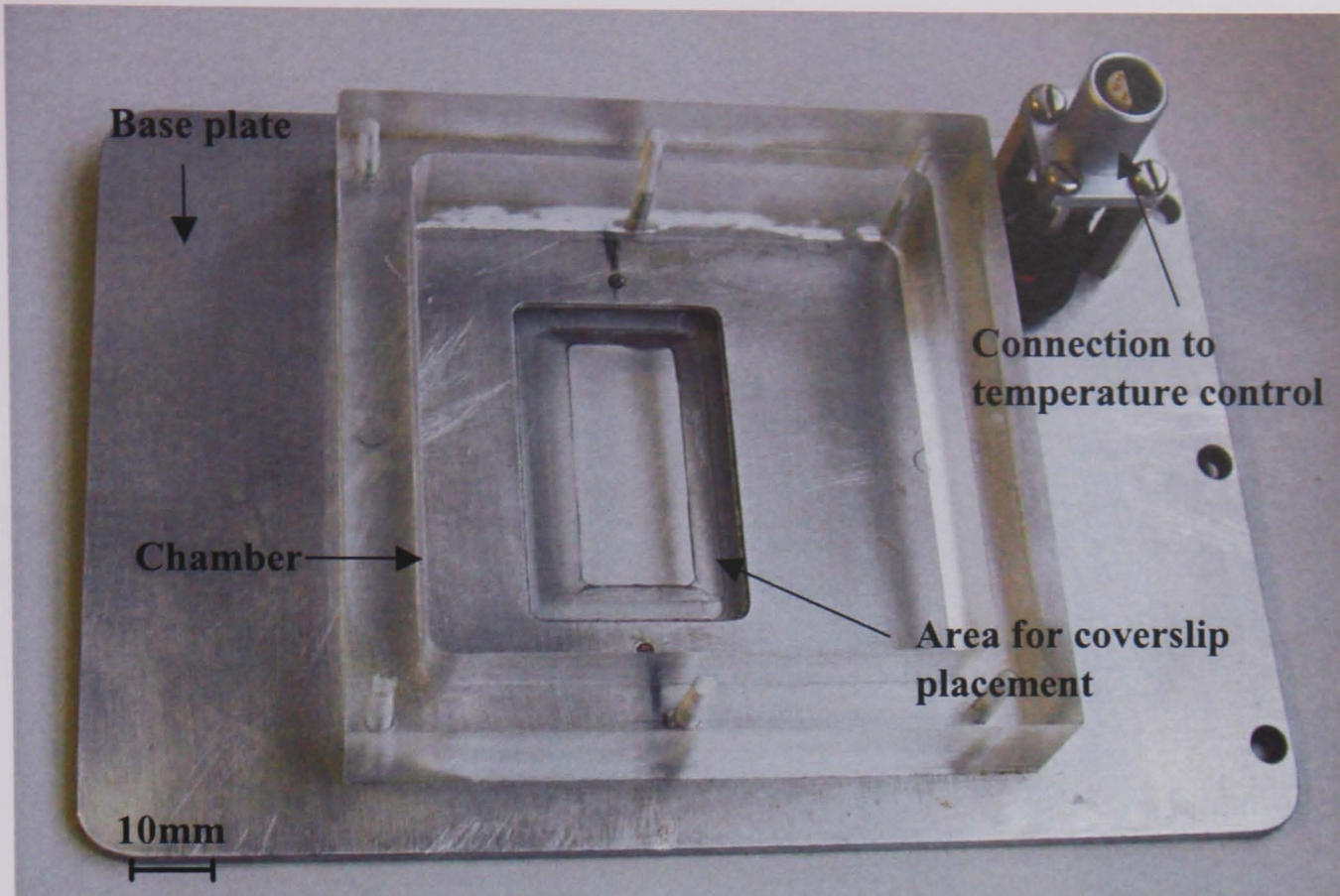


FIGURE 3.8: Chamber component of microscope rig. A 70x70mm perspex chamber was attached onto a pre-existing stainless steel base-plate.

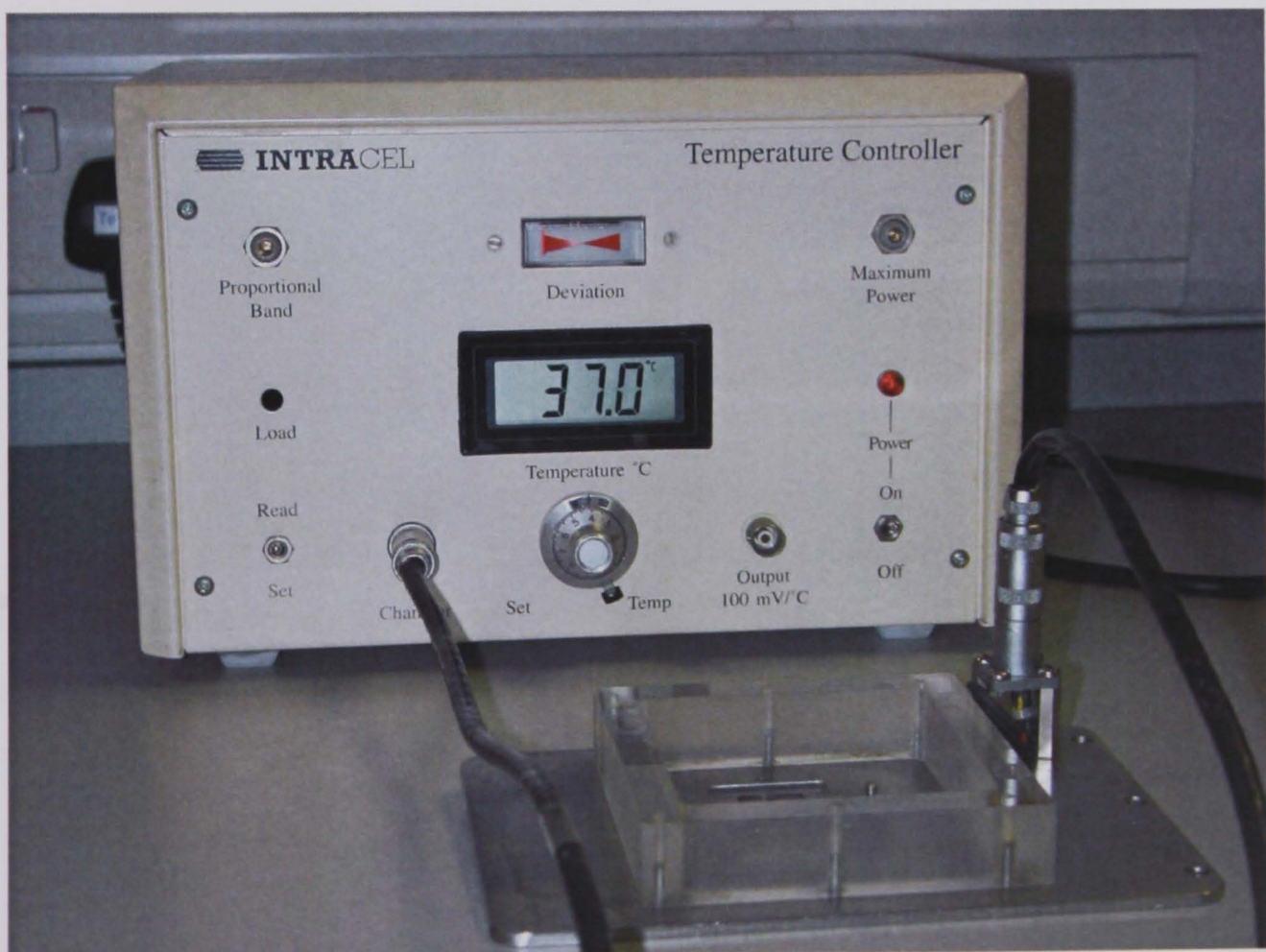
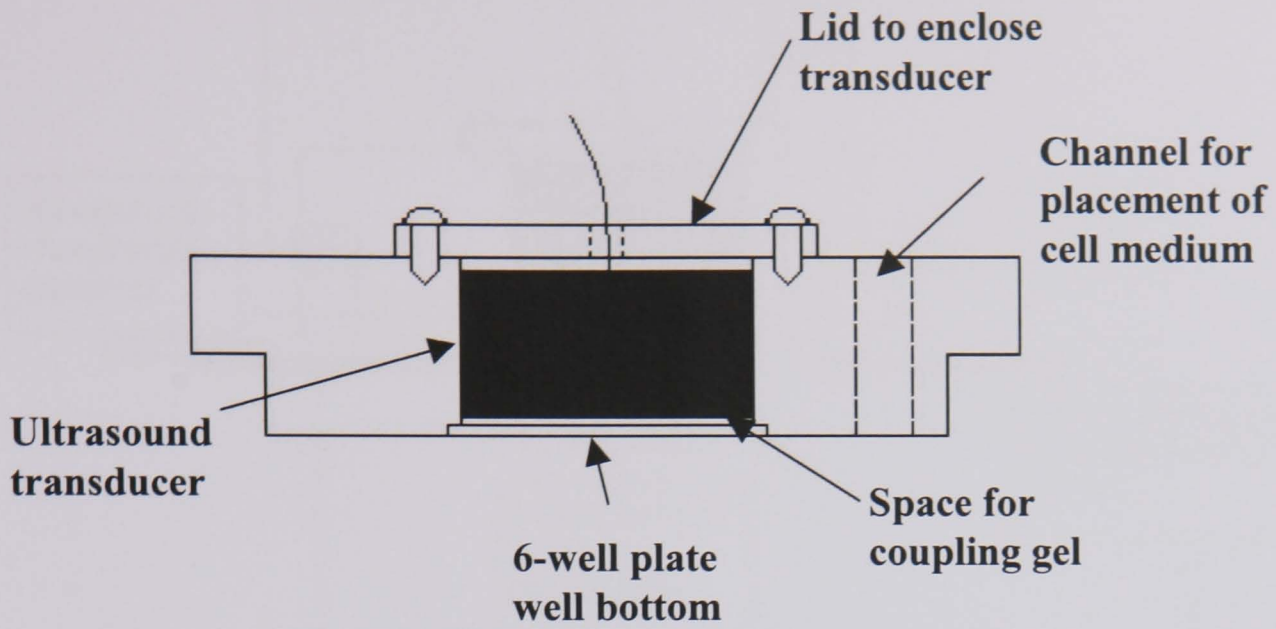


FIGURE 3.9: Photograph of the temperature control unit (Intracel, U.K.) attached to the base plate of the confocal rig.

A



B

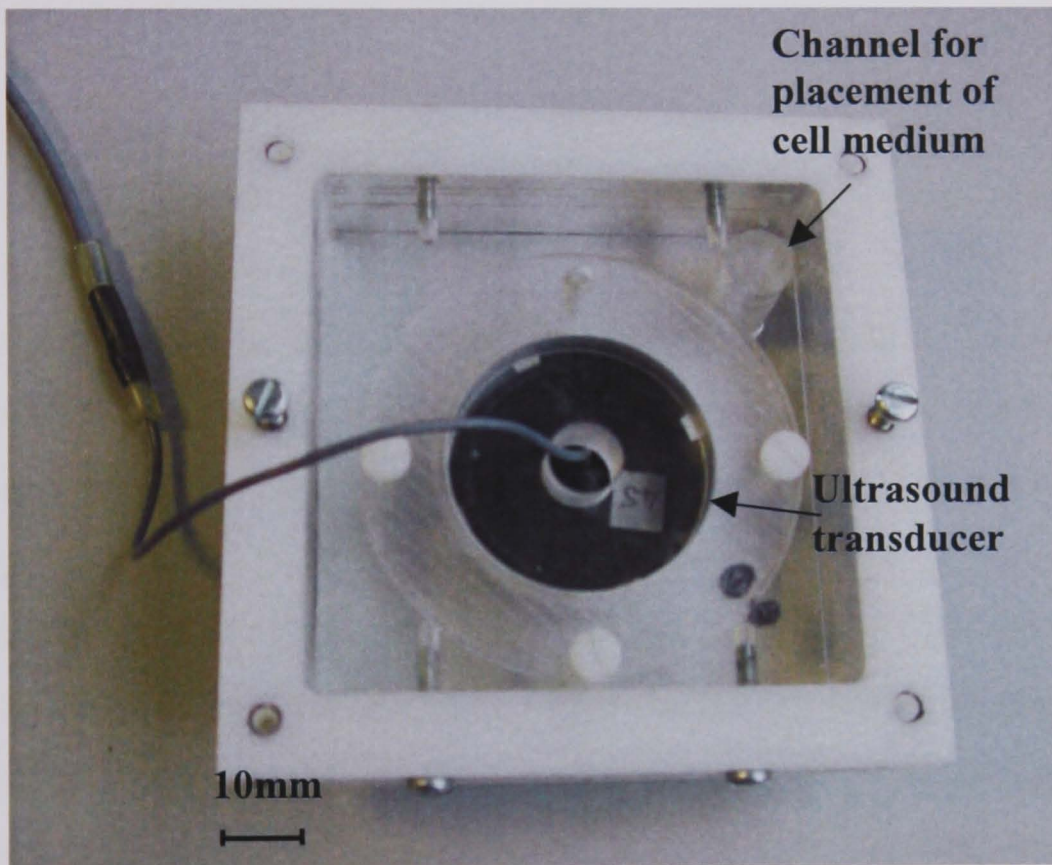


FIGURE 3.10: A) Diagram of a cross-section through the lid component of the rig and B) photo of plan view of lid component of rig.

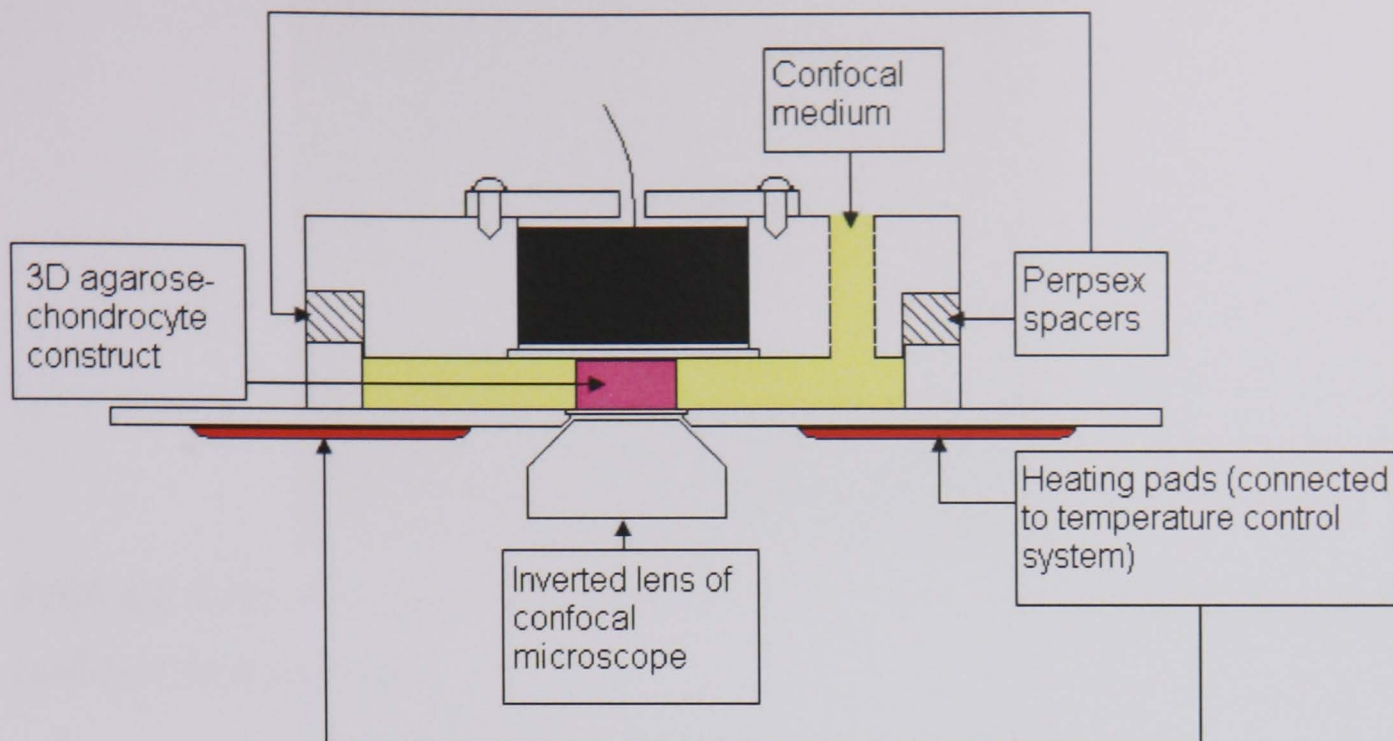


FIGURE 3.11: Schematic of confocal rig setup.

3.6.2 Preparation of 3D chondrocyte-agarose constructs for use in the microscope mounted test rig

Bovine chondrocytes were extracted and isolated as described in Section 3.2.3. Low gelling agarose (Sigma, UK) was used to prepare a final 10×10^6 cell/ml concentration in 3% (w/v) agarose suspension. A stainless steel mould was used to produce cylindrical constructs of dimensions 5mm diameter and 5mm depth (volume $98.5 \mu\text{l}$), one of which is shown in Figure 3.12. All mould components were sterilized beforehand in a clinical autoclave. A sterile glass slide was taped to the bottom surface of the mould before the chondrocyte/agarose suspension was pipetted into each well. A second glass slide was placed on top of the mould to remove excess gel and ensure correct dimensions, and all components taped together before placing the mould into a sterile 150mm diameter Petri dish (Falcon, Oxford, UK), which was subsequently placed at 4°C for 20 minutes. Once gelled, the constructs were removed from the mould using a 1ml pipette (Falcon, Oxford, UK). Each construct was placed in a 50mm Petri dish containing DMEM + 16.1% FCS and incubated overnight at $37^\circ\text{C}/5\% \text{CO}_2$, before the calcium imaging experiments were undertaken.



FIGURE 3.12: Photograph of a 5mm diameter x 5mm height chondrocyte-agarose construct on a coverslip.

3.6.3 Optimisation of microscope mounted test rig – prevention of specimen drift

The confocal rig was tested using the 3D chondrocyte-agarose constructs. A coverslip was fixed to the chamber using silicon grease, and a single construct was placed into the chamber. The lid was placed over the chamber after the 5mm spacers were positioned between them. However, two potential problems arose, both associated with construct location. When filling up the rig with ^{BF}DMEM + 16.1% FCS, previously heated to 37°C in a water bath, the construct tended to move due to movement of fluid. This makes continuous imaging of individual cells very difficult to achieve. Secondly, using the lid as the means to secure the construct proved both ineffective and also highlighted the fact that closing the lid could cause deformation of the construct, which might trigger an intracellular signalling response which could mask any effect of the pulsed ultrasound signal.

Thus, it was necessary for the constructs to be fixed in some way to the chamber of the rig. A perspex insert was designed into which the cell-agarose could be located and held in the chamber by means of a screw (Figures 3.13 and 3.15). The insert, used in conjunction with a mould for casting (Figure 3.14), enabled a 5x5x5mm cell-agarose construct to be gelled. Two 3mm diameter cylinders were drilled into the insert (Figure 3.13), so that the cell-agarose construct could be anchored in the insert, thereby stabilising the construct during the imaging period. A number of these Perspex inserts were made. The mould and insert assembly were made sterile by placing in 70% Industrial Methylated Spirit (70% IMS) and leaving it in the hood for two hours prior to use.

By holding the construct in this manner, it was now unnecessary for the lid of the rig to be in contact with the construct. Another set of Perspex spacers were used so that there was a fluid gap between the top of the construct and the lid.

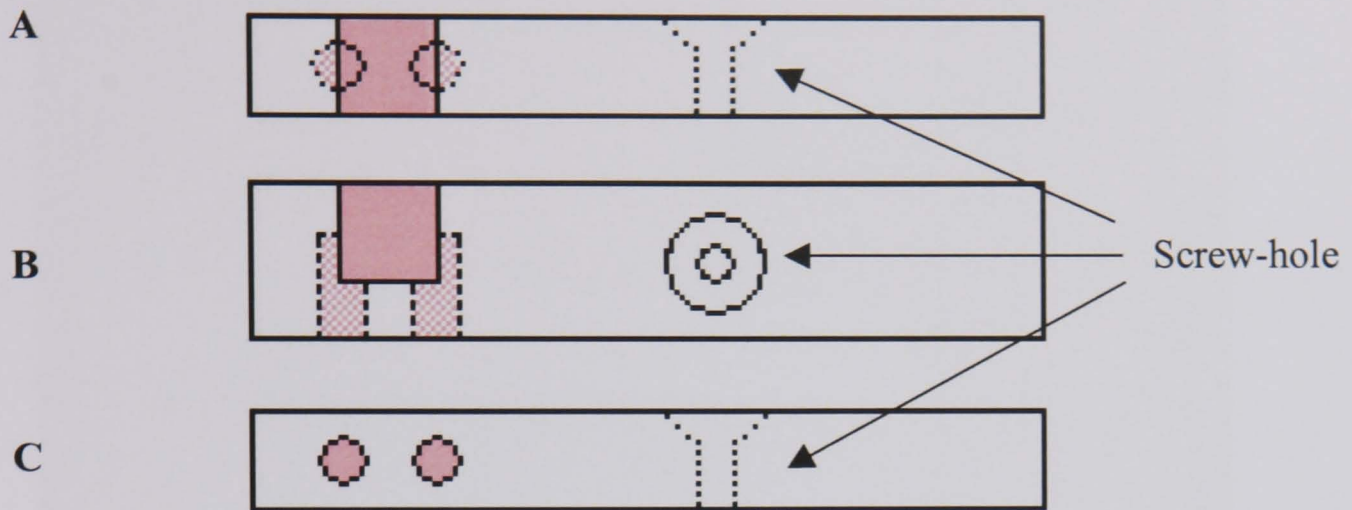


FIGURE 3.13: Construct mould/insert for the confocal rig. *A)* shows the top of the construct, *B)* side view of construct and *C)* base of the construct. A hole was made in the base of the rig chamber so that the insert could be held down by a screw. Pink denotes the 5x5x5mm chondrocyte-agarose construct and the two 5x3mm diameter 'anchors' for stabilising the construct..

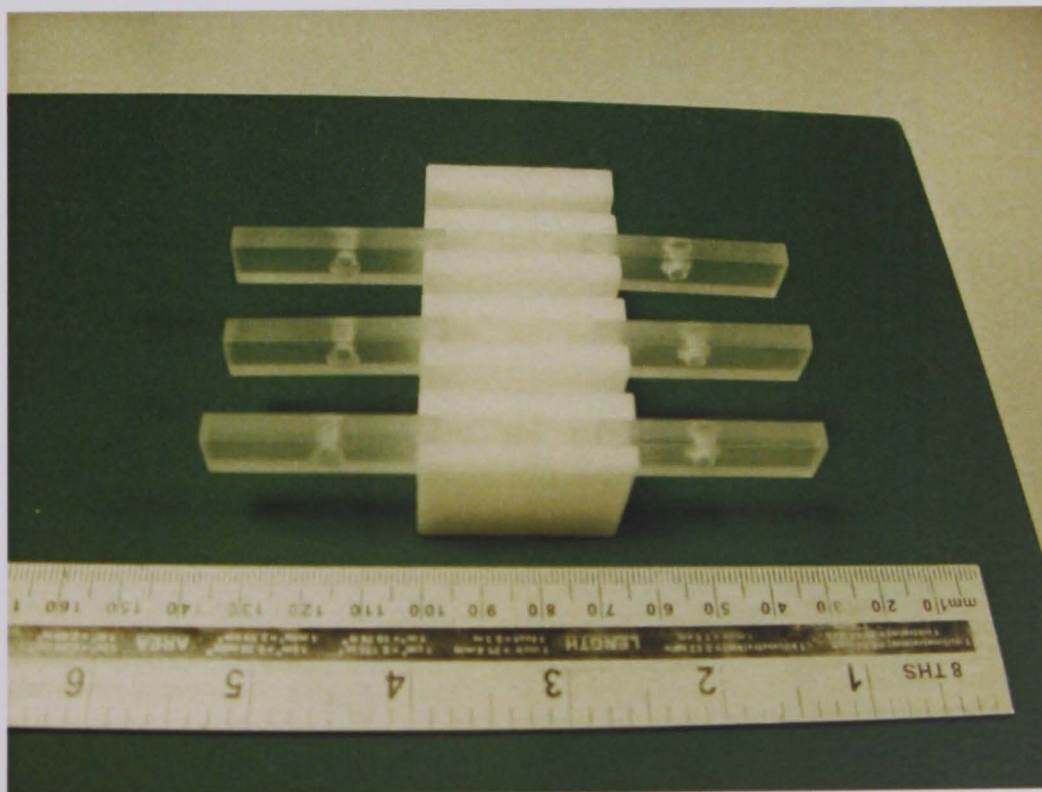


FIGURE 3.14: Perspex inserts positioned in mould for casting of cell-agarose suspension in inserts.

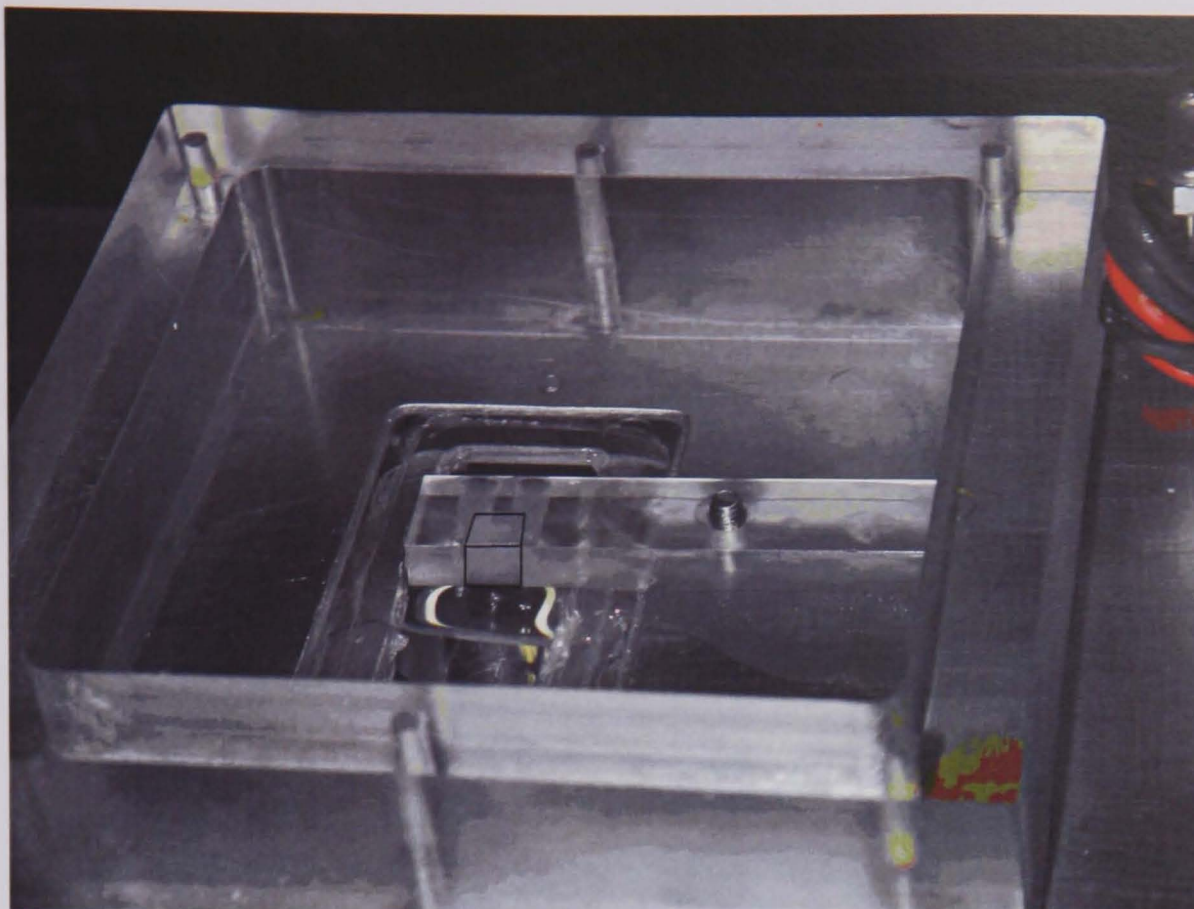


FIGURE 3.15: Photograph of construct insert, containing a 5x5x5mm cell-agarose construct (demarcated in black), in the chamber of the confocal rig.

3.7 3D model system for matrix synthesis experiments

For the matrix synthesis experiments, low gelling agarose (Sigma, UK) was used to prepare a final concentration of 4×10^6 cells/ml in 3% (w/v) cell-agarose suspension. Each well of a six-well plate was filled with cell-agarose suspension to yield a 3mm height gel using a positive displacement pipette. The gels were covered with 6.6ml of DMEM + 16.1%FCS and cultured for 24 hours in a 37°C 5% CO₂ incubator before being used in the experiments. At each prescribed experimental time-point, a 6mm diameter sterile corer was used to remove a number of cylindrical constructs from the central region of the agarose gels, in the manner shown in Figure 3.16.

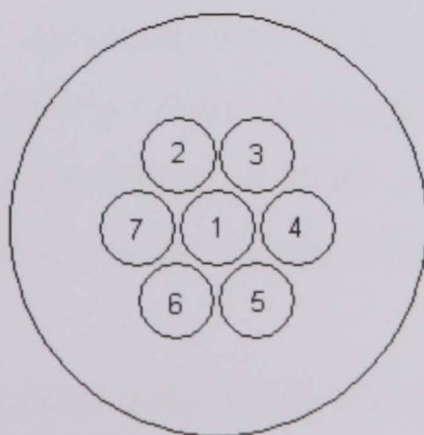


FIGURE 3.16: Schematic of well plate showing location of 6mm diameter cores removed from cell-agarose gels. Core 1: central core. Cores 2-7: peripheral cores. Well diameter is 34 mm while the underlying ultrasonic transducer is 30 mm.

3.8 Standard protocols for biochemical analysis

The following sub-sections will outline the standard methods used to analyse the 3D chondrocyte/agarose culture, as part of the investigation into the influence of PLIUS on cell metabolism.

3.8.1 Digest of chondrocyte-seeded agarose constructs

Prior to the biochemical assays, the cored cell-agarose constructs were digested to separate the chondrocytes and any associated extracellular matrix from the embedding agarose (Lee and Bader, 1997). This was achieved with a solution of papain digest buffer, made by adding 0.788g of cysteine hydrochloride and 0.403g of ethylenediaminetetraacetic acid (EDTA) (Sigma, UK) to 480ml of phosphate buffered saline (PBS) (Sigma, UK), and adjusted to pH6 before making up to 500ml with PBS.

A volume of 1ml papain digest buffer was added to each construct in a small bijoux tube and placed in a 70°C oven for 1 hr 30 minutes, samples being vortexed after 45 minutes. Samples were then cooled in a 37°C oven. 10µl agarase (1000 units.ml⁻¹, Sigma, UK), an enzyme that digests the polysaccharide backbone of molten agarose into alcohol soluble oligosaccharides, and 5µl papain (560 units.ml⁻¹, Sigma, UK), a proteolytic enzyme, were added to each construct and allowed to digest overnight at 37°C and then for an hour at 60°C. Once digested, samples could be assayed immediately or frozen at -20°C for later analysis.

3.8.2 DMB assay for total sGAG content in constructs

Digested constructs were assayed for sulphated GAG (sGAG) concentration using a spectrophotometric assay based on dimethyl-methylene blue (DMB) (Farndale *et al.*, 1982). DMB is a dye that complexes with sGAGs causing a metachromatic shift in absorbance maximum from 600 to 535nm. A solution of DMB was prepared in 1 litre of distilled water by weighing out 0.016g of DMB powder and adding 5ml ethanol, 2g sodium formate and 2ml formic acid (all Sigma, UK) before being adjusted to pH 3.0.

A set of standards were prepared using shark chondroitin 4-sulphate (Sigma, UK) at a stock concentration of 1mg.ml⁻¹, which was diluted using distilled water to concentrations of between 10 and 100µg.ml⁻¹, in increments of 10 µg.ml⁻¹. Distilled water was used as the 0 µg.ml⁻¹ standard. A 40µl volume of the standards was pipetted in duplicate into separate wells of a 96-well plate. The same volume of the digested

constructs and aspirated medium was also pipetted in duplicate in separate wells. Samples and standards were vortexed prior to pipetting to ensure that contents were well mixed. Pipette tips were changed regularly to prevent cross-contamination. A volume of 250 μ l DMB was added to each well containing the standards and samples and the 96-well plate placed into a spectrophotometer (Multiskan Ascent, Thermolifesciences, Hampshire UK) to measure the absorbance at 535nm using a programmed protocol. Absorbance values from the chondroitin sulphate standards were plotted and a linear model fitted to the data. A typical calibration curve is shown in Figure 3.17. This data was then used to calculate absolute concentrations of sGAG in each construct based on the measured absorbance values. These values were normalized to construct weight.

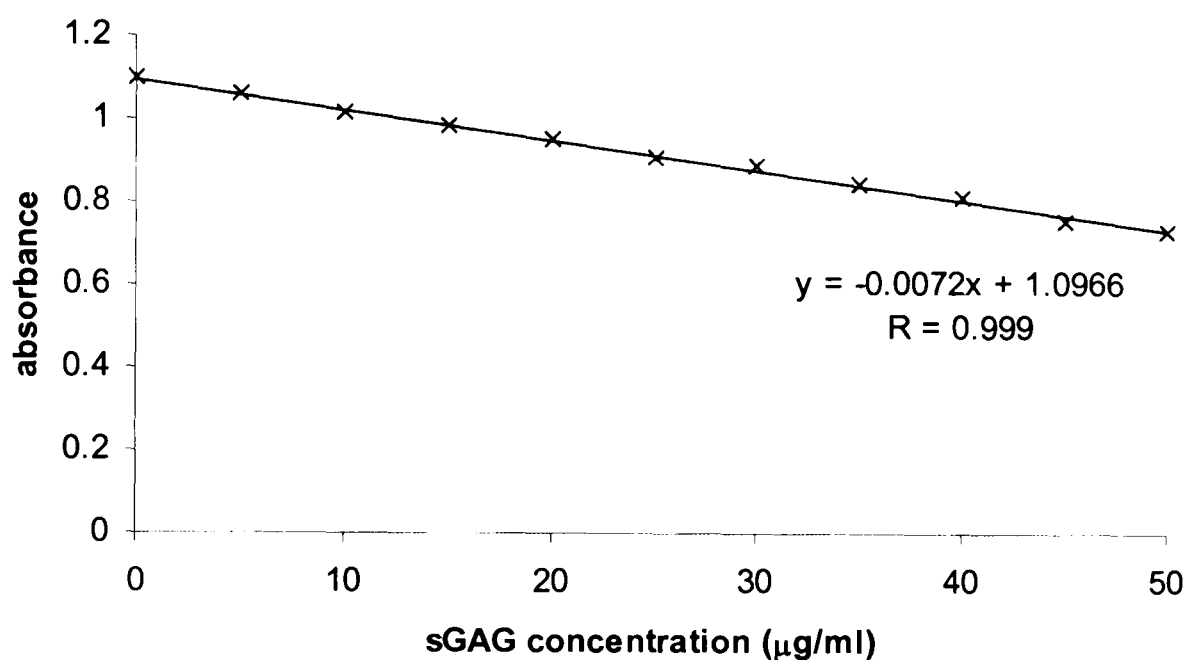


FIGURE 3.17: A typical standard curve obtained from chondroitin sulphate standards.

3.8.3 DMB assay for sGAG content in medium

Sulphated GAG content in the culture medium was assayed using DMB, in the same way as digested chondrocyte/agarose constructs described in Section 3.8.2. However, adjustments were made to the normalised spectrophotometer value of the concentration. The total sGAG values for medium obtained from the DMB assay gave a value that when corrected represented the concentration of sGAG in the 6ml of medium used to maintain the chondrocytes. However, it is invalid to associate this absolute medium value directly with the value ascertained for the construct, since the sGAG concentration contained in the medium was attributable to all the chondrocyte-agarose gel in the well. By contrast, the sGAG concentrations for the constructs were obtained

from those constructs cored from the chondrocyte-agarose gels in the well. Therefore a volume factor was used to correct for the medium values, using the following equation:

$$\text{corrected medium sGAG} = \text{total sGAG in medium} \times \left[\frac{\text{volume of construct}}{\text{total volume of agarose in well}} \right]$$

Equation 3.3

Therefore the sGAG in the medium was multiplied by a calculated value of 0.026. In addition, the total sGAG recorded at a time-point represented the cumulative of all medium collected up to that time-point, in order to correlate with the construct sGAG measured at each time-point. It is these corrected values that will be used throughout the thesis for 3D culture experiments. However, it should be noted that the sGAG measured in the medium is representative of the sGAG released by chondrocytes distributed throughout the well, whereas the constructs used for sGAG measurement originated from the central region of each well, directly above the ultrasound transducer. Therefore the final corrected sGAG content in the medium might reflect spatial differences in local ultrasound intensity.

3.8.4 Fluorimetric assay of DNA

Hoechst 33258 (Sigma, UK) is a DNA specific fluorimetric dye that is activated by binding to associated adenine-thymidine base pairs within DNA chains (Araki *et al.*, 1987). Binding causes a conformational change that emits fluorescence at 460nm. This assay uses two working solvents, namely papain digest buffer and Saline Sodium Citrate (SSC) Buffer. SSC buffer was prepared at a stock concentration of $\times 20$ by adding 87.65g of sodium chloride and 44.1g trisodium citrate to 480ml distilled water, adjusting the pH to 7.0 with 1M NaOH/ 1M HCl and making up to 500ml with further distilled water (all reagents Sigma, UK). The buffer was diluted to a $\times 2$ concentration. An equal volume of 2xSSC was added to papain digest buffer and this solution used to prepare a set of standards, using calf thymus DNA stock ($1 \mu\text{g}.\text{ml}^{-1}$, Sigma, UK). This stock solution was diluted to $20 \mu\text{g}.\text{ml}^{-1}$ and used to prepare serial double dilutions yielding concentrations of 20, 10, 5, 2.5, 1.25, 0.625 and $0.313 \mu\text{g}.\text{ml}^{-1}$. The 2xSSC: papain digest buffer was used as the $0 \mu\text{g}.\text{ml}^{-1}$ standard.

100 μl of standards were pipetted in triplicate into the separate wells of a 96-well plate and digested samples pipetted in duplicate into the remaining wells. Samples and

standards were vortexed before use and pipette tips changed regularly to prevent cross-contamination.

A working concentration of Hoechst ($1\mu\text{g}\cdot\text{ml}^{-1}$) was prepared by replacing $20\mu\text{l}$ of 20ml $2\times\text{SSC}$: papain digest buffer with $20\mu\text{l}$ of stock Hoechst 33258. $100\mu\text{l}$ of this was then added to every well containing standards and samples, and fluorescence measured at 460nm using a fluorimeter (Fluostar Galaxy, BMG Labtechnologies, Ayelsbury UK) and associated software. Fluorescence values from the Hoechst 33258 standards were plotted and a linear model fitted to the data, as shown in Figure 3.18. The standard curve was used to quantify the total DNA content in chondrocyte/agarose constructs in $\mu\text{g}\cdot\text{ml}^{-1}$. This method provided an approximation of cell number based on 7.7pg DNA per bovine chondrocyte (Kim *et al.*, 1988). DNA values were normalised to construct wet weight.

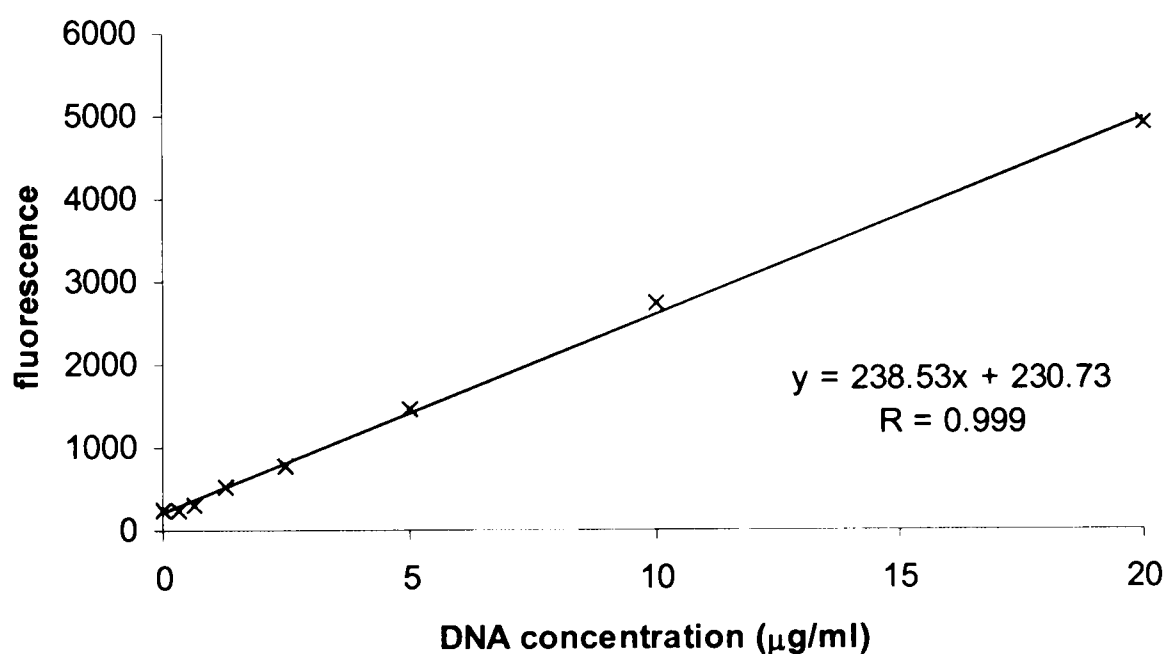


FIGURE 3.18: A typical standard curve obtained from Hoechst 33258 standards.

3.8.5 Cell viability determination

Cylindrical constructs were cut in half vertically and placed into $600\mu\text{l}$ of DMEM + 16.1% FCS supplemented with $5\mu\text{l}$ Calcein-AM and $5\mu\text{l}$ Ethidium Homodimer-2 (both Molecular Probes, UK) and incubated at 37°C for a period of 40-45 minutes. Calcein-AM is a non-fluorescent neutral membrane-permeable molecule, which enters the cytoplasm and is hydrolysed by endogenous esterase forming a highly negatively charged calcein, which is unable to diffuse out of the cell. This molecule binds with calcium and fluoresces green (wavelength $500\text{-}530\text{nm}$) when exposed to blue light (wavelength 488nm). In the absence of the enzyme, dead cells will not fluoresce.

Ethidium Homodimer-2 is a highly positively charged molecule that binds to both RNA and DNA. The molecule can only enter the cytoplasm through the compromised membranes of dead cells. By binding to the DNA, the fluorescence is increased more than 30 fold, emitting red fluorescence (wavelength 600-650nm) when exposed to green light (wavelength 568 nm).

After the incubation period, each construct was placed with its flat surface on a glass coverslip (22x40mm), and visualised using a fluorescence microscope (Nikon, UK) with a xenon lamp fluorescent light source. Live and dead cells were counted throughout the depth of the construct using a standard sampling area of 0.5 x 0.25mm, determined as the width and half the depth of a 1mm² eyepiece graticule in association with a x20 objective, using methodology developed in the host laboratory (Heywood *et al.*, 2004). Counting commenced from the top of a construct and continued down to the base to ascertain the viability in the area furthest from and closest to the PLIUS transducer, respectively. Chondrocyte viability for each sampling area was calculated using the following equation:

$$\text{Cell viability} = \left(\frac{\text{live cells}}{\text{live cells} + \text{dead cells}} \right) \times 100\% \quad \text{Equation 3.4}$$

3.9 PLIUS intensity and temporal changes in sulphated GAG content

Using the six-well plate model system set up for 3D chondrocyte-agarose culture described in Sections 3.2.2 and 3.7, a study was undertaken to determine the influence of PLIUS intensity on sGAG content, cell proliferation and cell viability in constructs over a culture period of 9 days.

3.9.1 Method

Gels were subjected to ultrasound intensities of 13, 30, 70, 100, 200 or 300 mW/cm² applied for 20 minutes once every 24 hrs, at 37°C/5% CO₂. Culture medium was changed every 2 days, and all aspirated medium was stored. At day 9, constructs were collected, weighed and assayed for total sGAG content using the DMB method (Section 3.8.2) normalised to construct wet weight, and total DNA content using the Hoescht 33258 method (Section 3.8.4). Culture medium was also assayed for total sGAG content (Section 3.8.3). The central core, labelled core 1 in Figure 3.16, was retained for cell viability measurements (Section 3.8.5).

3.9.2 Statistical analysis

Previous work in the host lab revealed data which was normally distributed for each cell activity parameter (Chowdhury et al., 2001). Accordingly, unpaired Student's t-tests were used for analysis to compare PLIUS-stimulated constructs with non-stimulated controls. A confidence level of 5% ($p < 0.05$) was considered statistically significant.

3.9.3 Results

Total sGAG content was calculated for each of the six constructs in the PLIUS groups and control groups. Values were normalised to wet weight, and means and standard deviations calculated. Figure 3.19 and Table 3.2 indicate the sGAG values in both the constructs and medium.

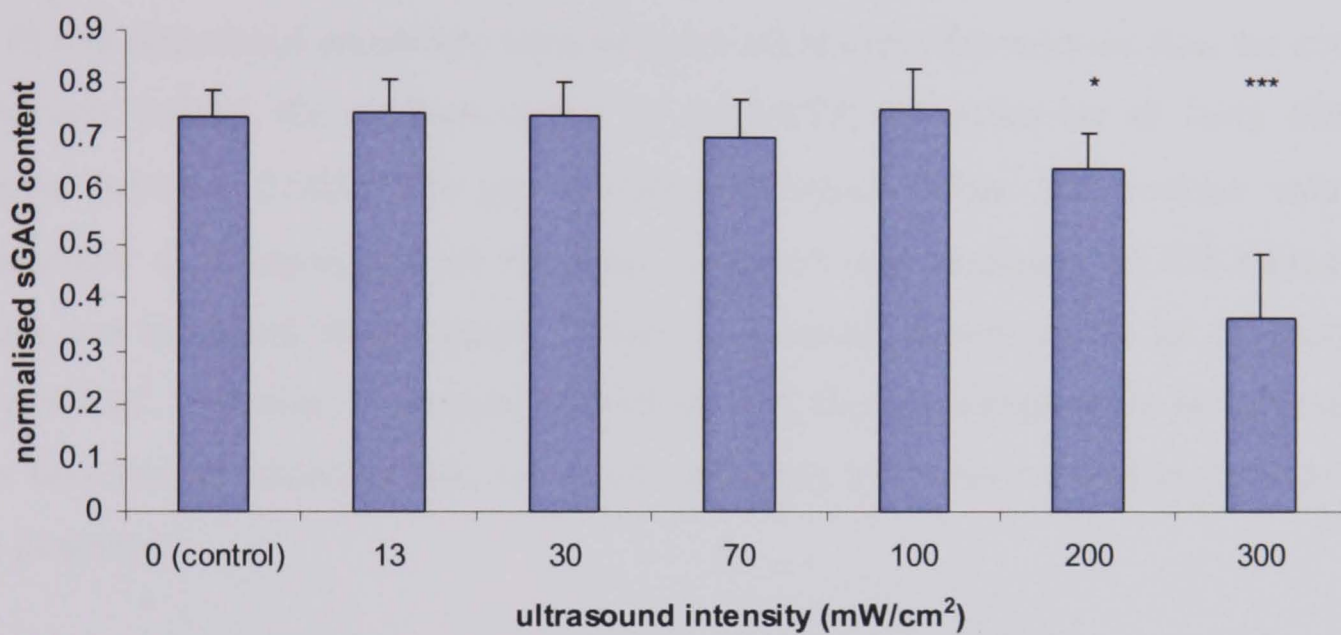


FIGURE 3.19: Effect of pulsed low intensity ultrasound (PLIUS) on total sGAG content in agarose-chondrocyte constructs. Cells were exposed to increasing PLIUS SATA intensities up to 300mW/cm² every 24 hours from day 1 to day 9. Data represents means sGAG content normalised to wet weight + standard deviation ($n=6$). Statistically significant differences are indicated at $p < 0.05$ (*) and $p < 0.001$ (***)

From Figure 3.19 it can be seen that for intensities up to and including 100mW/cm² sGAG values for PLIUS stimulated constructs are comparable to the control value ($p > 0.05$). However, at the two higher intensities, total sGAG was significantly lower than for the control ($p < 0.05$ for 200mW/cm² and $p < 0.001$ for 300mW/cm²).

TABLE 3.2: Effect of pulsed low intensity ultrasound (PLIUS) on normalised sGAG content in agarose-chondrocyte constructs. Cells were exposed to increasing PLIUS SATA intensities up to 300mW/cm² every 24 hours from day 1 to day 9. Values for construct represent mean (n=6). Values for medium (n=2) represent the cumulative of medium collected at days 2, 5, 7 and 9.

Mean normalised sGAG at day 9							
Ultrasound Intensity (mW/cm ²)	0 (control)	13	30	70	100	200	300
construct	0.740	0.749	0.744	0.705	0.756	0.647	0.364
medium	0.051	0.068	0.076	0.075	0.065	0.066	0.074
construct + medium	0.791	0.817	0.820	0.780	0.821	0.713	0.438
medium (% of total)	6.5	8.3	9.2	9.6	8.0	9.3	16.9

By examining the corrected medium sGAG values (Table 3.2), it can be seen that all of the PLIUS stimulated constructs released more sGAG into the medium than the control constructs. Indeed, the medium values for the SATA intensities are all fairly similar, ranging between 0.065-0.076 μg sGAG/ μg construct. When the medium value is represented as a percentage of the total (construct and medium), PLIUS-stimulated values are increased from control values by a small amount up to an intensity of 200mW/cm². However, in the case of 300mW/cm², this percentage value is increased to over two-fold of control values, associated primarily by the low sGAG in constructs at this intensity.

Figure 3.20 illustrates the total DNA results for the six PLIUS intensities and the control constructs. It can be seen that all DNA values for the PLIUS-stimulated constructs are lower than that of the control. Indeed, the majority of the mean values are statistically significantly lower than the control values. For example, the differences at SATA intensities of 13mW/cm² and 100mW/cm² were significant at the 5% level, whereas at intensities of 70, 200 and 300mW/cm², the differences were significant at the 0.1% level.

Using the previously mentioned conversion factor of 7.7pg of DNA per bovine chondrocyte (Kim *et al.*, 1988), the number of cells present in culture and the amount of sGAG produced per cell was estimated, as indicated in Table 3.3. It can be seen that for PLIUS stimulated systems there was a reduction in cell number, particularly at intensities of 70mW/cm² and greater. By contrast, the amount of sGAG produced per cell was generally higher for PLIUS-stimulated constructs compared to non-stimulated

constructs. The one exception to this trend was the lower sGAG produced per cell for the PLIUS intensity at 300mW/cm² (Table 3.3).

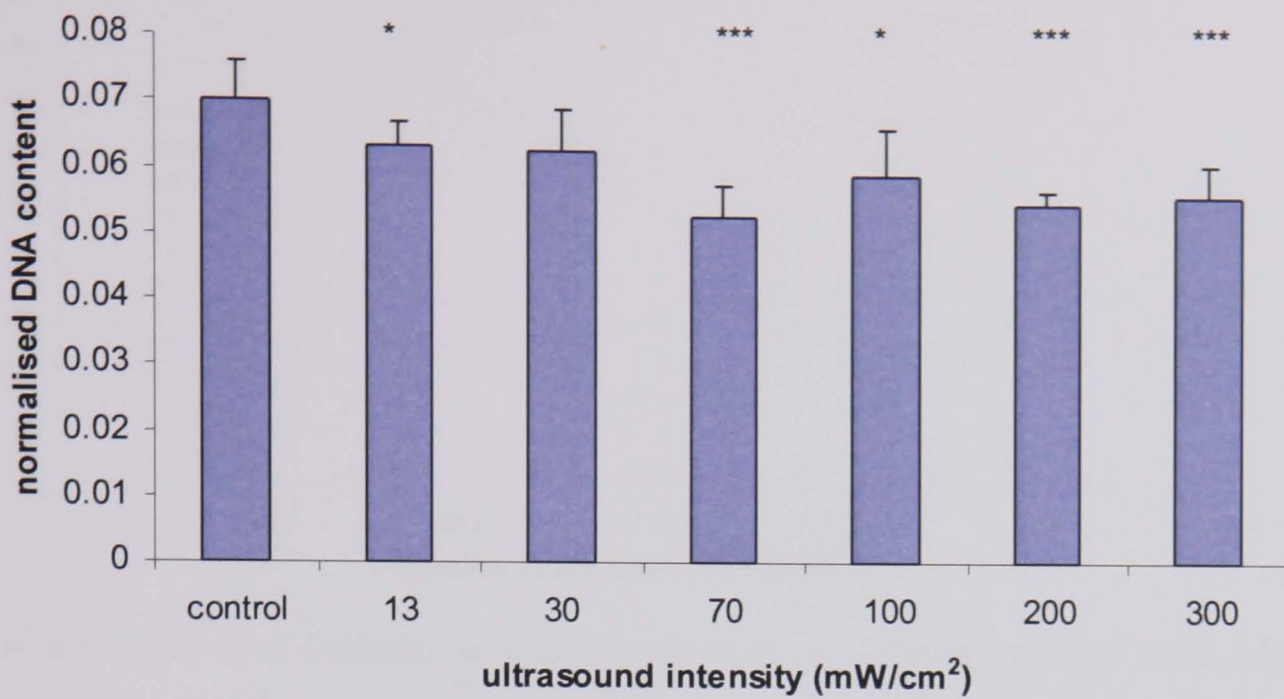


FIGURE 3.20: Effect of pulsed low intensity ultrasound (PLIUS) on DNA content in agarose-chondrocyte constructs. Cells were exposed to increasing PLIUS SATA intensities up to 300mW/cm² every 24 hours from day 1 to day 9. Data represents mean DNA content normalised to wet weight + standard deviation (n=6). Statistically significant differences are indicated at $p < 0.05$ (*) and $p < 0.001$ (***)

TABLE 3.3: Mean values of approximate cell number and amount of sGAG synthesised by each chondrocyte in agarose-chondrocyte constructs. Cells were exposed to 0, 13, 30, 70, 100, 200 or 300mW/cm² PLIUS every 24 hours from day 1 to day 9 (n=6).

	PLIUS intensity (mW/cm ²)						
	0	13	30	70	100	200	300
Cell number (x 10 ³)	908	822	811	682	765	711	723
sGAG produced/cell (g x 10 ⁻¹⁰)	0.87	1.00	1.01	1.14	1.07	1.00	0.61

Cell viability results, as summarised in Figure 3.21, showed that for both control and PLIUS-stimulated constructs of SATA intensities 13-100mW/cm², cell viability was maintained at greater than 85% throughout the depth of the construct. However, at a SATA intensity of 200mW/cm², a decrease in viability to approximately 60% was recorded. By contrast, a significant loss of cell viability was evident in the constructs subjected to 300mW/cm². It is evident that the values decrease with distance from the top of the construct. Thus in the bottom third of the construct, adjacent to the PLIUS transducer, viability values were less than 5% at a SATA intensity of 300mW/cm².

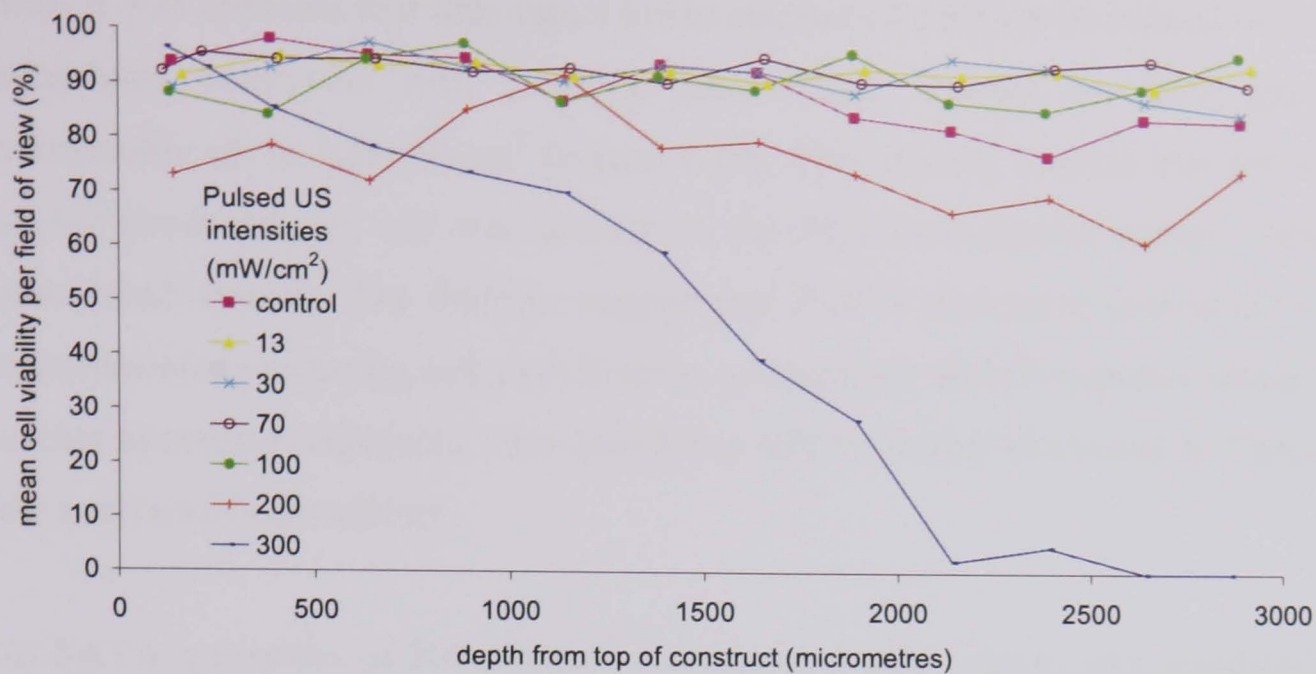


FIGURE 3.21: Cell viability in agarose-chondrocyte constructs at 9 days of culture. Cells were exposed to increasing PLIUS SATA intensities up to 300mW/cm² every 24 hours from day 1 to day 9. Values represent mean (n=6).

3.9.4 Discussion

The results of the study generally indicate that the application of PLIUS to chondrocytes seeded in 3D agarose constructs had no statistically significant effect on sGAG synthesis and cell proliferation over a nine day culture period at intensities up to and including 100mW/cm². Indeed, stimulated chondrocytes remained viable (Figure 3.21) and were able to produce comparable amounts of sGAG when compared to chondrocytes in non-stimulated constructs (Figure 3.19 and Table 3.2).

Table 3.2 indicates that PLIUS appears to increase the amount of sGAG released from the agarose constructs into the medium. This was evident at all intensities, suggesting that the pressure waves resulting from the ultrasound were promoting transport of sGAG molecules from the construct into the medium. However there was no systematic trend to suggest that sGAG levels in the medium increased with increasing PLIUS intensity.

The DNA content with chondrocyte-agarose constructs was measured at day 9 (Figure 3.20). The total DNA content in constructs was significantly lower in PLIUS-stimulated culture than control at all intensities, with the exception of the relative low intensity of 30mW/cm². From the results shown in Figure 3.20 and Table 3.3, it appears that PLIUS inhibits cell proliferation over the nine day period, particularly at higher SATA

intensities. However, when total sGAG content was normalised to cell number (Table 3.3), it was apparent that although a lower amount of cells are contained in the PLIUS-stimulated constructs than controls, total sGAG content for both groups were comparable up to $100\text{mW}/\text{cm}^2$ (Figure 3.19). This finding implies that the amount of sGAG produced per cell was greater in the PLIUS-stimulated groups than in non-stimulated controls. The findings suggest that PLIUS stimulated individual cells while simultaneously reducing cell proliferation, giving a net sGAG response which is similar to that in control constructs. This possibility will be further examined in Chapter 4 with the analysis of cell activity.

At SATA intensities of $200\text{mW}/\text{cm}^2$ and above, sGAG content was significantly lower than the control value (Figure 3.19). The viability results displayed in Figure 3.21 show that at these PLIUS intensities cell viability is severely compromised. However, the total DNA results (Figure 3.20) did not show the extent of cell death seen at 200 and $300\text{mW}/\text{cm}^2$. This can be attributed to the fact that the Hoescht 33258 used for the assay binds to associated adenine-thymidine base pairs within DNA chains, regardless of the status of the cell viability.

In many of the therapeutic and surgical applications of ultrasound, their effectiveness involves the generation of tissue heating, such as hyperthermia treatment and tissue ablation (Section 2.5.6). Therapeutic levels of ultrasound ($<10\text{W}/\text{cm}^2$) are used in cancer therapy, sometimes in conjunction with drug delivery (Feril *et al.*, 2002; Lagneaux *et al.*, 2002). Along with heat, cavitation (Section 2.5.8.2) has been proposed as a non-thermal effect of therapeutic ultrasound in cancer treatment, leading to mechanical shear stress, increased cell permeability and production of free-radicals (Tabuchi *et al.*, 2007; Feril and Kondo, 2005). It is well established that at high intensities cell lysis is induced, whereas at lower intensities apoptosis is the predominant mechanism of cell death (Feril *et al.*, 2005). A wide variety of ultrasound signals have been examined in studies using cell suspensions of human leukaemia cell lines (Feril *et al.*, 2002, 2003, 2005; Lagneaux *et al.*, 2002; Tabuchi *et al.*, 2007). Feril and colleagues found that non-thermal PLIUS treatment (1 MHz resonant frequency, 100Hz PRF, 1 minute) induced apoptosis at SATA intensities of greater than $200\text{mW}/\text{cm}^2$ (2005, Tabuchi *et al.*, 2007). Although the PLIUS parameters used in the present chapter (namely 1.5 MHz resonant frequency, 1 kHz PRF, 20 minutes) are different from those utilised by Feril and colleagues, it appears likely that PLIUS at

intensities as high as 200mW/cm^2 and 300mW/cm^2 can cause permanent damage leading to cell death in the chondrocyte-agarose constructs. This could be caused by a combination of heating and non-thermal effects. Progressive decrease in cell viability with increasing proximity to the well plate surface was demonstrated for 3D cultures exposed to 300mW/cm^2 (Figure 3.21). The lowest values for cell viability are evident within 1mm of the culture well plastic and the underlying ultrasound transducer. This suggests that absorption heating of the transducer and/or the plastic well plate may be the primary cause of cell damage. Any heat incurred at the base of the 6-well plate would dissipate through the construct towards the construct/medium interface. Accordingly, cells located closer to the medium would be less affected and would more likely maintain their viability levels.

Another factor to consider when examining the viability data was the availability of nutrients for the chondrocytes from the medium. The bioreactor arrangement was such that diffusion of nutrients could only occur via the top surface of the agarose gel; thus the diffusion distance was considerably greater for chondrocytes towards the bottom of the constructs. A study by Heywood *et al.* (2004) revealed that the optimum conditions for 3D chondrocyte culture to maintain high viability throughout the depth of a construct required a volume of 6.4ml per million cells. The present arrangement of the 3D-culture system precluded the use of such an equivalent high volume. Volumes of up to 10ml were initially used in preliminary experiments; however, it proved difficult to prevent the occurrence of infection due to spillage of medium, and a volume of 6.6ml was used. Accordingly, with a prescribed volume of 6.6ml, chondrocyte viability was maintained in the absence of PLIUS.

Studies in conjunction with Smith and Nephew Research Centre (York, UK) have investigated the attenuation and heating properties of the Exogen signal (1.5 MHz resonant frequency, 1 kHz PRF, 30mW/cm^2 SATA intensity), which can shed some light on the physics of the signal in relation to the set-up of the experimental system.

Attenuation studies were undertaken using equipment at the Physics Department of the University of Leeds (Chan *et al.*, 1978; Dyer *et al.*, 1992). The attenuation co-efficient of the well-base of a polystyrene six well plate was calculated to be 1.71 dB/cm/MHz. This value is equivalent to that measured in muscle, non-mineralised fibrocartilage and articular cartilage (Dowsett *et al.*, 1998), and provides a low level of attenuation when

compared to mineralised fibrocartilage, tendon and bone (Sano *et al.*, 2006) (Table 2.1). The thickness of a well-base was measured as 1.367mm. Therefore attenuation in the well base whilst using the Exogen signal could be estimated as 0.35dB. The relatively low level of attenuation seen in the well-plate plastic suggests that the effect of the higher PLIUS intensities on viability is unlikely to be caused by differential heating of the plastic well base.

Measurements were also made to investigate the temperatures encountered within the in-vitro apparatus in conjunction with the PLIUS transducer. Studies undertaken at the National Physical Laboratories, Teddington, used an infrared camera to examine the self-heating of the base of empty wells of a 6-well plate coupled to an ultrasonic transducer at room temperature. After 10 seconds of PLIUS, the temperature rose by 1.6°C, with a 10°C increase after 180 seconds. These temperatures were concentrated in the centre of the transducers. The actual transducers are approximately 22mm in diameter, and are encased in a thermosetting resin material of diameter 30mm. It is important to note that in a cell culture system, energy would be transferred from the transducer into the biological system. Thus, the high temperatures seen here are likely demonstrative of the high attenuation of ultrasound in air (Table 2.1).

Other experiments, involving gradually filling a PLIUS-stimulated well with water, indicated variation in the temperature rise occurring in the water with depth (Figure 3.22). One possible explanation for this temperature variation is that incident PLIUS is being periodically reflected at the interface of the well culture plastic and reflecting back into the transducer, interfering with its subsequent oscillations and therefore reducing the power output and causing increased heat production.

When Figure 3.22 is compared to the results of the standing wave study undertaken in Section 3.5.2 (Figure 3.7), some similarity can be seen. Due to the lack of data from Figure 3.23 (compared with that in Figure 3.7), a definitive conclusion cannot be made with respect to the periodicity of the temperature change cycle. However, it does appear that the wavelength of the temperature rise phenomena may well be approximately 0.5mm, as was seen in the standing wave study. Taking into consideration that both phenomena occur due to attenuation of the incident ultrasound signal, it is likely that that two do in fact correlate in terms of periodicity.

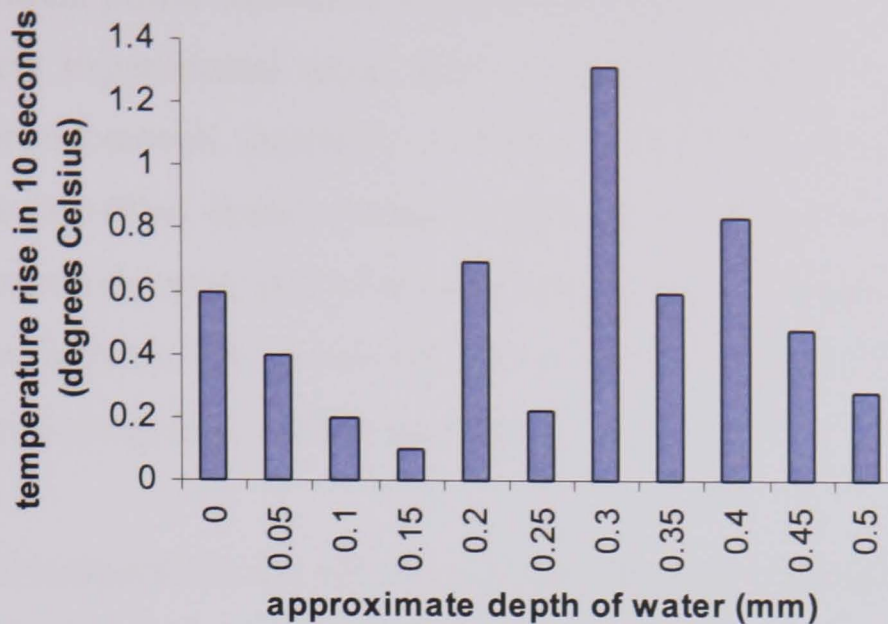


FIGURE 3.22: Graphical representation of temperature rise (after 10 seconds) with increasing depth of water placed in the well of a six well plate being stimulated with PLIUS. (Data adapted from that obtained courtesy of Smith and Nephew Research Centre, York, UK).

Researchers at Smith and Nephew investigated different well-plate configurations involving the use of water baths and tilting of the transducer (data not presented). Tilting of the transducer caused a reduction in recorded temperature. Of note was that when the transducer was positioned 8mm from the well in a water bath, the initial heat rise was approximately three times lower than that seen in the original configuration but, after one minute, the rate of increase was equivalent to that obtained when no water bath was used.

Kopakala-Tani *et al.* (2006) employed a 110mm water gap between ultrasound transducers and bovine chondrocytes cultured in monolayer, with the belief that increased water mass would reduce the temperature changes. However, after a ten minute exposure to an average intensity of $580\text{mW}/\text{cm}^2$ the temperature rise in the plastic bottom of the well plate was found to be 6.9°C . Observation of Figure 3.6 indicates that for a $30\text{mW}/\text{cm}^2$ transducer, the intensity seen in an equivalent distance in water is three times that of the incident intensity, namely between 80 and $90\text{mW}/\text{cm}^2$. This implies that there is no characteristic reduction of PLIUS intensity with distance, which would have an influence on heating effects.

Further investigations by Smith and Nephew indicated that the PLIUS power output decreased with increasing surrounding temperature. Between 21°C and 37°C it was

found that the incident power decreased at approximately 0.7% per degree. This implies that for the present experimental setup, there was approximately a 10% reduction in power at the transducer/well interface. A further experiment showed that a highly reflecting surface (air-filled foam) caused a high power output from the transducer, which was approximately twice that of an absorbing surface. Voltage changes measured in the transducer implied that these reflections can interfere with the transducer, changing the acoustic impedance of the material.

The wide range of temperature and attenuation investigations highlighted in this chapter show that significant changes can occur in the ultrasound signal when used in conjunction with a cell culture system. It is evident that variables such as distance from transducer, the temperature of the system, depth of fluid and the properties of material interfaces all play a major role in the final incident PLIUS power due to the attenuation of the ultrasound, a combination of scattering in heterogeneous media, reflection at interfaces and conversion of energy to heat (absorption). Indeed, it may be concluded that multiple reflections interfering with the transducer output may be a greater factor than the heat produced by absorption.

The system used in this thesis employs PLIUS coupled to the base of the transducer plate. The absence of a fluid gap between the two implies that any heat produced by the transducer would be directly transmitted to the well contents. There is likely to be a great deal of reflection and absorption in the chondrocyte agarose system, due to factors such as:

- The incidence of regular temperature variations and standing waves (periodicity ~0.493 mm in water)
- The heterogeneous nature of the cell culture system and the depths of each component
- The intensity of ultrasound used (and its efficiency)
- Heating of the ultrasound transducer

Although these attenuation effects are very difficult to interpret and display, the results of the study undertaken in this chapter indicates that PLIUS does not have an adverse effect on cell metabolism and sGAG synthesis of chondrocytes in the present 3D culture system, within a specified SATA intensity range.

3.10 Conclusion

From the above results and discussion (Sections 3.9.3 and 3.9.4 respectively), it appears that although PLIUS causes a decrease in chondrocyte proliferation, viability was maintained at over 85% throughout the depth of both control and PLIUS-stimulated constructs over a 9 day period for SATA intensities up to $100\text{mW}/\text{cm}^2$. Moreover, as there was no significant difference between control and PLIUS stimulated constructs in relation to sGAG content for these intensities, there was some indication that PLIUS may stimulate individual cells in the system, as the amount of sGAG produced per chondrocyte was greater for the PLIUS stimulated constructs than controls (significant at 70 and $100\text{mW}/\text{cm}^2$). However, cultures exposed to the higher intensity PLIUS of 200 and $300\text{mW}/\text{cm}^2$ were adversely affected causing cell death. From the extensive investigations completed in conjunction with Smith and Nephew (York, UK) and NPL (Teddington, UK), it is likely that the mechanism by which the PLIUS exerts cell death at higher intensities is due to a high degree of acoustic reflections in the system which interfere with the PLIUS signal and cause self-heating of the transducer, which transmits this heat to the substrate i.e. the well plate/culture interface. Cell death is unlikely to be caused by attenuation of the PLIUS signal in the well culture plastic/agarose as these materials only produce low attenuation.

The possible beneficial effect of PLIUS on sGAG synthesis in chondrocyte-agarose culture was shown for intensities up to $100\text{mW}/\text{cm}^2$ over a 9 day period. In order to investigate this further, temporal studies will be carried out to examine the effects of selected PLIUS intensities on cultures at various time-points over a 20 day period.

Chapter 4

Stimulation of Proteoglycan Synthesis by Pulsed Low Intensity Ultrasound in a 3D Agarose System

4.1	Introduction	98
4.2	Materials and methods	99
4.2.1	Preparation of chondrocyte-agarose constructs	99
4.2.2	PLIUS regime	99
4.2.3	Temporal changes in sGAG and DNA content	99
4.2.4	Incorporation of SO ₄ into sGAGs	100
4.2.5	Incorporation of [³ H]thymidine into DNA	101
4.2.6	Statistical analysis	102
4.3	Results	102
4.3.1	Total sGAG content	103
4.3.1.1	The effect of a SATA intensity of 30mW/cm ²	103
4.3.1.2	The effect of a SATA intensity of 100mW/cm ²	109
4.3.2	Total DNA content	113
4.3.3	Cell activity	116
4.3.4	SO ₄ incorporation	117
4.3.5	[³ H]thymidine incorporation	120
4.4	Discussion	124

4.1 Introduction

Previous studies examining the effects of pulsed low intensity ultrasound (PLIUS) on a variety of cell types in both monolayer and 3D model systems have shown that ultrasound influences cellular mechanisms (Dinno *et al.*, 1989; Pilla *et al.*, 1990; Parvizi *et al.*, 2002; Naruse *et al.*, 2003; Schumann *et al.*, 2006). In particular, studies using chondrocytes in both monolayer and gel systems have suggested that PLIUS may stimulate sulphated glycosaminoglycan (sGAG) synthesis (Parvizi *et al.*, 1999; Nishikori *et al.*, 2001)

This chapter tests the hypothesis that PLIUS stimulates the synthesis and elaboration of sGAG and that this response is influenced by the intensity of the ultrasound. Based on the developmental and intensity experiments in Chapter 3, an optimized chondrocyte-seeded agarose model system was exposed to PLIUS at intensities 30mW/cm^2 and 100mW/cm^2 over a period of 20 days. At specific times throughout this culture period biochemical assays were employed to quantify sGAG synthesis and cell proliferation.

4.2 Materials and methods

4.2.1 Preparation of chondrocyte-agarose constructs

Chondrocytes were isolated from bovine articular cartilage and seeded in agarose constructs according to the standard procedures described in Section 3.2. To review briefly, articular cartilage was digested with pronase and collagenase and the isolated chondrocytes seeded at a final concentration of 4×10^6 cells.ml⁻¹ in 3% (w/v) low gelling agarose (Sigma, UK). Each well of a six-well plate was filled with cell-agarose suspension to yield a 3mm height gel using a positive displacement pipette. The agarose was gelled at 4°C, then covered with 6.6ml of DMEM + 16.1% FCS and maintained at 37°C / 5% CO₂ for a period of up to 20 days. Medium was changed every 2-3 days.

4.2.2 PLIUS regime

Each sample of a six-well plate was stimulated with PLIUS by placement of the plate on the six transducers with the use of coupling gel and manipulation of the plate to eliminate any air bubbles (Figure 3.2). Constructs were incubated for a period of 24 hours before stimulation with PLIUS at one of two SATA intensities, 30mW/cm² and 100mW/cm², such that:

- Three separate chondrocyte isolations were performed at 30mW/cm², denoted by 0504, 1204 and 0305.
- Two chondrocyte isolations were performed at 100mW/cm² studies, denoted 0805 and 1005.

The six wells were exposed to one 20 minute period of PLIUS every 24 hours from day 1 to day 20 (where day 0 is the day of seeding into agarose).

- For the two isolations, 1204 and 0305, a subsequent group of specimens was exposed to 30mW/cm² PLIUS using a modified ultrasonic box, which enabled an additional set of 6 well plates to be exposed to a 20 minute period of PLIUS every 12 hours (twice a day).

For each experiment, control constructs remained non-stimulated in separate six-well plates.

4.2.3 Temporal changes in sGAG and DNA content

At days 1, 4, 8, 11, 15, 19, medium was removed from the wells and replaced with fresh medium supplemented with 10 µCi/ml ³⁵SO₄ and 1 µCi/ml [³H] thymidine (both Amersham Biosciences, UK) for a 24 hr period. This enabled the assessment of the rate of sGAG production and chondrocyte proliferation, respectively. After the 24 hour

incubation period the medium was removed and stored, and 6mm diameter constructs (n=6) were removed from the specimen in the well using a sterile corer in the manner described in Section 3.7. At day 1, constructs had not been exposed to PLIUS. At all other time-points, both constructs and medium were harvested from the well exposed to PLIUS and from the corresponding non-stimulated controls. All constructs were weighed and frozen. At the end of the experiment constructs were digested for the biochemical assays, as detailed in Section 3.8.1, with total sGAG content and total DNA content determined using the DMB and Hoescht 33258 methods, respectively. The standard protocols for incorporation assays are detailed below.

4.2.4 Incorporation of SO₄ into sGAGs

DMEM+16.1%FCS was supplemented with 10 μ Ci/ml ³⁵SO₄ and used to maintain chondrocyte/agarose constructs for the prescribed period, after which both medium and constructs were collected. Incorporation of SO₄ into newly synthesized GAG was determined in both digested agarose/chondrocyte constructs and the collected media, using the alcian blue precipitation method (Masuda *et al.*, 1994). Alcian blue is a cationic dye that binds to sulphate groups on the GAG chains of proteoglycan. The buffers in this assay are detailed in table 4.1.

75 μ l of acetate buffer, 25 μ l of sample and 150 μ l of alcian blue solution were added to individual wells of a multiscreen plate (0.45 μ m pore filter, Millipore, UK). The plate was agitated for 1 hour at room temperature, vacuum aspirated and the wells washed three times with acetate buffer supplemented with 0.1M sulphate. This washing step was designed to remove non-incorporated SO₄ molecules and unbound dye. The base of the plate was removed to expose the filters, which were allowed to dry at 37°C for 1 hour and punched out into scintillation vials, using a multiple-punch assembly (Millipore, UK). A volume of 0.5ml guanidine hydrochloride solution was added to each vial and agitated for 1 hour to dissociate and solubilise the SO₄-labelled proteoglycan molecules bound to the alcian blue. After this period 4ml of scintillation fluid (Ultima Gold MV, Perkin Elmer, USA) was added to the vials. Additionally, 10 μ l aliquots of original medium were measured out into separate scintillation vials with 4ml of scintillating fluid added, in order to provide a total measure of incorporation rate. All vials were placed into a scintillation counter (Wallac 1409 DSA, Perkin Elmer, USA) and a prewritten protocol used to measure radioactive counts.

TABLE 4.1: Details of buffers and reagents used for alcian blue assay for the measurement of SO_4 incorporation.

Buffer	Composition	Quantity	Source
Acetate Buffer (pH5.8)	Sodium Acetate	2.05g (0.05M)	Sigma, UK
	Magnesium Chloride.6H ₂ O	8.64g (0.085M)	Sigma, UK
	Distilled Water	500ml	
Alcian Blue	Alcian Blue 8GX	0.2g (0.2% w/v)	Sigma, UK
	Acetate Buffer (pH5.8)	100ml	
Acetate Buffer with 0.1M Sulphate	Sodium Acetate	2.05g (0.05M)	Sigma, UK
	Magnesium Chloride.6H ₂ O	5.08g (0.05M)	Sigma, UK
	Sodium Sulphate	7.10g (0.1M)	Sigma, UK
	Distilled Water	500ml	
4M Guanidine Hydrochloride in 33% Propan-2-ol	Guanidine Hydrochloride	190.6g	Merck, UK
	Propan-2-ol	166.7ml	Merck, UK
	Distilled Water	333.3ml	

The incorporation rate of SO_4 into newly synthesized GAG was calculated using the following equation (Lee *et al.*, 1998):

$$SO_4 \text{ incorporation} = \frac{(\text{bound counts of construct and medium}) \times 0.81}{(\text{total counts in control medium}) \times (h) \times \text{total DNA}} \times 1000$$

Equation 4.1

where:

- = hours that chondrocyte/agarose construct was exposed to the radiolabelled medium
- Total DNA = amount of DNA in μg in cells (calculated using Hoechst 33258 DNA assay)
- 0.81 = Concentration of SO_4 in labelled medium (mM)

Units of incorporation: $\mu\text{M } SO_4/\text{h}/\mu\text{g DNA}$.

4.2.5 Incorporation of [³H] thymidine into DNA

Thymidine is one of the four nucleotides which make up DNA. Radiolabelled [³H] thymidine incorporation into newly-synthesised chondrocyte DNA was measured by the trichloroacetic acid (TCA) precipitation method (Lee and Bader, 1997). TCA precipitates nucleic acid polymers longer than approximately 20 nucleotides, resulting

in a separation of the radiolabelled nucleotides incorporated into nucleic acid from the unincorporated label.

Solutions of 10% and 20% (w/v) TCA were prepared using TCA powder (Sigma, UK) and dH₂O. These were stored and used at 4°C in order to prevent dissolution of precipitated nucleotides. 100µl 10%TCA was pipetted into each well of a multiscreen plate (0.45µm pore filter, Millipore, UK) before being vacuum aspirated. 100 µl 20%TCA was then added to each well, prior to 100µl of digested construct sample and a further 100µl 20%TCA. The plate was agitated for 1 hour at room temperature, the wells then vacuum aspirated and washed once with 100 µl 10%TCA to remove excess non-incorporated [³H] thymidine. The base of the plate was removed to expose the filters, which were allowed to dry at 37°C for 1 hour, before being punched out into scintillation vials using a multiple-punch assembly (Millipore, UK). A volume of 0.5ml 0.01M potassium hydroxide solution was added to each vial and agitated for 2 hours to dissociate and solubilise the [³H] thymidine labelled DNA bound to the TCA. After this period, 4ml of scintillation fluid was added to the vials and placed into a scintillation counter and a prewritten protocol used to measure radioactive counts. The incorporation of [³H] thymidine into newly synthesized DNA was calculated by dividing the counts per minute by the amount of DNA ascertained from the Hoescht 33258 assay, giving units of incorporation in CPM/µg DNA.

4.2.6 Statistical analysis

Previous work in the host lab revealed data which was normally distributed for each cell activity parameter (Chowdhury et al., 2001). Accordingly, unpaired Student's t-tests were used to compare PLIUS-stimulated constructs with non-stimulated controls at each time-point. A confidence level of 5% (p<0.05) was considered statistically significant.

4.3 Results

The following results display the total sGAG content, total DNA content, SO₄ incorporation rate and [³H] thymidine incorporation following stimulation using PLIUS intensities of 30mW/cm² and 100mW/cm². It should be noted that those studies involving two cell isolations, 0504 and 0805, were terminated at day 16, due to a bacterial infection beyond that time point.

4.3.1 Total sGAG content

4.3.1.1 The effect of a SATA intensity of 30mW/cm²

Total sGAG content was estimated for each of the six constructs in both the PLIUS and control groups, normalized to weight wet, and a mean value and standard deviation determined. The results for the three 30mW/cm² isolations 0504, 1204 and 0305 are presented in Figure 4.1. Table 4.2 summarises the statistical data relating to the differences between the two stimulation groups and the non-stimulated control, for each time point. The corresponding data for sGAG released into the medium from the three isolations is presented in Figure 4.2 and Table 4.3.

Figure 4.1 shows an increase in total sGAG content over the 20 day culture period for agarose constructs from the control group and the groups exposed to once-daily ultrasound (termed PLIUSx1), and twice-daily ultrasound (termed PLIUSx2). Close examination of the results generally reveal few differences and no systematic trends in the mean total sGAG between the control and PLIUSx1-stimulated constructs. Indeed, Table 4.2 indicates only two cases of significant up-regulation of sGAG for stimulated constructs and two cases of significant down-regulation, from a possible seventeen time-points over the duration of the three isolations.

By contrast, the results for the two isolations in which constructs were stimulated twice per day, indicated that this regimen (PLIUSx2) consistently yielded the lower values for total sGAG. Indeed in 8 out of the 12 comparisons, PLIUSx2 yielded statistically significantly lower values of total sGAG in the construct compared to control values (Table 4.2). Indeed, there was only one comparison in which PLIUSx2 was significantly higher than the control value, namely day 5 values for isolation 1204. Comparison of the two stimulation groups revealed that the PLIUSx1 group generally yielded significantly higher mean total sGAG values (Figure 4.1B and C). The only exception was for isolation 0305 at day 9, where PLIUSx2 yielded a higher sGAG content than the PLIUSx1 group ($p < 0.05$, Figure 4.1C). However, this difference was only of the order of a few micrograms, and the other experimental data for total sGAG values with PLIUSx2 revealed significantly lower values than for the other two groups ($p < 0.01$ or $p < 0.001$, Figure 4.1C and Table 4.2).

Figure 4.2 presents the mean total sGAG released into the medium. The medium values for each time point are cumulative, so that comparisons could be made between sGAG

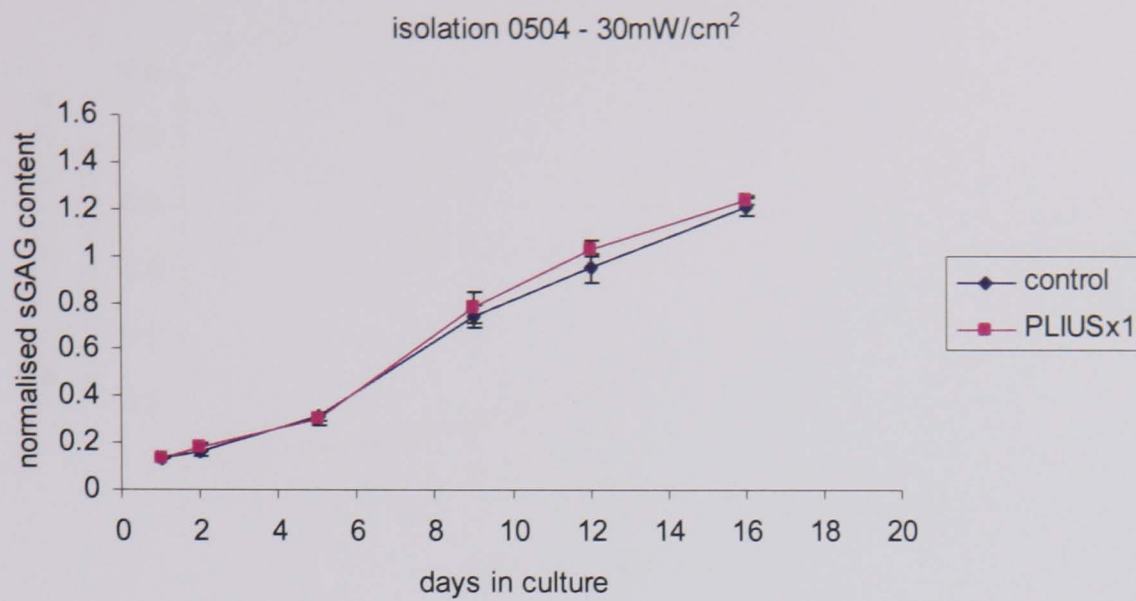
content in the constructs and medium at each time-point. It can be seen that there is a fairly constant rate of sGAG release over time. Generally, for the three separate isolations, the sGAG values for the medium at each time point were comparable for both experimental and control groups. However, beyond 12 days of culture, the differences in sGAG were more noticeable between groups, although there were no systematic trends. For example, a higher GAG content was released into the medium for the control group at day 16 for isolation 0504 (Figure 4.2A). By contrast, isolations 1204 and 0305 (Figures 4.2B and 4.2C respectively) indicate that the PLIUS-stimulated chondrocytes release slightly more sGAG into the medium than those in controls at days 16 and 20. Close examination of values between experiments reveal that the mean sGAG released in the medium corresponding to isolation 0305 is comparably higher than for the other two isolations (0504 and 1204).

TABLE 4.2: Summary of results investigating the effect of PLIUS on elaboration of total sGAG content in chondrocyte-agarose constructs exposed to once or twice daily $30\text{mW}/\text{cm}^2$ PLIUS, as determined by total sGAG content. $\uparrow(\downarrow)$ represents statistically significant up-regulation (down-regulation) of sGAG content compared to controls.

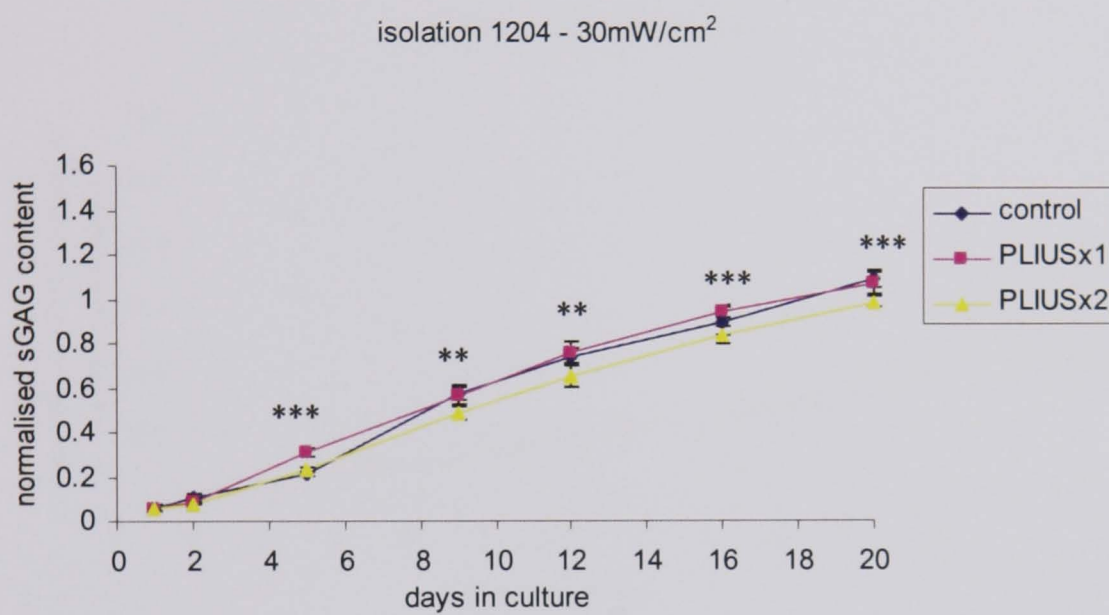
Isolation	PLIUS intensity/frequency	Time-point (day)					
		2	5	9	12	16	20
0504	$30\text{mW}/\text{cm}^2$ PLIUSx1	-	-	-	↑*	-	N/A
1204	$30\text{mW}/\text{cm}^2$ PLIUSx1	↓**	↑***	-	-	-	-
0305	$30\text{mW}/\text{cm}^2$ PLIUSx1	-	-	↓***	-	-	-
1204	$30\text{mW}/\text{cm}^2$ PLIUSx2	↓***	↑*	↓***	↓**	↓***	-
0305	$30\text{mW}/\text{cm}^2$ PLIUSx2	-	-	↓**	↓***	↓***	↓***

The significance levels $p < 0.05$, $p < 0.01$ and $p < 0.001$ are represented by one, two or three symbols, respectively, with red and blue highlighting up- and down-regulation from controls.

A



B



C

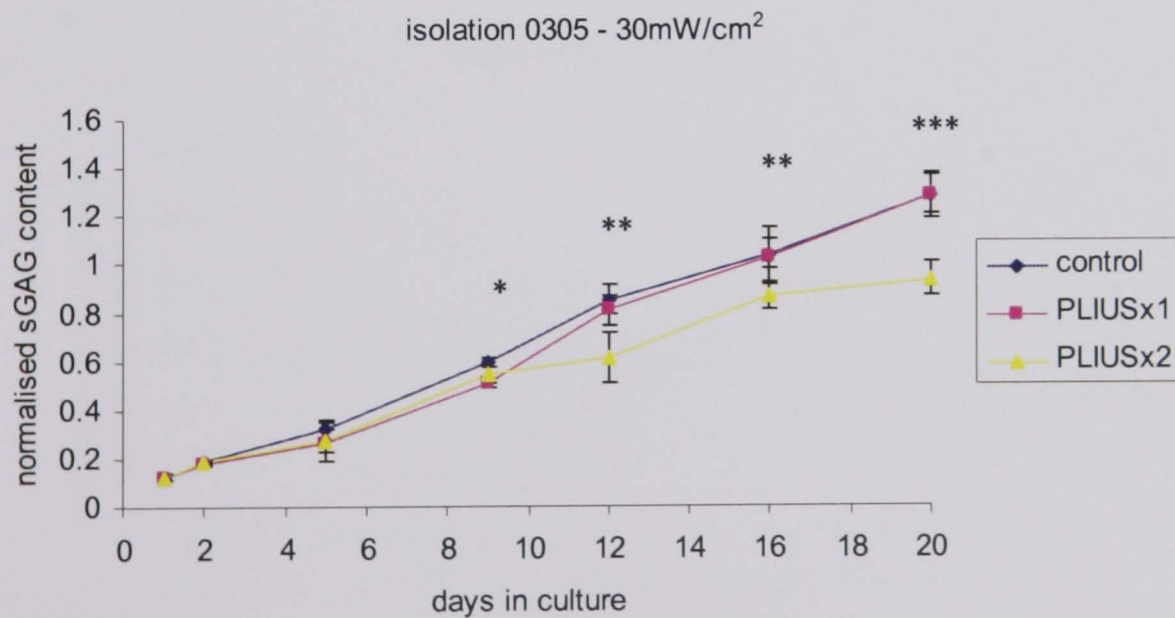
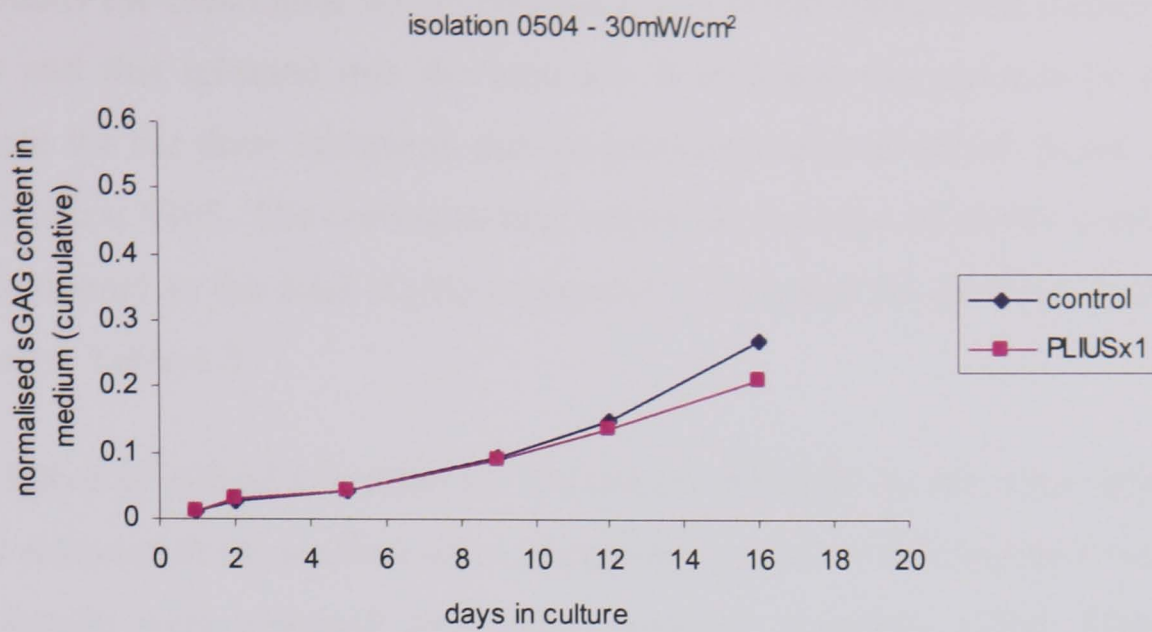
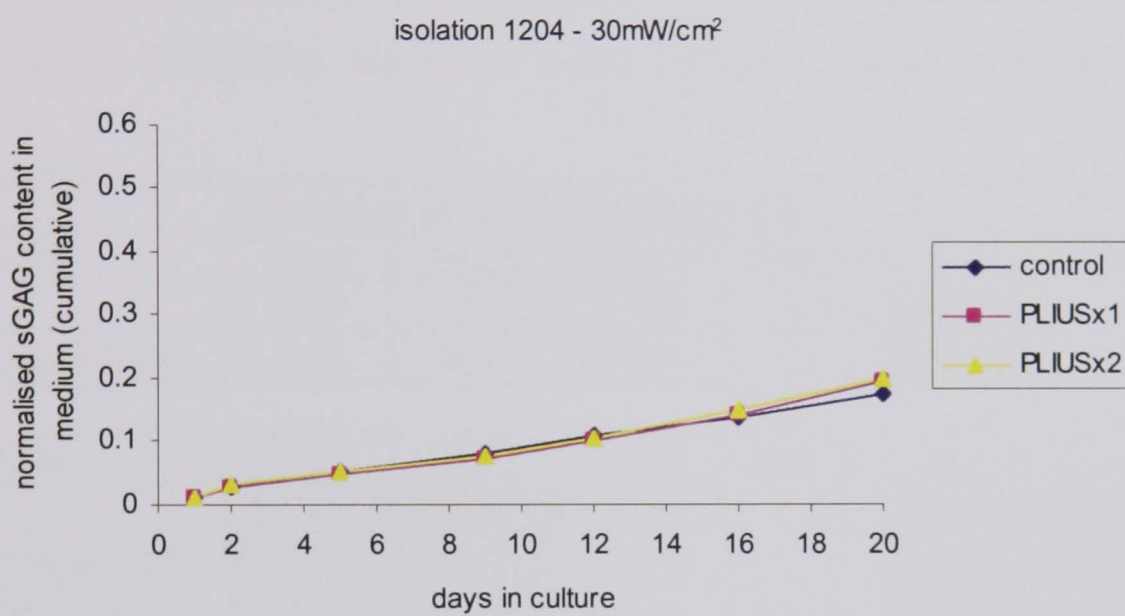


FIGURE 4.1: Effect of pulsed low intensity ultrasound (PLIUS) on total sGAG content in agarose-chondrocyte constructs undertaken from three separate isolations (0504, 1204 and 0305). Cells were exposed to 30mW/cm² PLIUS either every 24 or 12 hours (termed PLIUSx1 and PLIUSx2, respectively). Values represent mean \pm standard deviations ($n=6-7$). Statistical differences between PLIUSx1 and PLIUSx2 are indicated such that * $p < 0.05$; ** $p < 0.01$; *** $p < 0.001$.

A



B



C

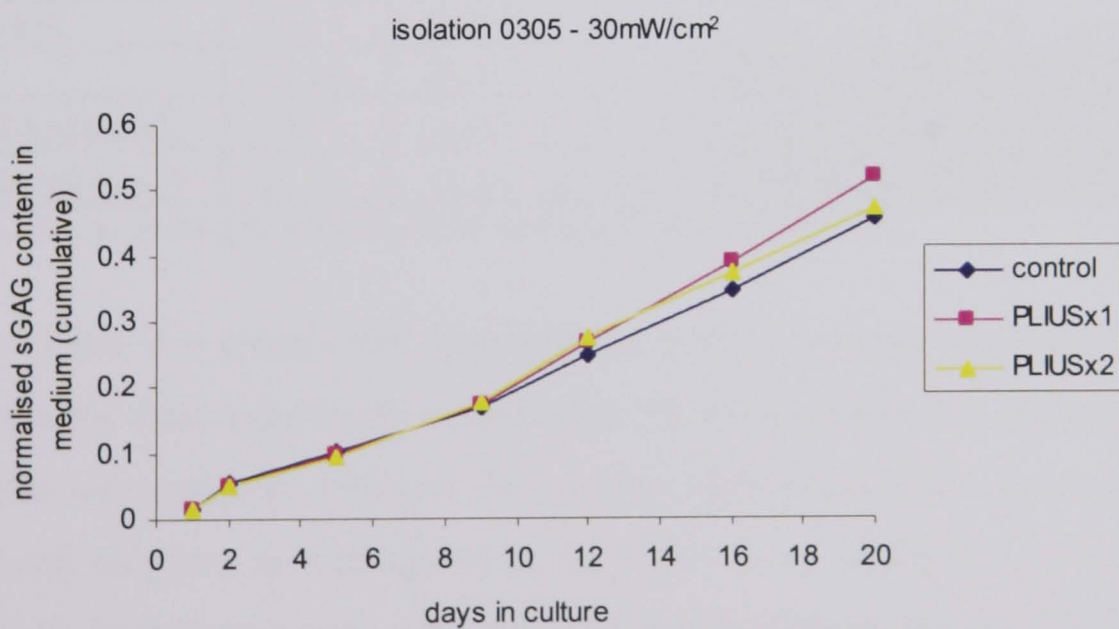


FIGURE 4.2: Effect of pulsed low intensity ultrasound (PLIUS) on total sGAG released into the medium from agarose-chondrocyte constructs from three separate isolations (0504, 1204 and 0305). Cells were exposed to 30mW/cm² PLIUS either every 24 or 12 hours (termed PLIUSx1 and PLIUSx2, respectively). Values are cumulative and represent the mean (n=2).

Figure 4.3 presents the mean total sGAG corresponding to the sum of that measured in the constructs and that released into the medium. It indicates the variance in sGAG values over time for the three isolations and the increased ratio of sGAG found in the medium for isolation 0305. The corresponding values for the ratio of sGAG content in the medium compared to the total sGAG (construct + medium) for all three isolations are summarised in Table 4.3.

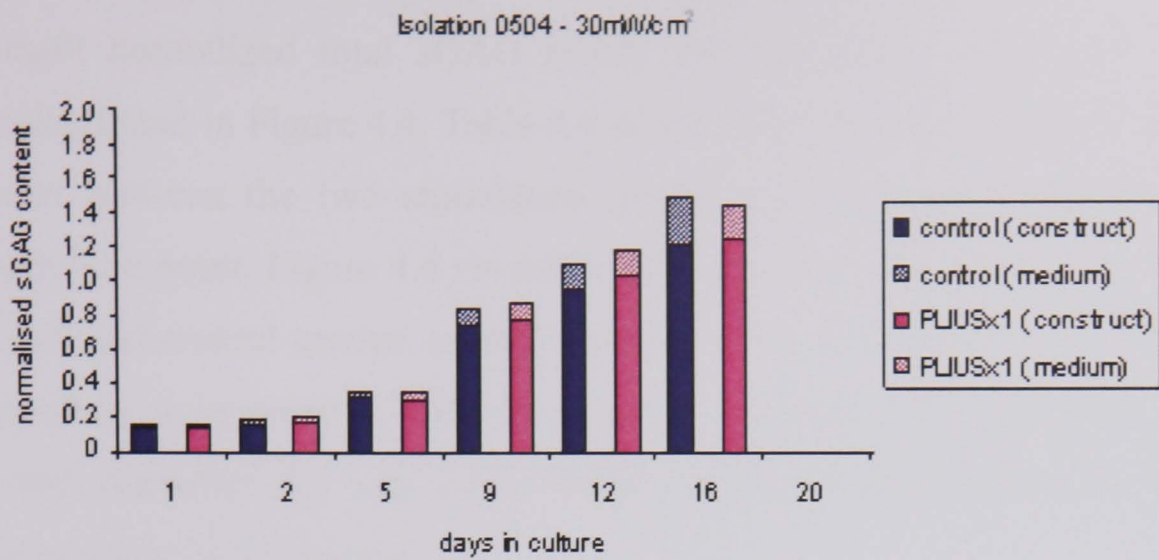
TABLE 4.3: *Effect of pulsed low intensity ultrasound (PLIUS) on the ratio values of sGAG content released in the medium when compared to total sGAG content (construct + medium). Results were obtained from three separate isolations (0504, 1204 and 0305). Experimental groups involved cell-seeded constructs exposed to 30mW/cm² once (PLIUSx1) or twice (PLIUSx2) every 24 hours. Control groups remained non-stimulated.*

Percentage of total sGAG in medium						
Isolation 0504	Day 2	Day 5	Day 9	Day 12	Day 16	Day 20
Control	13.97	12.42	11.44	13.45	18.23	n/a
PLIUSx1 (30mW/cm ²)	14.60	12.30	10.31	11.75	14.75	n/a
Isolation 1204	Day 2	Day 5	Day 9	Day 12	Day 16	Day 20
Control	21.16	19.98	12.23	12.87	13.49	13.93
PLIUSx1 (30mW/cm ²)	25.06	13.98	11.49	11.98	13.19	15.37
PLIUSx2 (30mW/cm ²)	28.48	18.73	13.79	13.96	15.38	16.77
Isolation 0305	Day 2	Day 5	Day 9	Day 12	Day 16	Day 20
Control	22.26	24.15	22.18	22.61	25.01	26.12
PLIUSx1 (30mW/cm ²)	22.41	26.42	25.38	24.85	27.31	28.93
PLIUSx2 (30mW/cm ²)	21.70	25.68	24.55	31.16	30.03	33.52

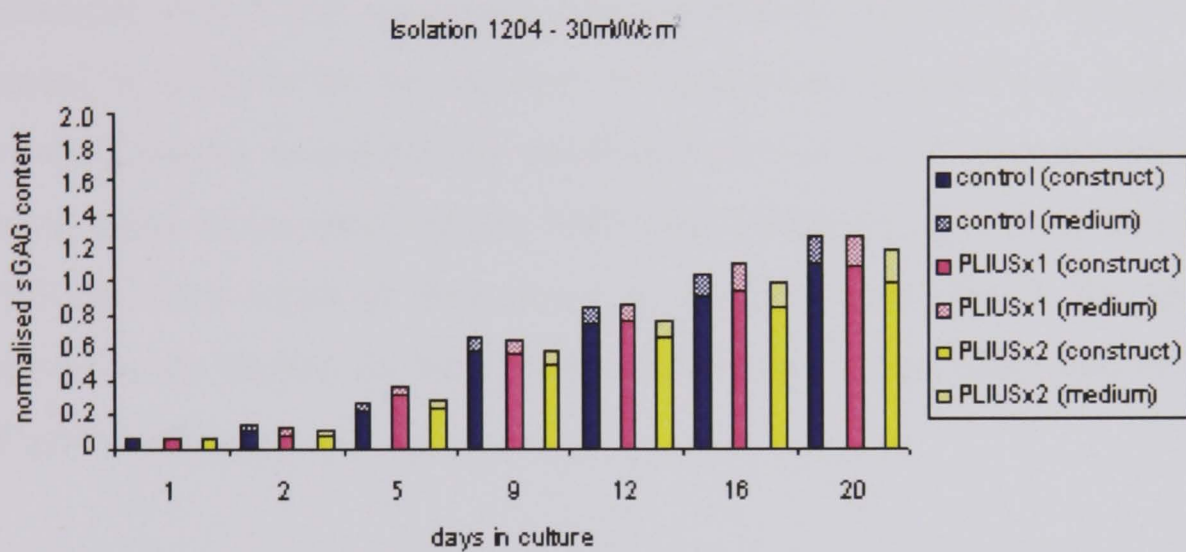
Highlighted entries indicate differences between stimulated and control values.

Examination of Table 4.3 reveals that generally no specific pattern could be seen in medium ratios for the three experimental conditions. However there were some cases in which differences were apparent between the medium sGAG levels for stimulated and non-stimulated cell cultures, as highlighted in the table. As an example, for isolations 1204 and 0305 at later time-points, the twice-daily stimulation regimen (PLIUSx2) yielded increased release of sGAG into the medium.

A



B



C

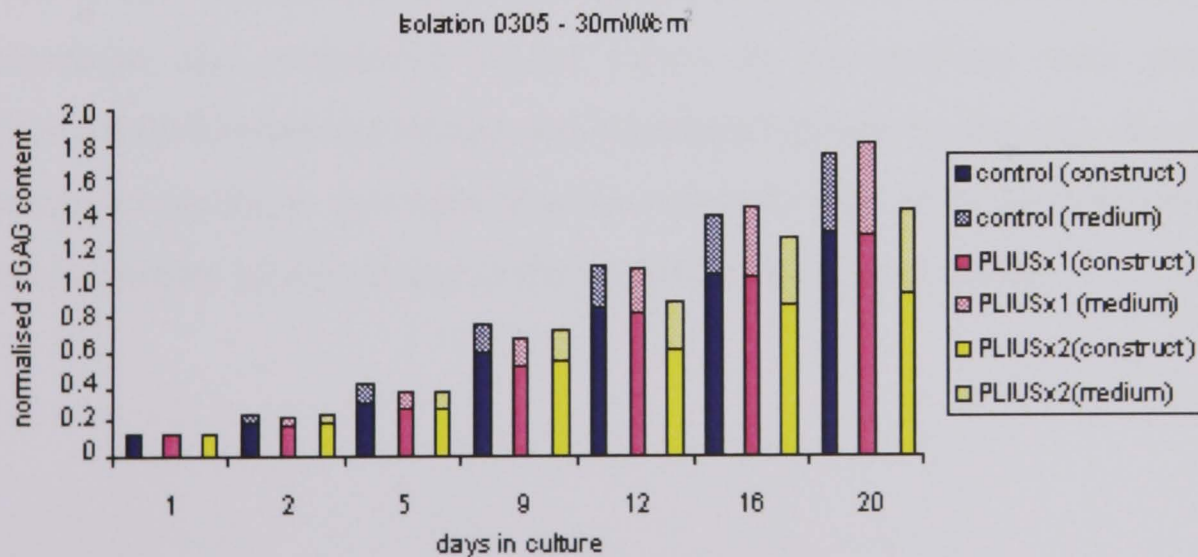


FIGURE 4.3: Effect of pulsed low intensity ultrasound (PLIUS) on total sGAG content in agarose-chondrocyte constructs and sGAG released into the medium undertaken from three separate isolations (0504, 1204 and 0305). Cells were exposed to 30mW/cm² PLIUS either every 24 or 12 hours (termed PLIUSx1 and PLIUSx2, respectively). Values for construct represent mean (n=6-7). Values for medium are cumulative and represent mean (n=2).

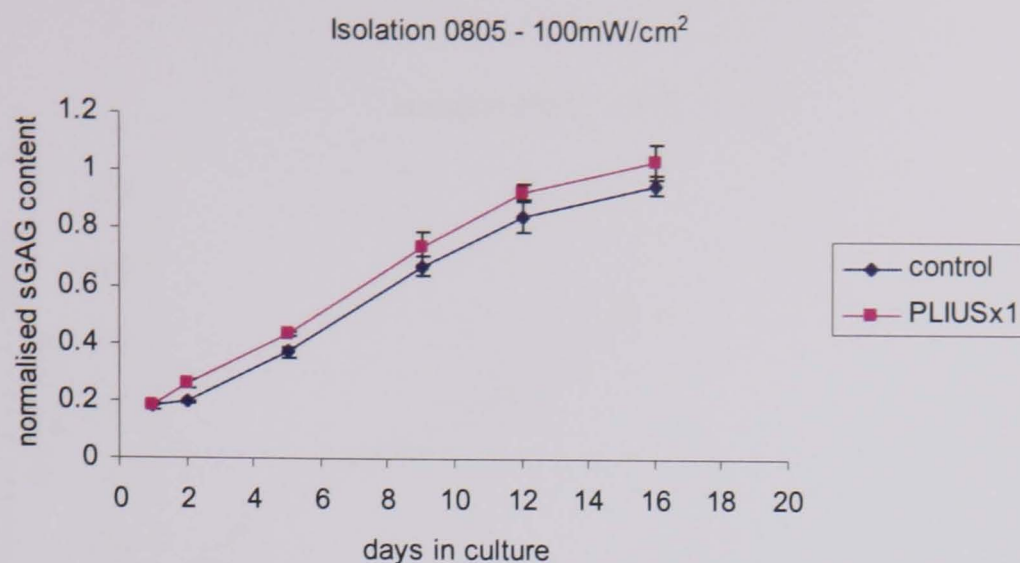
4.3.1.2 The effects of a SATA intensity of 100mW/cm²

The wet weight normalized total sGAG results for the higher 100mW/cm² SATA intensity are illustrated in Figure 4.4. Table 4.4 summarises the statistical data related to the differences between the two stimulation groups and the non-stimulated control group for each time point. Figure 4.4 reveals a general increase in sGAG over time for both the PLIUS and control groups, as was evident for the 30mW/cm² data. This trend is most pronounced with isolation 0805. By contrast, isolation 1105 yielded an increase up to day 9 and, thereafter, the total sGAG values remained fairly constant for both the experimental and the control groups.

For both isolations, PLIUS was associated with significantly higher total sGAG content when compared to controls for the majority of time-points (Figure 4.4). Indeed, the differences were found to be statistically significant for 9 of the 11 comparisons (Table 4.4). However, close examination of the 0805 data reveal that the main stimulatory effect of PLIUSx1 was achieved from day 1 to day 2. Beyond day 2, the temporal gradients appear to be similar for both groups indicating an equivalent rate of sGAG synthesis (Figure 4.4A).

The corresponding mean total cumulative sGAG released into the medium is presented in Figure 4.5. It can be seen that there is a fairly constant rate of sGAG release over time. Furthermore, the cumulative sGAG values in the medium were generally equivalent for the PLIUS-stimulated and non-stimulated groups for the majority of time points. The only exception to this trend was the values for day 20 in the isolation 1105, which revealed a higher sGAG release in the control group (Figure 4.5B).

A



B

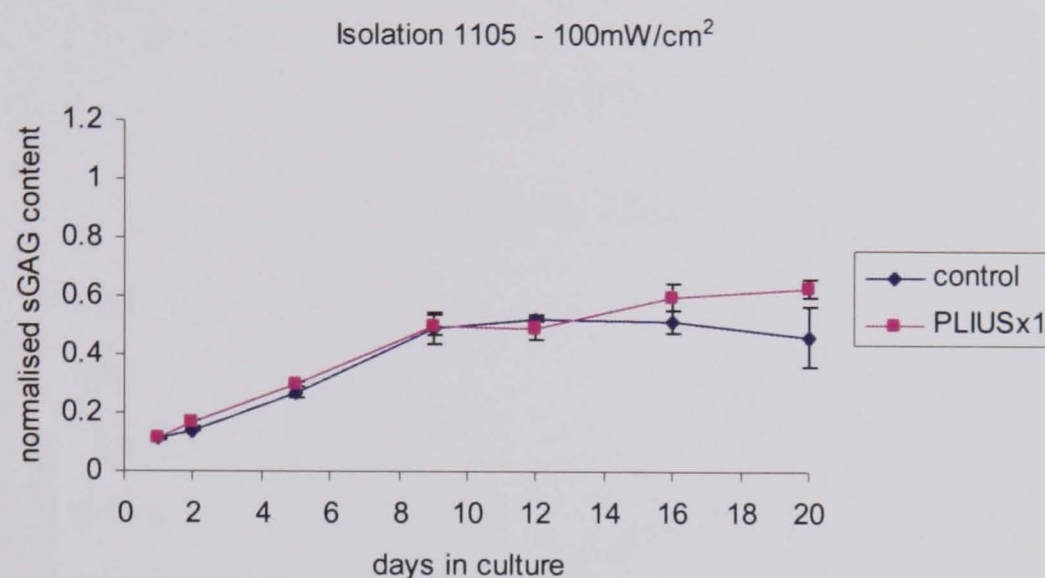


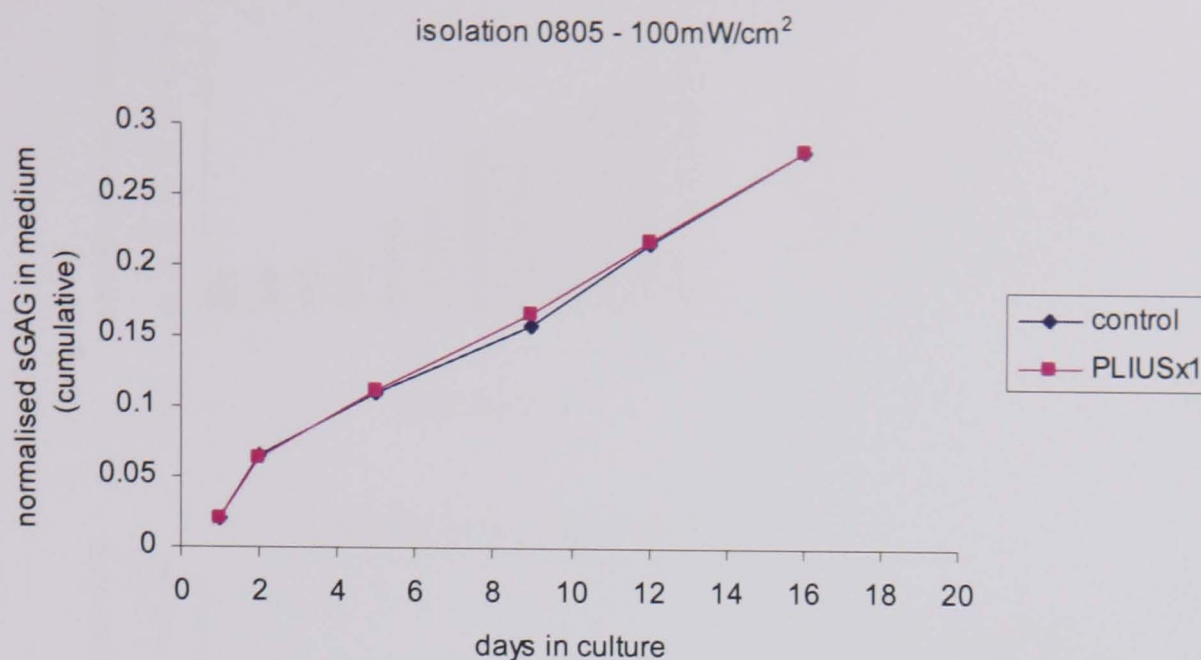
FIGURE 4.4: Effect of pulsed low intensity ultrasound (PLIUS) on total sGAG content in agarose-chondrocyte constructs undertaken from two separate isolations (0805 and 1105). Cells were exposed to 100mW/cm² PLIUS every 24 hours (termed PLIUSx1). Values represent mean \pm standard deviations ($n=6-7$).

TABLE 4.4: Summary of results investigating the effect of PLIUS on elaboration of sGAG elaboration in chondrocyte-agarose constructs exposed to once daily 100mW/cm² PLIUS, as determined by total sGAG content. \uparrow (\downarrow) represents statistically significant up-regulation (down-regulation) of sGAG content compared to controls.

Isolation	PLIUS intensity/frequency	Time-point (day)					
		2	5	9	12	16	20
0805	100mW/cm ² PLIUSx1	↑***	↑***	↑*	↑**	↑*	N/A
1105	100mW/cm ² PLIUSx1	↑***	↑**	-	-	↑***	↑***

The significance levels $p<0.05$, $p<0.01$ and $p<0.001$ are represented by one, two or three symbols, respectively, with red highlighting up-regulation from controls.

A



B

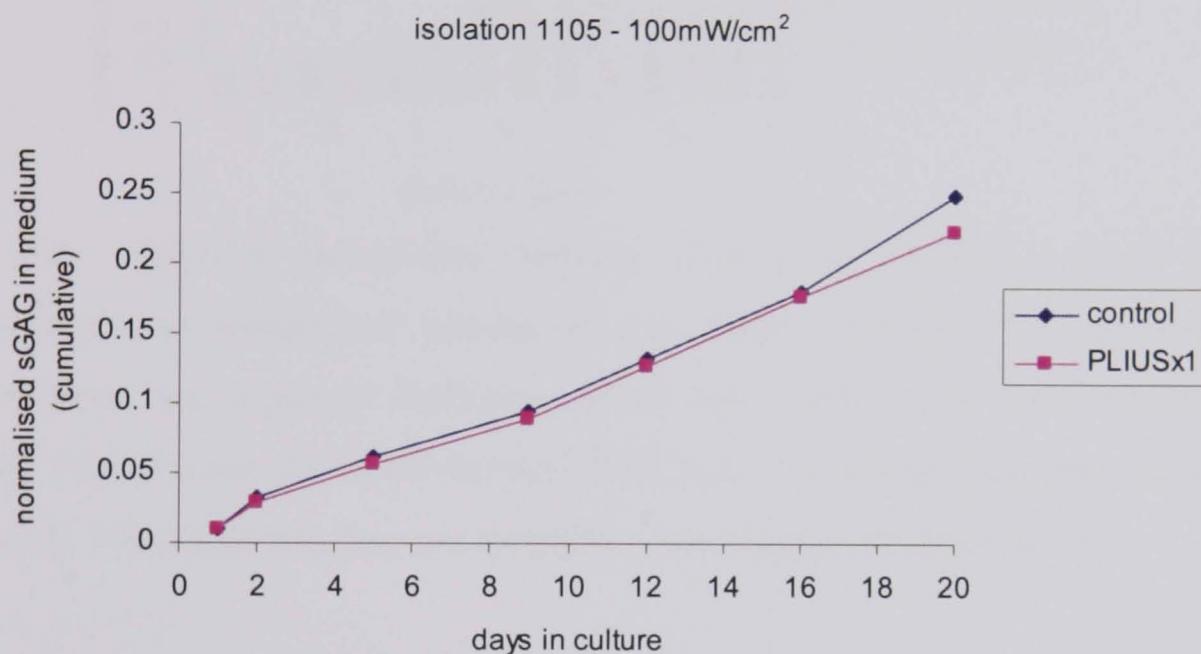
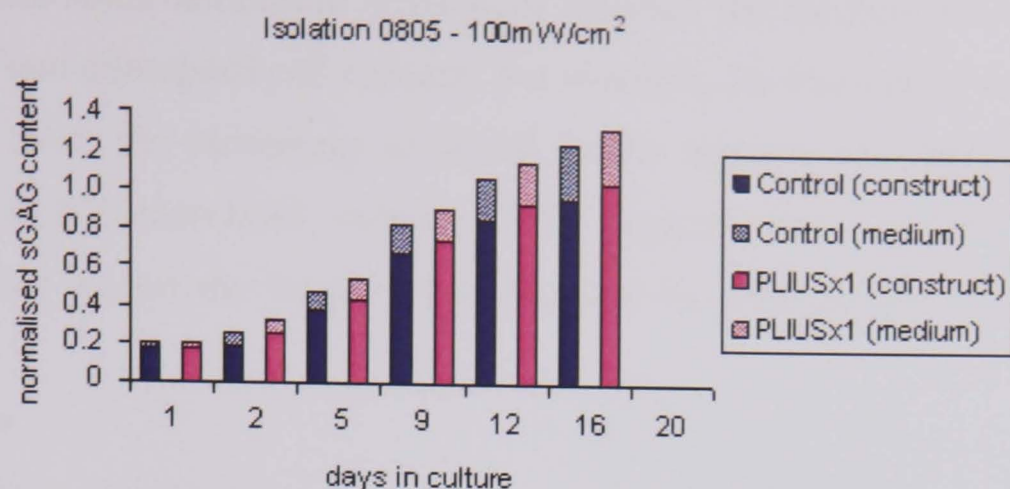


FIGURE 4.5: Effect of pulsed low intensity ultrasound (PLIUS) on total sGAG released into the medium for agarose-chondrocyte constructs from two separate isolations (0805 and 1105). Cells were exposed to 100mW/cm² PLIUS every 24 hours (termed PLIUSx1). Values are cumulative and represent the mean (n=2).

Figure 4.6 shows the mean total sGAG corresponding to the sum of that measured in the construct and that released into the medium. The corresponding values for the ratio of sGAG content in the medium compared to the total sGAG (construct + medium) for the two isolations are detailed in Table 4.5. It can be seen from Figure 4.6 that the total sGAG levels obtained from isolation 1105 are approximately 50% lower than those obtained from isolation 0805.

A



B

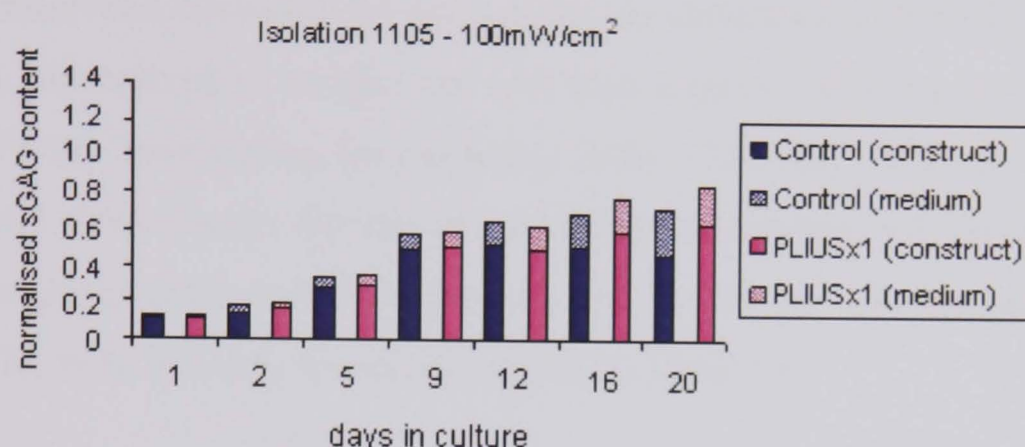


FIGURE 4.6: Effect of pulsed low intensity ultrasound (PLIUS) on total sGAG content in agarose-chondrocyte constructs and sGAG released into the medium undertaken from two separate isolations (0805 and 1105). Cells were exposed to 100mW/cm² PLIUS every 24 hours (termed PLIUSx1). Values for construct represent mean ($n=6-7$). Values for medium are cumulative and represent mean ($n=2$).

TABLE 4.5: Effect of pulsed low intensity ultrasound (PLIUS) on the ratio values of sGAG content released in the medium when compared to total sGAG content (construct + medium). Results were obtained from two separate isolations (0805 and 1105). Experimental groups involved cell-seeded constructs exposed to 100mW/cm² PLIUS every 24 hours (termed PLIUSx1). Control groups remained non-stimulated.

	Time-point (days)					
Isolation 0805	Day 2	Day 5	Day 9	Day 12	Day 16	Day 20
control	24.70	22.85	19.10	20.37	22.81	n/a
PLIUSx1 (100mW/cm ²)	19.58	20.38	18.50	18.91	21.42	n/a
Isolation 1105	Day 2	Day 5	Day 9	Day 12	Day 16	Day 20
control	18.99	18.50	16.24	20.10	26.10	35.03
PLIUSx1 (100mW/cm ²)	14.84	15.73	15.16	20.63	22.80	26.14

Highlighted entries indicate differences between stimulated and control values.

Table 4.5 reveals some noticeable differences between the medium sGAG levels for stimulated and non-stimulated cell cultures. For example, for four out of six time-points with isolation 1105, the percentage of sGAG in the medium was higher for control cultures than PLIUS-stimulated cultures. This suggests that once-daily PLIUS at $100\text{mW}/\text{cm}^2$ may inhibit the release of sGAG into the medium for this isolation of chondrocytes.

4.3.2 Total DNA content

Total DNA content was calculated for each of the six constructs in both the PLIUS and control groups, normalized to weight wet, and then a mean value was estimated. The results of $30\text{mW}/\text{cm}^2$ stimulation for isolations 0504, 1204 and 0305 are presented in Figure 4.7. Total DNA results for the two isolations undertaken for the $100\text{mW}/\text{cm}^2$ stimulation (isolations 0805 and 1105) are presented in Figure 4.8. A summary of the statistical data for both intensity levels is provided in Table 4.6.

Figures 4.7 and 4.8 show that overall, for the two PLIUS-stimulated groups (PLIUSx1 and PLIUSx2) and control group, there was only a moderate level of DNA increase over time, indicating low cell proliferation over the 20 day culture period. It is clear that different isolations yielded a marked variation in total DNA levels at day 1, despite the fact that the nominal seeding density was prescribed at 4×10^6 cells/ml. In particular, the DNA levels for chondrocytes used in isolation 0305 were much lower than those seen for the other four isolations over the 20 day period of culture (Figure 4.7C). The statistical data presented in Table 4.6 showed that in the majority of cases, PLIUS at $30\text{mW}/\text{cm}^2$ had no significant effect on DNA levels ($p > 0.05$). There was no systematic trend seen for the cases for which there were significant differences between PLIUS and control groups.

At an intensity of $100\text{mW}/\text{cm}^2$, some statistical differences in the DNA content were found between PLIUSx1 and control groups at equivalent time points (Figure 4.7, Table 4.6). In 5 out of a possible 11 time-points a down-regulation of DNA content was seen for PLIUS-stimulated constructs ($p < 0.05$), specifically at days 5 and 9, evident with both isolations (Figure 4.8, Table 4.6).

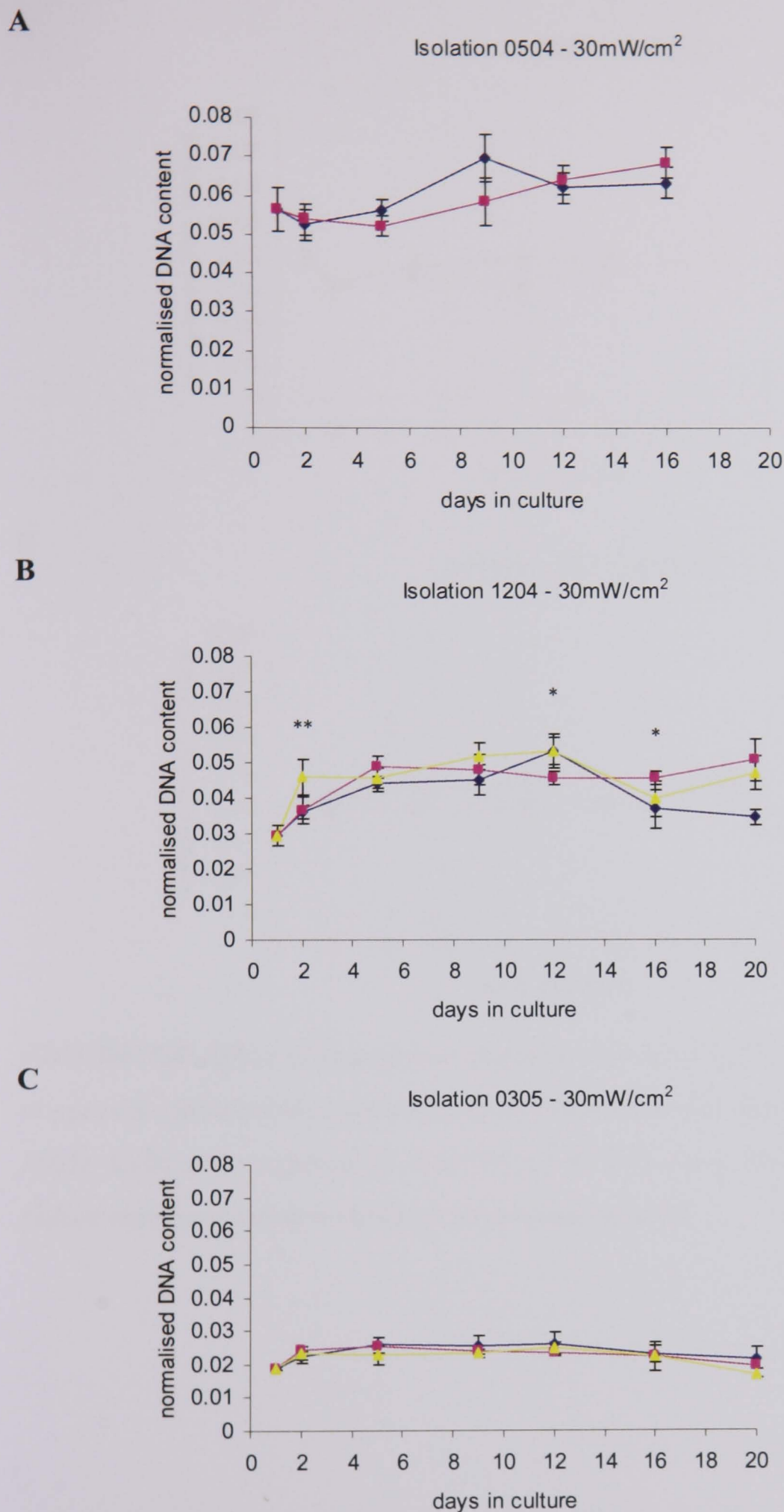
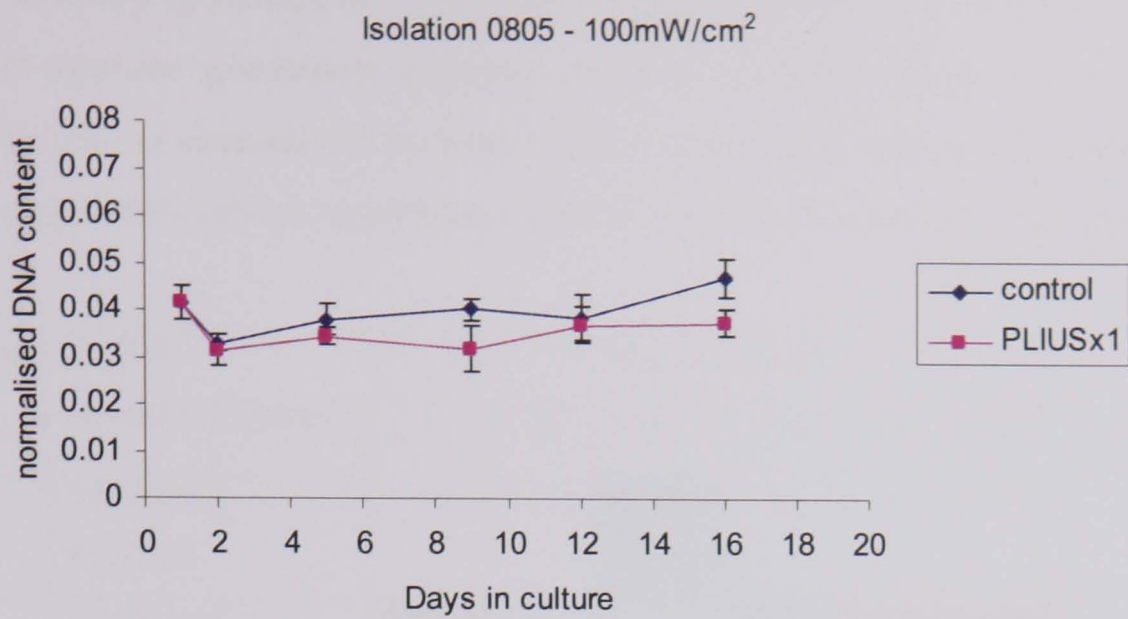


FIGURE 4.7: Effect of pulsed low intensity ultrasound (PLIUS) on total DNA content in agarose-chondrocyte constructs undertaken from three separate isolations (0504, 1204 and 0305). Cells were exposed to 30mW/cm² PLIUS either every 24 or 12 hours (termed PLIUSx1 and PLIUSx2, respectively). Values represent mean \pm standard deviations ($n=6-7$). Statistical differences between PLIUSx1 and PLIUSx2 are indicated such that * $p < 0.05$; ** $p < 0.01$; *** $p < 0.001$.

A



B

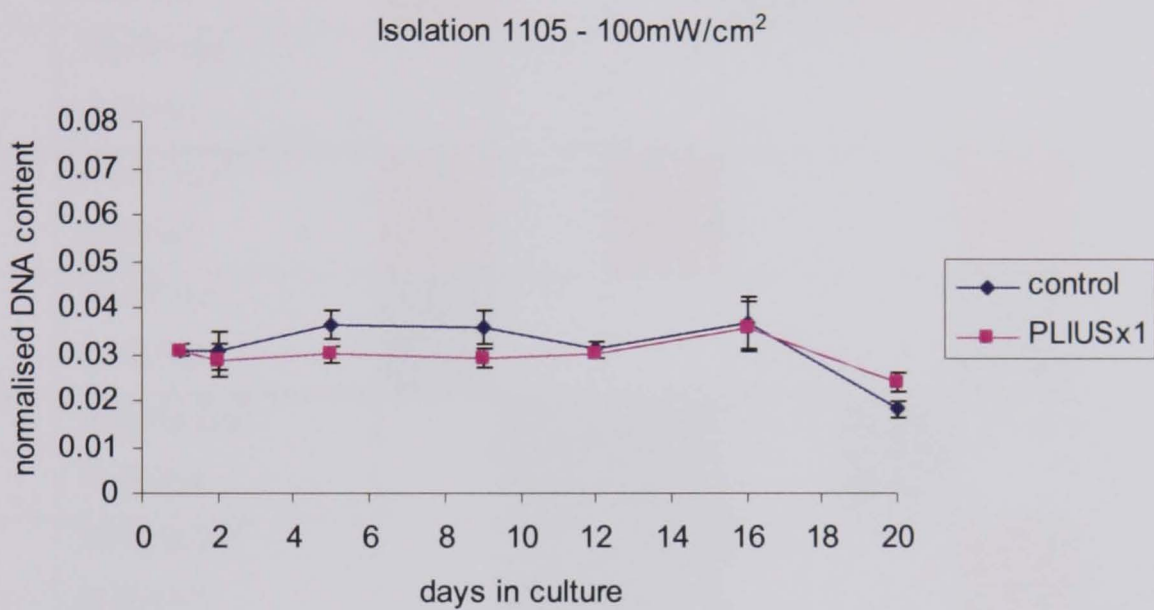


FIGURE 4.8: Effect of pulsed low intensity ultrasound (PLIUS) on total DNA content in agarose-chondrocyte constructs undertaken from two separate isolations (0805 and 1105). Cells were exposed to 100mW/cm² PLIUS every 24 hours (termed PLIUSx1). Values represent mean \pm standard deviations ($n=6-7$).

TABLE 4.6: Summary of results investigating the effect of PLIUS on cell proliferation in chondrocyte-agarose constructs exposed to once or twice daily 30mW/cm² or 100mW/cm² PLIUS, as determined by total DNA content. ↑(↓) represents statistically significant up-regulation (down-regulation) of sGAG content compared to controls.

Isolation	PLIUS intensity/frequency	Time point (day)					
		2	5	9	12	16	20
0504	30mW/cm ² PLIUSx1	-	-	↓***	-	-	N/A
1204	30mW/cm ² PLIUSx1	↑*	-	-	↓**	↑***	↑***
0305	30mW/cm ² PLIUSx1	-	-	-	-	-	-
1204	30mW/cm ² PLIUSx2	↑***	-	↑**	-	-	↑****
0305	30mW/cm ² PLIUSx2	↓*	-	-	-	-	↓**
0805	100mW/cm ² PLIUSx1	-	↓*	↓**	-	↓***	N/A
1105	100mW/cm ² PLIUSx1	-	↓****	↓**	-	-	↑****

The significance levels $p < 0.05$, $p < 0.01$ and $p < 0.001$ are represented by one, two or three symbols, respectively, with red and blue highlighting up- and down-regulation from controls.

4.3.3 Cell activity

The total sGAG and total DNA data detailed in the previous sections can be employed to provide an assessment on cell activity in terms of sGAG. The calculation is based on the conversion that bovine chondrocytes produce 7.7pg of DNA (Kim *et al.*, 1988). A summary of the data is presented in Table 4.7.

It can be seen that for all isolations the amount of sGAG produced per cell increases with time in culture. This might be predicted due to the greater increase in total sGAG over the culture period (Figures 4.3 and Figure 4.6) when compared to the relatively small DNA increase over time for all isolations. There were a few cases where PLIUS-stimulated chondrocytes produced significantly higher or lower sGAG amounts when compared to control cells. For constructs stimulated at 30mW/cm², it can be seen that there was no overall increase in sGAG productivity for cells subjected to either once- or

twice-daily PLIUS. For the higher intensity of $100\text{mW}/\text{cm}^2$, it can be seen that for the majority of time points (8 out of 11 cases) there was increased sGAG productivity in PLIUS-stimulated chondrocytes compared to controls.

TABLE 4.7: Mean amount of sGAG per cell in chondrocyte/agarose construct. Constructs exposed to once or twice daily $30\text{mW}/\text{cm}^2$ or $100\text{mW}/\text{cm}^2$ PLIUS ($n=6-7$).

Isolation	PLIUS intensity	Regimen	Mean sGAG/cell ($\times 10^{-10}$) at time point						
			1	2	5	9	12	16	20
0504	$30\text{mW}/\text{cm}^2$	Control	0.17	0.22	0.39	0.74	1.07	1.34	N/A
		PLIUSx1		0.23	0.41	0.99	1.13	1.25	N/A
1204	$30\text{mW}/\text{cm}^2$	Control	0.17	0.24	0.37	0.99	1.07	1.84	2.38
		PLIUSx1		0.19	0.52	0.88	1.24	1.67	1.61
		PLIUSx2		0.14	0.41	0.73	0.95	1.63	1.63
0305	$30\text{mW}/\text{cm}^2$	Control	0.5	0.65	0.96	1.82	2.57	3.56	4.72
		PLIUSx1		0.57	0.82	1.65	2.71	3.57	5.21
		PLIUSx2		0.62	0.94	1.82	1.9	3.12	4.25
0805	$100\text{mW}/\text{cm}^2$	Control	0.34	0.46	0.76	1.29	1.71	1.58	N/A
		PLIUSx1		0.64	0.97	1.80	1.96	2.13	N/A
1105	$100\text{mW}/\text{cm}^2$	Control	0.28	0.36	0.58	1.06	1.31	1.09	1.98
		PLIUSx1		0.45	0.77	1.33	1.23	1.31	2.04

Statistically significant differences from controls are highlighted in red or blue (up- or down-regulation respectively) ($p < 0.05$).

4.3.4 SO_4 incorporation

The rate of incorporation of SO_4 into newly synthesized GAG for chondrocytes exposed to 30 and $100\text{mW}/\text{cm}^2$ is presented graphically in Figures 4.9 and 4.10, respectively. Incorporation rates are represented as percentage of control values. Statistics relating to these data are included in Table 4.8.

Figure 4.9 indicates that at $30\text{mW}/\text{cm}^2$, for the majority of time points (22 out of 24 cases), both PLIUSx1 and PLIUSx2 systems exhibited either comparable or lower incorporation rates than control cultures. However, there was some variation between isolations and therefore no systematic pattern of incorporation rates could be discerned over the culture period.

The data for isolation 1204 yielded a maximum mean value at between days 8-9 and 11-12, where PLIUS-stimulated cultures reached an equivalent or higher incorporation rate

than controls. Thereafter, the values declined so that at the end of the culture period they were less than 75% of control values. It is worthy of note that between days 11-12, the PLIUSx2 stimulated culture exhibited a two fold increase in sulphate incorporation compared to controls ($p < 0.001$) (Table 4.8). Such an increase was not evident at any other time point or isolation at this SATA intensity.

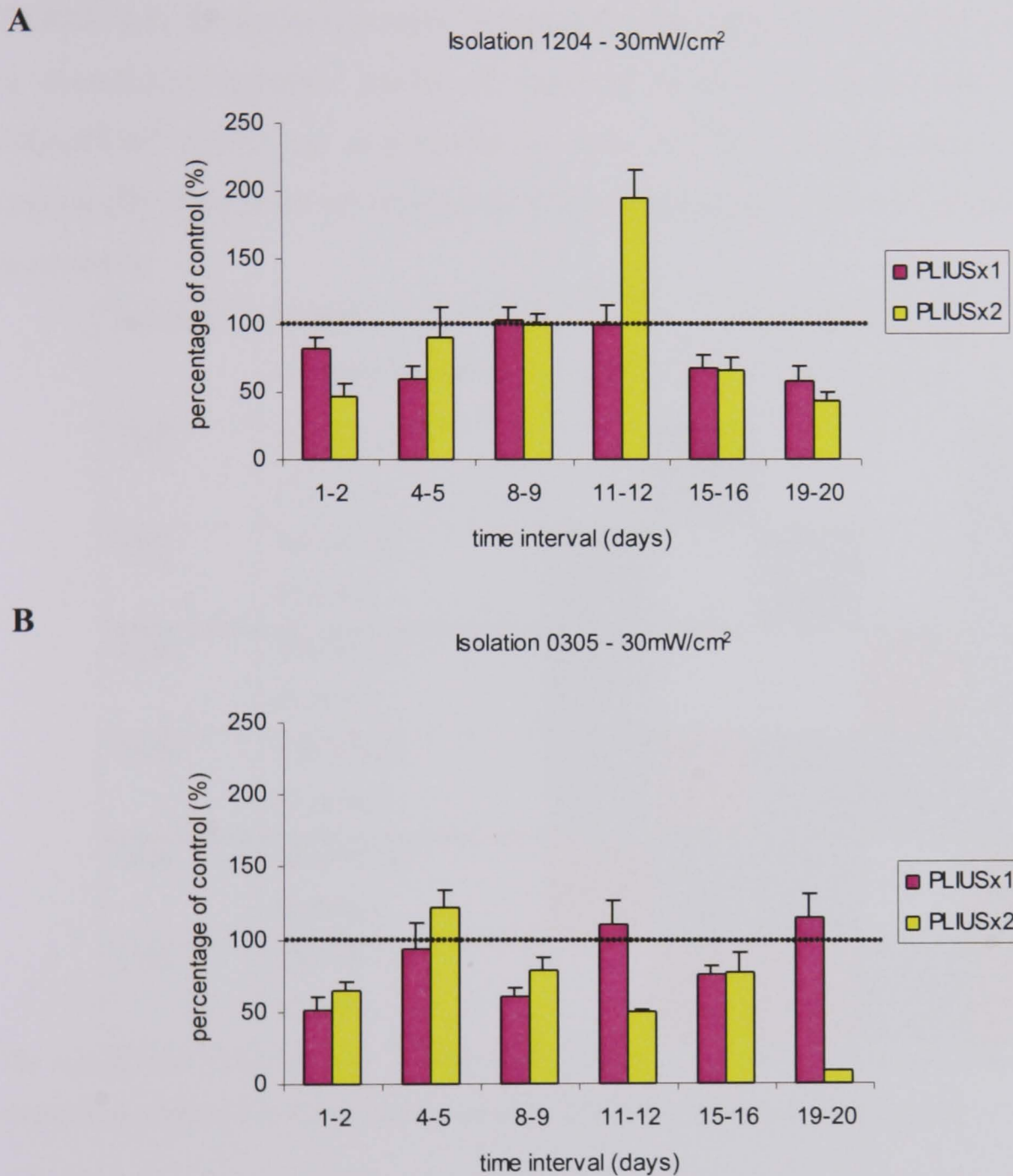


FIGURE 4.9: Relative effect of pulsed low intensity ultrasound (PLIUS) on the rate of ³⁵SO₄ incorporation in agarose-chondrocyte constructs undertaken from two separate isolations (1204 and 0305). Cells were exposed to 30mW/cm² PLIUS either every 24 or 12 hours (termed PLIUSx1 and PLIUSx2, respectively). Values represent mean PLIUS ³⁵SO₄ incorporation (units: $\mu\text{M } ^{35}\text{SO}_4/\text{h}/\mu\text{g DNA}$) as a percentage of control values with error bars showing standard deviation ($n=6-7$).

With isolation 0305, the majority of PLIUS-stimulated cultures appeared to fluctuate over time between 50% and 100% of the control incorporation rates. The only time point where a stimulatory effect was seen was between days 4-5, for the PLIUSx2 culture ($p < 0.01$). It is also worthy of note that at 19-20 days, the PLIUSx2 stimulated cultures yielded a sulphate incorporation of only 10% of that of the control value.

TABLE 4.8: Summary of results investigating the effect of PLIUS on sGAG production in chondrocyte-agarose constructs exposed to once or twice daily 30mW/cm² and 100mW/cm² PLIUS as determined by rate of ³⁵SO₄ incorporation. ↑(↓) represents statistically significant up-regulation (down-regulation) of incorporation rate compared to controls.

Isolation	PLIUS intensity/frequency	Time interval (days)					
		1-2	4-5	8-9	11-12	15-16	19-20
1204	30mW/cm ² PLIUSx1	-	↓***	-	-	↓***	↓***
0305	30mW/cm ² PLIUSx1	↓***	-	↓***	-	↓***	-
1204	30mW/cm ² PLIUSx2	↓***	-	-	↑****	↓***	↓***
0305	30mW/cm ² PLIUSx2	↓**	↑**	↓**	↓***	↓**	↓***
0805	100mW/cm ² PLIUSx1	↑***	↓**	↓***	-	↑*	N/A
1105	100mW/cm ² PLIUSx1	-	↑*	↑***	↓*	↑***	↓***

The significance levels $p < 0.05$, $p < 0.01$ and $p < 0.001$ are represented by one, two or three symbols, respectively, with red and blue highlighting up- and down-regulation from controls.

Figure 4.10 shows that for cultures stimulated with PLIUS at 100mW/cm², the majority of sulphate incorporation rates were between 75-125% of control values. It is worthy of note that the differences in most of the comparisons were statistically significant, with five exhibiting higher incorporation rates than controls, and four exhibiting lower rates. In a similar manner to the 30mW/cm² isolations, however, no discernible pattern of incorporation was evident, with contrasting findings between the two isolations at many time intervals (Table 4.8).

Comparison of the two PLIUS intensities revealed that, overall, 3D-cell cultures stimulated with $100\text{mW}/\text{cm}^2$ produced the greatest increase in sulphate incorporation rates when compared to non-stimulated controls. However, the differences were generally less than 50% and the pattern of change was variable between isolations.

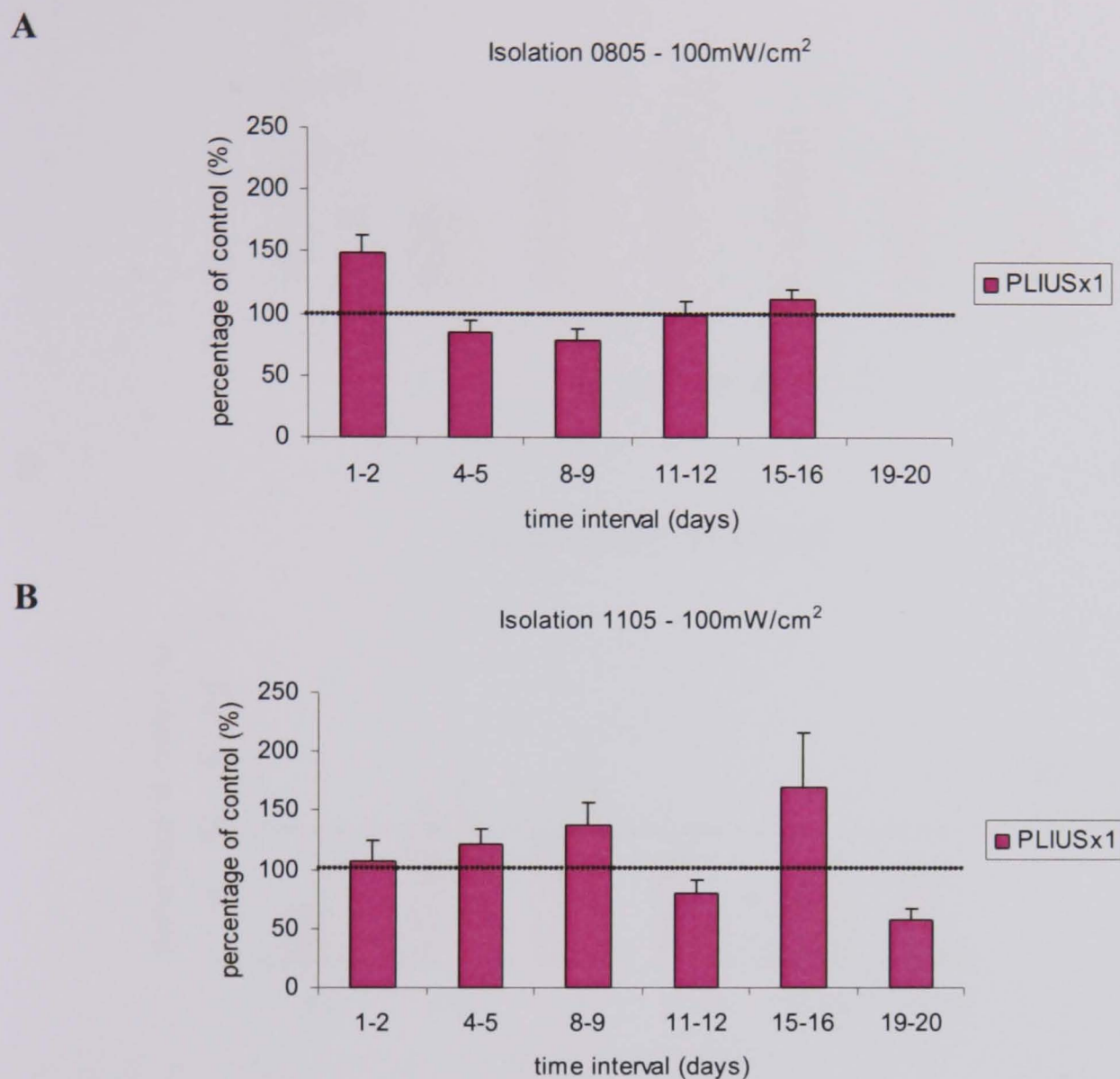
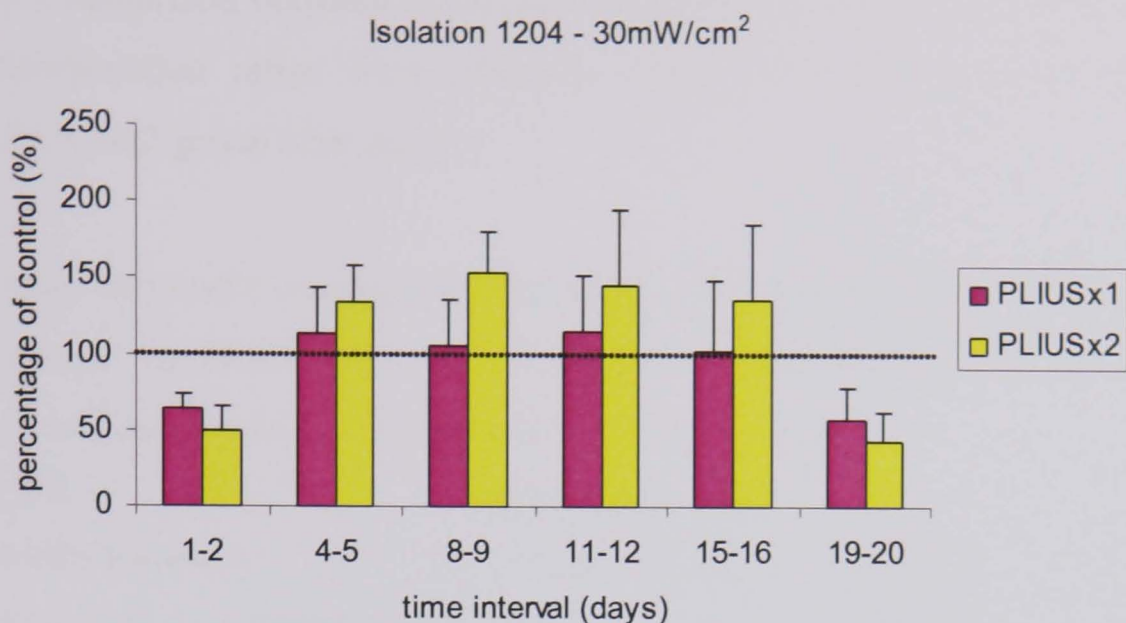


FIGURE 4.10: Relative effect of pulsed low intensity ultrasound (PLIUS) on the rate of $^{35}\text{SO}_4$ incorporation in agarose-chondrocyte constructs undertaken from two separate isolations (0805 and 1105). Cells were exposed to $100\text{mW}/\text{cm}^2$ PLIUS every 24 hours (termed PLIUSx1). Values represent mean PLIUS $^{35}\text{SO}_4$ incorporation (units: $\mu\text{M } ^{35}\text{SO}_4/\text{h}/\mu\text{g DNA}$) as a percentage of control with error bars showing standard deviation ($n=6-7$).

4.3.5 [^3H]thymidine incorporation

The rate of incorporation of [^3H]thymidine into newly synthesized DNA for chondrocytes exposed to 30 and $100\text{mW}/\text{cm}^2$ is presented graphically in Figure 4.11 and 4.12, respectively. Incorporation rates are represented as percentage of control values. Statistics relating to these data are presented in Table 4.9.

A



B

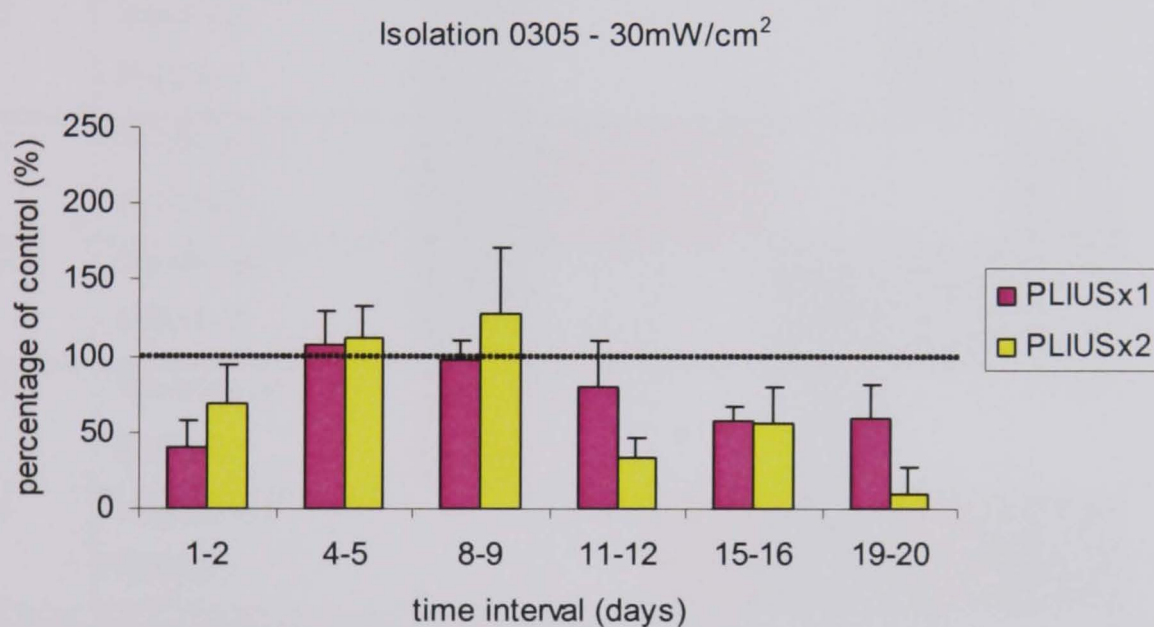


FIGURE 4.11: Relative effect of pulsed low intensity ultrasound (PLIUS) on the rate of [³H]thymidine incorporation in agarose-chondrocyte constructs undertaken from two separate isolations (1204 and 0305). Cells were exposed to 30mW/cm² PLIUS either every 24 or 12 hours (termed PLIUSx1 and PLIUSx2, respectively). Values represent mean PLIUS [³H]thymidine incorporation (units: CPM/μg DNA) as a percentage of control with error bars showing standard deviation (n=6-7).

Examination of Figure 4.11 suggested some consistency of data between the two stimulation regimens. Indeed for many of the time-points, PLIUS-stimulated groups yielded [³H]thymidine incorporation rates which were at least 100% of those of the corresponding controls. However, any increases were only found to be statistically significant in 2 out of 24 time-points over the two isolations (Table 4.9). Furthermore, these differences occurred in the same isolation, namely isolation 1204 for the PLIUSx2

group between days 4-5 and 8-9. Additionally, down-regulation of [³H]thymidine incorporation rates was seen for PLIUS-stimulated groups for 10 out of the 24 time points (Table 4.9). Comparison between isolations showed some variation, specifically that thymidine incorporation ratios were generally lower for isolation 0305, most noticeable for the PLIUSx2 group after day 9.

TABLE 4.9: Summary of results investigating the effect of PLIUS on cell proliferation in chondrocyte-agarose constructs exposed to once or twice daily 30mW/cm² or 100mW/cm² PLIUS, as determined by [³H]thymidine incorporation.

Isolation	PLIUS intensity/frequency	Time interval (days)					
		1-2	4-5	8-9	11-12	15-16	19-20
1204	30mW/cm ² PLIUSx1	↓***	-	-	-	-	↓**
0305	30mW/cm ² PLIUSx1	↓**	-	-	-	↓**	-
1204	30mW/cm ² PLIUSx2	↓***	↑***	↑****	-	-	↓***
0305	30mW/cm ² PLIUSx2	↓*	-	-	↓***	↓**	↓***
0805	100mW/cm ² PLIUSx1	↑**	-	-	↓**	-	N/A
1105	100mW/cm ² PLIUSx1	-	-	↑***	↓*	↑****	↓***

The significance levels $p < 0.05$, $p < 0.01$ and $p < 0.001$ are represented by one, two or three symbols, respectively, with red and blue highlighting up- and down-regulation from controls.

At the higher intensity of 100mW/cm² (Figure 4.12) it can be seen that there is a fairly similar pattern of [³H]thymidine incorporation over the culture period for the two isolations. However, isolation 0805 tended to have lower percentage values compared to controls than isolation 1105.

Although Figure 4.12 shows 6 cases in which PLIUS [³H]thymidine incorporation rates were at least 100% of control values, this was only statistically significant in three cases (Table 4.9, $p < 0.01$). Additionally, there were three observed cases of down-regulation (Table 4.9, $p < 0.05$), one of which occurred at days 19-20 for isolation 1105. Indeed, this value was very low compared to other time-points.

Comparison of Figure 4.11 and 4.12 revealed no noticeable difference in [^3H]thymidine incorporation between chondrocytes stimulated at $30\text{mW}/\text{cm}^2$ and $100\text{mW}/\text{cm}^2$.

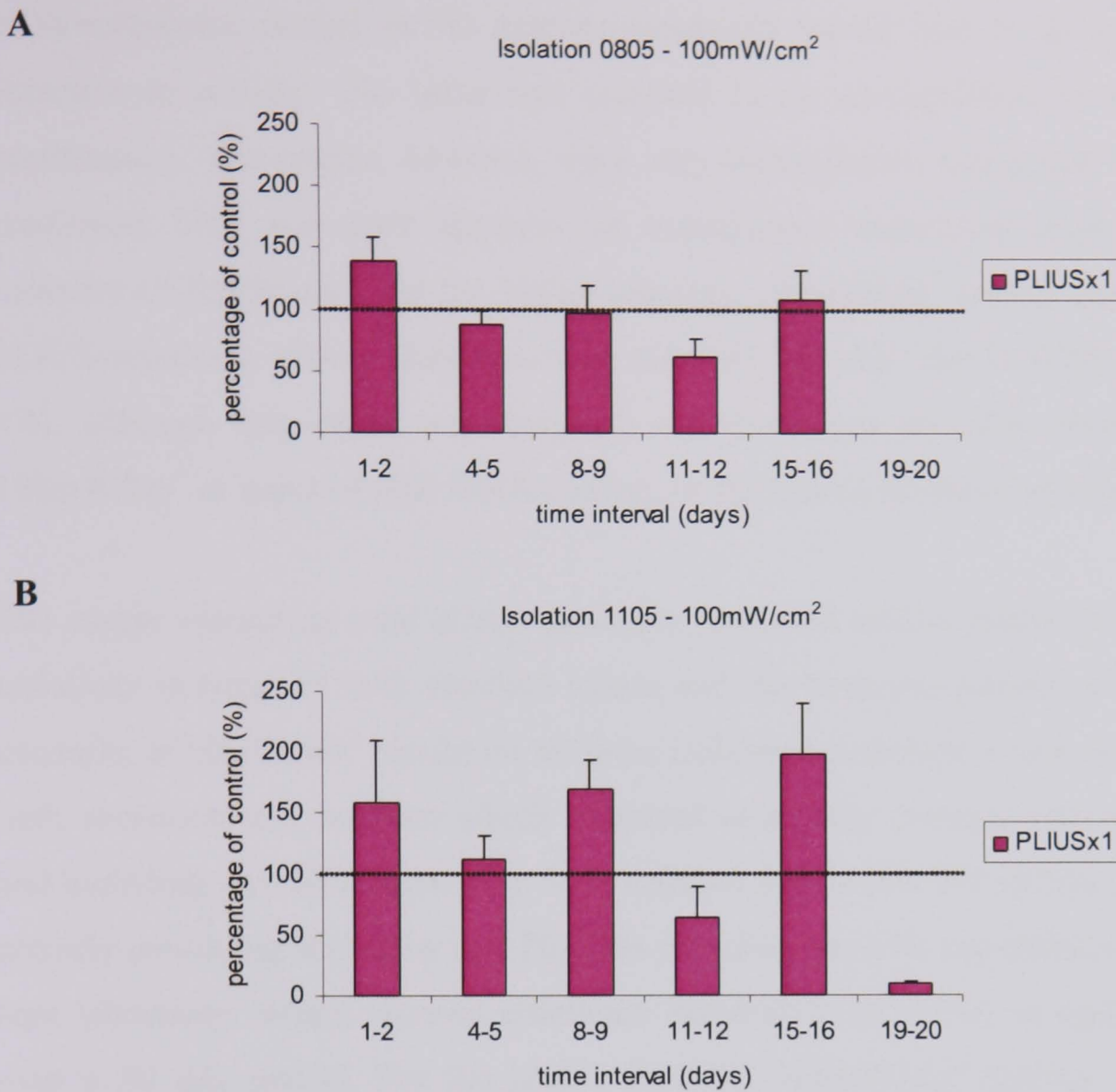


FIGURE 4.12: Relative effect of pulsed low intensity ultrasound (PLIUS) on the rate of [^3H]thymidine incorporation in agarose-chondrocyte constructs undertaken from two separate isolations (0805 and 1105). Cells were exposed to $100\text{mW}/\text{cm}^2$ PLIUS every 24 hours (termed PLIUSx1). Values represent mean PLIUS [^3H]thymidine incorporation (units: $\text{CPM}/\mu\text{g}$ DNA) as a percentage of control with error bars showing standard deviation ($n=6-7$).

4.4 Discussion

The hypothesis examined in the present set of experiments was that PLIUS stimulation of chondrocytes seeded in 3D agarose constructs would lead to an up-regulation of chondrocyte activity. The latter was assessed by an up-regulation of sGAG and cell proliferation. The results, however, were very inconclusive, and a null hypothesis was confirmed. This was more apparent for experiments undertaken employing a SATA intensity of $30\text{mW}/\text{cm}^2$. At the higher intensity $100\text{mW}/\text{cm}^2$ studies appeared to show PLIUS-enhanced sGAG elaboration as assessed by total sGAG DMB assay (Figure 4.4), although this effect was marginal and there was no other observed effect of $100\text{mW}/\text{cm}^2$ in terms of total DNA content, or the rate of synthesis of sGAG or DNA.

The assays measuring total sGAG generally produced similar results between separate isolations in terms of both absolute values and the temporal pattern of behaviour. For example, at $30\text{mW}/\text{cm}^2$ results for all three isolations indicated a total sGAG content in both constructs and medium which increased at a fairly constant rate with time up to and including day 20 (Figure 4.3). This inferred that in this 3D system, cells were still actively producing sGAG by day 20. This corroborates with unpublished data from the host laboratory, which showed continued elaboration of sGAG in agarose constructs over a 30 day period. For the higher intensity $100\text{mW}/\text{cm}^2$ studies, isolation 0805 showed a similar pattern of sGAG production to that evident with $30\text{mW}/\text{cm}^2$ (Figure 4.4A). Isolation 1105 however, indicated that sGAG content reached a plateau at day 9 and remained fairly constant thereafter (Figure 4.4B). Additionally, sGAG values for the latter isolation were approximately 60% of that of previous values. These observations were true for both PLIUS-stimulated and control cultures, indicating that these differences are attributable to the activity of the cell population isolated for a particular experiment. Indeed, a variance seen between separate isolations in terms of measured control values meant that separate responses to PLIUS could not be directly compared.

The aforementioned variation between isolations was also observed in terms of sGAG released into the medium by the 3D cultures. In most cases, however, very similar amounts of sGAG were measured in the medium between the experimental groups. Nevertheless there were a few cases in which an increased ratio of sGAG in the medium was noted in either PLIUS-stimulated cultures (for the $30\text{mW}/\text{cm}^2$ studies, Table 4.3) or the control studies (for the $100\text{mW}/\text{cm}^2$ studies, Table 4.5). There was no conclusive

evidence that PLIUS affected the transport of sGAG within the agarose construct and into the medium. However, of note is the difference between sGAG contents of cored agarose constructs and medium samples. As described in Sections 3.7, 6mm cylindrical constructs were cored from the chondrocyte-agarose gel at each time-point, and analysis done on these constructs. However, for medium calculations, all medium associated with the gel was collected, and the measured sGAG content value corrected to enable comparisons with the cored constructs, as described in Section 3.8.3. Therefore, whereas the measured sGAG contained in constructs is representative of that produced by chondrocytes located in the central region of the well, directly above the ultrasonic transducer, the sGAG located in the medium is that produced by chondrocytes throughout the 3D gel. A proportion of these cells would not have been directly exposed to the PLIUS signal, and it is therefore possible that local differences in sGAG release in relation to the position of the ultrasonic transducer may be undetectable in the total volume of culture medium.

The majority of the total DNA content data at both SATA intensities revealed no marked temporal change in DNA levels (Figures 4.7 and Figure 4.8). The one exception was seen at $30\text{mW}/\text{cm}^2$ with isolation 0504 (Figure 4.7A), which appeared to indicate a degree of cell proliferation. However, examination of the corresponding total sGAG data did not indicate that the proliferation translated into an associated increase in sGAG content (Figure 4.1). The chondrocyte, whose primary function is to produce matrix, is not known for detectable levels of cell proliferation in healthy adult articular cartilage (Mankin, 1964); the bovine steers obtained by the host lab from which chondrocytes were isolated are skeletally mature. Therefore, the relative constancy of DNA levels over time might be predicted. The application of either once- or twice-daily PLIUS in the majority of cases had no effect on DNA content when compared to controls at $30\text{mW}/\text{cm}^2$. However, at the higher $100\text{mW}/\text{cm}^2$ intensity, approximately 50% of time-points showed an inhibition in cell proliferation when compared to control cultures (Table 4.6).

Cell activity was measured, by normalizing sGAG content to the number of chondrocytes present (as determined by DNA content), to provide a more reliable indicator of cell production of sGAG (Table 4.7). All isolations indicated a temporal increase in the amount of sGAG produced per cell over time, which was predicted due to the associated low relative increase in DNA. The majority of results at $30\text{mW}/\text{cm}^2$

showed no increase in sGAG productivity for cells stimulated with either PLIUS regimen. However, at the higher intensity of $100\text{mW}/\text{cm}^2$, there was an increased sGAG synthesis in PLIUS stimulated chondrocytes compared to controls.

The radiolabelling protocols for SO_4 and [^3H]thymidine incorporation were undertaken to further investigate cell activity by assessing the rates at which chondrocytes were synthesising sGAG and DNA. SO_4 incorporation results showed a significant degree of down-regulation compared to controls (Table 4.8) for most time intervals. Comparison with the findings obtained from the total sGAG assays (shown in Tables 4.2 and 4.4), revealed some disparity between the two data sets. For cultures stimulated with PLIUSx1 at $30\text{mW}/\text{cm}^2$, the down-regulation seen in terms of SO_4 incorporation rate was not significant when estimated by total sGAG content. There was a greater degree of agreement between SO_4 incorporation rate and total sGAG content with the $30\text{mW}/\text{cm}^2$ PLIUSx2 and $100\text{mW}/\text{cm}^2$ cultures, the former corroborating a down-regulatory effect and the latter an up-regulatory effect. However, it is important to note that the two assays measure different indices of sGAG synthesis. Thus, total sGAG assay is a measure of the cumulative sGAG produced up to each time point from the beginning of the culture period, whereas incorporation of SO_4 measures the synthesis of new sGAG over a specified 24 hour period over the duration of the culture. Therefore the temporal effects observed with the incorporation assays may have little relationship to the total sGAG content. By overall examination of SO_4 incorporation it was evident that sGAG stimulation by PLIUS at $30\text{mW}/\text{cm}^2$ either had no effect (as seen for PLIUSx1 cultures) or a partial detrimental effect (as seen for PLIUSx2 cultures) on total sGAG content, both confirming a null hypothesis. At $100\text{mW}/\text{cm}^2$, however, there was a greater degree of significant sGAG elaboration for the PLIUS-stimulated groups, as evident from the results of both assays.

[^3H]thymidine incorporation results (Figures 4.11 and 4.12, Table 4.9) showed that for the majority of time-points there was no difference between PLIUS-stimulated groups and controls (17 out of 35 time-points), and a down-regulation in 13 time-points. There was some disparity between total DNA and [^3H]thymidine results when attempting to examine significant differences between PLIUS-stimulated and non-stimulated control constructs (Tables 4.6 and 4.9). However, in a similar manner to the discussion related to sGAG synthesis, total DNA and [^3H]thymidine incorporation assays measure cumulative and newly formed DNA, respectively. Overall it appeared that there was

minimal effect of PLIUS on DNA levels in 3D chondrocyte-agarose cultures, confirming a null hypothesis.

Cook *et al.* (2001) reported that increasing PLIUS treatment time from the standard 20 minutes to 40 minutes resulted in a statistically significant improvement in the histological appearance of cartilage in osteochondral defects in a rabbit model. In order to ascertain whether a similar finding could be achieved for chondrocytes in a 3D system, PLIUS at $30\text{mW}/\text{cm}^2$ was applied either once or twice daily (termed PLIUSx1 and PLIUSx2 respectively). The results generally indicated no marked difference between the two regimes. Indeed, in some cases PLIUSx1 results were significantly higher than PLIUSx2 results, although the reverse was also evident. The clearest differences between the two regimes could be related to the total sGAG data (Figure 4.1), where PLIUSx2 tended to yield lower sGAG contents than PLIUSx1 treated constructs. Isolation 0305 had a noticeable decrease in sGAG content for the PLIUSx2 group after day 9 compared to the two other groups. The corresponding sulphate and thymidine data at 19-20 days showed that incorporation rates for the PLIUSx2 stimulated cultures were only 10% of those of control cultures. This might be attributable to impaired viability due to early stages of infection by the end of the experimental period, as evidenced with other isolations e.g. 0504. Overall no advantage was seen in stimulating constructs in the present system twice a day with $30\text{mW}/\text{cm}^2$ PLIUS. These findings do not support the work of Cook and colleagues (2001), although their use of an *in-vivo* model system clearly precludes a direct comparison.

There were few instances with each assay where a stimulatory effect of PLIUS was consistently evident. It should be stated, however, that there was limited reproducibility between isolations. Indeed, it has been reported that different cell populations respond differently to ultrasound (Leskinen *et al.*, 2005). The steer hooves obtained weekly from the abattoir varied both in terms of age, condition and breed, and therefore it is likely that cell metabolism could have differed between isolations, although by choosing multiple hooves for chondrocyte isolations to make up a mixed cell population, this effect was minimalised.

Studies in the literature highlighting a stimulatory effect of PLIUS employed neonatal, embryonic and mesenchymal stem cells (Nishikori *et al.*, 2001; Zhang *et al.*, 2003; Ebisawa *et al.*, 2004; Cui *et al.*, 2006). Such populations are well established to be more

metabolically active than skeletally mature cells, such as those used in the present set of experiments. Indeed a number of studies employing adult chondrocytes showed no stimulatory effect of PLIUS, as ascertained from histological analysis, and [^3H]thymidine and SO_4 incorporation (Duda *et al.*, 2004 and Choi *et al.*, 2006, respectively).

It is important to reiterate that differences in cell-culture systems will have a major effect on the metabolic performance of cells. The present system involved casting a layer of chondrocyte-agarose gel in six-well plates and covering with a volume of medium. In this arrangement, only the top surface of the gel will be continually exposed to the medium. It is reasonable to assume that chondrocytes in the gel receive different amounts of nutrients depending on their position relative to the medium. Additionally, as discussed in Section 3.9.4, the amount of medium present per cell is lower than that recommended for chondrocytes in 3D-culture (Heywood *et al.*, 2004). Efficient nutrient delivery is essential to maintain optimum cell function. However, a depth-viability study, undertaken over a 16 day culture period with the 3D-culture, showed that at $30\text{mW}/\text{cm}^2$ the majority of cells remained viable over 90% throughout construct depth at day 16 (Figure 4.13). It is possible that a stimulatory effect of PLIUS at the lower intensity of $30\text{mW}/\text{cm}^2$ cannot be seen in this 3D system.

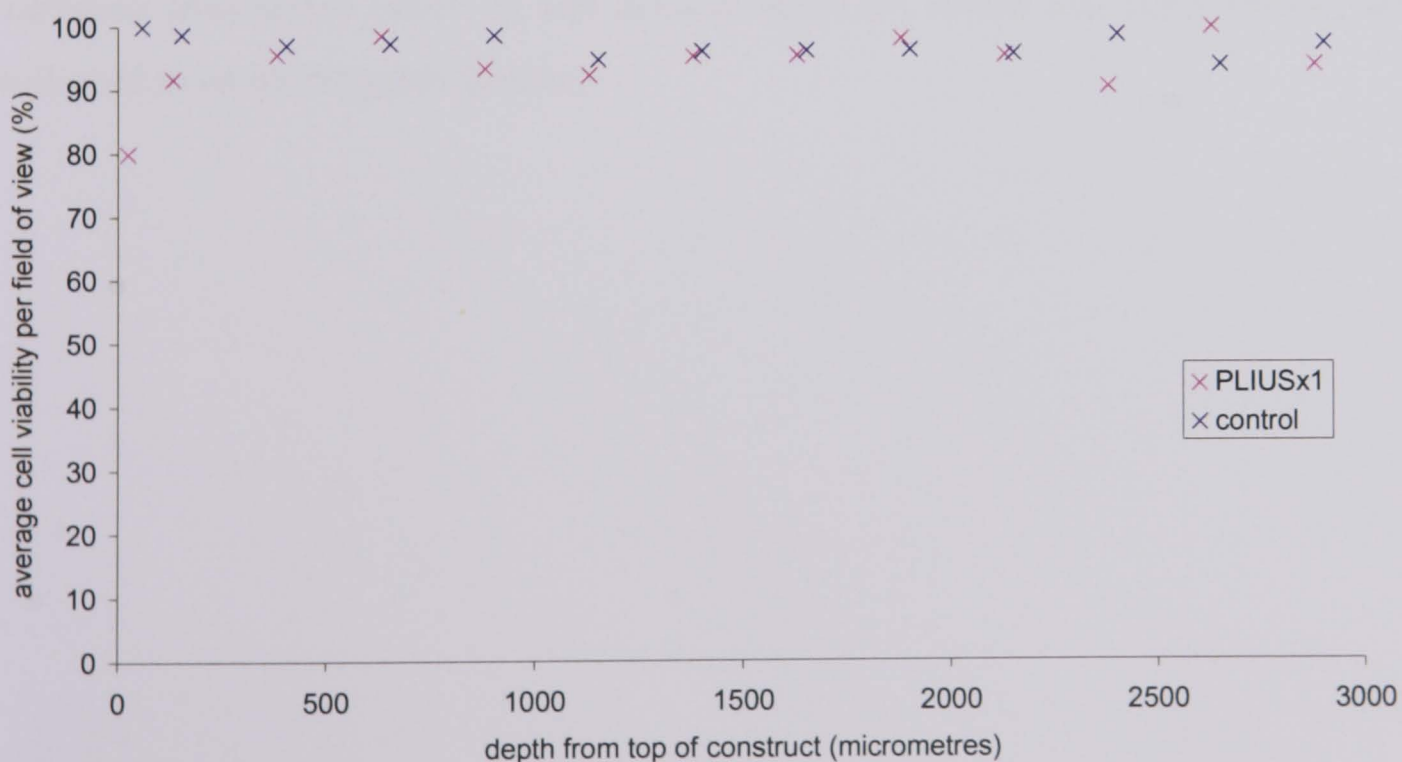


FIGURE 4.13: Cell viability at day 16 in agarose-chondrocyte constructs exposed to $30\text{mW}/\text{cm}^2$ PLIUS every 24 hours from day 1 to day 16. Values represent mean ($n=6$).

Another factor to consider is the distance between the ultrasound transducer and chondrocyte-agarose gel. The present system facilitates PLIUS application by using coupling gel to fix a six-well plate to transducers. The transducer is only a few millimeters distant from the chondrocytes. However, the use of the Exogen device for fracture healing works at a depth of penetration of 3.5cm from the bone (Nelson *et al.*, 2003). Figure 3.6 showed that the intensity of the PLIUS signal varied considerably with distance from the transducer, and along with attenuation of the signal by the various materials of the body, the ultrasound intensity on the bone may or may not actually be $30\text{mW}/\text{cm}^2$. Indeed, Zhang *et al.* (2003) found that the SATA intensity of $2\text{mW}/\text{cm}^2$ to be more effective than $30\text{mW}/\text{cm}^2$ when stimulating collagen synthesis in chick sterna explants. Additionally, the establishment of standing waves in the culture could inhibit cell activity, both at the construct/medium and medium/air interfaces. Indeed, a water bath has been used to maintain a working distance between the ultrasonic transducers and six-well plate (Kopakkala-Tani *et al.*, 2006). It is possible that such changes to the experimental system would generate an alternate set of data.

In conclusion, based on the present experimental arrangement, the application of once or twice-daily PLIUS at intensity $30\text{mW}/\text{cm}^2$ did not have a discernable effect on sGAG synthesis or proliferation of chondrocytes seeded in a 3D agarose system. Overall, application of PLIUS at a higher intensity of $100\text{mW}/\text{cm}^2$ did appear to have some increased stimulatory effect on cell activity based on sGAG and DNA results, which will need to be investigated further.

Chapter 5

Stimulation of Proteoglycan Synthesis by Pulsed Low Intensity Ultrasound in a Monolayer System

5.1	Introduction	131
5.2	Materials and methods	132
5.2.1	Preparation of chondrocyte monolayer culture	132
5.2.2	PLIUS regime	132
5.2.3	Temporal changes in sGAG and DNA content	132
5.2.4	Statistical analysis	133
5.3	Results	133
5.3.1	Total sGAG content	133
5.3.1.1	30mW/cm ² studies	133
5.3.1.2	100mW/cm ² studies	135
5.3.2	Total DNA content	135
5.3.3	Cell activity	138
5.3.4	SO ₄ incorporation	138
5.3.5	[³ H]thymidine incorporation	140
5.4	Discussion	141

5.1 Introduction

The results of the previous chapter revealed that for chondrocytes seeded in the 3D agarose system, pulsed low intensity ultrasound (PLIUS) at 30mW/cm^2 applied either once or twice-daily had no significant effect on sGAG synthesis or cell proliferation. However, use of a higher selected SATA intensity of 100mW/cm^2 appeared to have some increased stimulatory effect, although this was highly variable. These results appeared to conflict with previous work undertaken by two research groups (Parvizi *et al.*, 1999; Nishikori *et al.*, 2001), who found a stimulatory effect of PLIUS with regards to sGAG synthesis in rat chondrocyte monolayer and rabbit chondrocyte 3D collagen gel systems, respectively. Therefore, the studies described in the following chapter were undertaken to determine whether the nature of the response was highly dependent on the model system employed. Consequently, a bovine chondrocyte monolayer culture system was adapted with a protocol similar to that employed by Parvizi *et al.* (1999) in order to test the hypothesis that PLIUS stimulates the synthesis and elaboration of sGAG in a monolayer system. SATA intensities of 30mW/cm^2 and 100mW/cm^2 were used to examine whether the response was influenced by the intensity of the ultrasound. Biochemical assays were employed to quantify sGAG synthesis and cell proliferation over an eight day culture period.

5.2 Materials and Methods

5.2.1 Preparation of chondrocyte monolayer culture

Chondrocytes were isolated from bovine articular cartilage, according to the standard procedures described in Section 3.2. To review briefly, articular cartilage was isolated from the proximal surface of bovine metacarpal joints prior to digestion with pronase and collagenase. The isolated chondrocytes were then checked for viability (>95%) and seeded in the wells of six-well plates at approximately 1 million cells per well ($\sim 100,000$ cells/cm²), filled with 6ml of DMEM + 20% FCS and maintained at 37°C / 5% CO₂ for 72 hours before exposure to ultrasound.

5.2.2 PLIUS regime

Each six-well plate was stimulated with PLIUS by placement of the plate on the six transducers with the use of coupling gel and manipulation of the plate to eliminate any air bubbles (Section 3.3). Cultures were stimulated once daily with PLIUS at one of two SATA intensities, namely 30mW/cm² and 100mW/cm².

Two separate chondrocyte isolations were performed at an intensity of 30mW/cm² studies, labelled 0206 and 0306. Two chondrocyte isolations were undertaken at an intensity of 100mW/cm², labelled 0905 and 1205. After the initial 72 hour culture period, wells were exposed to a 20-minute period of PLIUS once at day 3, 5 or 7 (where day 0 is day of plating), based on the protocol adopted by Parvizi *et al.* (1999). Control cultures remained non-stimulated in separate six-well plates. Medium was changed on day 3, 5 and 7, and saved for subsequent analysis.

5.2.3 Temporal Changes in sGAG and DNA Content

After the final PLIUS stimulation, both test and control medium was removed and replaced with 2ml medium supplemented with 10 μ Ci ³⁵S-sulphate and 10 μ Ci [³H] thymidine for a 24 hr period, for the assessment of the rate of sGAG production and chondrocyte proliferation, respectively. After the 24 hour incubation period - occurring at days 4, 6 or 8 of culture - the medium was removed and chondrocytes were digested with 1 ml of papain digest buffer (see Section 3.8.1) with 5 μ l papain (560 units.ml⁻¹, Sigma, UK). Cell digests were then pipetted into bijoux tubes for subsequent analysis. Total sGAG content in both cell digest and culture medium was determined using the DMB method (Section 3.8.2) and total DNA content in the digest was determined using

the Hoescht 33258 method (Section 3.8.4). Incorporation of sulphate into newly synthesized GAG was determined using the alcian blue precipitation method (Section 4.2.4), and [^3H] thymidine incorporation into newly-synthesised chondrocyte DNA was measured by the trichloroacetic acid (TCA) precipitation method (Section 4.2.5).

5.2.4 Statistical Analysis

Previous work in the host lab revealed data which was normally distributed for each cell activity parameter. Accordingly, unpaired Student's t-tests were used for analysis to compare PLIUS-stimulated constructs with non-stimulated controls at each time-point. A confidence level of 5% ($p < 0.05$) was considered statistically significant.

5.3 Results

The following results display the total sGAG content, total DNA content, sulphate incorporation rate and [^3H]thymidine incorporation following stimulation using PLIUS at intensities of $30\text{mW}/\text{cm}^2$ and $100\text{mW}/\text{cm}^2$.

5.3.1 Total sGAG Content

5.3.1.1 $30\text{mW}/\text{cm}^2$ studies

Sulphated GAG content was estimated for each of the six samples of the PLIUS and control monolayer groups, normalized to wet weight, and a mean value and standard deviation determined. The sGAG content released into the medium was also calculated, as well as the ratio of sGAG content in the medium compared to the total sGAG (monolayer + medium). The results for the two $30\text{mW}/\text{cm}^2$ isolations 0206 and 0306 are presented in Figure 5.1 and Table 5.1. They indicate a consistent increase in sGAG content over the 8 day culture period for chondrocytes in both the control group and the group exposed to once-daily ultrasound (termed PLIUSx1) in terms of:

- total sGAG content (Figures 5.1C and D)
- content in the monolayer alone (Figure 5.1A and B) and
- percentage of total sGAG contained in the medium (Table 5.1). The medium values for each time point were cumulative, so that comparisons could be made between sGAG content in the monolayer and medium at each time-point.

Close examination of the results reveal that in the majority of cases there was no difference between the total sGAG content of stimulated and non-stimulated cells.

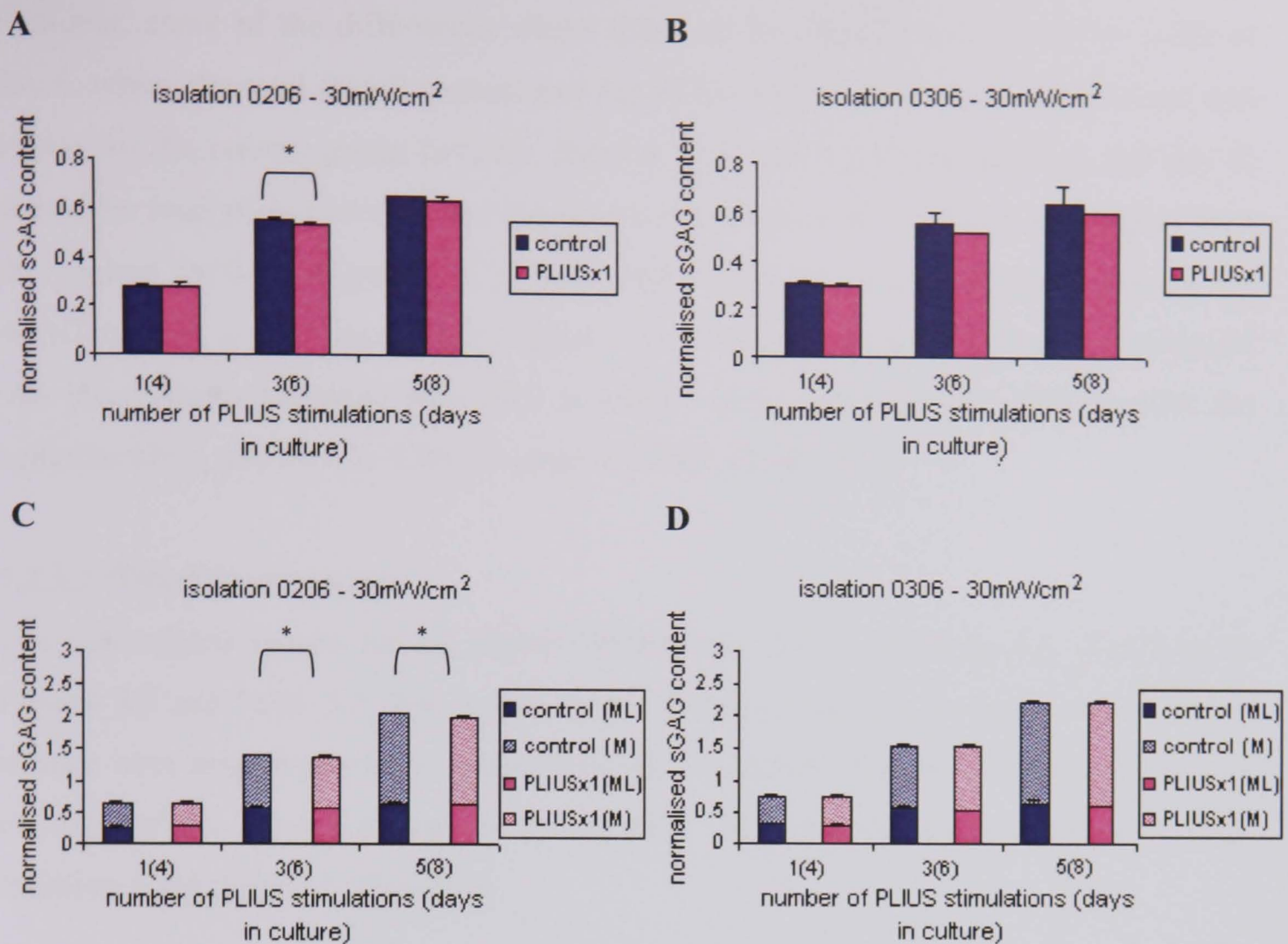


FIGURE 5.1: Effect of pulsed low intensity ultrasound (PLIUS) on total sGAG content in chondrocyte monolayer culture undertaken from two separate isolations (isolations 0206 and 0306). **A** and **B** show sGAG contained in monolayer alone. **C** and **D** show total sGAG content split between monolayer (ML) and that released into the medium (M). Experimental groups involved chondrocyte monolayer culture exposed to 30mW/cm² once every 24 hours (PLIUSx1) after a 72 hour initial culture period. Control groups remained non-stimulated. Values represent mean with error bars showing standard deviation ($n=6$). Values for medium are cumulative. Statistical differences between PLIUSx1 and control are indicated such that $*p<0.05$.

TABLE 5.1: Effect of PLIUS at 30mW/cm² on the ratio values of sGAG content released in the medium when compared to total sGAG content (monolayer + medium). Results were obtained from two separate isolations (0206 and 0306).

	Percentage of total sGAG in medium			
	Isolation 0206		Isolation 0306	
	Control	PLIUSx1	Control	PLIUSx1
Day 4	58	56	58	60
Day 6	60	60	64	66
Day 8	68	68	71	73

However, some of the differences were found to be significant for isolation 0206 at day 6, where the total sGAG content and the sGAG content in the monolayer alone was higher for the control group ($p < 0.05$, Figures 5.1C and 5.1A respectively), and day 8, where the total sGAG content and the sGAG contained in the medium was higher than the control ($p < 0.05$, Figure 5.1C). Both cell isolations gave comparable values for sGAG content at each time-point (Figure 5.1). The percentage of total sGAG released into the medium increased with time in culture from approximately 56% to 68% for isolation 0206, and 58% to 73% for isolation 0306 (Table 5.1).

5.3.1.2 100mW/cm² studies

The total sGAG results for the higher 100mW/cm² SATA intensity are illustrated in Figures 5.2 and Table 5.2. The results clearly indicate a general increase in total sGAG content over time for both the control and PLIUS groups (Figure 5.2C and D), as was evident for the lower intensity of stimulation. This trend is most pronounced with isolation 1205 (Figure 5.2B and D).

Table 5.2 shows an increasing ratio of sGAG content in the medium over time from 22% to 50% for isolation 0905, and 35% to 53% for isolation 1205. For both isolations, at all time-points, there was only one difference which was statistically significant, namely that for isolation 0905 at day 8, where more sGAG was released into the medium in the control monolayer ($p < 0.05$, Figure 5.2C).

5.3.2 Total DNA content

Total DNA content was calculated for each of the six samples of the PLIUS and control monolayer groups, normalized to weight wet, and then a mean value was estimated. The DNA content for the 30mW/cm² stimulations (isolations 0206 and 0306) and the 100mW/cm² stimulations (isolations 0905 and 1205) are presented in Figure 5.3, with corresponding controls.

For both the PLIUS-stimulated monolayer and control groups at both SATA intensities, there was an increase in total DNA content with increasing time in culture. The one exception to this trend was evident with isolation 0306, where there was a slight decrease in DNA content between days 6 and 8 for both control and PLIUS-stimulated groups (Figure 5.3B).

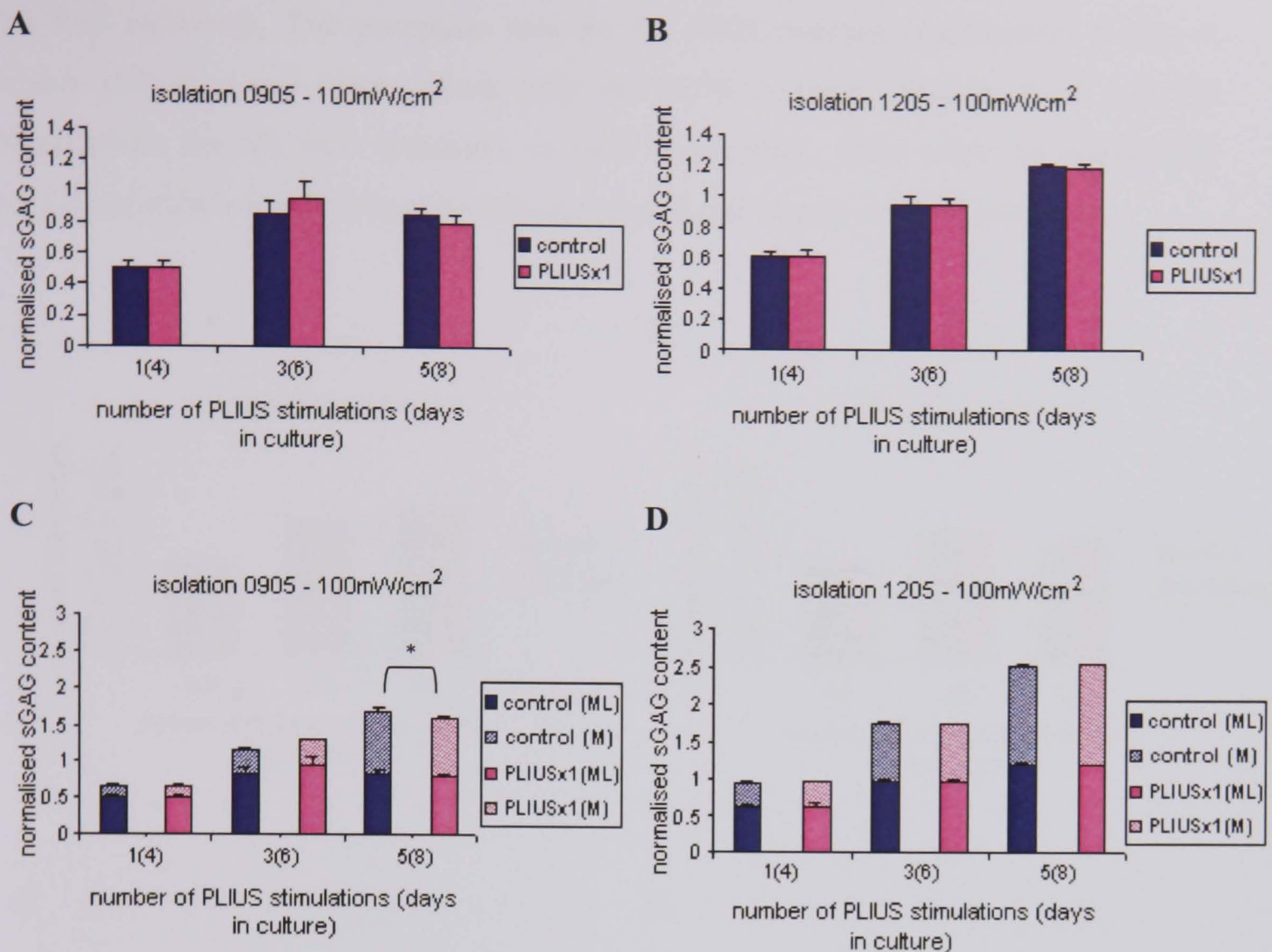


FIGURE 5.2: Effect of pulsed low intensity ultrasound (PLIUS) on total sGAG content in chondrocyte monolayer culture undertaken from two separate isolations (isolations 0905 and 1205). **A** and **B** show sGAG contained in monolayer alone. **C** and **D** show total sGAG content split between monolayer (ML) and that released into the medium (M). Experimental groups involved chondrocyte monolayer culture exposed to 100mW/cm² once every 24 hours (PLIUSx1) after a 72 hour initial culture period. Control groups remained non-stimulated. Values represent mean with error bars showing standard deviation (n=6). Values for medium are cumulative.

TABLE 5.2: Effect of PLIUS at 100mW/cm² on the ratio values of sGAG content released in the medium when compared to total sGAG content (monolayer + medium). Results were obtained from two separate isolations (0905 and 1205).

	Percentage of total sGAG in medium			
	Isolation 0905		Isolation 1205	
	Control	PLIUSx1	Control	PLIUSx1
Day 4	22	22	35	36
Day 6	28	26	45	45
Day 8	50	49	52	53

The values for DNA content were generally comparable for each time-point for three of the four isolations. The exception was for the 0905 isolation, particularly at day 4, which yielded lower DNA values than the 1205 isolation (Figures 5.3C and D). Nonetheless for all four isolations at each time point, there were no statistically significant differences between PLIUS-stimulated and control cultures ($p>0.05$).

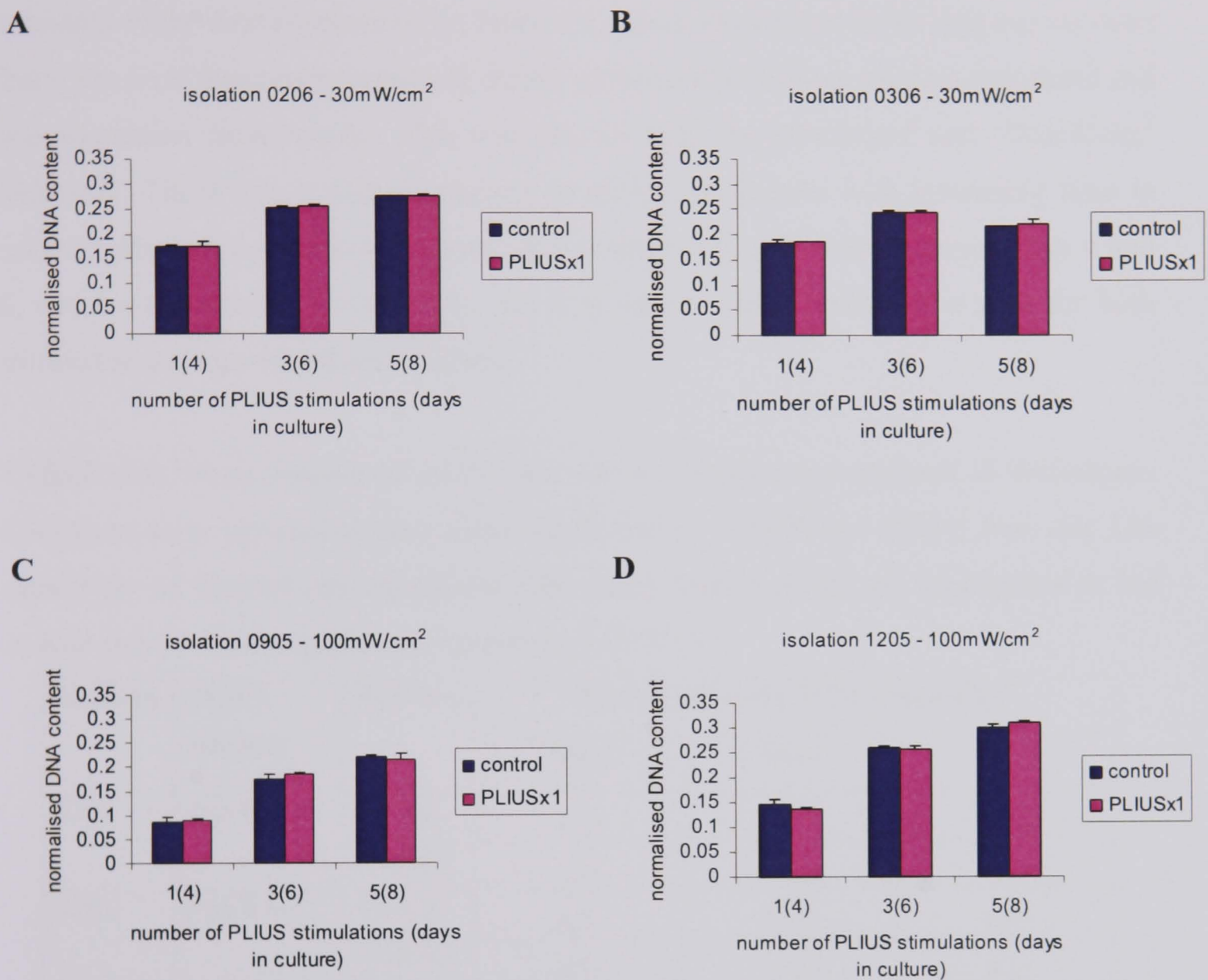


FIGURE 5.3: Effect of pulsed low intensity ultrasound (PLIUS) on total DNA content in chondrocyte monolayer culture undertaken from four separate isolations and at two PLIUS SATA intensities. Isolations 0206 and 0306 were stimulated with PLIUS at 30mW/cm² (Figures A and B respectively), and isolations 0905 and 1205 at 100mW/cm² (Figures C and D, respectively). Experimental groups involved chondrocyte monolayer culture exposed to PLIUS once every 24 hours after a 72 hour initial culture period. Control groups remained non-stimulated. Values represent mean with error bars showing standard deviation (n=6).

5.3.3 Cell activity

The total sGAG and total DNA data, detailed in the previous sections, can be employed to provide an assessment on cell activity in terms of sGAG productivity. Specifically, using the factor of one bovine chondrocyte produces 7.7pg of DNA (Kim *et al.*, 1988), the DNA values obtained from the Hoescht 33258 assay were used to calculate both the cell number and consequently the mean sGAG produced per cell (Section 4.3.2). A summary of the data is presented in Table 5.3, which shows that in the majority of cases there was no difference between cell sGAG productivity between PLIUS-stimulated and non-stimulated chondrocytes. This was true for both the 30mW/cm² and 100mW/cm² isolations. There was an overall increase in sGAG production with increasing time in culture, although for the 100mW/cm² studies there was a decrease between days 4 and 6, which subsequently increased by day 8 ($p < 0.05$). These trends were seen for both stimulated and non-stimulated cultures.

TABLE 5.3: Mean amount of sGAG per cell in chondrocytes cultured in monolayer. Constructs were exposed to once daily 30mW/cm² or 100mW/cm² PLIUS from day 3 in culture ($n=6$). Statistically significant differences from controls are highlighted in red or blue (up- or down-regulation respectively) ($p < 0.05$).

Isolation	PLIUS intensity	Regimen	Mean sGAG/cell ($\times 10^{-10}$) at time point		
			Day 4	Day 6	Day 8
0206	30mW/cm ²	Control	0.29	0.31	0.33
		PLIUSx1	0.28	0.30	0.32
0306	30mW/cm ²	Control	0.31	0.35	0.44
		PLIUSx1	0.31	0.34	0.43
0905	100mW/cm ²	Control	0.60	0.45	0.50
		PLIUSx1	0.56	0.47	0.45
1205	100mW/cm ²	Control	0.49	0.42	0.44
		PLIUSx1	0.53	0.42	0.43

5.3.4 SO₄ incorporation

The rate of incorporation of sulphate into newly synthesized GAG for chondrocytes exposed to 30 and 100 mW/cm² is presented graphically in Figure 5.4. Incorporation rates are represented as a percentage of control values.

Figure 5.4A and 5.4B, related to stimulation intensities of 30mW/cm², reveal no significant difference in sulphate incorporation rates between stimulated and non-

stimulated monolayer cultures. Indeed for both isolations the stimulated group was between 96% and 107% of the control values. At the higher $100\text{mW}/\text{cm}^2$ intensity, there was some variation between isolations 0905 and 1205 in terms of incorporation relative to controls at days 4 and 6 of culture. However, none of the differences were statistically significant between control monolayers and those stimulated with $100\text{mW}/\text{cm}^2$ (Figure 5.4C and D).

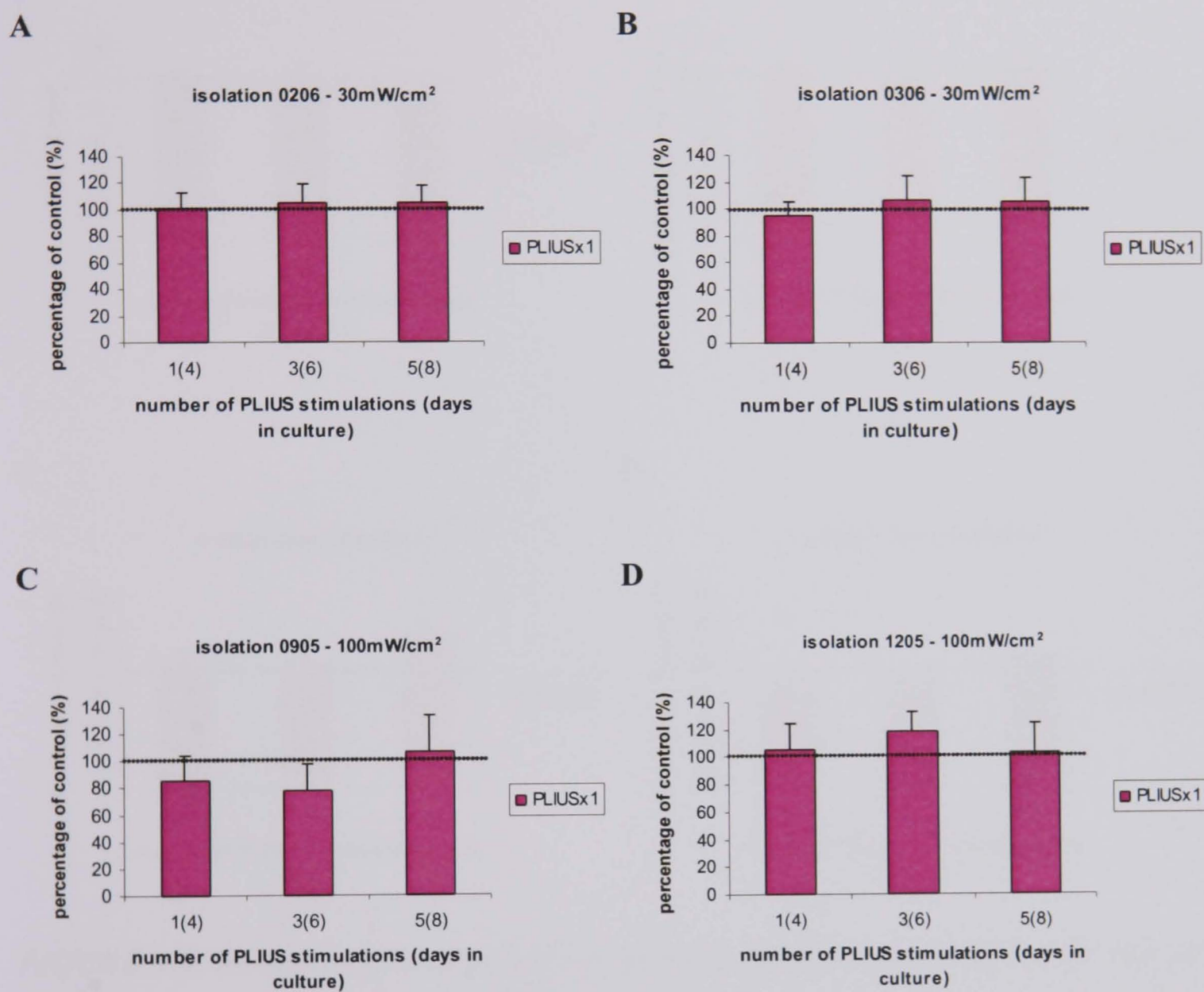


FIGURE 5.4: Relative effects of pulsed low intensity ultrasound (PLIUS) on the rate of SO_4 incorporation in chondrocytes in monolayer, undertaken from four separate isolations and at two PLIUS SATA intensities. Isolations 0206 and 0306 were stimulated with PLIUS at $30\text{mW}/\text{cm}^2$ (Figures A and B respectively), and isolations 0905 and 1205 at $100\text{mW}/\text{cm}^2$ (Figures C and D respectively). Experimental groups involved chondrocyte monolayer culture exposed to PLIUS once every 24 hours after a 72 hour initial culture period. Control groups remained non-stimulated. Values represent mean PLIUS SO_4 incorporation (units: $\mu\text{MSO}_4/\text{h}/\mu\text{g DNA}$) as a percentage of control with error bars showing standard deviation ($n=6$).

5.3.5 [^3H]thymidine incorporation

The rate of incorporation of [^3H]thymidine into newly synthesized DNA for chondrocytes exposed to 30 and 100 mW/cm² is presented graphically in Figure 5.5. Incorporation rates are represented as a percentage of control values.

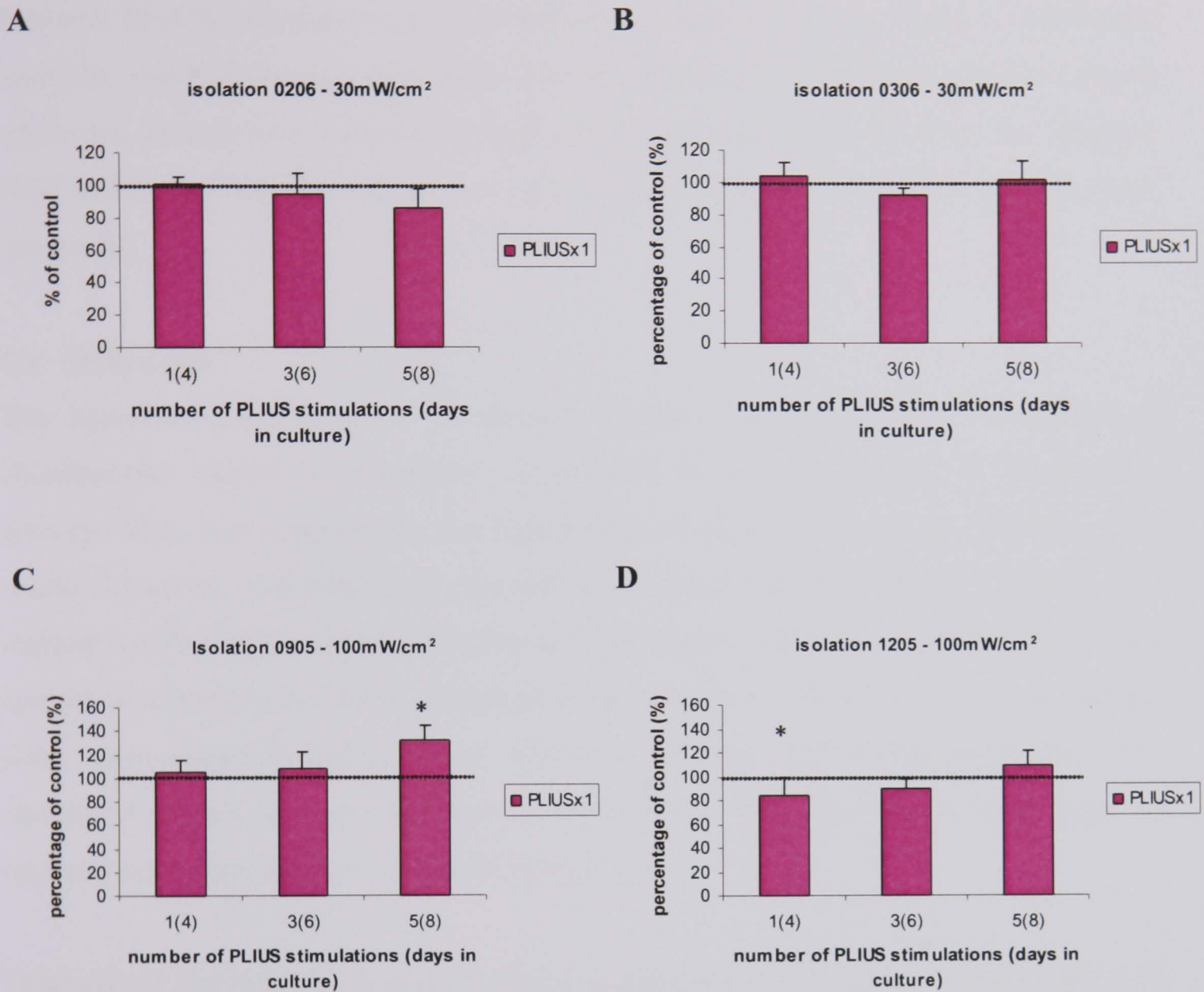


FIGURE 5.5: Relative effects of pulsed low intensity ultrasound (PLIUS) on the rate of [^3H]thymidine incorporation in chondrocytes in monolayer, undertaken from four separate isolations. Isolations 0206 and 0306 were stimulated with PLIUS at 30mW/cm² (Figures A and B respectively), and isolations 0905 and 1205 at 100mW/cm² (Figures C and D, respectively). Chondrocyte monolayer cultures were exposed to PLIUS once every 24 hours after a 72 hour initial culture period. Control groups remained non-stimulated. Values represent mean PLIUS [^3H]thymidine incorporation (units: CPM/ μg DNA) as a percentage of control with error bars showing standard deviation (n=6). Statistical differences between PLIUSx1 and control are indicated such that *p<0.05.

As with the sulphate incorporation data, Figure 5.5 shows that in 10 out of 12 cases there was no statistically significant difference in [³H] thymidine incorporation between PLIUS-stimulated and non-stimulated cultures. At both SATA intensities, there were marginal differences between isolations in terms of PLIUS-stimulated incorporation rates relative to controls. However, there were two cases for which the difference between PLIUS-stimulated and non-stimulated cultures at the higher 100mW/cm² intensity were statistically significant. One example involved isolation 0905 at day 8, where the former was significantly higher than the latter, and the other for isolation 1205 at day 4, where the former was significantly lower than the latter ($p < 0.05$ in both instances).

5.4 Discussion

The hypothesis examined in the present chapter was that PLIUS stimulation of chondrocytes seeded in monolayer would lead to an up-regulation of chondrocyte activity. This was assessed by the elaboration of sGAG and cell proliferation. The results, however, overwhelmingly support a null hypothesis. For all isolations, the vast majority of PLIUS-stimulated chondrocyte monolayers behaved very similarly to their control counterparts ($p > 0.05$). Although some variation was seen between isolations, these were generally found to be common for both PLIUS-stimulated and non-stimulated groups and can therefore be attributed to isolation-specific differences as opposed to changes specific to PLIUS stimulation.

Total sGAG and total DNA content, and to a lesser extent ³⁵S-sulfate incorporation and [³H] thymidine incorporation results, revealed a temporal increase in culture. However, by day 8, the cells were generally fully confluent in the wells (Appendices 1 and 2), which could account for the reduction in increase in sGAG and DNA content between days 6-8 in culture when compared to days 4-6 in culture (Figures 5.1, 5.2 and 5.3).

Minimal differences were found between PLIUS and control groups, with one case of significant difference in the sGAG results (Figure 5.1A), one case for the cell activity results (Table 5.3) and two cases with the [³H] results (Figure 5.5C and D) ($p < 0.05$). However, of the four cases, only two yielded a stimulatory effect of PLIUS on monolayer cultures (Table 5.3 and Figure 5.5C, $p < 0.05$). There was no significant PLIUS-induced promotion of sGAG release into the medium (Tables 5.1 and 5.2). In addition, comparison of the results from the two levels of ultrasound intensity revealed

no data to suggest that either was likely to consistently stimulate primary bovine chondrocytes cultured in monolayer cultures.

Examination of published studies employing chondrocytes in monolayer showed some differences in methodology when compared to the present work. For example, Parvizi and colleagues (1999) cultured chondrocyte monolayer using condyle cartilage from neonatal rats. They used PLIUS at SATA intensities of 50 and 120mW/cm², for 10 minutes daily from day 3 in culture. A water bath was used to apply PLIUS to the six-well plates with a 3mm water gap. A 2mm height of medium was used to culture the cells. Although different methods were used to measure proteoglycan and cell proliferation, these authors reported a temporal increase in proliferation. However, there were no significant differences between control and PLIUS-stimulated cultures at any time, which is consistent with the presented findings. Parvizi and colleagues (1999) reported that microscopic examination directly after PLIUS stimulation at day 4 with the higher 120mW/cm² SATA intensity revealed cell detachment from the plate. In the present study, a seeding density was utilized that was six-fold greater than in the previous study. By day 3 of culture, there were areas of confluence in the 6-well culture plates, although in the centre of the plate (where microscope images presented in Appendices 1 and 2 were taken) confluency was reached between days 6 and 8. No detachment of chondrocytes was seen after stimulation with PLIUS at either 30 or 100mW/cm² at any time-point up to day 8.

Parvizi and co-workers (1999) also reported no effect of PLIUS on levels of collagen I and II mRNA, although there was an increase in aggrecan gene expression at days 6 and 8 for stimulated cultures, at both 50 and 120mW/cm². In terms of the downstream synthetic response of these cells, the authors noted that SO₄ incorporation was enhanced by PLIUS, as shown by the greater rate of increase between days 4 and 6 for stimulated cultures when compared to controls (p<0.001). However, closer examination of these results, which are reproduced in Figure 5.6, revealed that there were no significant differences in the absolute values of SO₄ incorporation between experimental groups at any time-point. Furthermore, the apparent 'increased' SO₄ incorporation rate seen between days 4 and 6 for PLIUS-stimulated cultures was mainly due to a slightly raised value for the control culture at day 4 (circled in red in Figure 5.6). Therefore, a PLIUS-stimulated increase in SO₄ incorporation is not substantiated from their results. Indeed, the only clear influence that PLIUS has on rat chondrocyte monolayer culture involves

enhanced expression of the aggrecan gene at days 6 and 8 of culture. Clearly, this increased gene expression did not translate into significant increases in proteoglycan synthesis as indicated in Figure 5.6.

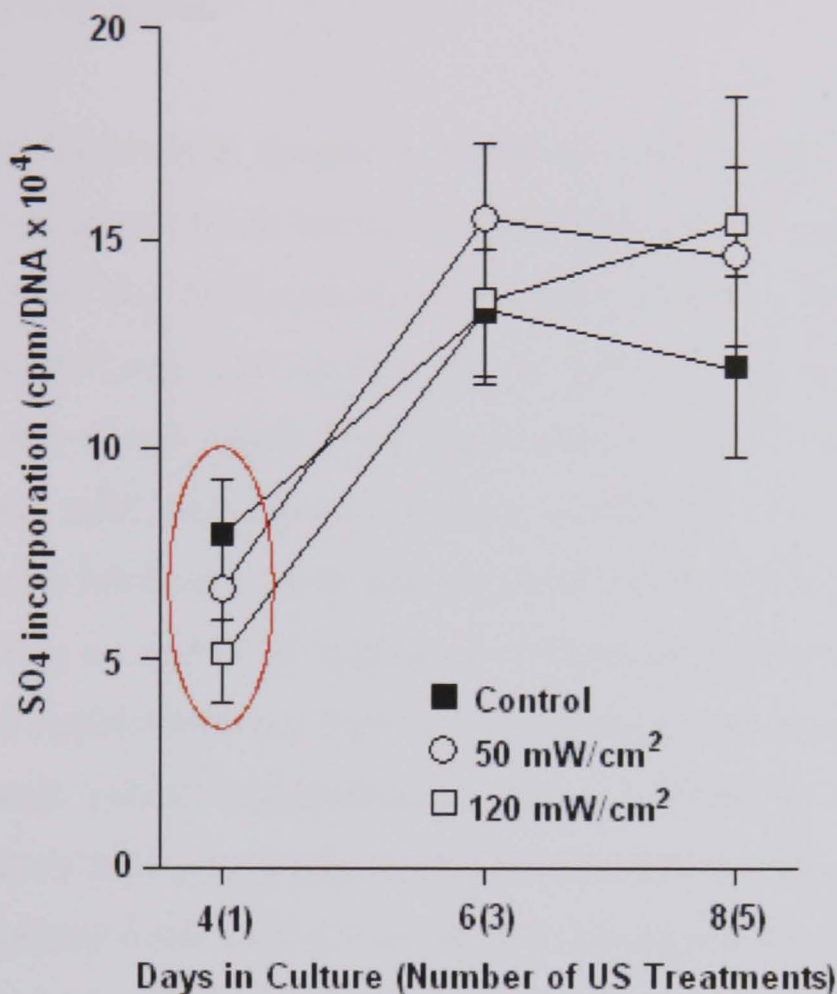


FIGURE 5.6: Sulphate incorporation data obtained by Parvizi and colleagues (1999). The red circle highlights initial incorporation values at day 4, where control rates were slightly raised compared to PLIUS-stimulated cultures.

A more recent study undertaken by Kopakkala-Tani and co-workers (2006) employed bovine chondrocytes cultured in monolayer, in a similar manner to that presented in the present chapter. They reported that a PLIUS of SATA intensity 580mW/cm², applied once daily for 10 minutes, was able to stimulate sulphate incorporation over a five day period.

There were a number of differences between Kopakkala-Tani's study and the present study, namely:

- A higher PLIUS intensity was employed in the previous study
- A 10 minute stimulation period was used, as opposed to the 20 minutes used in the present work

- Kopakkala-Tani and colleagues (2006) initiated the PLIUS stimulation regimen after 9 days of monolayer culture, whereas the present study commenced stimulation after 3 days of culture
- The authors employed a 110mm water gap between the ultrasonic transducers and culture well plates.

The intensity study described in chapter 3, found that an intensity of $300\text{mW}/\text{cm}^2$ was sufficient to cause gross cell death throughout the depth of a 3D agarose construct. The use of a 110mm water gap by Kopakkala-Tani and colleagues (2006) would have, to some extent, dissipated any heat production by such a high intensity and thereby reduced the incidence of cell death. Their application of PLIUS after 9 days in culture suggested that their cells had already attained confluence. As such, they reported significant differences between control and stimulated cultures after the second PLIUS-stimulation, occurring on day 10 of culture. In contrast, in the present experimental set up, ultrasound was applied between days 3-7. Confluency was attained toward the end of this experimental period (Appendices 1 and 2). There is the possibility that monolayer confluency may play a role in PLIUS-stimulation. However, the intensities employed in the present work and by Parvizi and colleagues are much lower than that used by Koppakala-Tani and colleagues in their study. It is possible that intensities up to $120\text{mW}/\text{cm}^2$ may be lower than the threshold for chondrocytes in monolayer to appreciably sense the ultrasonic signal and respond accordingly in terms of stimulatory sGAG synthesis. Additionally the use of a water bath by the latter group may alter the PLIUS signal in such a way, both in terms of incident signal and reduction of residual heating, as to cause promotion of extracellular matrix synthesis.

In conclusion, based on the present experimental arrangement, the application of once-daily PLIUS at intensities of 30 and $100\text{mW}/\text{cm}^2$ had no effect on sGAG synthesis or proliferation of chondrocytes seeded in a monolayer system.

Chapter 6

Calcium Signalling in Pulsed Low Intensity Ultrasound-stimulated Chondrocytes

6.1	Introduction	146
6.2	Materials and methods	147
6.2.1	Preparation of bicarbonate-free chondrocyte medium	147
6.2.2	Preparation of 3D chondrocyte-agarose constructs	147
6.2.3	Preparation of chondrocyte monolayer culture	147
6.2.4	Fluo-4 labelling of constructs and monolayers	148
6.2.5	Application of PLIUS to chondrocytes	149
6.2.6	Ultrasound regime	150
6.2.7	Confocal system and experimental parameters for calcium signalling	150
6.2.8	Cell selection and identification of calcium transients	151
6.2.9	Statistical analysis	152
6.2.10	Summary of experimental test procedures	153
6.3	Results	154
6.3.1	Effect of PLIUS on calcium signalling in chondrocytes in 3D culture	154
6.3.2	Effect of PLIUS on calcium signalling in chondrocytes cultured in monolayer	157
6.3.3	Influence of PLIUS intensity on calcium signalling in chondrocytes in 3D culture	160
6.3.4	Influence of PLIUS intensity on calcium signalling in chondrocytes cultured in monolayer	164
6.4	Discussion	169

6.1 Introduction

Mechanotransduction, as highlighted in section 2.3 of this thesis, involves events at the tissue level, the cellular level and the intracellular level. Intracellular calcium ($[Ca^{2+}]_i$) is a ubiquitous second messenger involved in many cellular processes. Mechanical perturbation of the cell membrane has been shown to cause increases in the $[Ca^{2+}]_i$ concentration of several cell types, including chondrocytes (Guilak *et al.*, 1994; 1999; Xia and Ferrier, 1995; Hung *et al.*, 1996a and 1996b; Eifler *et al.* 2006). Pulsed low intensity ultrasound (PLIUS), equivalent to high frequency micromechanical perturbations of the order of kPa, may produce the same intracellular changes seen with compressive and cyclic mechanical loading (Pinggwan-Murphy *et al.*, 2006). Indeed, one study reported that calcium signalling mediated ultrasound-stimulated aggrecan synthesis in rat chondrocyte monolayer cultures (Parvizi *et al.*, 2002). In addition, they reported that ultrasonic intensity influenced calcium response. However, an equivalent study examining the effects on chondrocytes seeded in 3D constructs exposed to PLIUS has not been reported.

The present chapter tests the hypothesis that pulsed low intensity ultrasound activates $[Ca^{2+}]_i$ signalling in bovine chondrocytes, both in monolayer and 3D culture, and that this response is influenced by the intensity of the ultrasound. This will be undertaken by labelling chondrocytes with Fluo-4, a fluorescent indicator dye, and recording changes in $[Ca^{2+}]_i$ using confocal microscopy techniques. As detailed in Section 3.6, a rig was designed which could be mounted onto the stage of a confocal microscope enabling simultaneous ultrasonic stimulation of chondrocytes and confocal imaging. Briefly, cells were labelled with Fluo-4 and then exposed to PLIUS for a period of 10 minutes. Temporal confocal imaging examined the calcium levels in cells of interest in real-time over the experimental period. Separate constructs/monolayers served as controls in the absence of PLIUS exposure. In a separate set of experiments investigating the effects of PLIUS intensity on $[Ca^{2+}]_i$ levels, cells were exposed to a regimen in which the intensity of PLIUS was increased over a 20-minute exposure period.

6.2 Materials and methods

The following sections detail the preparation of the chondrocyte cultures, cell labelling and imaging techniques, and calcium measurement protocols.

6.2.1 Preparation of bicarbonate-free chondrocyte medium

Bicarbonate-free DMEM (D5030, Sigma, UK) (Pingguan-Murphy, 2006) was reconstituted according to manufacturer's instructions. 800ml of distilled water (dH₂O) was added to the powder and mixed using a magnetic stirrer. Small amounts of HCl or NaOH were added to adjust the pH to 7.4, as measured using an electronic pH meter (Fisherbrand, Hydrus 300, Orion Research Inc., USA). A further 200ml of dH₂O was added to make the volume up to 1 litre. Serum and other additives were used to supplement the medium, as previously described in table 4.1. In addition 1g/litre glucose (Sigma-Aldrich, Poole, UK) was added. The medium (termed ^{BF}DMEM + 16.1% FCS) was filtered using a 0.22µm pore cellulose acetate filter before being aliquoted and stored at -20°C.

6.2.2 Preparation of 3D chondrocyte-agarose constructs

Chondrocytes were isolated from bovine articular cartilage and seeded in agarose constructs, according to the standard procedures described in Sections 3.2. and 3.6. Briefly, articular cartilage was digested with pronase and collagenase and the isolated chondrocytes seeded at a final concentration of 10×10^6 cells.ml⁻¹ in 3% (w/v) low gelling agarose (Sigma, UK). Constructs were gelled at 4°C for 20 minutes in specially made perspex moulds that could be held inside the chamber of the microscope-mounted ultrasound rig (both detailed in Section 3.6). Construct dimensions were 5x5x5mm. The constructs were placed in a 140mm Petri dish (Sterilin, UK), covered with 60ml of DMEM + 16.1% FCS and maintained at 37°C / 5% CO₂ for up to 24 hours prior to the start of the calcium imaging experiments.

6.2.3 Preparation of chondrocyte monolayer culture

Bovine chondrocytes were isolated as described in Section 3.2.2, cultured in monolayer at a concentration of 20,000 cells/cm² area and maintained in DMEM + 16.1% FCS at 37°C / 5% CO₂ for a 72 hour period prior to the start of the calcium imaging experiments.

Initially, monolayers were cultured on 22x40mm glass coverslips, for subsequent placement into the appropriate gap at the base of the confocal mounted rig, using silicon grease as a seal. However, when the coverslips were removed from culture, their underside needed to be dry in order for the silicon grease seal to remain airtight. Attempts were made to dry the underside of the coverslip with tissue paper, but this proved difficult without disrupting the monolayer, and inevitably there were problems with leaking of the rig once the confocal medium was added to the chamber. This compromised the transmission of PLIUS and made imaging impossible.

For this reason the use of the rig was discontinued for use with monolayer imaging experiments, and was replaced by a system involving 35mm glass-bottomed sterile Petri dishes (MaTtek Corp., USA), the glass component of which permitted high resolution microscopic images to be taken. Chondrocytes were seeded into these dishes as described above and made up to a total volume of 2ml. They were incubated at 37°C / 5% CO₂ for a 72 hour period prior to the calcium imaging experiments.

6.2.4 Fluo-4 labelling of constructs and monolayers

Fluo-4, a single-wavelength indicator, was chosen for calcium imaging experiments as it had been successfully used to label chondrocytes in previous studies in the host lab (Knight et al, 2003; Pinguan-Murphy et al, 2005).

The acetoxymethyl (AM) ester form of Fluo-4, termed Fluo-4AM, was used for calcium imaging experiments. Fluo-4 is a predominantly negatively charged molecule, and therefore impermeable to the lipid bilayer membrane of the cell. However, the uncharged hydrophilic nature of the AM ester masks the negative charge on the carboxyl groups, enabling transportation across the cell membrane. Inside the cell esterase enzymes hydrolyse the ester to expose the carboxyl groups, allowing the Fluo-4 to become fluorescent and preventing its transport back out of the cell. Fluo-4 is maximally excited at a wavelength of 494nm, with excitations between approximately 425nm and 525nm (Gee *et al.*, 2000). However, the fluorescence intensity is proportional to the concentration of Ca²⁺, as shown in Figure 6.1, thereby enabling the use of Fluo-4 as a [Ca²⁺]_i indicator.

A 5µM solution of Fluo-4AM was made up using ^{BF}DMEM + 16.1% FCS. Chondrocyte-agarose constructs were incubated at 37°C in this solution for 1 hour,

before being incubated for 10 minutes in BF DMEM + 16.1% FCS, termed the post-staining period, to remove excess label immediately prior to imaging. Monolayer cultures were stained with the same concentration of Fluo-4AM for 30, 45, or 60 minutes. An acceptable level of staining of chondrocyte monolayer cultures was achieved in 30 minutes, followed by a 10 minute post-staining period.

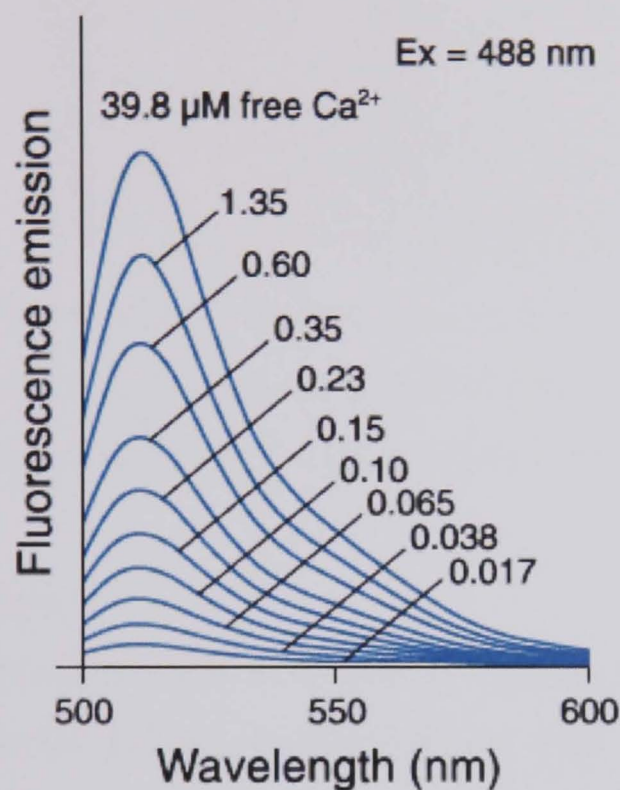


FIGURE 6.1: Fluorescence emission spectra of Fluo-4 in solution with free Ca^{2+} concentrations as labelled. Adapted from the InvitrogenTM website.

6.2.5 Application of PLIUS to chondrocytes

The microscope mounted test rig described in Section 3.6 was used to apply PLIUS to chondrocyte-agarose constructs, while enabling simultaneous visualisation of cells labelled with Fluo-4.

As discussed in Section 6.2.3, the ultrasound rig proved to be unsuitable for monolayer experiments. Instead, 35mm glass-bottomed sterile Petri dishes were used to culture the chondrocytes. An ultrasonic transducer, with a diameter of 30mm fitted into each dish. Elastic bands were wrapped around the diameter of the transducer to increase its effective diameter, so that it could be positioned and stabilised inside the dish while leaving a fluid-gap between chondrocytes and transducer (Figure 6.2).

After post-staining, the Petri dish was placed onto the stage of the confocal microscope and the transducer appropriately positioned. Preheated BF DMEM + 16.1% FCS was

added to the dish using a 1ml syringe with an attached needle to ensure complete contact between the fluid and the transducer. This arrangement permitted continuous PLIUS transmission to the chondrocyte monolayer.

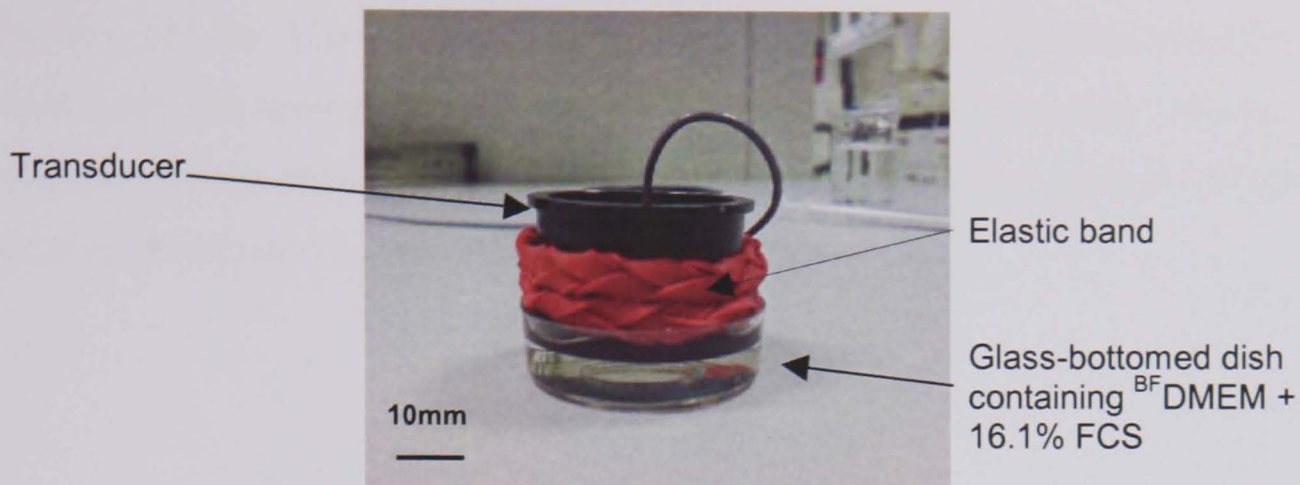


FIGURE 6.2: Glass-bottomed dish (MaTtek Corp., USA) and adapted transducer for application of ultrasound to dish contents. A syringe was used to add additional fluid to the dish to ensure continuous PLIUS transmission to chondrocytes.

6.2.6 Ultrasound regime

In the first set of experiments, PLIUS at $30\text{mW}/\text{cm}^2$ was applied to chondrocyte cultures for a continuous 10 minute period. Control cultures were left non-stimulated for 10 minutes. In separate experiments, the effects of PLIUS intensity were investigated. PLIUS intensity was incremented over 20 minutes, divided into 5 four minute periods corresponding to exposures of 0, 30, 70, 100 and $200\text{mW}/\text{cm}^2$ PLIUS respectively, as using the regimen shown in Figure 6.3. Control cultures were left non-stimulated for a 20 minute period.

Confocal imaging for both sets of experiments involving both monolayer and 3D constructs took place simultaneously over the 10 or 20 minute experimental period.

6.2.7 Confocal system and experimental parameters for calcium imaging

Visualisation of labelled chondrocytes took place using a confocal microscope system (UltraVIEW LCI, Perkin Elmer, Cambridge, UK) with an associated inverted fluorescent microscope (TE Eclipse, Nikon, Kingston-upon-Thames, UK) and a computer workstation for image analysis.

Laser excitation was set at 488 nm with fluorescent emission detected above 500 nm. Images containing at least 15 cells per field of view were captured every 4 seconds over the imaging period with a 20x Plan Apo objective lens, yielding a pixel size of $1.01\mu\text{m}$.

6.2.8 Cell selection and identification of calcium transients

The UltraVIEW Temporal software was used to analyse the calcium signalling experiments. Chondrocytes were selected for analysis that had a homogeneous distribution of the Fluo-4 label. Cells that indicated compartmentalisation were excluded from the analysis due to compartment-specific environmental effects on the fluorescence spectra (Diliberto *et al.*, 1994). Circular regions of interest (ROIs) were placed around individual cells, as shown in Figure 6.4.

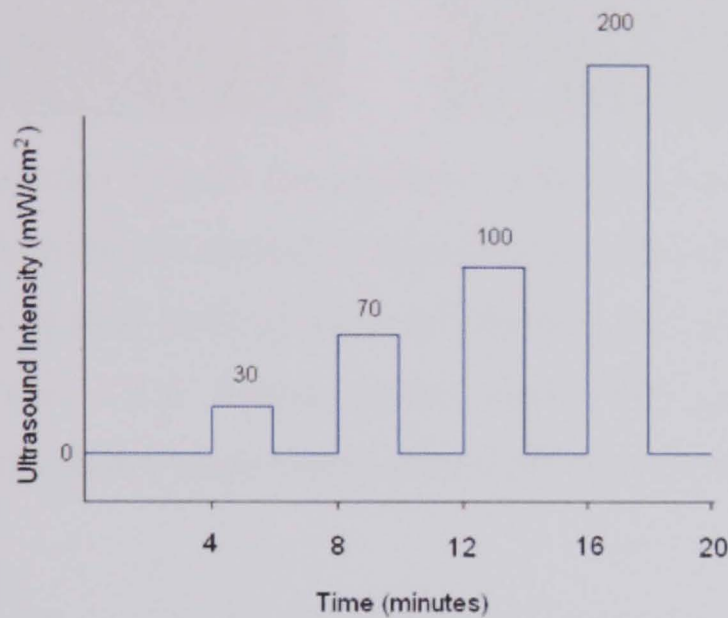


FIGURE 6.3: Schematic diagram showing the nature of the increasing PLIUS intensity applied to chondrocytes cultured in either monolayer or 3D-agarose constructs over a 20-minute period for calcium signalling experiments investigating the influence of PLIUS intensity.

The mean intensity within each ROI was calculated at each time point, and an intensity greyscale was plotted against time to show the temporal variation in $[Ca^{2+}]_i$ concentration. Figure 6.5 illustrates two typical greyscale plots, one from a chondrocyte cultured in 3D-agarose, and the other from a chondrocyte cultured in monolayer. Both responses indicated that the individual chondrocyte utilised $[Ca^{2+}]_i$, characterised by a rapid increase in greyscale intensity followed by a rapid decrease to baseline levels, the spiked shape termed a $[Ca^{2+}]_i$ transient. These transients were manually identified by observation of the greyscale plots, and both the number of transients and the time of the peak of each transient was recorded for each cell (Pingguan-Murphy *et al.*, 2005). The apparent increase in baseline intensity seen in Figure 6.5A may represent an element of specimen drift (as discussed in Section 3.6.3) and had no influence on data retrieval.

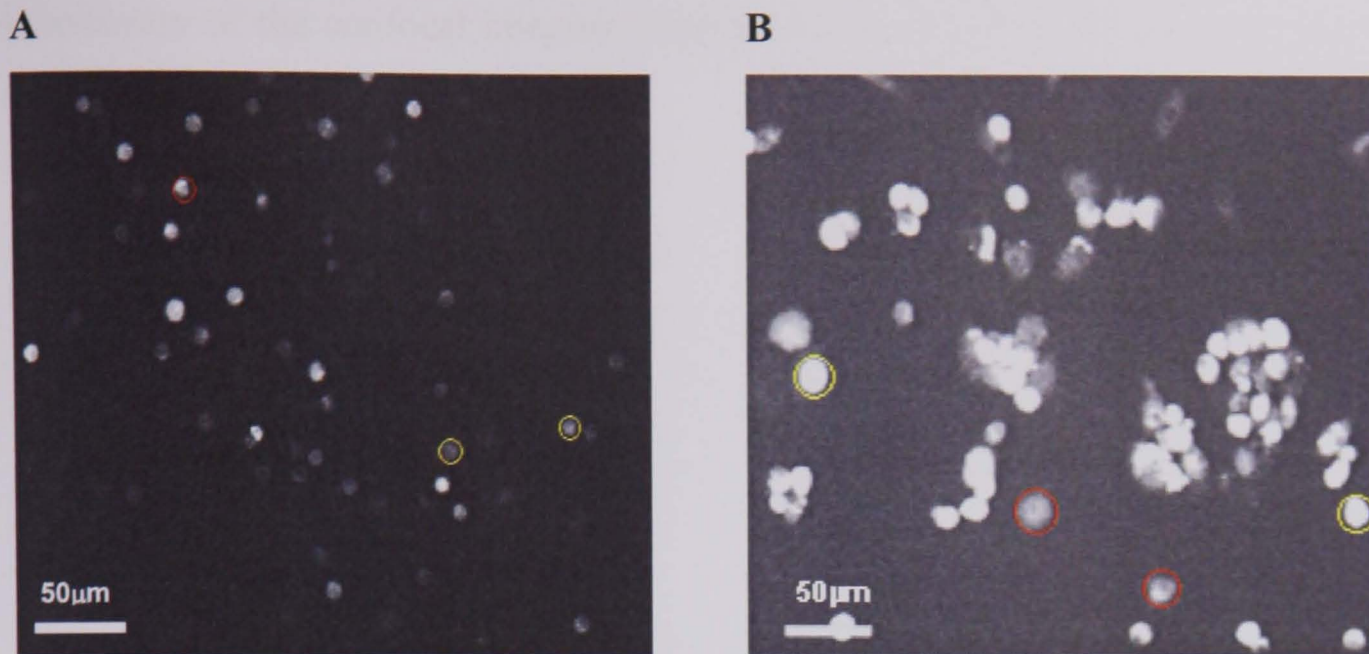


FIGURE 6.4: Selection of cells for calcium signalling analysis. *A* shows a typical field of view of chondrocytes seeded in agarose gel, cultured as described in Section 6.2.2. *B* shows a typical field of view of chondrocytes in monolayer culture, as described in Section 6.2.3. Yellow circles show ROIs around cells chosen for analysis. Red circles show compartmentalised cells which were not used for analysis.

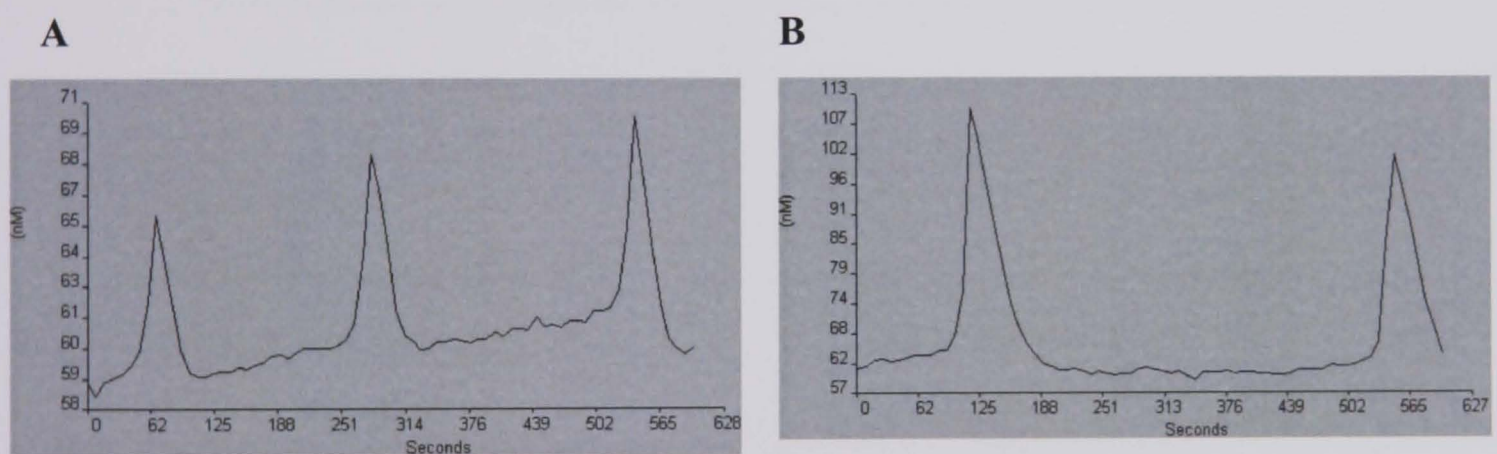


FIGURE 6.5: Two typical greyscale plots, *A* from a chondrocyte in 3D agarose culture, where the cell underwent three $[Ca^{2+}]_i$ transients, and *B* from a chondrocyte in monolayer, where the cell underwent two $[Ca^{2+}]_i$ transients.

6.2.9 Statistical analysis

Experiments were repeated over a number of weeks in order to yield a minimum of ten samples each for PLIUS-stimulated and control conditions. Previous work in the host lab revealed data which was normally distributed for each cell activity parameter (Pinguan-Murphy et al., 2006). Accordingly, unpaired Student's t-tests were used for analysis to compare PLIUS-stimulated constructs with non-stimulated controls. A confidence level of 5% ($p < 0.05$) was considered statistically significant.

6.2.10 Summary of experimental test procedures

A summary of the confocal imaging experiments described in the previous sections is shown in Figure 6.6.

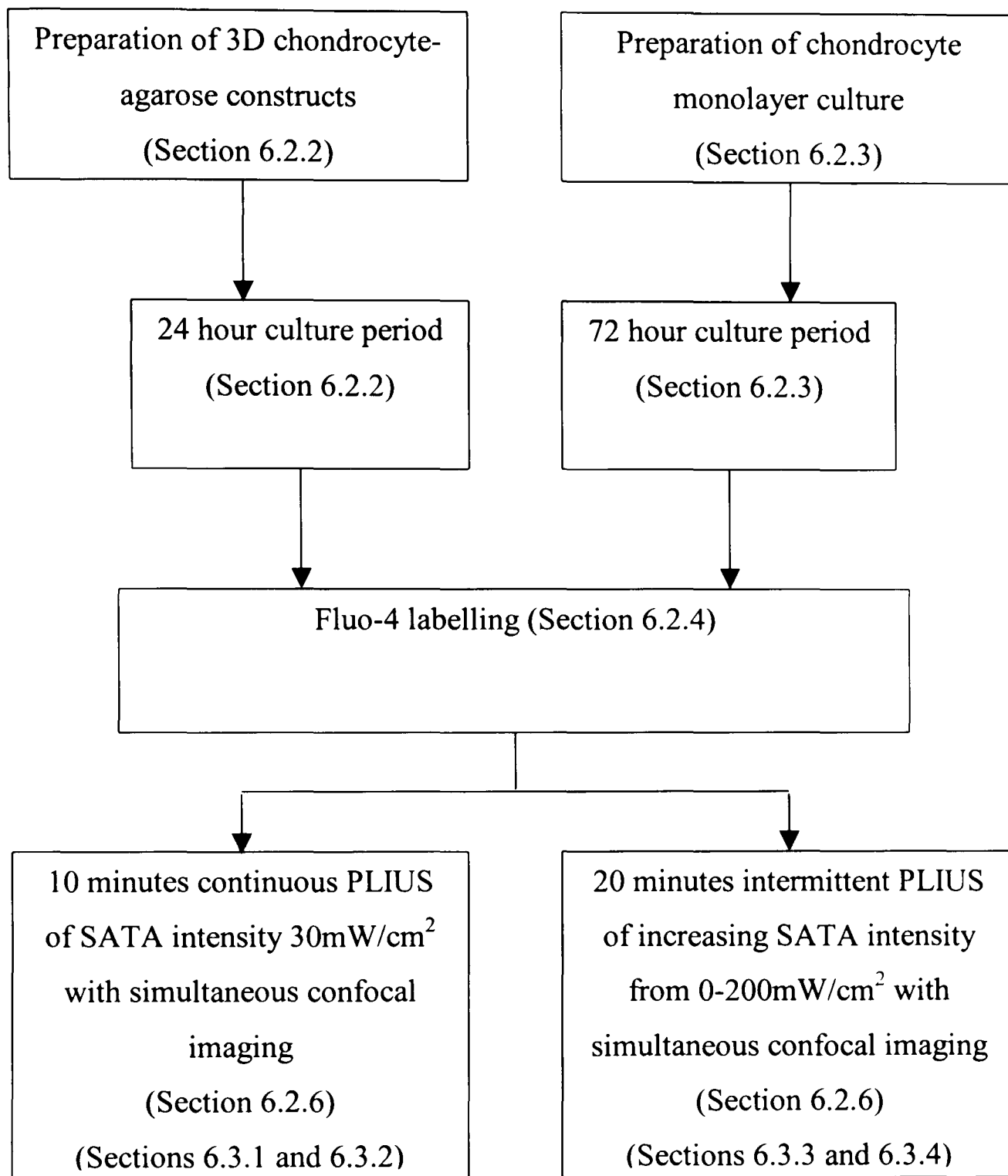


FIGURE 6.6: Summary of experimental procedures with relevant sections.

6.3 Results

6.3.1 Effect of PLIUS on calcium signalling in chondrocytes in 3D culture

A total of ten experiments were conducted for control and PLIUS-stimulated constructs, using three separate cell isolations. The subsequent data for the 10 minute calcium signalling experiments was pooled, representing a total of 200 chondrocytes each for both the PLIUS-stimulated and control constructs.

Figure 6.7 represents a cumulative plot showing the percentage number of cells exhibiting at their first $[Ca^{2+}]_i$ transient over the experimental period. Overall, there was a similar shape for both conditions, with between 30 and 35% of chondrocytes exhibiting their first calcium transient over the 600 second experimental period. It can also be seen for both PLIUS-stimulated and non-stimulated control chondrocytes, there was a similar percentage of cells, approximately 10%, responding for the first time during the initial 60 second imaging period. Thereafter, up to 540 seconds subtle differences between group responses were evident. For example, the rate of increase of cell number eliciting a $[Ca^{2+}]_i$ response appeared greater between 180-540 seconds in the PLIUS stimulation group. However beyond 540 seconds no additional cells elicited a response for either of the groups.

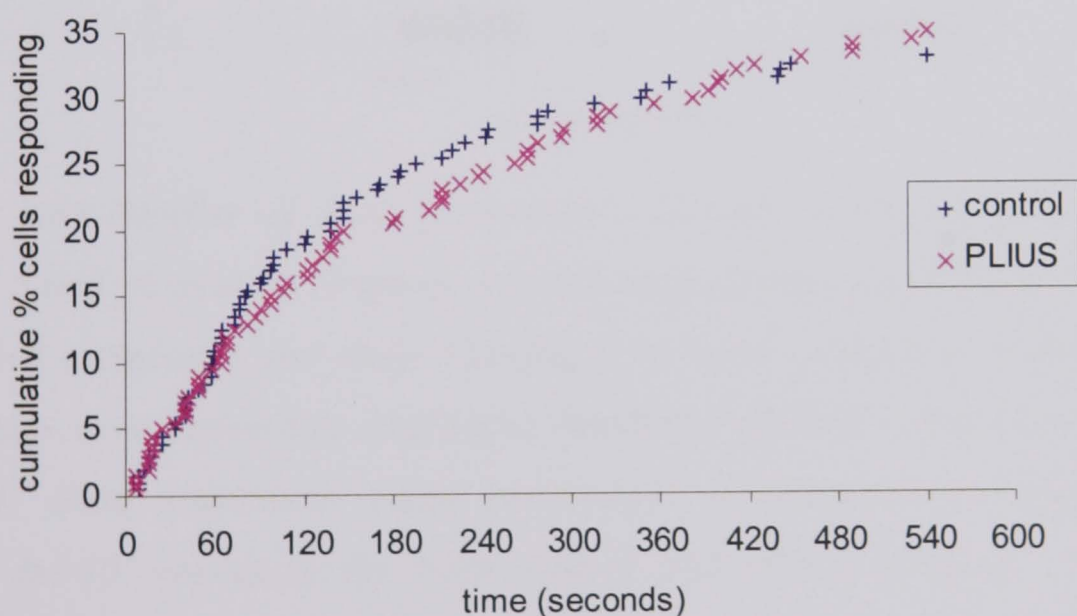


FIGURE 6.7: Cumulative number of chondrocytes in agarose constructs exhibiting a $[Ca^{2+}]_i$ transient over the 10 minute experimental period. PLIUS-stimulated chondrocytes were exposed to continuous $30mW/cm^2$ PLIUS. Controls remained non-stimulated. A total of 200 cells were analysed for each experimental group.

The total percentage of cells exhibiting $[Ca^{2+}]_i$ transients at 5 and 10 minutes are illustrated in Figure 6.8A and 6.8B, respectively. The data has been further divided into

those cells showing 1-3 transients and those showing $[Ca^{2+}]_i$ oscillations of 4 or more transients. This classification has previously been adopted in the host laboratory (Pingguan-Murphy *et al.*, 2005, 2006).

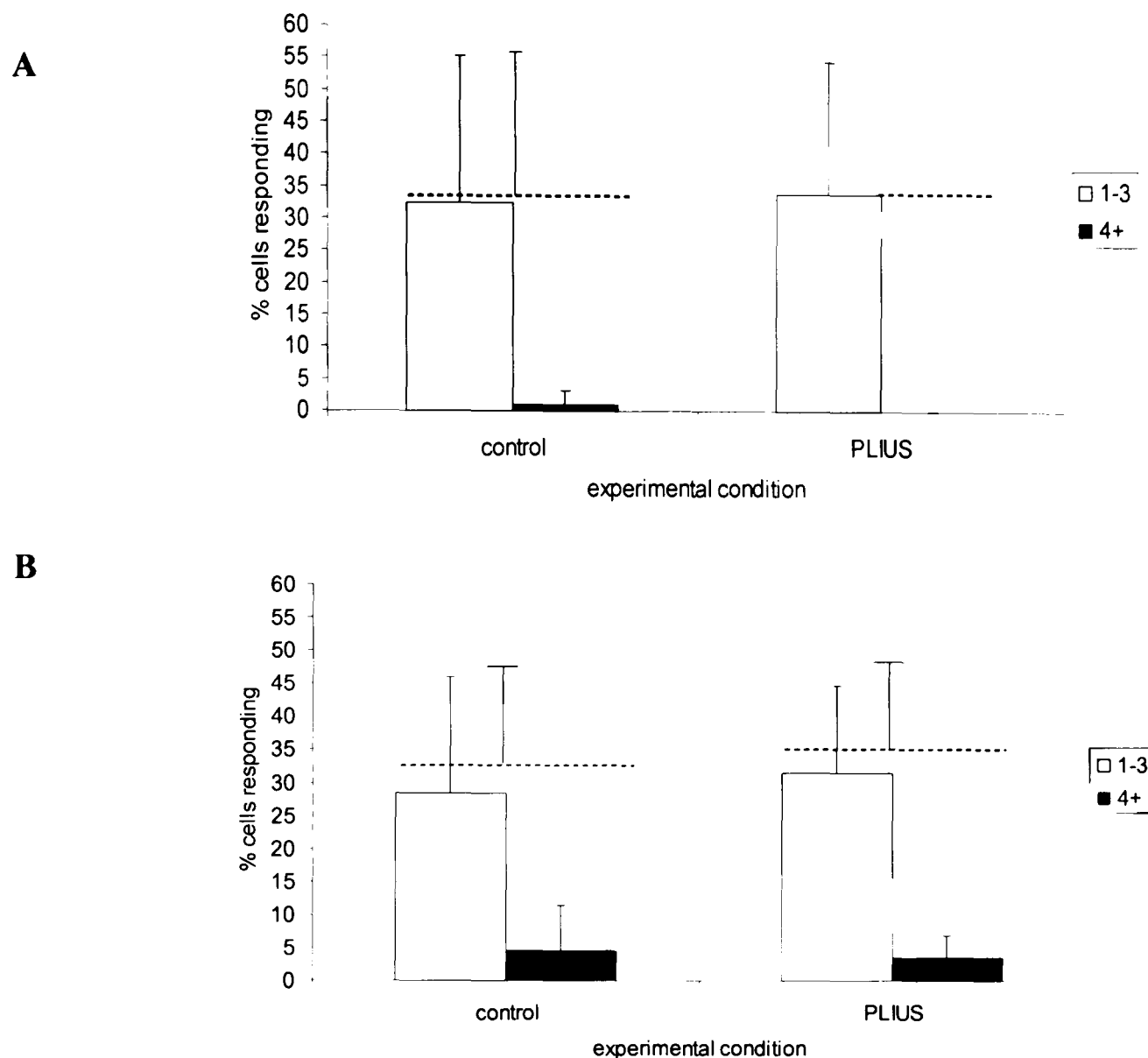


FIGURE 6.8: Number of $[Ca^{2+}]_i$ transients elicited by chondrocytes in agarose culture at 5 and 10 minutes (Figures A and B respectively), divided into cells eliciting between 1-3 transients, and those eliciting 4 or more transients. PLIUS-stimulated chondrocytes were exposed to continuous $30mW/cm^2$ PLIUS. Controls remained non-stimulated. Data represents mean percentage of chondrocytes responding per construct ($n=10$ constructs for both control and PLIUS groups). Dotted lines represent total percentage of cells responding for each given experimental condition. Error bars represent standard deviation for each parameter.

At five minutes, it can be seen that there was very little difference between the total percentage of cells responding in PLIUS and control groups, with mean values of 34% and 32.5%, respectively ($p>0.05$, Figure 6.8A). Additionally, 1% of control chondrocytes elicited 4 or more $[Ca^{2+}]_i$ transients, whereas none were seen for the stimulated group.

At ten minutes, there was again no significant difference between the experimental groups in terms of total percentage of cells responding ($p>0.05$, Figure 6.8B), with 35% of PLIUS-stimulated chondrocytes showing a response compared to 33% of controls. There was a slight increase in the number of cells exhibiting 1-3 $[Ca^{2+}]_i$ transients in the PLIUS-stimulated group (31.5% compared to 28.5% for controls). Conversely, there was a slightly higher proportion of chondrocytes in the control group that exhibited 4 or more $[Ca^{2+}]_i$ transients (4.5% compared to 3.5% for the PLIUS-stimulated cells). However, none of the differences were statistically significant ($p>0.05$)

The temporal nature of $[Ca^{2+}]_i$ signalling, divided into five 2 minute intervals, is presented in Figure 6.9. A general decrease in calcium response was seen with time in terms of the percentage of cells responding over a given time period, from 18.5% to 6% for control chondrocytes, and 16% to 9% for PLIUS-stimulated chondrocytes. There were no statistically significant differences between PLIUS-stimulated and control chondrocytes over any two minute interval ($p>0.05$).

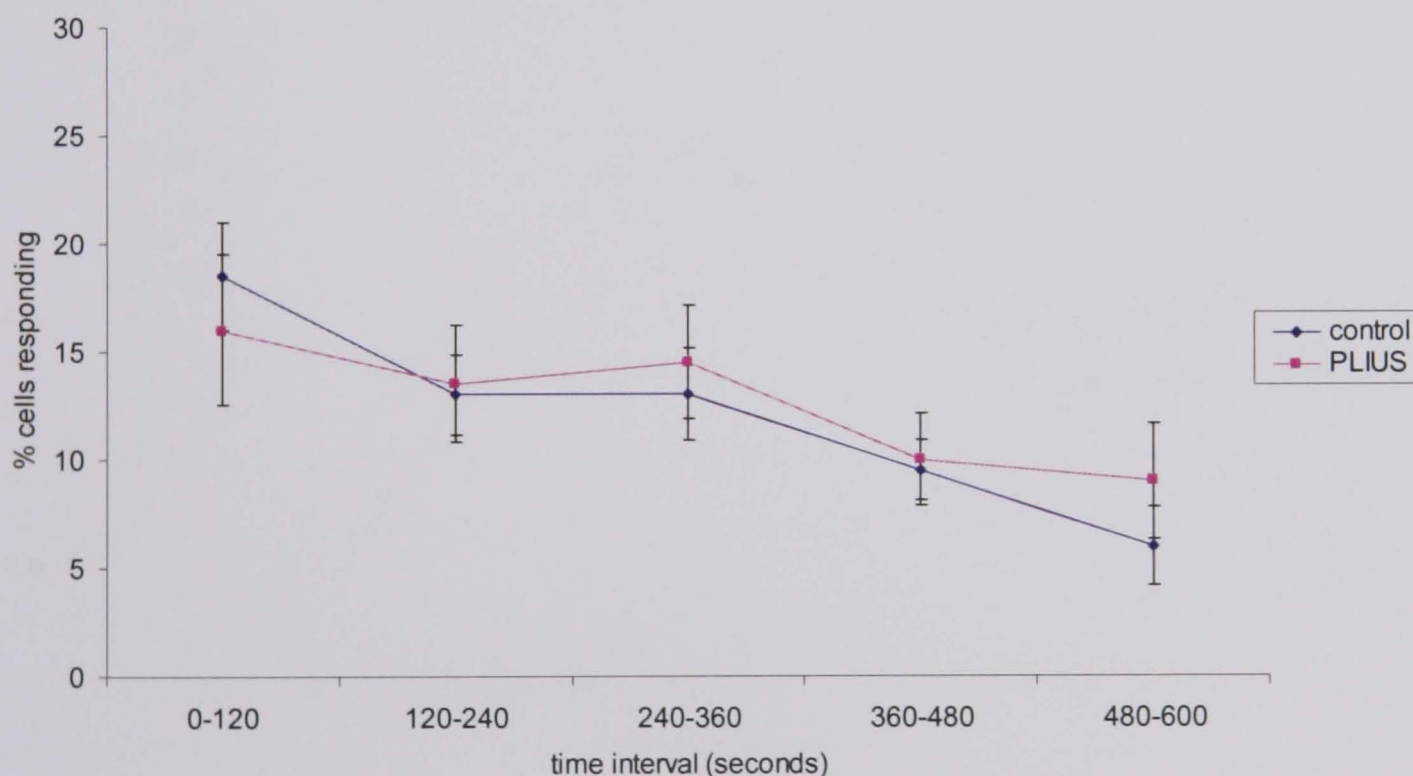


FIGURE 6.9: Temporal profile of $[Ca^{2+}]_i$ signalling exhibited by chondrocytes in agarose over the 600 second imaging period, divided into two minute intervals. Data represents the mean percentage of chondrocytes exhibiting a transient within each two minute interval. Error bars represent \pm SEM for $n=10$ constructs, for both control and PLIUS groups. None of the comparisons were statistically significant ($p>0.05$).

6.3.2 Effect of PLIUS on calcium signalling in chondrocytes cultured in monolayer

A total of ten experiments were conducted for control and PLIUS-stimulated monolayers, using three separate cell isolations. The data was pooled, representing a total of 200 chondrocytes for each experimental group.

Figure 6.10 represents a cumulative plot showing the percentage of cells exhibiting at least one $[Ca^{2+}]_i$ transient over the experimental period. It can be seen that there was a difference between groups with regard to the percentage of cells responding over the 600 second experimental period. PLIUS-stimulated chondrocytes at all times elicited a reduced number of transients than non-stimulated controls. Indeed, the first instances of $[Ca^{2+}]_i$ response occurred at earlier time-points for control cells than for PLIUS-stimulated cells. However, the rate of increase of cell number eliciting a $[Ca^{2+}]_i$ response, as demonstrated by the gradient of the curves, is similar for both groups over the first 240 seconds. Nonetheless, beyond 360 seconds of imaging, the curves appear to converge. Overall, approximately 47.5% of control chondrocytes and 45% of PLIUS-stimulated cells demonstrated a $[Ca^{2+}]_i$ response over the 600 second experimental period.

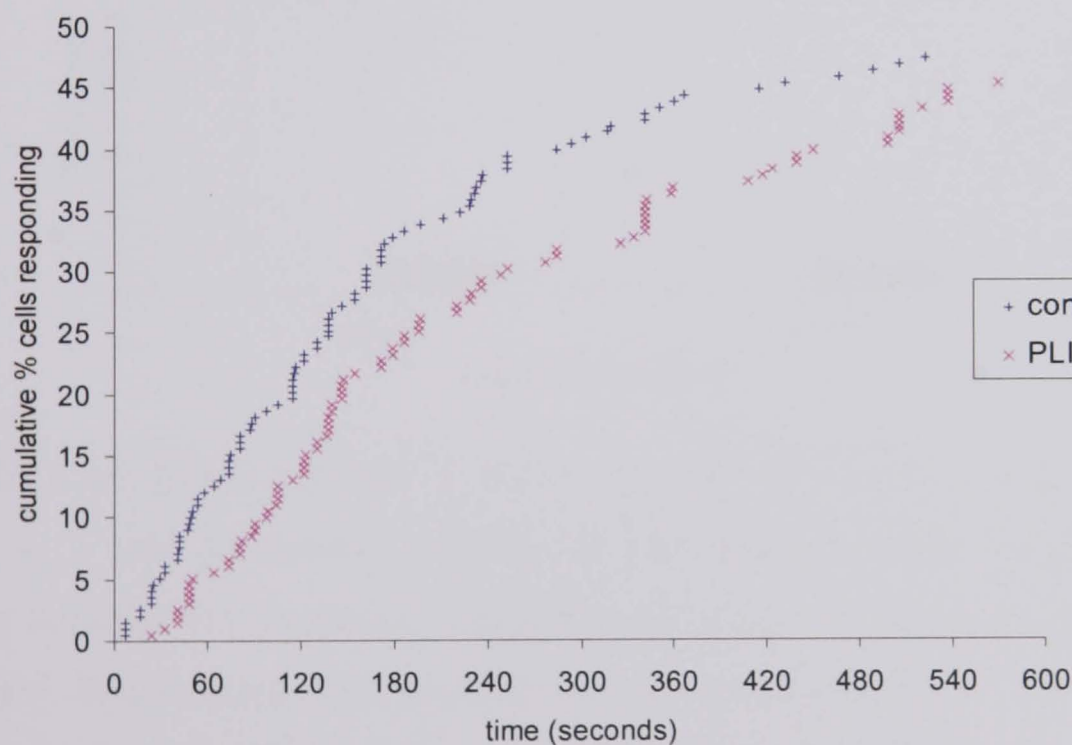
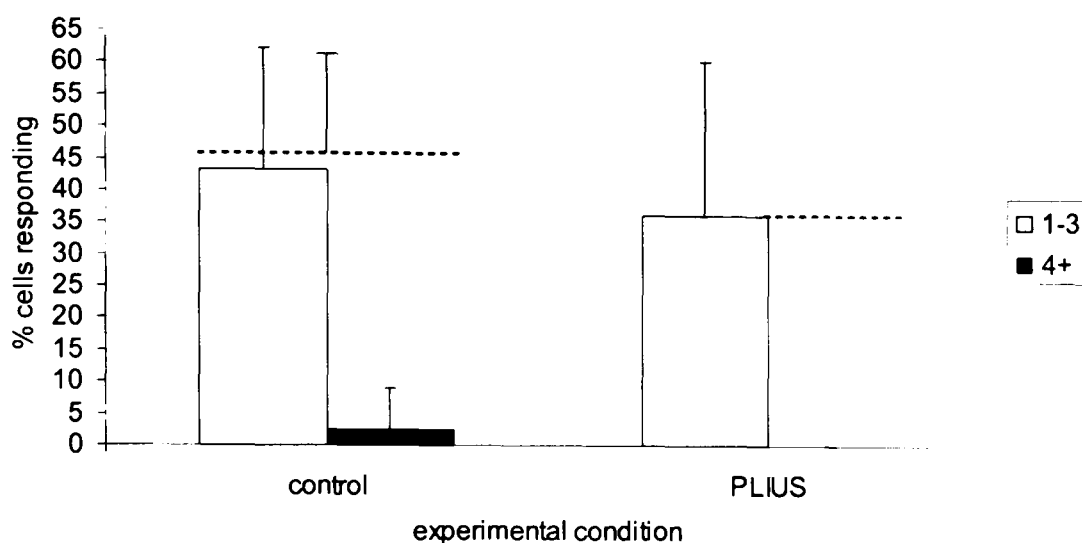


FIGURE 6.10: Cumulative number of chondrocytes in monolayer exhibiting a $[Ca^{2+}]_i$ transient over the 10 minute experimental period. PLIUS-stimulated chondrocytes were exposed to continuous $30mW/cm^2$ PLIUS. Controls remained non-stimulated. A total of 200 cells were analysed for each experimental group.

The total percentage of cells exhibiting $[Ca^{2+}]_i$ transients at 5 and 10 minutes are illustrated in Figures 6.11A and 6.11B, respectively. The data has been further divided

into those cells showing 1-3 transients and those showing $[Ca^{2+}]_i$ oscillations of 4 or more transients.

A



B

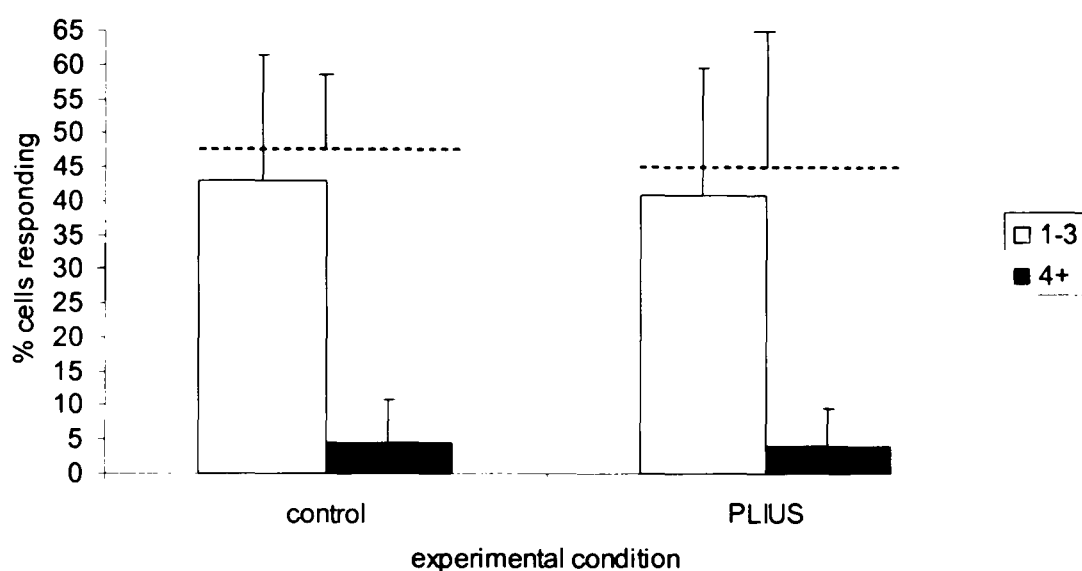


FIGURE 6.11: Number of $[Ca^{2+}]_i$ transients elicited by chondrocytes in monolayer culture at 5 and 10 minutes (Figures A and B respectively), divided into cells eliciting between 1-3 transients, and those eliciting 4 or more transients. PLIUS-stimulated chondrocytes were exposed to continuous $30mW/cm^2$ PLIUS. Controls remained non-stimulated. Data represents mean percentage of chondrocytes responding per construct ($n=10$ monolayers for both control and PLIUS groups). Dotted lines represent total percentage of cells responding for each given experimental condition. Error bars represent standard deviation for each parameter.

At five minutes, it can be seen that control chondrocytes elicited a higher total percentage of $[Ca^{2+}]_i$ transients than the PLIUS-stimulated cells (46% compared to 36%, Figure 6.11A), although this difference was not statistically significant ($p>0.05$).

Additionally, 2.5% of control chondrocytes elicited 4 or more $[Ca^{2+}]_i$ transients, whereas no cells exhibited these number of transients in the stimulated group.

However, by ten minutes there was minimal difference between experimental conditions, with respect to both the number of cells exhibiting 1-3 transients and those exhibiting 4 or more transients (Figure 6.11B). A total of 47.5% of control chondrocytes elicited a calcium response, compared to 44% of PLIUS-stimulated chondrocytes, a difference which was not statistically significant ($p>0.05$). The percentage of cells eliciting 4 or more transients was approximately 5% for both groups.

The temporal nature of $[Ca^{2+}]_i$ signalling, in terms of the percentage of cells responding in 2 minute intervals over the 10 minute period, is presented in Figure 6.12.

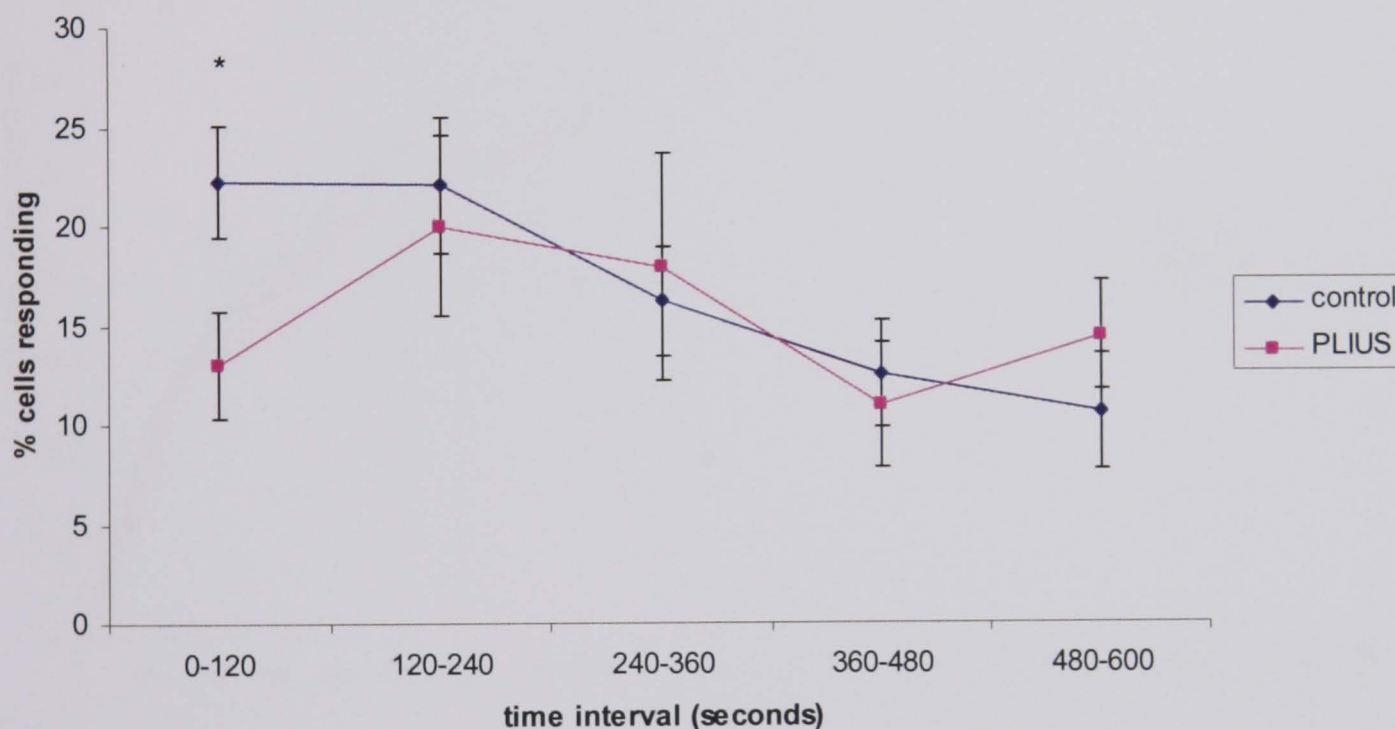


FIGURE 6.12: Temporal profile of $[Ca^{2+}]_i$ signalling exhibited by chondrocytes in monolayer culture over the 600 second imaging period, divided into two minute intervals. Data represents the mean percentage of chondrocytes exhibiting one or more transients within each two minute interval. Error bars represent \pm SEM for $n=10$ monolayers for both control and PLIUS groups. Only one comparison was statistically significant with $*$ = $p<0.05$.

Comparison of both groups revealed that PLIUS-stimulated cells were less responsive than control cells for the first two minute interval ($p<0.05$). There were no further significant differences between experimental conditions after this time, with both

PLIUS-stimulated and control groups having a similar range of absolute values over the imaging period, between 11-20% for the former and 11-22% for the latter group.

6.3.3 Influence of PLIUS intensity on calcium signalling in chondrocytes in 3D culture

A total of fifteen experiments were undertaken for control and twenty-four experiments for PLIUS-stimulated constructs from five separate cell isolations. The pooled data represents a total of 323 control and 478 PLIUS-stimulated chondrocytes.

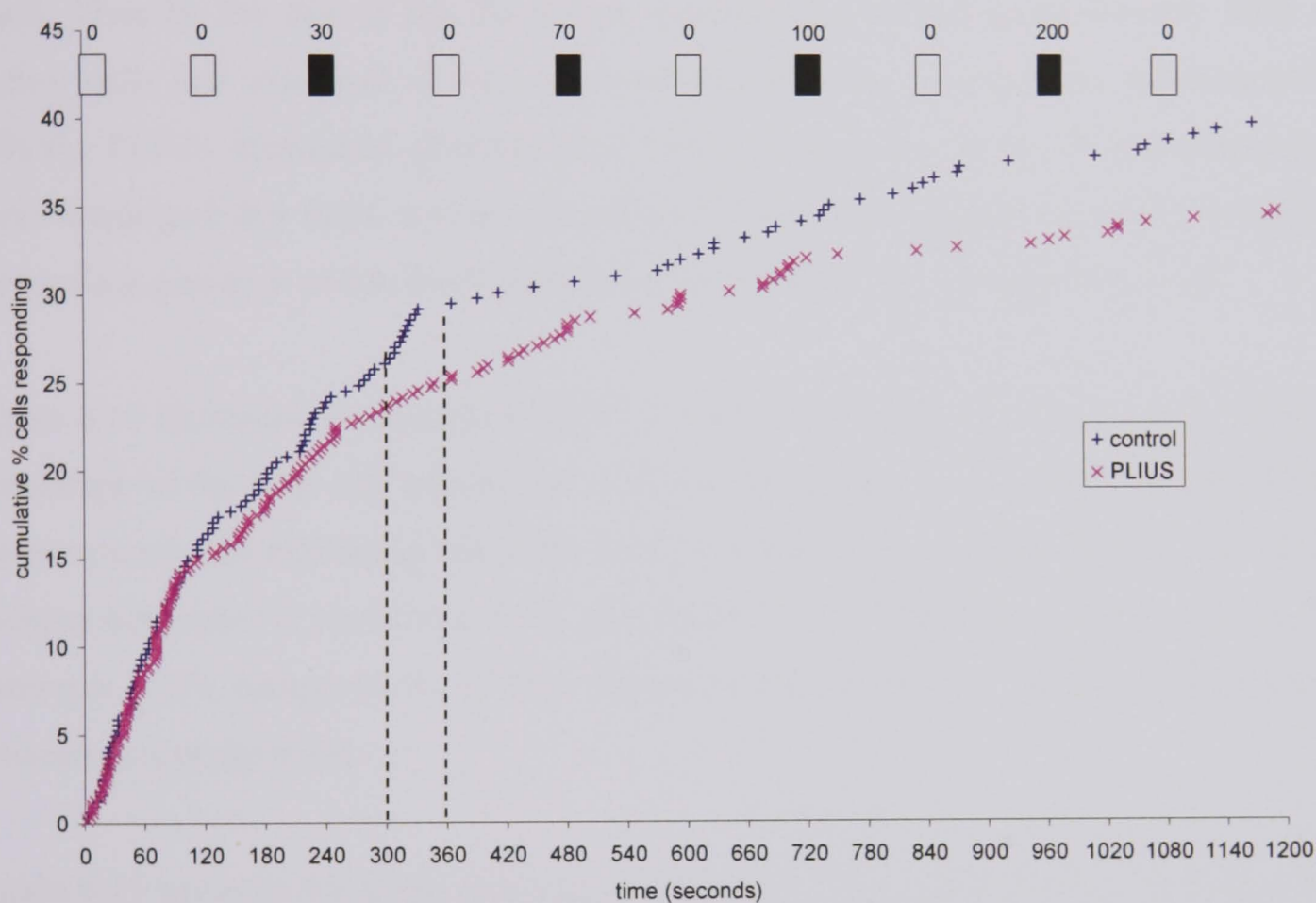


FIGURE 6.13: Cumulative number of chondrocytes in 3D agarose constructs exhibiting a $[Ca^{2+}]_i$ transient over the 20 minute experimental period. PLIUS-stimulated chondrocytes were exposed to PLIUS of increasing intensity from 0-200mW/cm² as displayed in Figure 6.2. Controls remained non-stimulated. White and black legends represent the PLIUS SATA intensity being employed for a given 2 minute period in mW/cm². Dotted lines indicate time period 300-360 seconds. A total of 323 control cells and 478 PLIUS-stimulated cells were analysed.

Figure 6.13 is a cumulative plot showing the percentage number of cells exhibiting at least one $[Ca^{2+}]_i$ transient over the twenty minute imaging period. Both groups exhibited some increase in the percentage number of cells responding throughout the experimental period. Indeed, both groups behaved similarly for the first 120 seconds,

with approximately 15% of cells exhibiting a $[Ca^{2+}]_i$ transient. Thereafter, PLIUS-stimulated chondrocytes elicited fewer transients than non-stimulated controls for all subsequent time-points. This is most noticeable between 300 and 360 seconds, as depicted by dotted lines in Figure 6.13, where there is an increase in the gradient of response for non-stimulated chondrocytes compared to the response of cells which, during this period, were being stimulated with PLIUS at an intensity of $30mW/cm^2$. Between 480 and 720 seconds, the increase in cell percentages eliciting their first $[Ca^{2+}]_i$ transient was similar for both groups. During this period, stimulated chondrocytes were exposed to $70mW/cm^2$ PLIUS. After 720 seconds the two rates of response diverge again. Thus by the end of the 20 minute experimental period approximately 40% of control cells had exhibited at least one calcium transient, compared to approximately 35% for PLIUS stimulated chondrocytes. Close examination of the PLIUS-stimulated curve suggested that there was no consistent instantaneous change in $[Ca^{2+}]_i$ response during time-points at which the PLIUS stimulation was either switched on or off.

Figure 6.14 illustrates the number of $[Ca^{2+}]_i$ transients exhibited per cell, presented as a percentage of the total cell population. It shows that there was a small reduction in the proportion of cells exhibiting transients in the stimulated group, when divided into cells eliciting between 1-3 transients (24% compared to 27%) and those eliciting 4 or more transients (11% compared to 12.5%). However there were no significant differences between groups ($p>0.05$).

Figure 6.15 presents the mean percentage response of PLIUS-stimulated chondrocytes, in terms of $[Ca^{2+}]_i$ transient, normalised to control chondrocytes over the 20 minute imaging period, which has been divided into ten 2 minute intervals. Figure 6.15A-E shows the mean values for each of the five separate cell isolations used for the imaging experiments. In addition, the data was pooled for all five experiments, and mean values were estimated as illustrated in Figure 6.15F. A normalisation process was established to accommodate any temporal change in the non-stimulated controls over the imaging period. For example, Figures 6.9 and 6.12 reveal a decline in the total number of cell

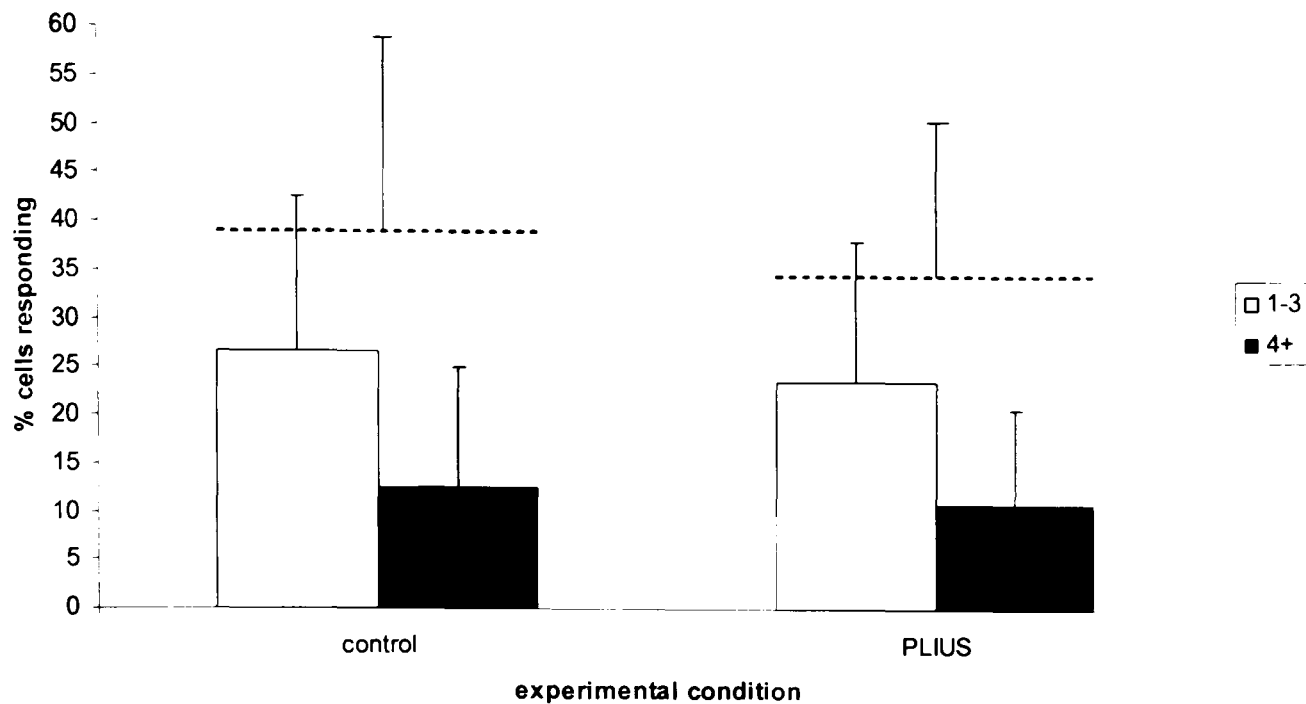


FIGURE 6.14: Number of transients elicited by chondrocytes in 3D agarose constructs over a 20 minute period, divided into cells eliciting between 1-3 transients, and those eliciting 4 or more transients. PLIUS-stimulated chondrocytes were exposed to intermittent PLIUS of increasing SATA intensity between 0-200 mW/cm². Controls remained non-stimulated. Data represents mean percentage of chondrocytes responding per construct (n=15 for control constructs and n=24 for PLIUS-stimulated constructs). Dotted lines represent total percentage of cells responding for each given experimental condition. Error bars represent standard deviation.

responders in non-stimulated constructs and monolayers, respectively. Hence, for each of the selected two minute intervals, the mean number of chondrocytes exhibiting one or more $[Ca^{2+}]_i$ transients in the stimulated group was divided by the corresponding mean number of cells in the control group, and a percentage value estimated.

Figures 6.15A-E clearly indicate that the cell response varied with different cell isolations. Figure 6.15A and Figure 6.15E show that for the majority of time-points the calcium response of PLIUS stimulated chondrocytes were inhibited, with values of approximately 50-70% of the corresponding controls. Indeed, in Figure 6.15E, six out of ten time-intervals were significantly lower than controls ($p < 0.05$), corresponding to three "on" (PLIUS stimulation) and three "off" periods. Figure 6.15A appears to show the inhibitory effect of PLIUS on chondrocytes at all intensities, although only at 100mW/cm² were the differences statistically significant. This effect is temporary, however, as chondrocytes recover in the subsequent two minute period with higher mean percentages of responders than for the periods where PLIUS was applied.

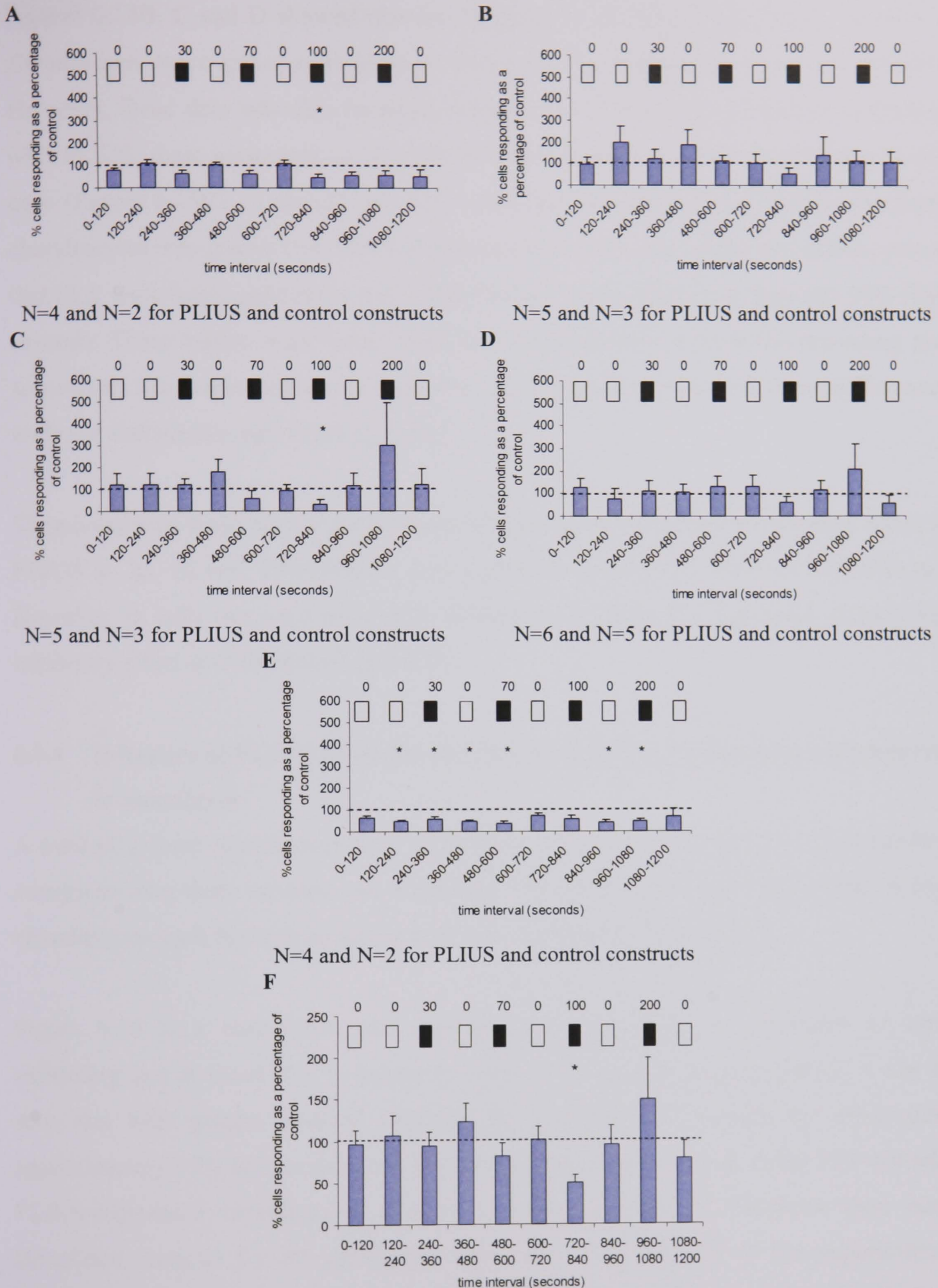


FIGURE 6.15: Temporal profile of $[Ca^{2+}]_i$ signalling over the 1200 second imaging period, split into 2 minute intervals. White and black legends represent the PLIUS SATA intensity being employed for a given 2 minute period in mW/cm^2 . Bars on graphs represent the percentage of PLIUS-stimulated chondrocytes in 3D agarose culture responding over a given time as a percentage of control. A through to E represent results obtained from five separate cell isolations. F is the mean of the five isolations.

Figures 6.15B, C and D showed that for the majority of time-points PLIUS-stimulated chondrocytes were either equivalent or above the corresponding values for controls. However, these data sets also revealed some cases of temporary inhibition associated with PLIUS, most noticeably at $100\text{mW}/\text{cm}^2$, which was statistically significant in one case (Figure 6.15C). It should also be noted that the response of PLIUS-stimulated chondrocytes was greater than 200% compared to controls during the two minute period that they were being stimulated with $200\text{mW}/\text{cm}^2$, corresponding to between 960-1080 seconds. These values were higher than the responses seen in both the preceding and subsequent two minute intervals (Figures 6.15C and 6.15D). However, these differences were not statistically significant ($p>0.05$).

The pooled data from the five experiments (Figure 6.15F) indicates an inhibitory effect of PLIUS at 30, 70 and $100\text{mW}/\text{cm}^2$, and a possible stimulatory effect at $200\text{mW}/\text{cm}^2$. However, in only one case were these differences statistically significant, namely the inhibitory effect at $100\text{mW}/\text{cm}^2$ ($p<0.05$).

6.3.4 Influence of PLIUS intensity on calcium signalling in chondrocytes cultured in monolayer

A total of sixteen experiments were undertaken for both control and PLIUS-stimulated constructs over three separate cell isolations. The pooled data represents a total of 240 chondrocytes each for both control and PLIUS-stimulated chondrocytes.

Figure 6.16 is a cumulative plot showing the percentage of occurrence of cells exhibiting one or more $[\text{Ca}^{2+}]_i$ transients over the 20 minute imaging period. It can be seen that both groups behaved similarly for the first 240 seconds, by which time approximately 35% of chondrocytes had elicited their first response. After 240 seconds, PLIUS-stimulated chondrocytes elicited a greater number of transients than non-stimulated controls for all subsequent time-points. By the end of the experimental period approximately 65% of PLIUS-stimulated chondrocytes had exhibited their first calcium transient, compared to approximately 60% for control cells. Close examination of the stimulated curve revealed changes in the rate of increase of cell numbers exhibiting a $[\text{Ca}^{2+}]_i$ transient occurring at 240 and 480 seconds, coinciding with the onset of PLIUS stimulation of $30\text{mW}/\text{cm}^2$ and $70\text{mW}/\text{cm}^2$, respectively. However, at later times there appeared to be periods where no new PLIUS-stimulated cells were responding, for example, between 540 and 600 seconds and between 660 and 900

seconds. Furthermore, there were no additional stimulated responders after 1020 seconds, whereas control chondrocytes continued to respond for the vast majority of the imaging period.

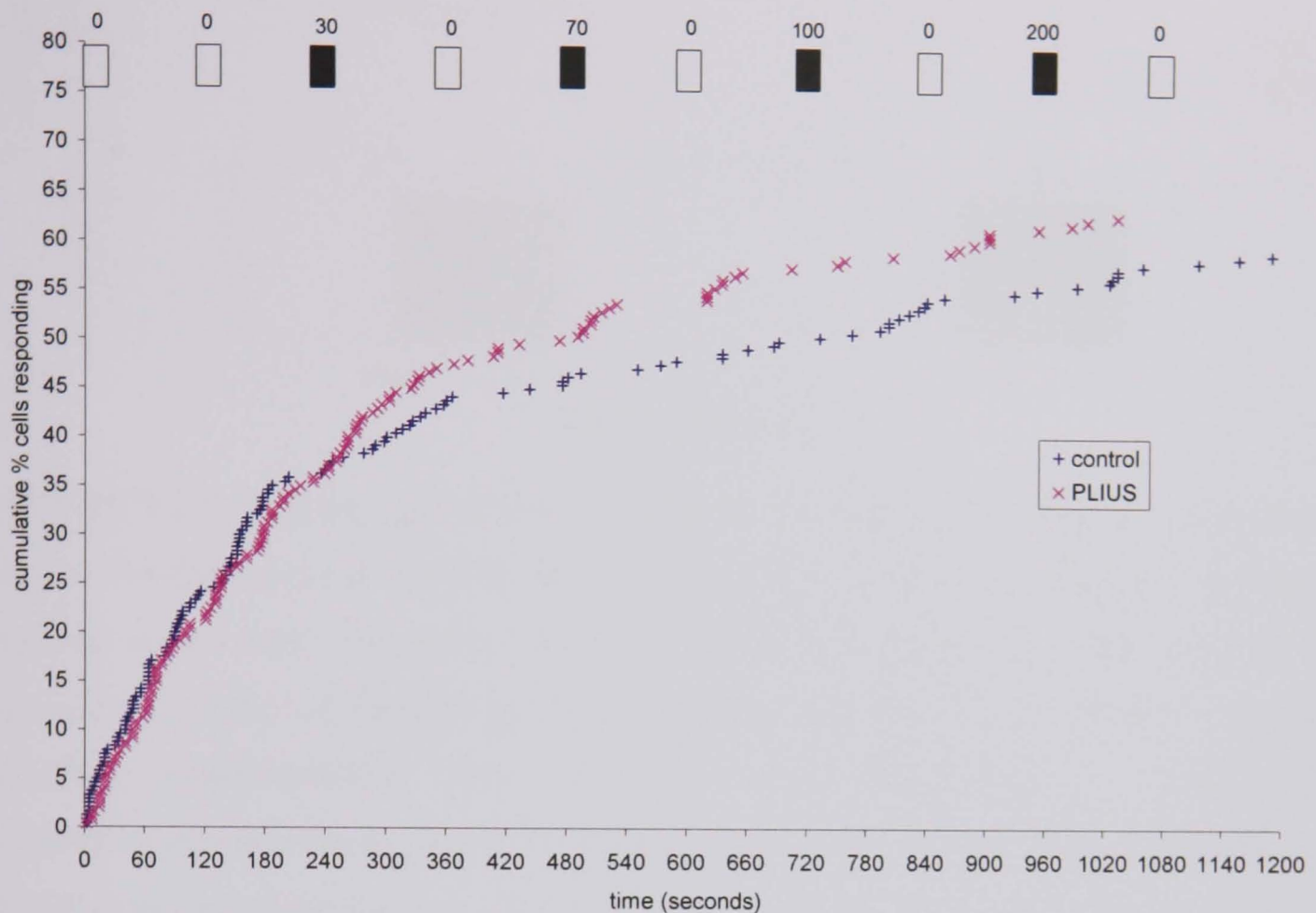


FIGURE 6.16: Cumulative number of chondrocytes in monolayer culture exhibiting a $[Ca^{2+}]_i$ transient over the 20 minute experimental period. PLIUS-stimulated chondrocytes were exposed to PLIUS of increasing intensity from 0-200mW/cm² as displayed in Figure 6.2. Controls remained non-stimulated. White and black legends represent the PLIUS SATA intensity being employed for a given 2 minute period in mW/cm². A total of 240 cells were analysed for each experimental group.

Figure 6.17 illustrates the number of $[Ca^{2+}]_i$ transients exhibited per cell over the 20 minute period, presented as a percentage of the total cell population. It can be seen that there was a slightly higher proportion of chondrocytes exhibiting transients in the stimulated group when compared to controls. This was the case for both cells eliciting between 1-3 transients (37.5% compared to 35%) and for cells eliciting 4 or more transients (25% compared to 24%). However, neither of these differences were significantly different ($p > 0.05$).

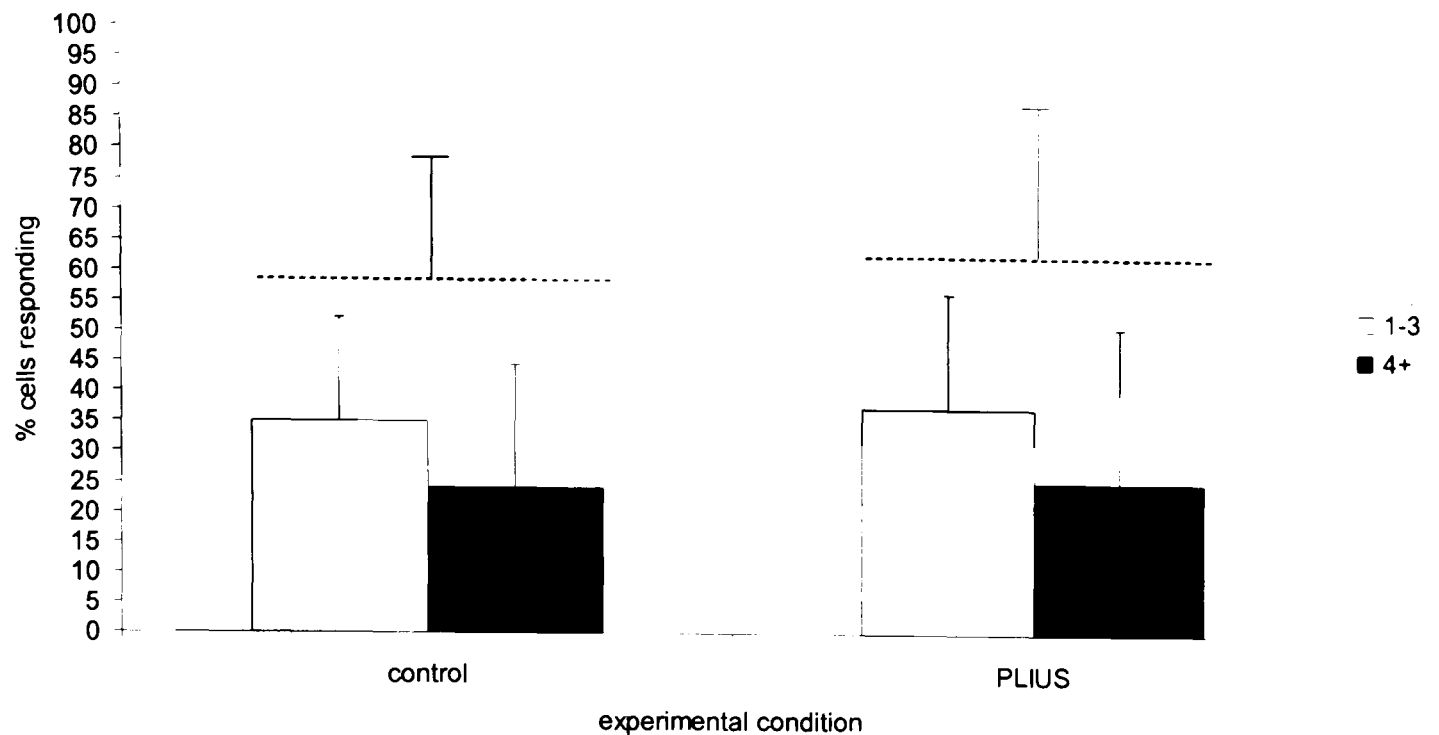


FIGURE 6.17: Number of transients elicited by chondrocytes cultured in monolayer over a 20 minute period, divided into cells eliciting between 1-3 transients, and those eliciting 4 or more transients. PLIUS-stimulated chondrocytes were exposed to intermittent PLIUS of increasing SATA intensity between 0-200 mW/cm². Controls remained non-stimulated. Data represents mean percentage of chondrocytes responding per monolayer (n=16 for both control and PLIUS-stimulated monolayers). Dotted lines represent total percentage of cells responding for each given experimental condition. Error bars represent standard deviation.

Figure 6.18 presents the mean cell $[Ca^{2+}]_i$ transient response as a percentage of control for each of the three times that experiments were undertaken (Figure 6.18A-C), as well as the pooled data for the three cell isolations (Figure 6.18D). As explained in Section 6.3.3, the mean number of stimulated cells was normalised to the mean number of non-stimulated cells for each two minute period.

Figures 6.18A-C show that cell response varied considerably between cell isolations. Figure 6.18A shows that for the majority of time-points the $[Ca^{2+}]_i$ response of PLIUS stimulated chondrocytes was comparable or higher than controls. However, differences were only significant during the interval 480-600 seconds, during which time chondrocytes were exposed to 70mW/cm² (p<0.05). During the final two minutes of imaging in this isolation, stimulated chondrocytes showed a significant decrease in $[Ca^{2+}]_i$ transients when compared to control cells (p<0.05). Figure 6.18B shows a more variable pattern of response. It appeared that during periods where PLIUS was applied there was generally an inhibitory response for all intensities up to and including

100mW/cm². However, none of the differences were statistically significant ($p>0.05$). Figure 6.18C also showed a varied pattern in terms $[Ca^{2+}]_i$ response. Indeed in the first four minutes, there was an apparent difference between groups ($p>0.05$), even though PLIUS stimulation was not active. During periods where cells were exposed to 30mW/cm² and 70mW/cm² mean percentages exceeded 100% of the control values, whereas the opposite trend was evident when cells were exposed to 100mW/cm² and 200mW/cm². However, none of these differences were statistically significant ($p>0.05$).

The pooled data from the three experiments (Figure 6.18D) generally indicated that, for the majority of time periods, stimulated cells exhibited a $[Ca^{2+}]_i$ response which was equivalent or in excess of control values. This was found to be significant at 600-720 seconds, during which time chondrocytes were not experiencing PLIUS ($p<0.05$). By contrast, for two intervals, stimulated cells exhibited responses less than 75% of control values (Figure 6.18D). These differences were only statistically significant during the last two minutes of the imaging period between and 1080 and 1200 seconds.

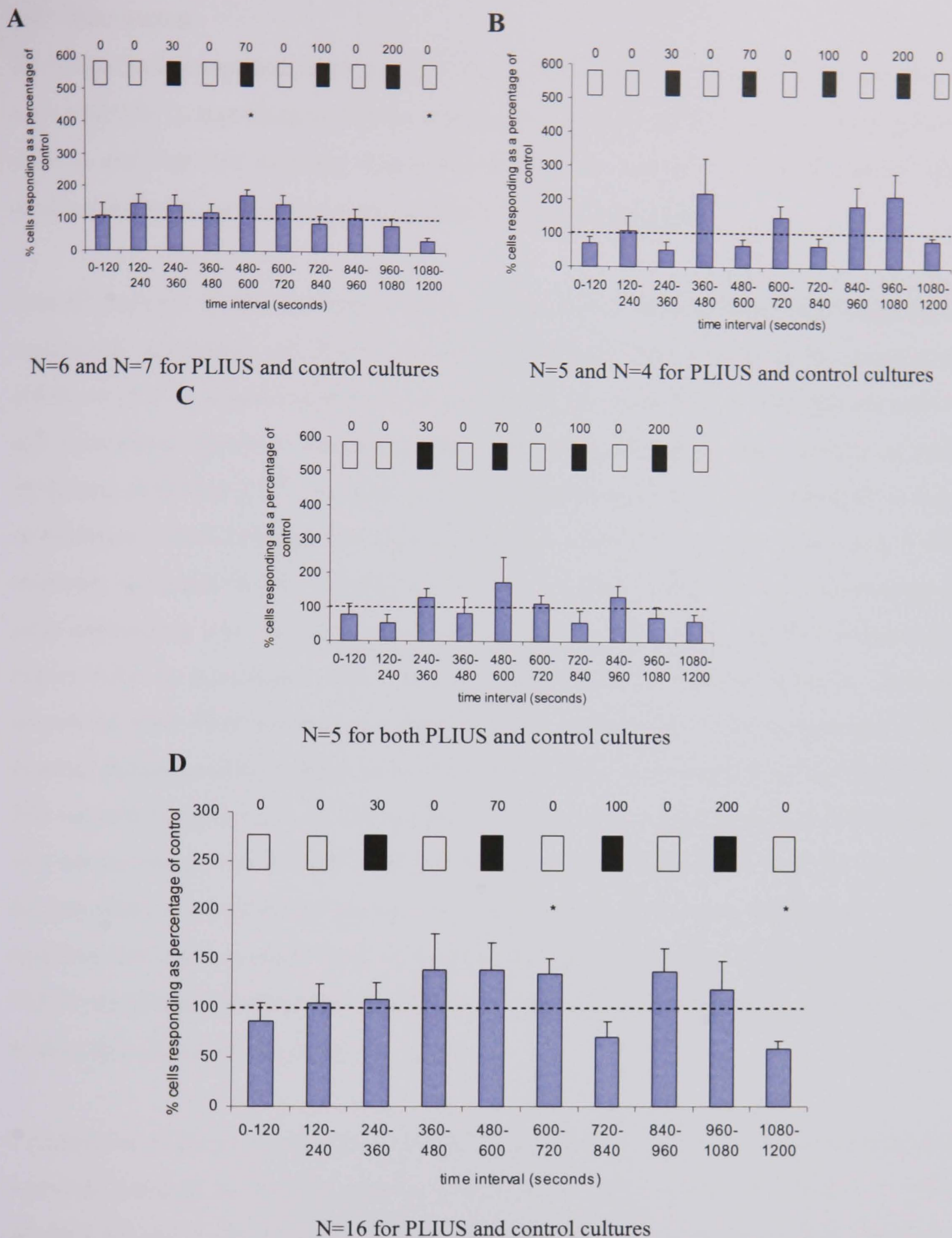


FIGURE 6.18: Temporal profile of $[Ca^{2+}]_i$ signalling over the 1200 second imaging period, split into 2 minute intervals. White and black legends represent the PLIUS SATA intensity being employed for a given 2 minute period in mW/cm^2 . Bars on graphs represent the percentage of PLIUS-stimulated chondrocytes in monolayer responding over a given time as a percentage of control. **A** through to **C** represent results obtained from three separate cell isolations. **D** is the mean of the three isolations.

6.4 Discussion

The hypothesis examined in the present set of experiments was that PLIUS stimulation activated $[Ca^{2+}]_i$ signalling in bovine chondrocytes seeded in 3D agarose and monolayer culture, and that this response was influenced by the intensity of the ultrasound. The results detailed in sections 6.3.1-6.3.4 confirm a null hypothesis.

Overall analysis of the ten minute experiments, where chondrocytes were exposed to continuous application of $30mW/cm^2$ PLIUS, showed that there was no stimulatory effect on $[Ca^{2+}]_i$ signalling behaviour, evidenced for cells both in 3D agarose culture and monolayer culture. Cumulative plots illustrating the percentage number of cells exhibiting their first $[Ca^{2+}]_i$ over time showed that in agarose, PLIUS appeared to have an inhibitory effect between 180 and 300 seconds. However, the rate of increase of cell response was such that by the end of the experimental period the total percentage of cells responding was comparable for both groups, in the region of 35% (Figure 6.7, Figure 6.8). In monolayer, there was an approximate 20 second delay in response associated with PLIUS-stimulated chondrocytes, although the rate of increase of cell number eliciting a $[Ca^{2+}]_i$ response was similar for both experimental groups for the first 240 seconds (Figure 6.10). A divergence in curves, seen at approximately 300 seconds, was not translated into a PLIUS-related inhibitory effect (Figure 6.11A). At the end of the ten minute experimental period, the total percentage of cells exhibiting a $[Ca^{2+}]_i$ response was approximately 45% for both groups (Figure 6.11B). A small proportion of PLIUS-stimulated chondrocytes continued to respond after 540 seconds, which was not evident in control cells in monolayer culture.

Comparison of the temporal nature of $[Ca^{2+}]_i$ signalling in both culture systems revealed a general decrease in calcium response over the ten minute period, of between 7-12.5% (Figures 6.9 and 6.12). The only exception to the pattern was seen for PLIUS-stimulated chondrocytes in the monolayer system, during the first and last two minute interval (Figure 6.12). However, by examining the corresponding cumulative plot (Figure 6.10), these differences can be attributed to the fact that stimulated chondrocytes began responding at a later time than controls, and continued responding in the last sixty seconds of the experimental period, after controls had ceased to respond.

Exposing chondrocytes to an increasing PLIUS intensity signal over a 20 minute period (Figure 6.3) failed to highlight any stimulatory effect on $[Ca^{2+}]_i$ signalling behaviour.

For chondrocytes cultured in agarose, the cumulative percentage of cells exhibiting $[Ca^{2+}]_i$ transients was lower for stimulated cells than for controls for the majority of the experimental period. However, this difference was seen during the period before the onset of PLIUS stimulation (Figure 6.13). The rate of increase of cell number eliciting $[Ca^{2+}]_i$ response did decrease at 240 seconds, coinciding with the onset of $30mW/cm^2$. However, this apparent inhibition was not statistically significant when examining the total percentage of cells eliciting $[Ca^{2+}]_i$ transients at 20 minutes (Figure 6.14). By contrast, PLIUS-stimulated cells cultured in monolayer exhibited a higher cumulative percentage of $[Ca^{2+}]_i$ transients than controls at all times after 240 seconds (Figure 6.16). However, as with the 3D system, there was no statistically significant difference between groups when observing the total percentage of cells exhibiting $[Ca^{2+}]_i$ transients at 20 minutes (Figure 6.17).

Figures 6.15 and 6.18, illustrating the normalised temporal profiles of $[Ca^{2+}]_i$ signalling of stimulated chondrocytes cultured in agarose and monolayer respectively, highlights the variation in cell signalling behaviour with separate cell isolations. In the vast majority of cases, no significant differences were seen between PLIUS-stimulated and non-stimulated systems. When data was pooled (Figure 6.15F and Figure 6.18D), the two culture systems exhibited different responses in relation to PLIUS stimulation. Chondrocytes in agarose appeared to show a dose dependent inhibition in $[Ca^{2+}]_i$ signalling during the periods where PLIUS was applied at SATA intensities 30, 70 and $100mW/cm^2$, which recovered in subsequent two minute periods when the PLIUS was removed. However, the difference was only significant for the latter intensity. The relative increase in $[Ca^{2+}]_i$ signalling evident on stimulation with $200mW/cm^2$ was not significant. In monolayer, $[Ca^{2+}]_i$ response was more varied, and no particular pattern was evident with relation to increasing PLIUS intensity. The only instance of an apparent dose dependent inhibition of $[Ca^{2+}]_i$ signalling was observed at $100mW/cm^2$, although this was not significant ($p>0.05$).

Comparison of the $[Ca^{2+}]_i$ signalling behaviour of the two cell culture systems revealed that for both groups, an increased subpopulation of chondrocytes responded in monolayer as opposed to in agarose, which was evident for both the 10 and 20 minute experiments. Comparable data is summarised in Table 6.1. For the 10 minute imaging experiments, it can be seen that the higher percentages seen in monolayer were attributable to those cells eliciting 1-3 transients. In both agarose and monolayer,

approximately 5% of cells exhibited 4 or more transients, irrelevant of experimental condition. Table 6.1 also highlights that for the 20 minute imaging experiments, there is an approximate twofold increase in the percentage of monolayer chondrocytes exhibiting 4 or more transients when compared to those in agarose, observed for both control and PLIUS-stimulated cells.

TABLE 6.1: Summary of results illustrating signalling behaviour for all experimental conditions in terms of percentage $[Ca^{2+}]_i$ transients. Of note, the 10 and 20 minute imaging periods cannot be directly compared due to the difference in employed PLIUS intensity profiles.

		% $[Ca^{2+}]_i$ transients			
Agarose	No. $[Ca^{2+}]_i$ transients	10 minutes (Figure 6.8B)		20 minutes (Figure 6.14)	
		Control	PLIUS	Control	PLIUS
	Total	33	35	39.5	35
	1-3	28.5	31.5	27	24
	4+	4.5	3.5	12.5	11
Monolayer	No. $[Ca^{2+}]_i$ transients	10 minutes (Figure 6.11B)		20 minutes (Figure 6.17)	
		Control	PLIUS	Control	PLIUS
	Total	47.5	45	59	62.5
	1-3	43	41	35	37.5
	4+	4.5	4	24	25

The 10 and 20 minute imaging periods cannot be directly compared in terms of the response of PLIUS-stimulated chondrocytes, due to the difference in SATA intensity profiles that cells are exposed to. However, some differences were noted. In agarose, there was an increase in the percentage of control cells responding, from 33% to 39% for 10 and 20 minutes, respectively. The total percentage of PLIUS-stimulated cells responding remained approximately 35%. Additionally, there was an increase in the percentage of cells exhibiting 4 or more transients by 20 minutes to approximately 12%, three times that evident at 10 minutes, for both PLIUS-stimulated and control groups. For monolayer cultures, there was an approximate 10% increase in the total percentage of cell responders for control chondrocytes at 20 minutes compared to at 10 minutes, from 47.5% to 59%, with an approximate 20% increase for PLIUS-stimulated cells, from 45% to 62.5%. Again, a greater proportion of chondrocytes exhibited 4 or more

transients at 20 minutes, at approximately 25%, representing a 5 fold increase to that found after 10 minutes of imaging.

In both agarose and monolayer, only a subpopulation of chondrocytes elicited a calcium response. Full depth cartilage is used for cell isolation, representing a heterogeneous chondrocyte population (Aydelotte *et al.*, 1988, 1992). It is possible that the observed $[Ca^{2+}]_i$ signalling behaviour is due to this heterogeneity. The increased level of $[Ca^{2+}]_i$ signalling seen in monolayer compared to agarose may be due to differences in culture conditions. In monolayer, the relative increase in cell-cell contact as well as attachment of chondrocytes to the well plate surface, may yield a greater level of $[Ca^{2+}]_i$ signalling. A previous study (Parvizi *et al.*, 2002) reported an increase in $[Ca^{2+}]_i$ levels in neonatal rat chondrocyte monolayer cultures when applying PLIUS in the range of 25-100mW/cm². Fura-2 was used as the fluorescent label, which gave an estimate of $[Ca^{2+}]_i$ concentration. The present experimental method employed Fluo-4, which did not measure $[Ca^{2+}]_i$ concentrations but rather enabled the amount and frequency of $[Ca^{2+}]_i$ transients to be measured, which could then be compared to control chondrocytes. It is unlikely that PLIUS would increase $[Ca^{2+}]_i$ concentrations without altering $[Ca^{2+}]_i$ transient behaviour, especially as Parvizi and colleagues appeared to show changes to both variables. As well as the difference in cell type and age used, the group did not use a control population of chondrocytes in their study. Therefore a direct comparison could not be made. However, it is evident from the current work that pulsed low intensity ultrasound was unable to stimulate $[Ca^{2+}]_i$ signalling in bovine chondrocytes in both monolayer and 3D agarose culture using the present system. In fact, an inhibitory dose-dependent response was evident in agarose that was significant at 100mW/cm². Monolayer cultures remained largely unaffected.

The implications of the present findings with regard to mechanotransduction are discussed in the following chapter.

Chapter 7

Discussion and Future Work

7.1	Introduction	174
7.2	Rationale for methodology	175
7.2.1	PLIUS regime	175
7.2.2	Rig and system design for PLIUS transmission	175
7.2.3	Cell source	177
7.2.4	Cell model systems	177
7.2.5	Cell seeding densities	178
7.3	PLIUS-induced mechanotransduction	179
7.3.1	Variability issues	179
7.3.2	Effect of PLIUS intensity	181
7.3.3	Comparison of monolayer and 3D culture	183
7.3.4	Influence of PLIUS on chondrocyte biosynthesis	185
7.3.5	PLIUS-induced diffusion in agarose culture	190
	7.3.5.1 Materials and methods	191
	7.3.5.2 Results	191
	7.3.5.3 Discussion	194
7.3.6	Use of PLIUS in bone and cartilage repair strategies	194
7.4	Future work	195
7.4.1	Further investigation of the 100mW/cm ² signal	195
7.4.2	Influence of PLIUS on other ECM molecules	196
7.4.3	Other intracellular mechanotransduction events	196
7.4.4	Alteration of the model system and PLIUS signal	197
7.5	Final summary	198

7.1 Introduction

The previous chapters of this thesis examined the potential use of pulsed low intensity ultrasound (PLIUS) for cartilage repair interventions by determining its influence on proteoglycan synthesis, cell proliferation and calcium signalling in chondrocytes seeded in 3D agarose and monolayer systems. This involved designing a system for application of PLIUS to chondrocytes cultured in agarose, as well as a rig that enabled microscopic evaluation of cells subjected to PLIUS.

This chapter will evaluate the model systems and experimental techniques employed in this thesis before discussing the implications of the results with regard to PLIUS-induced mechanotransduction effects and the use of PLIUS for enhancement of cartilage repair. Suggestions for future work are proposed as well as a summary of the key findings of the thesis.

7.2 Rationale for methodology

7.2.1 PLIUS regime

The ultrasound system used in this thesis (Figure 3.3) was provided by Smith and Nephew Inc. (York, UK), and exhibited a characteristic output signal of a 1.5 MHz frequency pulsed 200 μ s sine wave repeating at 1000 μ s (Figure 3.2). As detailed in Chapter 2, this output, or similar, has been used extensively in research investigating the influence of PLIUS on bone and cartilage tissues (Sections 2.3.9 and 2.3.10 respectively). The system routinely employed a SATA intensity of 30mW/cm², equivalent to that of the commercially available Exogen Sonic Accelerated Fracture Healing System (SAFHS). Additional equipment, also provided by Smith and Nephew Inc., allowed for the variation of the SATA intensity between 13-300mW/cm². A number of other published studies investigating possible cartilage modification by PLIUS have employed SATA intensities ranging from 2mW/cm² (Zhang *et al.*, 2002) to 580mW/cm² (Kopakkala-Tani *et al.*, 2006). Based on the results of an initial study described in Section 3.9, an additional SATA intensity of 100mW/cm² was chosen for the sGAG elaboration studies described in chapters 4 and 5. In addition, SATA intensities up to 200mW/cm² were employed to examine the effect of PLIUS intensity on calcium signalling in chondrocytes in agarose (Chapter 6).

Within the overall study, culture systems were subjected to single PLIUS exposures of between 2 and 20 minutes. A once-daily twenty minute exposure represents the current recommendation for those employing SAFHS treatment for fracture healing (Smith and Nephew, Inc.). However, in a study involving osteochondral defect repair in a rabbit model, a beneficial effect was reported if the daily PLIUS dose was doubled to 40 minutes (Cook *et al.*, 2001). Accordingly, PLIUS was employed twice a day at 12-hour intervals for the 30mW/cm² temporal agarose studies undertaken in Chapter 4.

7.2.2 Rig and system design for PLIUS transmission

The equipment provided by Smith and Nephew Inc. was operable in conjunction with the use of a six well plate, whereby PLIUS was transmitted via the base of each well. Therefore, the 3D agarose system used to investigate effect of PLIUS on temporal sGAG elaboration in agarose needed to be cultured in such plates. In addition, the gel was required to remain fixed or stationary during ultrasonic stimulation to remove any other factors, such as enhanced mass transport, that could contribute to the elaboration of extracellular matrix components. This made it difficult to employ the 5 × 5 mm

cylindrical or cube-shaped agarose constructs commonly utilised for mechanotransduction studies in the host laboratory. As a consequence, it was decided to cast the chondrocyte/agarose suspension directly into the individual wells of a six well plate to a 3mm height, and cover the gel with DMEM + 16.1% FCS.

At selected time-points, 6mm diameter cylindrical constructs were removed from the centre of the chondrocyte/agarose gel using a sterile corer (Figure 3.17). Outer regions were not used due to the non-uniformity of the PLIUS intensity field (Figure 3.6) and the fact that with a 22mm diameter transducer, the central region of the construct was more likely to be exposed to the nominal PLIUS signal intensity specified by the system. By contrast, such site-specific selection for biochemical analysis was not possible when exposing monolayer culture to ultrasound.

For calcium signalling experiments, a custom-designed microscope mounted rig was required in order to visualise viable cells in chondrocyte/agarose constructs exposed to PLIUS stimulation. The design and developmental process of this rig is detailed in Section 3.6 (Figures 3.8-3.16). To review briefly, 5×5×5 mm constructs were cast in a Perspex insert that was held in the chamber of the rig, covered with medium, and exposed to ultrasound using a single PLIUS transducer positioned in the lid component of the rig.

The main difference in the PLIUS transmission between the two systems is that with the former, ultrasound was transmitted directly from the transducer to well contents via the base of the well plate. However, due to the use of an inverted confocal microscope used for calcium imaging experiments, the transducer needed to be placed above cells. In order to maintain some consistency between the systems, the base of a well of a six well plate was cut out and used as the component of the lid through which the PLIUS was transmitted (Figure 3.10). Additionally, a fluid gap was employed so that the lid of the rig was not in direct contact with the construct to minimise the possibility of construct compression during insertion into the rig. Both designed systems fulfilled the aims of the thesis, namely to investigate the effects of PLIUS on chondrocyte biosynthesis and calcium signalling in a 3D model system.

7.2.3 Cell source

The cells used throughout this thesis were chondrocytes obtained from the proximal surface of the metaphalangeal joints of bovine steers aged between 18 and 24 months. This cell source is readily available, and a typical joint can provide 40 million cells. Skeletally mature bovine articular cartilage has been utilised in a number of studies investigating cartilage properties (Kerin *et al.*, 1998; Schinagl *et al.*, 1997) and the associated chondrocytes have been used in mechanotransduction studies by a variety of groups (Li *et al.*, 2001; Langelier and Buschmann, 2003; Browning *et al.*, 2004; Kerrigan *et al.*, 2006) including the host laboratory (Lee and Bader 1995; Lee *et al.*, 2000a and 2000b; Knight *et al.*, 2001; Lee *et al.*, 2003; Heywood *et al.*, 2004; Pinguann-Murphy *et al.*, 2005; Knight *et al.*, 2006a and 2006b; Campbell *et al.*, 2007; Akanji *et al.*, 2008). Although the use of bovine chondrocytes limits extrapolation to the clinical setting, alternative human allogenic sources are restricted in availability and there is an inherent variability associated with factors such as age and clinical history.

7.2.4 Cell model systems

The chondrocyte/agarose system used in Chapters 3, 4 and 6 is well characterised, having been used in a range of studies investigating chondrocytic phenotype and biosynthesis (Benya and Shaffer, 1982; Buschmann *et al.*, 1992; Kelly *et al.*, 2004). Indeed, chondrocytes seeded in low concentration agarose gel can maintain their phenotype in long-term culture for up to 70 days in culture (Buschmann *et al.*, 1992), with cytoskeletal organization similar to that seen *in situ* (Idowu *et al.*, 2000). This system has been utilised for mechanotransduction studies both in the absence and development of extracellular matrix (Freeman *et al.*, 1994; Buschmann *et al.*, 1995; Lee and Bader 1995; Knight *et al.*, 1998a and 1998b; Quinn *et al.*, 2002), and has been widely used in the host laboratory to investigate downstream mechanotransduction effects of dynamic compression (Lee and Bader, 1997; Chowdhury *et al.*, 2003; Pinguann-Murphy *et al.* 2005).

Agarose represents only one of the options for a 3D scaffold material. As described in Section 2.1.2.3, alginate, a negatively charged polysaccharide, has some structural and chemical similarity to GAG, which makes it advantageous for tissue engineering applications, and has been employed within some studies in the host lab (Knight *et al.*, 2002; Heywood *et al.*, 2004; Campbell *et al.*, 2006). However, it is this similarity to GAG that can prove a disadvantage when investigating specific aspects of chondrocyte

mechanotransduction. For example, a charged extracellular environment may undoubtedly influence transduction channels and the deposition of extracellular matrix. Furthermore, the gelation process may introduce some degree of heterogeneity to alginate gels, which can influence factors such as cell organisation and morphology (Aydelotte *et al.*, 1998). Thus, the agarose system was considered to represent a more suitable and easy to use 3D model environment for monitoring the biosynthetic behaviour of chondrocytes exposed to PLIUS.

As described in Section 2.1.2.2, the use of monolayer culture for investigation of chondrocyte mechanotransduction events can be problematic due to the loss of chondrocytic phenotype with time and passage in culture, and the difficulty of applying physiological levels of strain. However, a number of studies employing PLIUS have used this culture system to investigate extracellular matrix synthesis (Parvizi *et al.*, 1999; Saito *et al.*, 2004) and a number of associated signalling pathways (Kokubu *et al.*, 1999; Parvizi *et al.*, 2002; Chen *et al.*, 2003; Hsu *et al.*, 2007; Choi *et al.*, 2007) in both osteoblasts and chondrocytes.

7.2.5 Cell seeding densities

At present there is no defined optimum initial cell density for cartilage tissue engineering, with reported values ranging from 0.4×10^6 cells.ml⁻¹ up to 130×10^6 cells.ml⁻¹ (Ruggiero *et al.*, 1993; Vunjak-Novakovic *et al.*, 1999; Mauck *et al.*, 2003; Ng *et al.*, 2006). The continued viability and functionality of cells of a given concentration are dependent on factors such as the volume of nutrients available to cells and the presence of media supplements (Mauck *et al.*, 2003). For the temporal biosynthesis studies undertaken in Chapters 3 and 4, a cell concentration of 4×10^6 cells.ml⁻¹ was chosen for culture in agarose, which is commonly used in the host lab for 48 hour dynamic strain experiments (Lee and Bader, 1997; Lee *et al.*, 2000b; Chowdhury *et al.*, 2003, 2006, 2008). This cell concentration was sufficient to produce quantifiable levels of sGAG and DNA over a 20 day period, using the standard biochemical assays described in Section 3.8.

As previously mentioned, the cell culture system designed for investigation of PLIUS effects on chondrocyte biosynthesis involved a 34mm diameter cylindrical 'slab' of gel of 3mm in depth covered with 6.6ml DMEM + 16.1% FCS. A study conducted in the host laboratory by Heywood and colleagues (2004), employing various chondrocyte

densities ranging from $5\text{-}40 \times 10^6$ cells.ml⁻¹, reported that a ratio of 6.4 ml of medium per million cells maintained homogeneous viability in alginate constructs of dimension $50 \times 25 \times 4$ mm. For the present system, this ratio was equivalent to 0.5ml of medium per million cells. However, chondrocyte viability was maintained throughout the depth of the agarose gels over a 16 day period (Figure 4.13), thus indicating that the medium, which was changed every 2-3 days, could maintain the culture over the length of the experimental period.

For the calcium signalling experiments, a cell seeding density in agarose of 10×10^6 cells.ml⁻¹ was selected. This represented a ratio of 4ml of medium per million cells. This higher concentration enabled approximately 20 chondrocytes per field of view to be visible with a $\times 20$ objective (Figure 6.4), thereby facilitating an adequate population size per construct for appropriate data analysis (Roberts *et al.*, 2001; Pinguan-Murphy *et al.*, 2005 and 2006). Cells were cultured for up to a 24 hour period before being used.

A number of studies have investigated the effect of PLIUS in a monolayer primary chondrocyte system, employing cell densities ranging from 6×10^3 cells.cm⁻² to 10×10^4 cells.cm⁻² (Parvizi *et al.*, 1999 and 2002; Kopakkala-Tani *et al.*, 2006; Hsu *et al.*, 2006 and 2007). Two seeding concentrations for monolayer culture were used in the present work. 10×10^4 cells.cm⁻² was adopted for the 8 day sGAG elaboration experiments undertaken in Chapter 5. However, for the calcium signalling experiments in Chapter 6, a reduced seeding concentration of 2×10^4 cells.cm⁻² was selected to improve visualisation and analysis of isolated chondrocytes during confocal imaging.

7.3 PLIUS-induced mechanotransduction

It is important to address 1) the individual factors impacting on the nature of the chondrocyte response to PLIUS stimulation, 2) the possible mechanisms by which PLIUS influences cell function, and 3) the implications of the present work on the use of PLIUS for bone and cartilage tissue engineering applications.

7.3.1 Variability issues

The chondrogenic response to a given stimuli, and its relevance to the clinical situation, is dependent on various factors such as the species of the cell source, the location from which it was derived, and the age and health of the donor, as well as the subsequent

culture method (Urban, 2000; Giannoni *et al.*, 2005; Isogai *et al.*, 2006 Lee *et al.*, 2006; Choi *et al.*, 2006). The cells used for this thesis were bovine chondrocytes isolated from the full depth of the cartilage of skeletally mature metacarpal joints. In order to ensure appropriate cell numbers for each study, cells were pooled from a number of joints. Moreover, this served to eliminate any donor-specific differences in response, which has been reported following PLIUS exposure of the same cell type (Kopakkal-Tani *et al.*, 2006). However, when comparing results from replicate studies, it became clear that there was variation in chondrocyte metabolic behaviour between separate cell isolations. Indeed, for chondrocytes cultured in the 3D agarose system, total sGAG content (Figures 4.3 and 4.6), sGAG release into the medium (Tables 4.2, 4.4, 5.1 and 5.2), DNA levels (Figures 4.7 and 4.8) and the incorporation rates of SO_4 (Figures 4.11 and 4.12) and [^3H]thymidine (Figures 4.13 and 4.14) over the test period varied between replicate studies, independently of PLIUS stimulation. In addition, cell activity levels, in terms of sGAG produced per cell, estimated with chondrocytes cultured in both agarose and monolayer (Tables 4.7 and 5.3, respectively) reaffirmed the batch-to-batch variation.

Accordingly, the results from each isolation were presented separately, as opposed to pooling the data between batches. The same approach was adopted for the monolayer data in Chapter 5, although the variability between replicate cultures was not as pronounced in this culture system. Variability was also evident in the calcium signalling behaviour of chondrocytes from the same isolation, seen for those cultured in both constructs and monolayers. However, for the purposes of analysis, the data was pooled for both the 10 minute studies (Figures 6.7-6.12) and the 20 minute intensity studies (Figures 6.13-6.18). The 20 minute temporal profiles for the intensity studies (Figures 6.15 and 6.18 for agarose and monolayer, respectively) were presented both for separate isolations and as a mean of the experiments, highlighting both the variability and specific trends in chondrocyte calcium signalling observed over the experimental period.

The metabolism of the chondrocytes is known to differ between the sub-populations present in cartilage. Indeed, data published from the host laboratory found that superficial and deep bovine chondrocytes were responsible for different synthetic mechanotransduction effects and uncoupled pathways when exposed to dynamic loading (Lee *et al.*, 1998 and 2000b). Although the chondrocytes used for the presented

work were isolated from full depth cartilage, the ratio of chondrocyte sub-populations was not controlled. This could explain the observed variation in chondrocyte metabolic behaviour, which has been previously reported in the host laboratory (Chowdhury *et al.*, 2003; Akanji *et al.*, 2008).

7.3.2 Effect of PLIUS intensity

An initial nine day study using chondrocytes seeded in agarose revealed a decrease in viable cells at SATA intensities of 200 and 300mW/cm² (Figures 3.20-3.22). Furthermore, at 300mW/cm², the degree of viability was directly proportional to the distance from the transducer. Studies undertaken by Smith and Nephew Inc. demonstrated a range of thermal effects even when operating at a SATA intensity of 30mW/cm², including self-heating of the transducer, and temperature rises of 1°C within 10 seconds occurring in the well plate (see Section 3.10 and Figure 3.23). Although these studies were not carried out on cell culture systems, it is apparent using the present apparatus and associated chondrocyte models, cells will be exposed to a degree of heating during PLIUS stimulation.

A recent study by Kopakkala-Tani and colleagues (2006), employing a 110mm water gap between the transducer and well plate, found that after 10 minutes of PLIUS (average SATA intensity 580mW/cm², 1 MHz frequency, 1s PRP, 20% duty cycle), a temperature rise of 6.9°C was found at the base of a well plate containing culture medium. This temporal rise in temperature was comparable to that caused by equivalent direct heat, transmitted via a water bath; however, accumulation of the heat shock protein 70 (Hsp70) was reported for bovine chondrocytes cultured in monolayer after direct heat exposure that was not elicited by PLIUS exposure. A PLIUS-induced heat rise appeared not to have a detrimental effect on these cultures, which showed increased SO₄ incorporation compared to untreated controls over a five day period. These findings are in contrast to those presented in Chapter 3, which showed reduced sGAG elaboration at the higher SATA intensities. A direct comparison cannot be made, however, due to the difference in experimental arrangements. The use of a water bath by Kopakkala-Tani and colleagues permitted the transfer of PLIUS-induced heat to the surroundings at a greater rate than that in the present system. The loss of cell viability seen for higher intensities may be due to the effect of heat as opposed to the ultrasonic intensity per se, as the SATA intensity used by Kopakkala-Tani and co-workers was approximately twice that employed in the present work; based on the intensity field

characterisation study undertaken by Smith and Nephew Inc. (Figure 3.6), the effective intensity experienced by chondrocytes in their study could be even higher.

Based on the results of the study in chapter 3, subsequent experiments utilised the 100mW/cm² SATA intensity as well as 30mW/cm². However, the enhanced sGAG per cell in PLIUS-stimulated agarose cultures exposed to up to 200mW/cm² for 9 days (Table 3.3) was not reproduced for subsequent experiments at 30mW/cm² data in chapter 4 (Table 4.7). In fact, the majority of experiments undertaken in chapters 4 and 6 showed that chondrocytes were not stimulated by exposure to PLIUS at 30mW/cm², whether cultured in agarose or in monolayer. The employment of an additional 20 minute daily PLIUS stimulation for agarose cultures (termed PLIUSx2 in chapter 4) also did not lead to an up-regulation of matrix synthesis. Indeed, for sGAG content in particular, a down-regulation was evident for the majority of time-points (Figure 4.1). This finding is in contrast to previous studies for which a longer/more frequent period of PLIUS stimulation caused an increased biosynthesis (Cook *et al.*, 2001; Schumann *et al.*, 2006; Park *et al.*, 2007). It is possible that additional PLIUS exposure may inhibit cell activity in the present experimental system.

At the higher intensity of 100mW/cm², the results are inconsistent. Although a marginal stimulatory effect was observed in terms of sGAG elaboration in agarose constructs (Figures 4.4 and Table 4.3), no such stimulatory effect was seen in the monolayer system. Furthermore, the results of the calcium signalling experiments indicated an inhibitory chondrocyte response at 100mW/cm² in both agarose and monolayer cultures (Figures 6.15F and 6.18D, respectively), which was statistically significant in the former ($p < 0.05$). Whether this inhibitory calcium transient behaviour was due to the 100mW/cm² SATA intensity alone, or an accumulation of effects from exposures to lower magnitude intensities is unclear. However, most notably for the chondrocytes cultured in agarose, cells appeared to recover in the two minute period between successive PLIUS exposures, based on the normalised percentage of chondrocytes eliciting a calcium transient (Figure 6.15 and 6.17). Parvizi and colleagues (2002), in their investigation of the events underlying ultrasound-stimulated aggrecan synthesis in neonatal rat chondrocyte monolayer cultures, reported an increased intracellular calcium concentration resulting from PLIUS intensities between 25-100mW/cm². Furthermore, their use of calcium channel blockers, that depleted both intra- and extracellular calcium stores, led to an inhibition of ultrasound-stimulated proteoglycan synthesis. This implies

coupling of the two processes in their work. Therefore, the apparent up-regulation of sGAG elaboration seen for chondrocyte-agarose cultures exposed to the higher $100\text{mW}/\text{cm}^2$ SATA intensity in the present work is unlikely to be due to any calcium signalling mechanism, based on the results obtained in Chapter 6.

It has been suggested that different intensities of PLIUS may elicit different pathways of cell response, as seen with mineralization of osteoblasts in monolayer (Saito *et al.*, 2004), and cell proliferation and proteoglycan synthesis in intervertebral disc cells cultured in alginate (Iwashina *et al.*, 2006). Therefore it is possible that there is some mechanism by which chondrocytes in agarose transduce the $100\text{mW}/\text{cm}^2$ signal into increased elaboration of sGAG not apparent at the lower $30\text{mW}/\text{cm}^2$ intensity. However, whether there are any beneficial effects of increasing SATA intensity is not clear from the literature, with some studies reporting a directly proportional relationship between intensity and cell activity (Harle *et al.*, 2005; Choi *et al.*, 2006; Hsu *et al.*, 2006), while others suggest that lower intensities were more effective (Tien *et al.*, 2008; Ebisawa *et al.*, 2004; Zhang *et al.*, 2003), and other studies indicate little difference between intensity levels (Parvizi *et al.*, 1999). What is evident is that the relationship between ultrasonic intensity and promotion of cell activity varies widely between specific culture systems, the nature of the PLIUS signals employed, and the markers of cell activity under investigation.

The stimulation of sGAG elaboration at the higher $100\text{mW}/\text{cm}^2$ SATA intensity, as assessed by DMB assay, remains questionable. This marginal effect may be attributed to an isolated cell-donor specific response as opposed to a generic indication of the effectiveness of PLIUS at this intensity, particularly as the rate of sGAG production was very similar for one of the cell isolations (Figure 4.4A). Further investigations are required to elucidate any stimulatory processes at this intensity.

7.3.3 Comparison of monolayer and 3D culture

PLIUS was not generally found to stimulate bovine chondrocytes in either agarose or monolayer culture. However, the employment of the two culture systems highlighted differences with regard to metabolic response, that was unaffected by PLIUS stimulation or cell isolations. The results from the biosynthesis experiments undertaken in chapters 4 and 5 could not be directly compared due to differences in the experimental set up and methods for sample harvest. However, in general, monolayer

systems showed approximately 50-100% greater sGAG and DNA content and incorporation rates compared to chondrocytes cultured in agarose. In addition, a greater sub-population of monolayer chondrocytes exhibited changes in calcium concentration compared to those in agarose constructs (approximately 30% greater at 10 minutes and 15% greater at 20 minutes).

In an agarose culture environment, chondrocytes produce extracellular matrix that is trapped in the 3D framework and can accumulate pericellularly. The formation of this pericellular matrix creates a steric hindrance that limits the movement of newly-synthesised further matrix molecules out into free space, and results in altered mechanotransduction effects with time and a decreased synthetic response. This effect is not as pronounced in monolayer culture, as synthesised matrix molecules are more able to be released into the culture medium. Indeed, as much as 70% of monolayer produced sGAG was released into the medium (Tables 5.1 and 5.2), in comparison with 15-30% seen for in the agarose system (Tables 4.3 and 4.5). However, as monolayers approached confluency, a decrease in synthetic response was observed.

The phenotypic status of chondrocytes cultured in monolayer is known to alter over time in culture (Lee *et al.*, 2003; Barlic *et al.*, 2008). The extent to which chondrocytes lose their phenotype is dependent on the initial seeding density (Murata *et al.*, 1998; Galois *et al.*, 2006). For example, four month old bovine calf chondrocytes exhibited a reduction in collagen II and aggrecan expression and induction of collagen I expression compared to native cartilage when cultured in monolayer for twelve days at both low and high seeding densities of 4×10^4 cells.cm⁻² and 60×10^4 cell.cm⁻², indicating partial dedifferentiation which was generally more marked at the lower seeding density (Galois *et al.*, 2006). However, in another study, phenotype was maintained for neonatal rat chondrocytes seeded at 1.7×10^4 cell.cm², and cultured for eight days (Parvizi *et al.*, 1999). It is likely that the adult bovine monolayer cultures utilised for the metabolic studies undertaken in Chapter 5, at a cell density of 10×10^4 cell.cm⁻², as well as the 2×10^4 cells.cm⁻² monolayers used for the calcium signalling experiments in Chapter 6, would have experienced a loss of chondrocytic phenotype over the respective eight and three day experimental periods. A number of studies have shown that PLIUS stimulates chondrogenic gene markers in mesenchymal stem cells and primary chondrocytes, cultured in both monolayer and aggregate form (Parvizi *et al.*, 1999; Mukai *et al.*, 2005; Ikeda *et al.*, 2006; Schumann *et al.*, 2006). Whether PLIUS is able to stimulate aggrecan

gene expression in the present system requires investigation. However, any up-regulation of GAG specific genes in monolayer did not lead to increased protein synthesis, as demonstrated by both SO_4 incorporation and DMB results.

It is well documented that cell behaviour can vary in 2D and 3D culture (Gruber and Handley, 2000; Pederson and Swartz, 2005; Martins and Kolega, 2006). Thus the increased chondrocyte proliferation occurring due to expansion in monolayer culture would enhance the telomeric age of cells in this system compared to that in agarose, which may influence the response of cells to a given stimulus. Additionally, the cell spreading associated with monolayer culture would influence the nature of focal adhesion formation, and the resulting chondrocyte mechanosensitivity. Physical aspects of the PLIUS signal, such as the production of standing waves, substrate heating, and purported microstreaming, may have a greater effect on monolayer chondrocyte systems due to all cells existing in one plane on the surface of the well plate, which, in the present system, was in direct contact with the transducer. However, the studies undertaken in Chapter 5 were unable to elicit any PLIUS-induced effects. In any case, it is possible that the ultrasonic signal may need to be altered between 2D and 3D cultures in order for both systems to experience a biosynthetic response after exposure to PLIUS. Whether any of the above influences the sensitivity of 2D or 3D cell systems to PLIUS-induced phenomenon is still open to question based on the present findings.

7.3.4 Influence of PLIUS of chondrocyte biosynthesis

The findings of a number of *in-vitro* studies investigating PLIUS influence on chondrocyte behaviour, including those presented in this thesis, are summarised in Table 7.1. It can be seen that some of the present findings contrast with those from the published literature, for which markers of sGAG synthesis, namely aggrecan gene expression, incorporation rates of SO_4 into newly formed sGAG, and downstream sGAG accumulation, were found to be up-regulated by PLIUS. With the exception of marginal increase in total sGAG content seen in agarose culture at $100\text{mW}/\text{cm}^2$ (discussed in Section 7.3.2), PLIUS did not stimulate chondrocyte sGAG synthesis in the present model systems. The present findings were, however, in accordance with those of most other studies demonstrating minimal effects of PLIUS on cell proliferation. The exceptions to this trend was reported in one study employing a SATA intensity of $2\text{mW}/\text{cm}^2$ on chondrocytes isolated from chick embryos (Zhang *et al.*, 2003, Table 7.1), and another involving 20 minutes daily PLIUS stimulation at $30\text{mW}/\text{cm}^2$ for

TABLE 7.1: *The influence of pulsed low intensity ultrasound (PLIUS) on the metabolic behaviour of chondrocytes.*

Study	Culture system	Cell source	PLIUS signal	Daily PLIUS dose	Effect of PLIUS
Present work - Chapter 3	Agarose	18-24 month primary MCPJ BACs	1.5 MHz, 20% duty cycle 13-300mW/cm ²	20 mins daily D1-D9	nc viability or sGAG content 13-100 mW/cm ² ; ↓210-300mW/cm ² . ↓total DNA content
Present work - Chapter 4	Agarose	18-24 month primary MCPJ BACs	1.5 MHz, 20% duty cycle 30 & 100mW/cm ²	20/40 mins daily D1-D20	nc sGAG synthesis except ↑100mW/cm ² , nc DNA synthesis, nc total sGAG or DNA content. ↓ 40 min stimulation
Present work - Chapter 6	Agarose	18-24 month primary MCPJ BACs	1.5 MHz, 20% duty cycle 30-200mW/cm ²	10/20 mins on D1	nc [Ca ²⁺] _i signalling behaviour except ↓100mW/cm ²
Nishikori <i>et al.</i> (2001)	Collagen gel	10-wk-old hip, knee, shoulder rabbit chondrocytes	1.5MHz 20% duty cycle 30mW/cm ²	20 mins daily D1-D21	↑ sGAG synthesis nc cell proliferation nc gel stiffness
Zhang <i>et al.</i> (2003)	Alginate beads	16-day-old chick embryo sternal chondrocytes	1.5MHz 20% duty cycle 2mW/cm ² 30mW/cm ²	20 mins on D2	nc viability or aggrecan exp. ↑PLIUS coll II exp Cell proliferation: ↑2, ↓30 Coll X exp: ↓2
Present work - Chapter 5	Monolayer	18-24 month primary MCPJ BACs	1.5 MHz, 20% duty cycle 30 & 100mW/cm ²	20 mins daily D3-D8	nc sGAG synthesis, NE DNA synthesis, nc total sGAG or DNA content
Kopakkala-Tani <i>et al.</i> (2006)	Monolayer	12-24 month primary femoral BACs	1 MHz, 20% duty cycle 580mW/cm ²	10 mins daily D9-D13	↑ sGAG synthesis nc HSP70 induction
Parvizi <i>et al.</i> (1999)	Monolayer	3-5 day old rat femoral chondrocytes	1 MHz, 20% duty cycle 50 & 120mW/cm ²	10 mins daily D3-D8	↑ aggrecan exp. ↑ sGAG synthesis nc cell proliferation nc Coll I or Coll II exp.
Present work - Chapter 6	Monolayer	18-24 month primary MCPJ BACs	1.5 MHz, 20% duty cycle 30-200mW/cm ²	10/20 mins on D3	nc [Ca ²⁺] _i signalling behaviour
Parvizi <i>et al.</i> (2002)	Monolayer	2-3 day old rat femoral chondrocytes	1 MHz, 20% duty cycle ~25-100mW/cm ²	2-10 mins on D3	PLIUS ↑[Ca ²⁺] _i conc. Chelating [Ca ²⁺] _i , ↓PLIUS induced sGAG synthesis.

MCPJ = metacarpal joint, BAC = bovine articular chondrocytes. ↑, ↓ and nc denotes up-regulation, down-regulation and no change, respectively.

10 days, which induced a marginal increase in DNA content in neonatal rat chondrocyte aggregate cultures (Mukai *et al.*, 2005; see Table 2.5). Given that these two studies show a disparity at 30mW/cm^2 , it is evident that the nature, duration and intensity of the PLIUS signal are critical in this process. Indeed, Zhang and colleagues reported a down-regulation of cell proliferation one week after one single 20 minute PLIUS dose at this higher intensity. Of note, this study additionally implies the promotion of collagen II expression in chick chondrocytes. By contrast, no such PLIUS-induced effect on collagen expression was seen in neonatal rat chondrocytes (Parvizi *et al.*, 1999).

It should be noted that the majority of studies reporting PLIUS-induced up-regulation employed immature chondrocytes (Table 7.1). The main function of chondrocytes during development are mitosis and matrix production to increase tissue mass (Section 1.3.1). Indeed cellularity and cell organisation in bovine articular chondrocytes (BACs) *ex-vivo* have been shown to alter with age (Jadin *et al.*, 2005). Additionally, fetal, calf and adult BAC explants have been shown to respond differently to static and dynamic loading (Li *et al.*, 2001), implying that these younger cells may be more sensitive to a given mechanical stimulus. Although the role of PLIUS in cell proliferation remains in question, from Table 7.1 it is probable that sGAG synthesis is stimulated by PLIUS in immature cells.

BACs have been classed as 'adult' from 12 months, implying that at that stage they are skeletally mature (Galois *et al.*, 2006). This paper further reported an inversely proportionality relationship between sGAG deposition in collagen gels and cell age. From Table 7.1, the only other study employing skeletally mature cells is that of Kopakkala-Tani and colleagues (2006). However, their study demonstrated a PLIUS-induced up-regulation of sGAG synthesis in monolayer culture, in contrast to the present work. Possible reasons for this difference have already been described in Sections 5.4, 7.3.1 and 7.3.2.

Dynamic compression studies conducted in the host laboratory utilise time courses of stimulation ranging from 1.5-48 hours, frequencies between 0.3-3Hz and cyclic compressive strain amplitudes of between 0-15%, equivalent to a range of compressive stress from 0-5MPa. It has been estimated that a 1.0MHz PLIUS signal of SATA intensities from 25 to 100mW/cm^2 translates to average peak pressures of 111-351 kPa (Parvizi *et al.*, 2002). Therefore, the ultrasonic signal presented in this thesis applies a

level of compressive strain at least 14 times lower than that experienced by cells during dynamic compression studies, and as such be described as a high frequency micromechanical perturbation. Despite the differences in culture set up between the dynamic compression studies and the present work, it is apparent that these two types of mechanical stimulation lead to vastly diverse effects on the metabolic and biosynthetic behaviour of chondrocytes cultured in agarose constructs.

In terms of the PLIUS signal, it is unclear as to which aspect contributes to the metabolic effects seen for the majority of the studies presented in Sections 2.5.9, 2.5.10 and Table 7.1. Although a number of recent studies have examined a variety of ultrasonic signals, employing both pulsed and continuous wave, no definitive relationship has been confirmed. Edlich and colleagues (2001), investigating oscillating fluid flow in BAC monolayers, proposed that high oscillation frequencies would lead to minimal flow-induced cell changes, due to the reduction in net fluid transport. Concordantly, Parvizi and colleagues (2002) speculated that their 1.0MHz ultrasonic signal would introduce cells to an effective hydrostatic pressure due to the large 1.5mm wavelength in comparison to chondrocyte dimension, and that it was the pulsed 200ms pulsed signal (20% duty cycle, repeated at 1.0kHz) that may provide cell perturbations and/or deformations. Another facet of the PLIUS signal employed in the present system is the formation of standing waves in the wells of the six well plates due to the medium-air interface (see Section 3.5.2), which may contribute to the temperature distribution in the well plate (see Section 3.10), and, in turn, influence cell metabolism. The occurrence of standing waves every $\sim 0.5\text{mm}$ meant that they were unavoidable when establishing the height of the culture medium in the present system. Some studies have employed systems whereby no liquid-air interface is present in order to have increased control of the PLIUS signal, as well as using ultrasound-absorbing material to eliminate reflections (Harle *et al.*, 2001; Zhang *et al.*, 2003; Mukai *et al.*, 2005; Iwashina *et al.*, 2006). However, the precise effects of standing waves on a cell system, such as chondrocytes in 2D or 3D culture, are largely unknown and require further investigation.

The pathways by which PLIUS may induce downstream chondrocyte biosynthesis, and the factors affecting this, which have been highlighted in Chapters 2, 3 and the present chapter, are summarized in Figure 7.1.

The possibility of cell deformation due to PLIUS has not been broadly investigated. In a recent study, a 5MHz continuous ultrasonic signal elicited alteration of cell morphology in HAC-seeded chitosan scaffolds, with associated up-regulation of cell proliferation, viability and gene expression (Noriega *et al.*, 2007). However, a lower 1.5MHz pulsed frequency did not elicit an equivalent effect. The possible involvement of integrins and stretch-activated channels implies that the acoustic energy from the PLIUS signal may have the ability to modify cell membrane permeability without inducing alteration of cell shape, involving microstreaming and/or fluid shear.

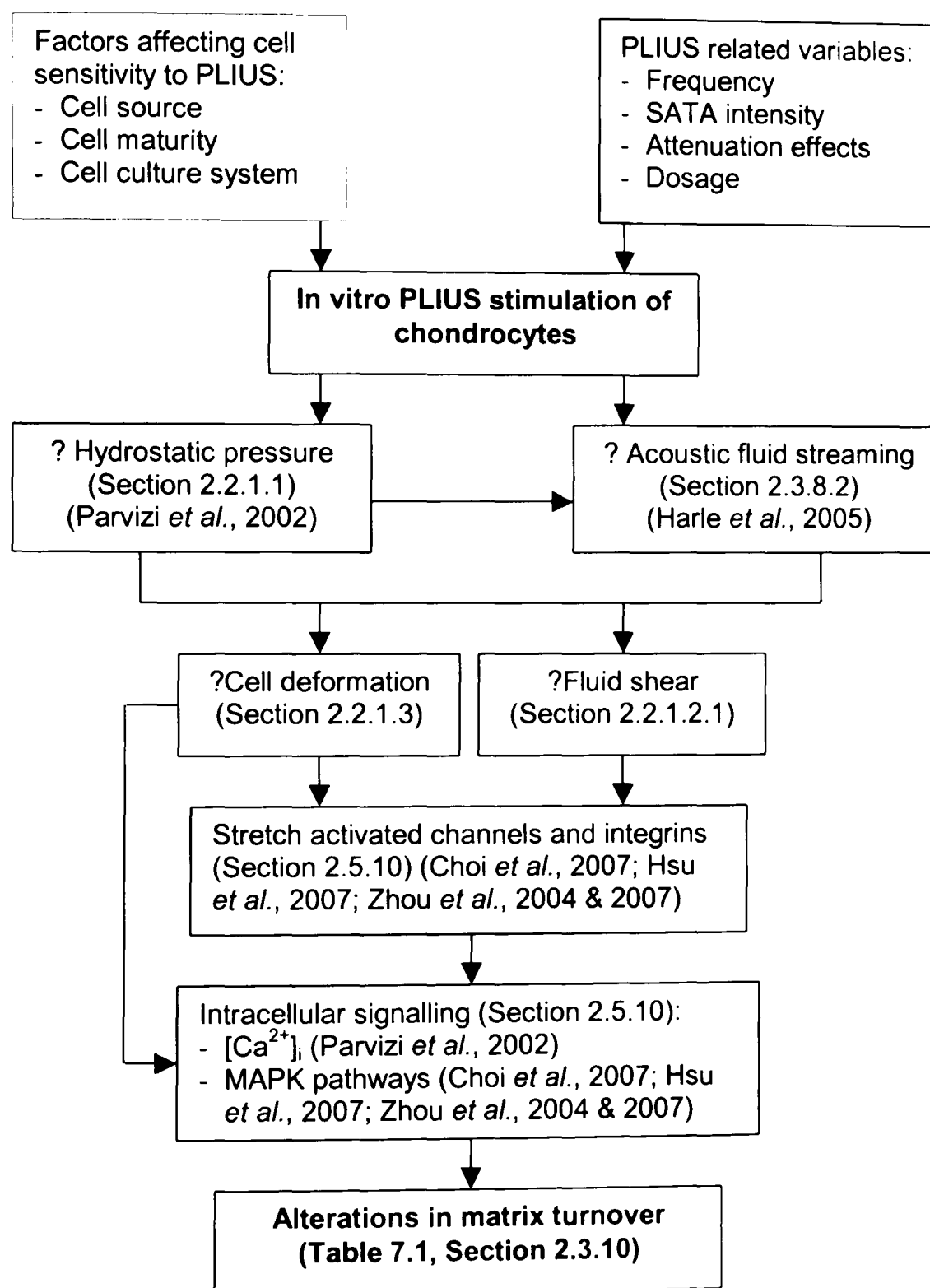


FIGURE 7.1: Possible pathways by which pulsed low intensity ultrasound (PLIUS) affects matrix biosynthesis in cultured chondrocytes.

The results of the present work did not confirm any of the pathways in Figure 7.1. There is a possibility that PLIUS is able to elicit non-calcium related signalling, which would require further investigation in both agarose and monolayer systems. However, based on the present results, any perceived signalling pathway did not give rise to an enhanced matrix synthesis. However PLIUS may affect catabolic as well as anabolic pathways, which may result in a net positive, net negative or no effective change with respect to sGAG elaboration in the presented systems. Catabolic markers may thus be investigated in future work.

The enhanced fluid movement by PLIUS may result in an increased nutrient delivery and removal of waste products in a cell culture system. Indeed, Cui and coworkers (2006), who exposed rabbit MSCs seeded in PGA constructs to 0.8 MHz continuous ultrasound at SATA intensity $200\text{mW}/\text{cm}^2$ in an *in-vivo* nude rat model, reported a more widely distributed and dense ECM deposition compared to control constructs. They attributed this to increased transport in the stimulated constructs. The role of diffusion and mass transport in *in-vitro* PLIUS-related activity was investigated in a preliminary study.

7.3.5 PLIUS-induced diffusion in agarose culture

An additional hypothesis was proposed through which PLIUS may influence chondrocyte biosynthesis in agarose culture and particularly in intact tissue; namely that PLIUS enhances diffusion and thereby influences cell metabolism by:

- 1) Enhancing nutrient delivery to cells, and/or
- 2) Increasing matrix transport away from cells, so reducing steric inhibition.

A preliminary study was performed in a cell-free agarose system to investigate the influence of PLIUS on diffusion of fluid, using the microscope technique of fluorescent recovery after photobleaching (FRAP). Fluorescent molecules are allowed to permeate into the sample, and then an intense laser beam is focused on a small area, eliciting irreversible fluorophore breakdown, termed *photobleaching*, that creates a dark region in the subsequent fluorescence images. Fluorescence gradually returns to this bleached region at a rate dependent on the diffusion characteristics of the fluorescent molecules.

7.3.5.1 Materials and Methods

Low-gelling agarose was made up as described in Section 3.2.3, in the absence of cells. PBS (Sigma) was used in place of DMEM to dilute the agarose to 3% (w/v). The cell-free agarose was gelled in the perspex inserts described in Section 3.6.3 to form 5x5x5mm constructs. These were then incubated for 24 hours at 37°C in 0.001% w/v solutions of fluorescein isothiocyanate (FITC) labelled dextrans of molecular weights 4kDa, 70kDa and 500kDa. The smallest 4kDa dextran is equivalent to the molecular weights of growth factors and hormones such as TGF-β and IGF-1, while 70kDa is representative of small non-aggregating proteoglycan molecules, such as biglycan and decorin, and 500kDa the larger proteins such as cartilage oligomeric matrix protein (COMP) and fibronectin (Leddy and Guilak, 2003).

After incubation, the construct and its respective FITC dextran solution were placed in the test rig, described in Section 3.6, and mounted on the stage of a confocal microscope (Leica SP2). An optimised FRAP protocol, similar to that previously used in the host laboratory (Campbell *et al.*, 2007a and 2007b), was used to quantify dextran diffusion with and without exposure to PLIUS at 30mW/cm². A series of five pre-bleach confocal images were recorded at 3% of maximum laser power. A 50µm diameter bleach region was then created, and a sequence of images recorded at a rate of one every 0.844s up to approximately 30 seconds post-bleach, at 3% laser power. Mean intensities measured within the bleached region at time t (I_t) were normalized to the mean pre-bleached intensity (I_p) and the first post bleach intensity (I_1) using the equation:

$$I_{normalised} = \frac{I_t - I_1}{I_p - I_1} \times 100 \quad \text{Equation 7.1}$$

All experiments were performed at room temperature. Ten FRAP procedures were conducted for each experimental condition.

7.3.5.2 Results

Figure 7.2 illustrates a typical FRAP process for 70kDa FITC-dextran in the absence of PLIUS, showing both the confocal image sequence (Figure 7.2A) and the resulting normalized FRAP curve (Figure 7.2B) over the 30 second post bleaching period. It can

be seen that by 30 seconds there is approximately 85% recovery, and that by extrapolating the curve the mobile fraction is likely to be 100% (Figure 7.2B).

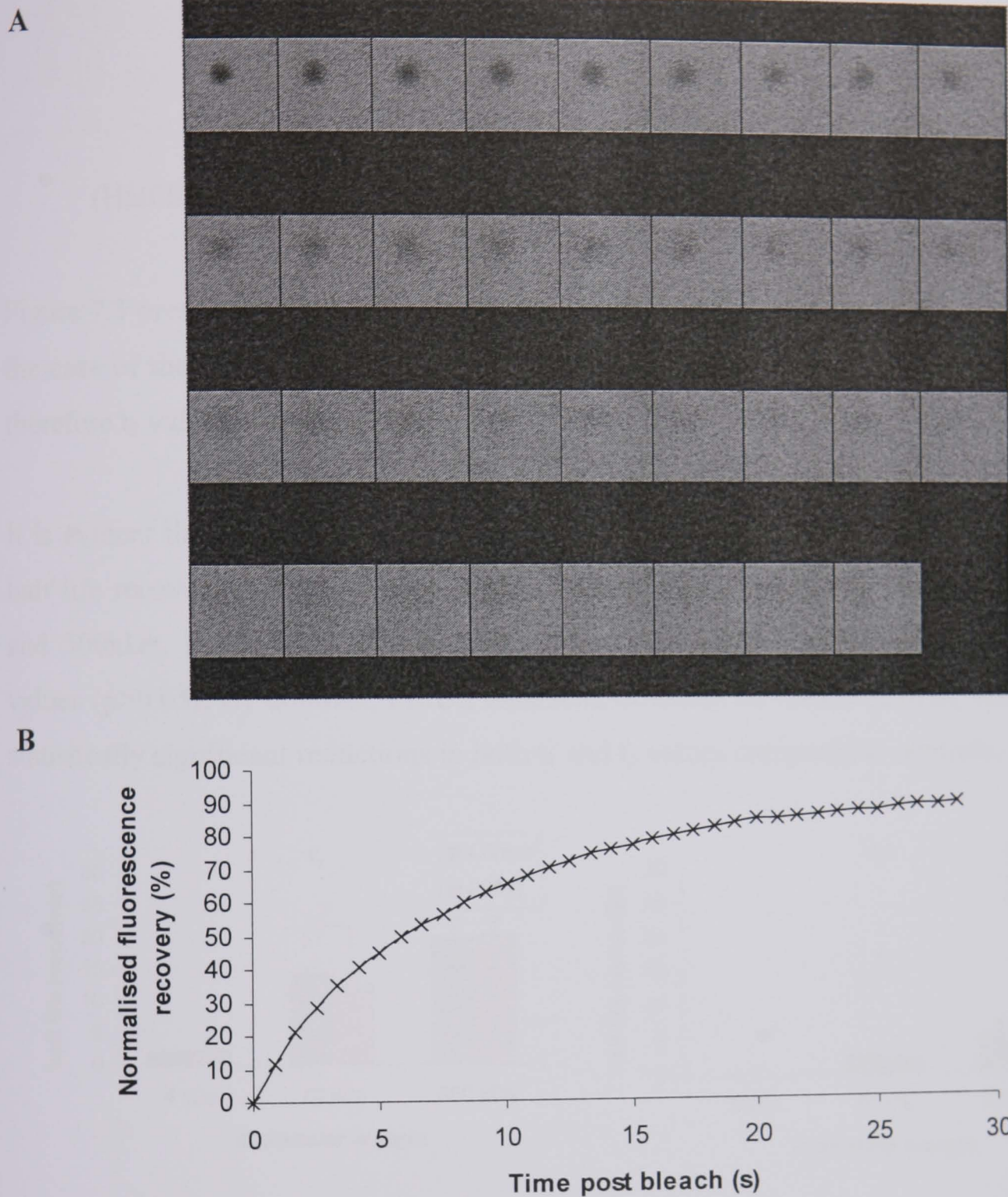


FIGURE 7.2: Representative FRAP analysis for 70kDa FITC-dextran showing **A)** confocal time series over the approximate 30 second post bleach period and **B)** the resulting normalized FRAP curve. The $50\mu\text{m}$ bleach region is clearly visible in the initial images but after 30 seconds fluorescence returns almost completely to pre-bleach levels.

A two phase exponential was fitted to the raw data (Equation 7.2) from which the half lives of fluorescent recovery, in seconds, were calculated (Equation 7.3):

$$I_t = I_p - ([A1 \times \exp(-t/T1)] + [A2 \times \exp(-t/T2)] + C) \quad \text{Equation 7.2}$$

Where: $A1/A2$ = amplitude of exponential term 1/term 2
 $T1/T2$ = time constant of exponential term 1/term 2
 C = pre-bleach intensity for $t \rightarrow$ infinity.

$$(\text{Half life})_t = \ln 2 \times T_t \quad \text{Equation 7.3}$$

Figure 7.3 presents the half-lives (t_1 and t_2) for each dextran with and without PLIUS. In the case of the 4kDa dextran, the recovery was best fitted by a single exponential, and therefore t_2 values are not presented.

It is evident that there is a proportional relationship between the molecular weight and half-life recovery of the dextrans, evident with and without PLIUS exposure. At 4kDa and 500kDa, PLIUS had no significant effect on diffusion in terms of the half live values ($p > 0.05$). By contrast, PLIUS enhanced diffusion of 70kDa dextran, reflected by statistically significant reductions in both t_1 and t_2 values compared to controls.

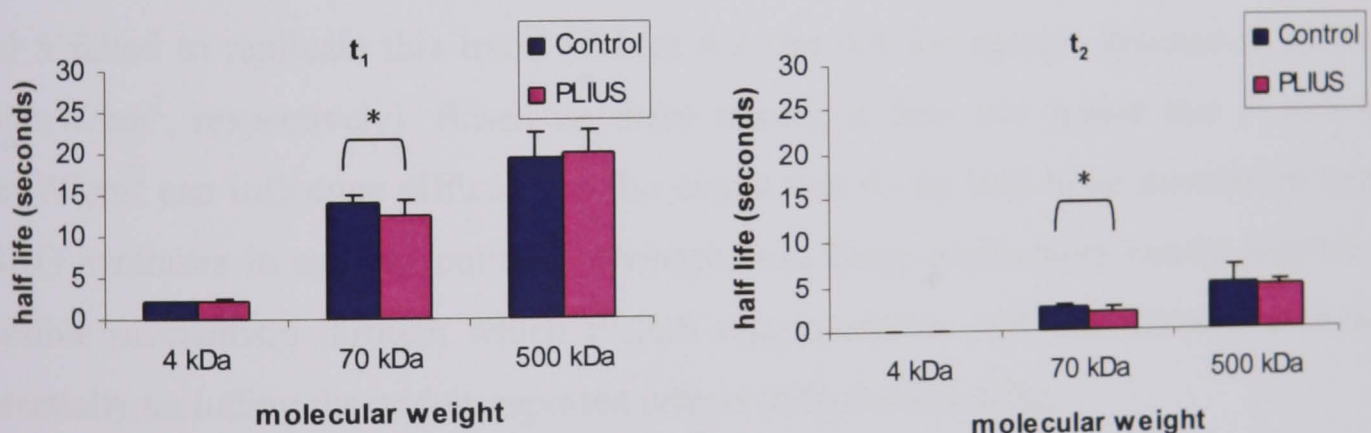


FIGURE 7.3: Effect of PLIUS on diffusion quantified using FRAP. Values represent the mean half lives (t_1 and t_2) for recovery of FITC-dextrans with molecular weights of 4, 70 and 500 kDa, with or without exposure to PLIUS (1.5MHz, 200ms pulsed at 1.0kHz, SATA intensity 30mW/cm²) ($n=10$). In the majority of cases, the 4kDa recovery was best fitted by a single exponential, and hence t_2 values are not shown. Error bars indicate standard deviations. Statistically significant differences between PLIUS and control groups are indicated (* = $p < 0.05$).

7.3.5.3 Discussion

FRAP analysis demonstrated that increasing molecular weight was associated with a reduced diffusion, as denoted by statistically significant differences in half life. In addition, PLIUS at 30mW/cm^2 promoted diffusion of 70kDa dextran molecules ($p<0.05$), but not 4kDa and 500kDa. The reason for this molecular weight dependent effect of PLIUS on diffusion is unclear, as are any resulting biological consequences. PLIUS may enhance the diffusion/transport of molecules such as biglycan and decorin, which are of a similar molecular weight and have a role in stabilizing cartilage extracellular matrix (Taylor and Gallo, 2006; Poole *et al.*, 2001). Consequently PLIUS may influence the formation of the pericellular matrix within the agarose cultures. Furthermore, this could potentially reduce matrix-induced steric inhibition of matrix synthesis, although the present studies found no overall effect on total sGAG production (Section 4.3.1).

In addition, PLIUS enhanced diffusion at 70kDa may increase the loss of matrix molecules from the agarose constructs. Indeed, the preliminary intensity study undertaken in Section 3.9 appeared to show that PLIUS promoted sGAG release into the medium from agarose constructs (Table 3.2). However, further assessment in Chapters 4 and 5 failed to replicate this trend (Tables 4.2 and 4.4 for agarose systems at 30 and 100mW/cm^2 , respectively). Based on these results, it does not appear that PLIUS at 30mW/cm^2 can influence diffusion to the extent that it can lead to an increase in total sGAG synthesis in agarose cultures. Nevertheless, these preliminary results suggest a possible mechanism through which PLIUS may modulate cell and tissue behaviour, potentially including the widely reported effects in fracture healing.

7.3.6 Use of PLIUS in cartilage repair strategies

The rationale for the present work was to identify some of the processes by which PLIUS could stimulate cartilage metabolism in order to assess how this may be activated during the bone healing process, and furthermore, to assess the potential use of PLIUS in cartilage repair and cartilage tissue engineering applications.

The present work has demonstrated that primary chondrocytes cultured in agarose or in monolayer were not stimulated into increased sGAG synthesis. This is in contrast with *in vivo* studies involving the healing fracture callus, where increased aggrecan expression was demonstrated after stimulation with PLIUS (Yang *et al.*, 1996).

Research into the use of PLIUS for cartilage repair has mainly concentrated on *in-vitro* studies with an aim of using this form of mechanical stimulation for bioreactor conditioned tissue engineered cartilage constructs for surgical intervention of cartilage defects. However, the literature is confusing in terms of whether low intensity continuous or pulsed ultrasound can positively affect long-term cartilage biosynthesis, as would be necessary for tissue engineered 3D scaffolds. The use of skeletally mature cells, as employed in this thesis, is relevant to the clinical situation, where the majority of patients seeking surgical intervention for cartilage injury are adults, and a tissue engineered approach to cartilage repair is likely to involve the use of autologous cells. However, a recent paper by Tien and co-workers (2008), evaluating the effect of PLIUS on human child articular chondrocytes cultured in agarose, found that cells harvested from older donors were less responsive to PLIUS stimulation. This highlights the possibility that PLIUS of the present parameters may have at most a limited effect on tissue culture of skeletally mature chondrocytes. An alternative tissue engineering approach may be to employ the present PLIUS signal to stimulate autologous mesenchymal stem cells (MSCs) into chondrogenesis, given that the cartilaginous tissue formed during the endochondral ossification process in bone develops from this cell type. A recent study by Schumann and colleagues (2006) demonstrated some stimulatory effect of PLIUS on proteoglycan and collagen marker expression and matrix deposition in hMSCs cultured in 3D scaffolds.

7.4 Future work

There are several directions in which future work on the PLIUS-induced mechanotransduction effects can proceed. These are briefly discussed in separate subsections.

7.4.1 Further investigation of the 100mW/cm² signal

The present findings reveal only marginal stimulation of chondrocyte sGAG accumulation in agarose culture when employing a SATA intensity of 100mW cm². In order to investigate if this finding is reproducible with additional chondrocyte batches, further experiments at the higher SATA intensity are proposed. These include twice-daily stimulation (PLIUSx2) as used in Chapter 4. This could be followed up by examination of calcium signalling behaviour and diffusion.

7.4.2 Influence of PLIUS on other ECM molecules

Although the present work has indicated that PLIUS has no effect on total sGAG production as assessed by total sGAG and incorporation assays, further work could investigate whether the size and type of sGAG found in PLIUS-stimulated cultures differ from that in a non-stimulated system. Additionally, the effect of PLIUS on production of the other major extracellular matrix molecule, collagen, could be examined. Due to the fact that collagen has a relatively low turnover compared to sGAG, it may be more suitable to assess collagen at a gene expression level by observing chondrogenic markers such as aggrecan and collagen II, as well as collagens I and X, using real-time quantitative PCR as undertaken in the host laboratory (Chowdhury *et al.*, 2008; Akanji *et al.*, 2008). However, it is important to note that up-regulation of these markers does not necessarily lead to synthesis of the protein molecules.

7.4.3 Other intracellular mechanotransduction events

As mentioned in Section 7.3.4, SACs, integrins and MAP kinases have been implicated as possible pathways involved in PLIUS-induced mechanotransduction. In the event of a PLIUS-induced stimulation of extracellular matrix synthesis (Sections 7.4.1 and 7.4.2), the signalling pathways could be investigated in agarose constructs, as well as in monolayer. The role of both anabolic and catabolic cytokines could also be investigated. For example, TGF-1 β has been implicated in PLIUS-induced up-regulation of collagen II and aggrecan gene expression in neonatal rat aggregate culture (Mukai *et al.*, 2005), and in chondrogenesis of hMSCs (Ebisawa *et al.*, 2004). Two recent studies have demonstrated a down-regulation of MMP-1 gene by employment of low intensity ultrasound in chondrocytes cultured in aggregate and alginate culture (Park *et al.*, 2007; Choi *et al.*, 2006). Other studies have implicated downstream COX-2 and prostaglandin production after exposure to PLIUS (Kokubu *et al.*, 1999; Hsu *et al.*, 2007). These studies imply a possible role for PLIUS in regulation of the processes associated with osteoarthritis.

Possible PLIUS-induced changes to organelle morphology and organisation could also be investigated. Indeed, confocal imaging and FRAP studies undertaken in the host laboratory have investigated the effects of mechanical compression and hydrostatic pressure on actin cytoskeletal, mitochondrial organisation and nuclear distortion in BACs cultured in agarose and monolayer (Lee *et al.*, 2000a; Knight *et al.*, 2006a and

2006b; Campbell *et al.*, 2007a and 2007b). These methodologies could be adopted for use in the present systems.

7.4.4 Alteration of the model system and PLIUS signal

The main drawbacks of using the current 6-well plate system with which to stimulate chondrocytes with PLIUS are:

- the proximity of the well plate to the transducer
- the attenuation of the signal in air leading to likely residual heating effects, and
- reflection at the air/liquid interface, leading to standing waves.

The employment of a water bath to distance the transducers from cells, similar to that used by Kopakkala-Tani and colleagues (2006), would enable use of the far field ultrasonic signal which is more stable and closest to the nominal SATA intensity (Section 3.5.1).

Other measures for minimising these effects could also be examined such as elimination of the air/liquid interface and use of absorbing materials to eliminate reflection back into the ultrasonic transducer/culture system (Harle *et al.*, 2001; Zhang *et al.*, 2003; Mukai *et al.*, 2005; Iwashina *et al.*, 2006). Investigation would be required in order to assess the effective PLIUS signal after the incorporation of such changes.

PLIUS parameters per se could also be varied, such as alteration of the daily dose to cell systems, changing the duty cycle of the pulsed signal, and elimination of the pulsed component entirely, with modification to a continuous ultrasonic signal. However, the latter two suggestions would again require some modifications to the existing system. Zhang and colleagues (2003) use of a PLIUS signal of $2\text{mW}/\text{cm}^2$ SATA intensity led to some interesting observations, particularly with reference to cell proliferation. The authors did not explain their use of this lower intensity, but it is possible that it is a reflection of attenuation through the tissue of a major articular joint. This may therefore represent a more realistic signal to employ for investigation of PLIUS for mechanotransduction in tissue engineering applications.

Additionally, cell source could be altered to employ primary human chondrocytes or mesenchymal stem cells to investigate the role of PLIUS in chondrocyte biosynthesis and chondrogenesis.

7.5 Final summary

Pulsed low intensity ultrasound (PLIUS) is used clinically to accelerate fracture healing. However, the mode of action is unclear although studies suggest that it may stimulate bone healing processes such as endochondral ossification (Claes and Willie, 2007). Consequently PLIUS may also be beneficial for cartilage regeneration either *in vivo* or as part of an *in vitro* tissue engineered approach. Previous studies by Parvizi and colleagues (1999, 2002) using chondrocytes cultured in monolayer have suggested that PLIUS may stimulate sGAG synthesis, and that calcium signalling is implicated in this process. However, this model system is far from ideal in terms of both maintaining chondrocyte phenotype and providing pure PLIUS without artifactual heating or fluid flow (Section 7.3.3). Furthermore, close inspection of the original previously published data (Parvizi *et al.*, 1999) indicate that it is not as robust as suggested (Section 5.4 and Figure 5.6). Therefore the present studies attempt to investigate the influence of PLIUS on chondrocytes within a more appropriate 3D agarose model system, as well as repeating the original monolayer experiments. The hypotheses proposed were that PLIUS stimulated the synthesis and elaboration of sGAG, that this was influenced by the intensity of the ultrasound, and that calcium signaling mediated these processes. In order to perform this investigation, a bioreactor system was designed so that agarose cultures could be subjected to PLIUS stimulation. In addition, a separate test rig was developed enabling calcium signalling experiments to be undertaken on the stage of a confocal microscope.

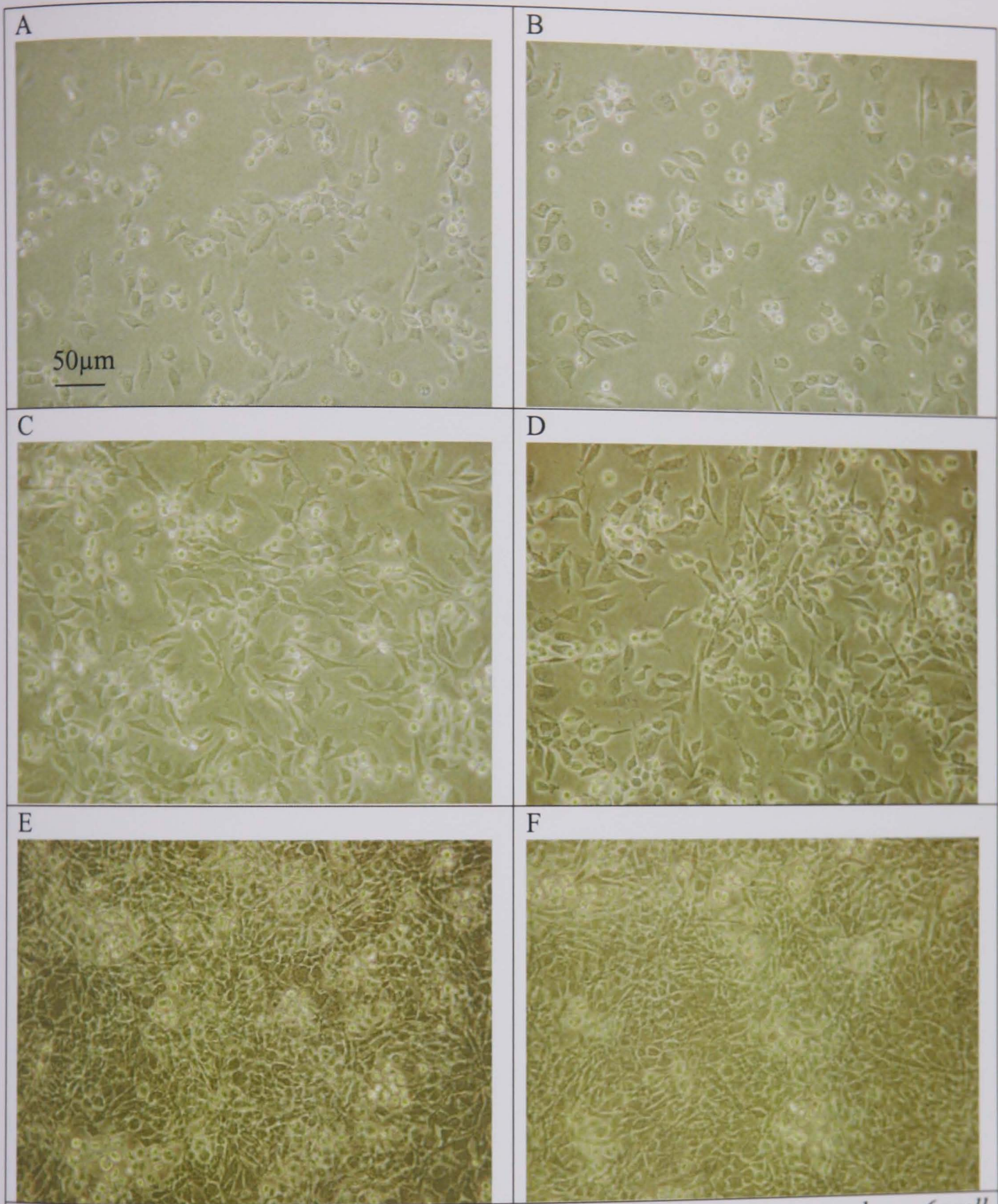
Chondrocytes in agarose were stimulated with PLIUS at SATA intensities ranging from 13-300mW/cm² for periods of up to 20 days, and biosynthesis was examined by assessment of extracellular matrix elaboration and cell proliferation using standard biochemical protocols. Additionally, calcium signalling in these cells was investigated as a possible mechanotransduction pathway, as in other forms of mechanical loading (Roberts *et al.*, 2001, Pinguan-Murphy *et al.*, 2005 & 2006). However, the experimental studies revealed that PLIUS had no stimulatory effect on chondrocyte metabolism based on the parameters explored, and a null hypothesis was confirmed. Further studies involving chondrocytes cultured in monolayer (Chapters 5 and 6) also failed to highlight any stimulatory effect of PLIUS in this system.

The findings of the present study may be summarised by the following statements:

- PLIUS did not influence chondrocyte viability in agarose constructs over a nine day culture period for SATA intensities up to and including $100\text{mW}/\text{cm}^2$. Cultures exposed to the higher 210 and $300\text{mW}/\text{cm}^2$ intensities were adversely affected causing cell death. This is likely to be due to attenuation in the transducer casing material, resulting in heat production.
- PLIUS at $30\text{mW}/\text{cm}^2$ did not stimulate sGAG production or proliferation in bovine chondrocytes seeded in a 3D agarose or monolayer system.
- Increasing the daily dose of $30\text{mW}/\text{cm}^2$ PLIUS from 20 to 40 minutes had no influence on sGAG synthesis or cell proliferation in agarose cultures.
- PLIUS at $100\text{mW}/\text{cm}^2$ had a marginal stimulatory effect on total sGAG content seen in agarose. However, this was not seen in monolayer culture. At this power there was also no stimulation of total DNA content or rates of sGAG or DNA production in bovine chondrocytes seeded in a 3D agarose or monolayer system.
- PLIUS at $30\text{mW}/\text{cm}^2$ had no significant effect on intracellular calcium signalling in a 3D agarose or monolayer system.
- Calcium signalling experiments involving an incremental PLIUS SATA intensity increase over a 20 minute period demonstrated a significant inhibitory response, when agarose constructs were stimulated at $100\text{mW}/\text{cm}^2$ ($p < 0.05$).
- PLIUS at $30\text{mW}/\text{cm}^2$ caused increased diffusion of 70kDa FITC dextrans through cell-free agarose compared with control constructs. There was no effect at 4 or 500kDa.

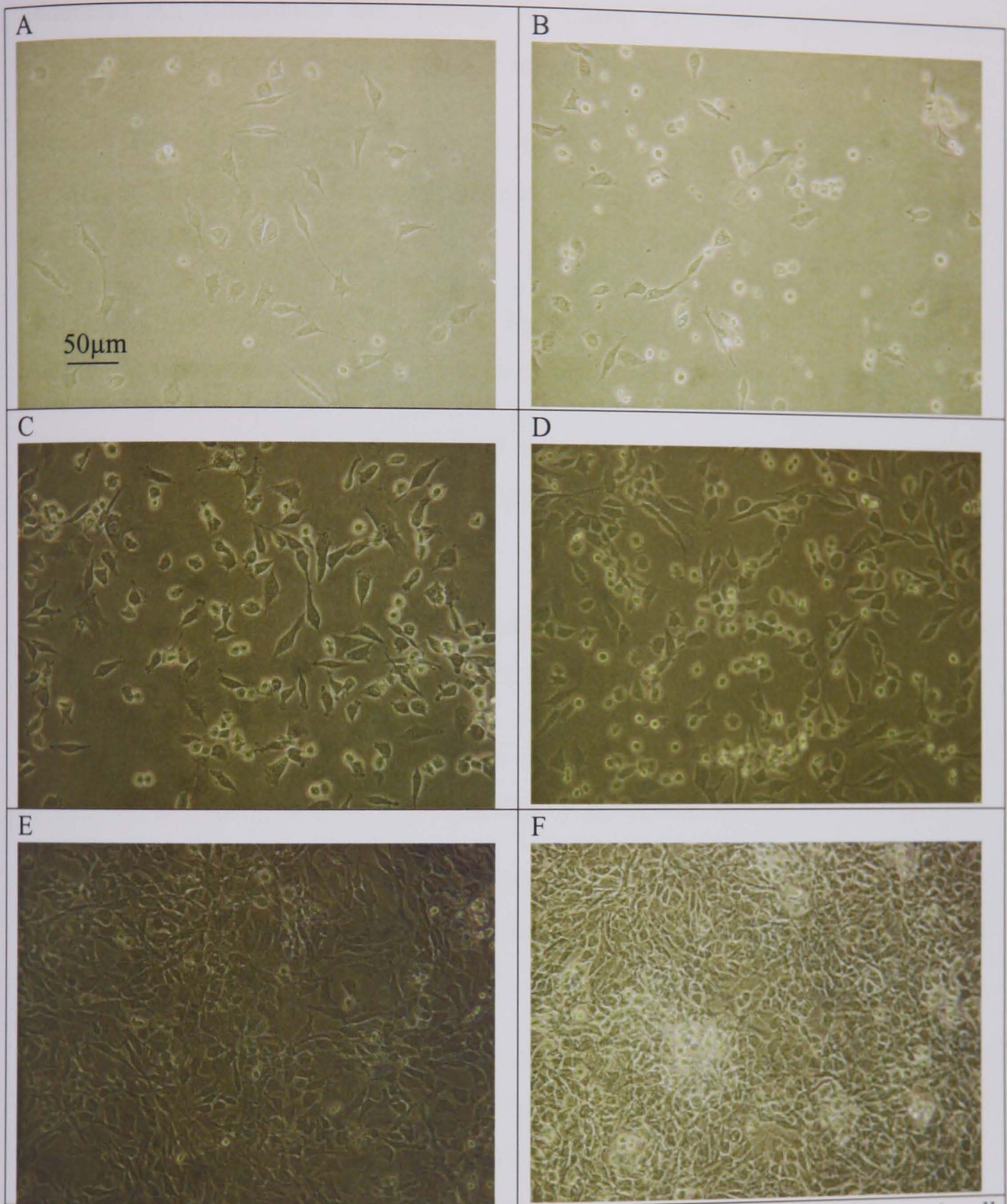
The presented results, along with a number of others (Duda *et al.*, 2004; Hsu *et al.*, 2006) suggest that PLIUS has limited potential for stimulating proteoglycan synthesis in 3D constructs as part of a tissue engineering repair strategy. Indeed, the proposed use of PLIUS in cartilage tissue engineering may be more limited than previously suggested.

APPENDIX 1: Microscope images taken to accompany $30\text{mW}/\text{cm}^2$ monolayer study in Chapter 5



Microscope images showing central region of well of chondrocyte monolayer 6-well plate culture. A, C, E show control monolayer culture at days 3, 5, and 7 of culture respectively. B, D, F show monolayers after application of 20 minutes $30\text{mW}/\text{cm}^2$ PLIUS at days 3, 5, and 7 of culture respectively.

APPENDIX 2: Microscope images taken to accompany $100\text{mW}/\text{cm}^2$ monolayer study in Chapter 5



Microscope images showing central region of well of chondrocyte monolayer 6-well plate culture. A, C, E show control monolayer culture at days 3, 5, and 7 of culture respectively. B, D, F show monolayers after application of 20 minutes $100\text{mW}/\text{cm}^2$ PLIUS at days 3, 5, and 7 of culture respectively.



REFERENCES

- Addonizio JC, Choudhury MS, Sayegh N, Chopp RT. 1984. Cavitron ultrasonic surgical aspirator. Applications in urologic surgery. *Urology*. 23(5): 417-20.
- Agemura DH, O'Brien WD Jr, Olerud JE, Chun LE, Eyre DE. 1990. Ultrasonic propagation properties of articular cartilage at 100MHz. *Journal of Acoustical Society of America*. 87: 1786-1791.
- Akanji OO, Lee DA, Bader DA. 2008. The effects of direct current stimulation on isolated chondrocytes seeded in 3D agarose constructs. *Biorheology*. 45(3-4): 229-43.
- Araki T, Yamamoto A, Yamada M. 1987. Accurate determination of DNA content in single cell nuclei stained with Hoechst 33258 fluorochrome at high salt concentration. *Histochemistry*. 87(4): 331-8.
- Archer CW and Francis-West P. 2003. Cells in focus: The chondrocyte. *International Journal of Biochemistry & Cell Biology*. 35: 401-404.
- Armstrong CG, Lai WM, Mow VC. 1984. An analysis of the unconfined compression of articular cartilage. *Journal of Biomechanical Engineering*. 106(2): 165-73.
- Aydelotte MB, Kuettner KE. 1988. Differences between sub-populations of cultured bovine articular chondrocytes. I. Morphology and cartilage matrix production. *Connective Tissue Research*. 18(3): 205-22.
- Aydelotte MB, Raiss RX, Caterson B, Kuettner KE. 1992. Influence of interleukin-1 on the morphology and proteoglycan metabolism of cultured bovine articular chondrocytes. *Connective Tissue Research*. 28(1-2): 143-59.
- Aydelotte MB, Thonar EJMA, Mollenhauer J, Flechtenmacher J. 1998. Culture of chondrocytes in alginate gel: Variations in conditions of gelation influence the structure of the alginate gel, and the arrangement and morphology of proliferating chondrocytes. *In Vitro Cellular & Developmental Biology - Animal*. 34(2): 123-130.
- Bachrach NM, Valhmu WB, Stazzone E, Ratcliffe A, Lai WM, Mow VC. 1995. Changes in proteoglycan synthesis of chondrocytes in articular cartilage are associated with the time-dependent changes in their mechanical environment. *Journal of Biomechanics*. 28(12): 1561-1569.

- Bader DL, Lee DA. 2000. Structure-properties of soft tissues. Articular cartilage. In: *Structural Biological Materials*. Ed: Elices M. Oxford, Pergamon. 75-103.
- Bader DL, Ohashi T, Knight MM, Lee DA, Sato M. 2002. Deformation properties of articular chondrocytes: a critique of three separate techniques. *Biorheology*. 39(1-2): 69-78.
- Baker KG, Robertson VJ, Duck FA. 2001. A review of therapeutic ultrasound: biophysical effects. *Physical Therapy*. 81(7): 1351-8.
- Barlic A, Drobnic M, Malicev E, Kregar-Velikonja N. 2008. Quantitative analysis of gene expression in human articular chondrocytes assigned for autologous implantation. *Journal of Orthopaedic Research*. 26(6): 847-53.
- Barnett SB, ter Harr G, Ziskin MC, Rott H-D, Duck FA, Maeda K. 2000. International recommendations and guidelines for the safe use of diagnostic ultrasound in medicine. *Ultrasound in Medicine & Biology*. 26(3): 355-366.
- Benjamin M, Ralphs JR, Archer CW, Mason RM, Chambers M. 1995. Cytoskeletal changes in articular fibrocartilage are an early indicator of osteoarthritis in STR ORT mice. *Transactions of the Orthopaedic Research Society*. 41: 246.
- Benjamin M., 1999. An introduction to synovial joints. In: *Biology of the Synovial Joint*. Ed: Archer CW, Caterson B, Benjamin M, Ralphs JR. Harwood Academic Publishers. 1-11.
- Benwell DA, Bly SHP. 1987. Sources and applications of ultrasound. In: *Ultrasound: Medical Applications, Biological Effects, and Hazard Potential*. Ed: Repacholi MH. Grandolfo M, Rindi A. Plenum Press, New York. 29-47.
- Benya PD, Shaffer JD. 1982. Dedifferentiated chondrocytes reexpress the differentiated collagen phenotype when cultured in agarose gels. *Cell*. 30(1): 215-24.
- Beris AE, Lykissas MG, Papageorgiou CD, Georgoulis AD. 2005. Advances in articular cartilage repair. *Injury*. 36S: S14-S23.
- Berridge MJ, Lipp P, Bootman MD. 2000. The versatility and universality of calcium signalling. *Nature reviews: Molecular Cell Biology*. 1(1): 11-21.

Blain EJ, Gilbert SJ, Hayes AJ, Duance VC. 2006. Disassembly of the vimentin cytoskeleton disrupts articular cartilage chondrocyte homeostasis. *Matrix Biology*. 25(7): 398-408.

Bootman MD, Collins TJ, Peppiatt CM, Prothero LS, MacKenzie L, De Smet P, Travers M, Tovey SC, Seo JT, Berridge MJ, Ciccolini F, Lipp P. 2001. Calcium signaling - an overview. *Seminars in Cell & Developmental Biology*. 12(1): 3-10.

Boustany NN, Gray ML, Black AC, Hunziker EB. 1995. Correlation between synthetic activity and glycosaminoglycan concentration in epiphyseal cartilage raises questions about the regulatory role of interstitial pH. *Journal of Orthopaedic Research*. 13(5): 733-9.

Brighton CT, Cronkey JE, Osterman AL. 1976. In vitro epiphyseal-plate growth in various constant electrical fields. *The Journal of Bone and Joint surgery. American Volume*. 58(7): 971-8.

Brighton CT, Wang W, Clark CC. 2006. Up-regulation of matrix in bovine articular cartilage explants by electric fields. *Biochemical and Biophysical Research Communications*. 342(2): 556-61.

Brittberg M, Tallheden T, Sjögren-Jansson E, Lindahl A, Peterson L. 2001. Autologous chondrocytes used for articular cartilage repair. *Clinical Orthopaedics and Related Research*. 391S: S337-S348.

Broom ND, Myers DB. 1980. A study of the structural response of wet hyaline cartilage to various loading situations. *Connective Tissue Research*. 7(4): 227-37.

Browning JA, Saunders K, Urban JP, Wilkins RJ. 2004. The influence and interactions of hydrostatic and osmotic pressures on the intracellular milieu of chondrocytes. *Biorheology*. 41(3-4): 299-308.

Buckwalter JA, Hunziker EB, Rosenberg L, Coutts R, Adams M, and Eyte D. 1987. Articular cartilage: Composition and structure. In: *Injury and Repair of Musculoskeletal Soft Tissue*. Ed: Woo S and Buckwalter JA. American Academy, Park Ridge, Illinois. 405-425.

Buckwalter JA, Hunziker EB, Rosenberg L, Coutts R, Adams M, and Eyre D. 1987. Articular cartilage: Injury and repair. In: *Injury and Repair of Musculoskeletal Soft Tissue*. Ed: Woo S and Buckwalter JA. American Academy, Park Ridge, Illinois. 465-482.

Buckwalter JA, Mow VC. 1992. Cartilage repair in osteoarthritis. In: *Osteoarthritis: Diagnosis and Medical/Surgical Management*. Ed: Moskowitz RW, Altman RD, Buckwalter JA, Goldberg VM, Hochberg MC. Second Edition. WB Saunders Company. 71-107.

Buckwalter JA, Mankin HJ. 1998. Articular cartilage: Tissue design and chondrocyte-matrix interactions. In: *AAOS Instructional Course Lectures*. 47: 447-486.

Buckwalter JA, Hunziker EB. 1999. Articular cartilage morphology and biology. In: *Biology of the Synovial Joint*. Ed: Archer CW, Caterson B, Benjamin M, Ralphs JR. Harwood Academic Publishers. 75-99.

Buechel FF. 2004. The infected total knee arthroplasty: just when you thought it was over. *Journal of Arthroplasty*. 19(4 Suppl 1): 51-5.

Buehler MJ. 2006. Nature designs tough collagen: Expanding the nanostructure of collagen fibrils. *Proceedings of the National Academy of Sciences of the United States of America*. 103(33): 12285-90.

Buschmann MD, Gluzband YA, Grodzinsky AJ, Kimura JH, Hunziker EB. 1992. Chondrocytes in agarose culture synthesize a mechanically functional extracellular matrix. *Journal of Orthopaedic Research*. 10: 745-758.

Buschmann MD, Gluzband YA, Grodzinsky AJ, Hunziker EB. 1995. Mechanical compression modulates matrix biosynthesis in chondrocyte/agarose culture. *Journal of Cell Science*. 108: 1497-1508.

Buschmann MD, Hunziker EB, Kim Y-J, Grodzinsky AJ. 1996. Altered aggrecan synthesis correlates with cell and nucleus structure in statically compressed cartilage. *Journal of Cell Science*. 109: 499-508.

- Buschmann MD, Kim Y-J, Wong M, Frank E, Hunziker EB, Grodzinsky AJ. 1999. Stimulation of aggrecan synthesis in cartilage explants by cyclic loading is localized to regions of high interstitial fluid flow. *Archives of Biochemistry and Biophysics*. 366(1): 1-7.
- Bushong, SC. 1999. *Diagnostic Ultrasound*. McGraw-Hill.
- Busse JW, Bhandari M, Kulkarni AV, Tunks E. 2002. The effect of low-intensity pulsed ultrasound therapy on time to fracture healing: a meta-analysis. *Canadian Medical Association Journal*. 166(4): 437-41.
- Campbell JJ, Lee DA, Bader DL. 2006. Dynamic compressive strain influences chondrogenic gene expression in human mesenchymal stem cells. *Biorheology*. 43(3-4): 455-70.
- Campbell JJ, Blain EJ, Chowdhury TT, Knight MM. 2007a. Loading alters actin dynamics and up-regulates cofilin gene expression in chondrocytes. *Biochemical and Biophysical Research Communications*. 361(2): 329-34.
- Campbell JJ, Knight MM. 2007b. An improved confocal FRAP technique for the measurement of long-term actin dynamics in individual stress fibres. *Microscopy Research and Technique*. 70(12): 1034-40.
- Carvalho DCL, Cliquet A. 2004. The action of low-intensity pulsed ultrasound in bones of osteopenic rats. *Artificial Organs*. 1: 114-118.
- Chan OK, Chen FC, Choy CL, Ward IM. 1978. The elastic constants of extruded polypropylene and polyethylene terephthalate. *Journal of Physics D: Applied Physics*. 11: 617-629.
- Chao PH, West AC, Hung CT. 2006. Chondrocyte intracellular calcium, cytoskeletal organization, and gene expression responses to dynamic osmotic loading. *American Journal of Physiology: Cell Physiology*. 291(4): C718-25.
- Chaussy C, Schüller J, Schmiedt E, Brandl H, Jocham D, Liedl B. 1984. Extracorporeal shock-wave lithotripsy (ESWL) for treatment of urolithiasis. *Urology*. 23(5): 59-66.

Chaussy C, Thüroff S. 2003. The status of high-intensity focused ultrasound in the treatment of localized prostate cancer and the impact of a combined resection. *Current Urology Reports*. 4(3): 248-52.

Chen YJ, Wang CJ, Yang KD, Chang PR, Huang HC, Huang YT, Sun YC, Wang FS. 2003. Pertussis toxin-sensitive Gai protein and ERK-dependent pathways mediate ultrasound promotion of osteogenic transcription in human osteoblasts. *FEBS Letters*. 554(1-2): 154-8.

Choi BH, Woo JI, Min BH, Park SR. 2006. Low-intensity ultrasound stimulates the viability and matrix gene expression of human articular chondrocytes in alginate bead culture. *Journal of Biomedical Materials Research. Part A*. 79(4): 858-64.

Choi BH, Choi MH, Kwak MG, Min BH, Woo ZH, Park SR. 2007. Mechanotransduction pathways of low-intensity ultrasound in C-2812 human chondrocyte cell line. *Proceedings of the Institution of Mechanical Engineers: Part II, Journal of Engineering in Medicine*. 221(5): 527-35.

Chowdhury TT, Bader DL, Lee DA. 2001. Dynamic compression inhibits the synthesis of nitric oxide and PGE₂ by IL-1 β -stimulated chondrocytes cultured in agarose constructs. *Biochemical and Biophysical Research Communications*. 285(5):1168-74.

Chowdhury TT, Bader DL, Shelton JC, Lee DA. 2003. Temporal regulation of chondrocyte metabolism in agarose constructs subjected to dynamic compression. *Archives of Biochemistry and Biophysics*. 417(1): 105-11.

Chowdhury TT, Bader DL, Lee DA. 2006. Anti-inflammatory effects of IL-4 and dynamic compression in IL-1 β stimulated chondrocytes. *Biochemical and Biophysical Research Communications*. 339: 241-247.

Chowdhury TT, Knight MM. 2006. Purinergic pathway suppresses the release of NO and stimulates proteoglycan synthesis in chondrocyte/agarose constructs subjected to dynamic compression. *Journal of Cellular Physiology*. 209(3): 845-53.

Chowdhury TT, Arghandawi S, Brand J, Akanji OO, Bader DL, Salter DM, Lee DA. 2008. Dynamic compression counteracts IL-1 β induced inducible nitric oxide synthase and cyclo-oxygenase-2 expression in chondrocyte/agarose constructs. *Arthritis Research & Therapy*. 10(2): R35.

- Claes L, Willie B. 2007. The enhancement of bone regeneration by ultrasound. *Progress in Biophysics and Molecular Biology*. 93(1-3): 384-98.
- Clark AL, Votta BJ, Kumar S, Liedtke W, Guilak F. 2008. In situ chondrocyte calcium signaling in response to osmotic stress: The role of TRPV4 ion channel. *54th Annual Meeting of the Orthopedic Research Society*, 480.
- Clement GT. 2004. Perspectives in clinical uses of high-intensity focused ultrasound. *Ultrasonics*. 42(10): 1087-93.
- Cook SD, Ryaby JP, McCabe J, Frey JJ, Heckman JD, Kristiansen TK. 1997. Acceleration of tibia and distal radius fracture healing in patients who smoke. *Clinical Orthopaedics and Related Research*. 337: 198-207.
- Cook SD, Salkeld SL, Popich-Patron LS, Ryaby JP, Jones DG, Barrack RL. 2001. Improved cartilage repair after treatment with low-intensity pulsed ultrasound. *Clinical Orthopaedics and Related Research*. 391S: S231-S243.
- Cui JH, Park K, Park SR, Min BH. 2006. Effects of low-intensity ultrasound on chondrogenic differentiation of mesenchymal stem cells embedded in polyglycolic acid: an in vivo study. *Tissue Engineering*. 12(1): 75-82.
- Culav EM, Clark CH, Merrilees MJ. 1999. Connective tissues: Matrix composition and its relevance to physical therapy. *Physical Therapy*. 79: 308-319.
- Cunningham JL, Kenwright J, Kershaw CJ. 1990. Biomechanical measurement of fracture healing. *Journal of Medical Engineering and Technology*. 14(3): 92-101.
- D'Andrea P, Calabrese A, Capozzi I, Grandolfo M, Tonon R, Vittur F. 2000. Intercellular Ca^{2+} waves in mechanically stimulated articular chondrocytes. *Biorheology*. 37(1-2): 75-83.
- De Witt MT, Handley CJ, Oakes BW, Lowther DA. 1984. In vitro response of chondrocytes to mechanical loading: The effect of short term mechanical tension. *Connective Tissue Research*. 12: 97-109.
- Diliberto PA, Wang XF, Herman B. 1994. Confocal imaging of Ca^{2+} in cells. *Methods in Cell Biology*. 40: 243-62.

- Dinno MA, Dyson M, Young SR, Mortimer AJ, Hart J, Crum LA. 1989. The significance of membrane changes in the safe and effective use of therapeutic and diagnostic ultrasound. *Physics in Medicine and Biology*. 34(11):1543-52.
- Donahue TL, Haut TR, Yellowley CE, Donahue HJ, Jacobs CR. 2003. Mechanosensitivity of bone cells to oscillating fluid flow induced shear stress may be modulated by chemotransport. *Journal of Biomechanics*. 36(9): 1363-71.
- Dowsett DJ, Kenny PA, Johnston RE. 1998. *The Physics of Diagnostic Imaging*. Hodder Arnold. Chapter 17.
- Drury JL, Dennis RG, Mooney DJ. 2004. The tensile properties of alginate hydrogels. *Biomaterials*. 25: 3187-3199.
- Duance VC, Vaughan-Thomas A, Wardale RJ and Wotton SF. 1999. The collagens of articular and meniscal cartilages. In: *Biology of the Synovial Joint*. Ed: Archer CW, Caterson B, Benjamin M, Ralphs JR. Harwood Academic Publishers. 135-163.
- Duck FA. 2007. Medical and non-medical protection standards for ultrasound and infrasound. *Progress in Biophysics and Molecular Biology*. 93: 176-91.
- Duda GN, Kliche A, Kleeman R, Hoffman JE, Sittinger M, Haisch A. 2004. Does low-intensity pulsed ultrasound stimulate maturation of tissue-engineered cartilage? *Journal of Biomedical Materials Research Part B: Applied Biomaterials*. 68B: 21-28.
- Dumont J, Ionescu M, Reiner A, Poole AR, Tran-Khanh N, Hoemann CD, McKee MD, Buschmann MD. 1999. Mature full-thickness articular cartilage explants attached to bone are physiologically stable over long-term culture in serum-free media. *Connective Tissue Research*. 40(4): 259-272.
- Durrant LA, Archer CW, Benjamin M, Ralphs JR. 1999. Organisation of the chondrocyte cytoskeleton and its response to changing mechanical conditions in organ culture. *Journal of Anatomy*. 194: 343-353.
- Dyer SRA, Lord D, Hutchinson IJ, Ward IM, Duckett RA. 1992. Elastic Anisotropy in Unidirectional fibre reinforced composites. *Journal of Physics D: Applied Physics*. 25: 66-73.

- Dyson M, Suckling J. 1978. Stimulation of tissue repair by ultrasound: a survey of the mechanisms involved. *Physiotherapy*. 64(4): 105-8.
- Dyson M, Brookes M. 1983. Stimulation of bone repair by ultrasound. *Ultrasound in Medicine and Biology*. Supplement. 2: 61-6.
- Dyson M. 1985. Therapeutic applications of ultrasound. In: *Clinics in Diagnostic Ultrasound Volume 16. Biological Effects of Ultrasound*. Ed: Nyborg WL, Ziskin MC. Churchill Livingstone. 121-133.
- Ebersson CP, Hogan KA, Moore DC, Ehrlich MG. 2003. Effect of low-intensity ultrasound stimulation of consolidation of the regenerate zone in a rat model of distraction osteogenesis. *Journal of Pediatric Orthopaedics*. 23: 46-51.
- Ebisawa K, Hata K, Okada K, Kimata K, Ueda M, Torii S, Watanabe H. 2004. Ultrasound enhances transforming growth factor β -mediated chondrocyte differentiation of human mesenchymal stem cells. *Tissue Engineering*. 10(5-6): 921-9.
- Edlich M, Yellowley CE, Jacobs CR, Donahue HJ. 2001. Oscillating fluid flow regulates cytosolic calcium concentration in bovine articular chondrocytes. *Journal of Biomechanics*. 34(1): 59-65.
- Edlich M, Yellowley CE, Jacobs CR, Donahue HJ. 2004. Cycle number and waveform of fluid flow affect bovine articular chondrocytes. *Biorheology*. 41(3-4): 315-22.
- Eggl PS, Hunziker EB, Schenk RK. 1988. Quantitation of structural features characterizing weight- and less-weight-bearing regions in articular cartilage: a stereological analysis of medial femoral condyles in young adult rabbits. *The Anatomical Record*. 222(3): 217-27.
- Eifler RL, Blough ER, Dehlin JM, Haut Donahue TL. 2006. Oscillatory fluid flow regulates glycosaminoglycan production via an intracellular calcium pathway in meniscal cells. *Journal of Orthopaedic Research*. 24(3): 375-84.
- Erdoğan O, Esen E, Ustün Y, Kürkçü M, Akova T, Gönluşen G, Uysal H, Cevlik F. 2006. Effects of low-intensity pulsed ultrasound on healing of mandibular fractures: an experimental study in rabbits. *Journal of Oral and Maxillofacial Surgery*. 64(2): 180-8.

- Erickson GR, Alexopoulos LG, Guilak F. 2001. Hyper-osmotic stress induces volume change and calcium transients in chondrocytes by transmembrane, phospholipid, and G-protein pathways. *Journal of Biomechanics*. 34(12): 1527-35.
- Erickson GR, Northrup DL, Guilak F. 2003. Hypo-osmotic stress induces calcium-dependent actin reorganization in articular chondrocytes. *Osteoarthritis and Cartilage*. 11(3): 187-97.
- Eyre D. 2002. Collagen of articular cartilage. *Arthritis Research*. 4: 30-35.
- Eyre DR, Weis MA, Wu J-J. 2006. Articular cartilage collagen: An irreplaceable framework? *European Cells and Materials*. 12: 57-63.
- Farndale RW, Sayers CA, Barrett AJ. 1982. A direct spectrophotometric microassay for sulfated glycosaminoglycans in cartilage cultures. *Connective Tissue Research*. 9(4): 247-8.
- Farr RF and Allisy-Roberts PJ. 1998. *Physics for Medical Imaging*. WB Saunders Company Ltd.
- Fauza DO. 2003. Tissue engineering: Current state of clinical application. *Current Opinion in Pediatrics*. 15: 267-271.
- Ferguson SJ, Ito K, Nolte LP. 2004. Fluid flow and convective transport of solutes within the intervertebral disc. *Journal of Biomechanics*. 37(2): 213-21.
- Feril LB Jr, Kondo T, Zhao QL, Ogawa R, Tachibana K, Kudo N, Fujimoto S, Nakamura S. 2003. Enhancement of ultrasound-induced apoptosis and cell lysis by echo-contrast agents. *Ultrasound in Medicine and Biology*. 29(2): 331-7.
- Feril LB Jr, Kondo T, Zhao QL, Ogawa R. 2002. Enhancement of hyperthermia-induced apoptosis by non-thermal effects of ultrasound. *Cancer Letters*. 178(1): 63-70.
- Feril LB Jr, Kondo T, Cui ZG, Tabuchi Y, Zhao QL, Ando H, Misaki T, Yoshikawa H, Umemura S. 2005. Apoptosis induced by the sonomechanical effects of low intensity pulsed ultrasound in a human leukemia cell line. *Cancer Letters*. 221(2): 145-52.
- Feril LB Jr, Kondo T. 2006. Ultrasound liberates nitric oxide (NO) from the caged NO compound N,N'-bis(carboxymethyl)-N,N'-dinitroso-p-phenylenediamine sodium salt. *Ultrasonics Sonochemistry*. 13(5): 397-400

- Fragonas E, Valente M, Pozzi-Mucelli M, Toffanin R, Rizzo R, Silvestri F, Vittur F. 2000. Articular cartilage repair in rabbits by using suspensions of allogenic chondrocytes in alginate. *Biomaterials*. 21: 795-800.
- Francis DA. 2007. Medical and non-medical protection standards for ultrasound and infrasound. *Progress in Biophysics and Molecular Biology*. 93: 176–191.
- Freeman PM, Natarajan RN, Kimura JH, Andriacchi TP. 1994. Chondrocyte cells respond mechanically to compressive loads. *Journal of Orthopaedic Research*. 12(3): 311-320.
- Frenkel SR, Di Cesare, PE. 2004. Scaffolds for articular cartilage repair. *Annals of Biomedical Engineering*. 32(1): 26-34.
- Fry FJ, Johnson LK. 1978. Tumor irradiation with intense ultrasound. *Ultrasound in Medicine and Biology*. 4(4): 337-41.
- Fujisato T, Sajiki T, Liu Q, Ikada Y. 1996. Effect of basic fibroblast growth factor on cartilage regeneration in chondrocyte-seeded collagen sponge scaffold. *Biomaterials*. 17: 155-162.
- Galois L, Hutasse S, Cortial D, Rousseau CF, Grossin L, Ronziere MC, Herbage D, Freyria AM. 2006. Bovine chondrocyte behaviour in three-dimensional type I collagen gel in terms of gel contraction, proliferation and gene expression. *Biomaterials*. 27(1): 79-90.
- Gee KR, Brown KA, Chen WN, Bishop-Stewart J, Gray D, Johnson J. 2000. Chemical and physiological characterization of fluo-4 Ca²⁺-indicator dyes. *Cell Calcium*. 27(2): 97-106.
- Giannoni P, Crovace A, Malpeli M, Maggi E, Arbico R, Cancedda R, Dozin B. 2005. Species variability in the differentiation potential of in vitro-expanded articular chondrocytes restricts predictive studies on cartilage repair using animal models. *Tissue Engineering*. 11(1/2): 237-248.
- Glogauer M, Arora P, Yao G, Sokholov I, Ferrier J, McCulloch CA. 1997. Calcium ions and tyrosine phosphorylation interact coordinately with actin to regulate cytoprotective responses to stretching. *Journal of Cell Science*. 110(1): 11-21.

- Goldring MB. 2006. Update on the biology of the chondrocyte and new approaches to treating cartilage diseases. *Best Practice and Research Clinical Rheumatology*. 5: 1003-1025.
- Görtz S, Bugbee, WD. 2006. Allografts in articular cartilage repair. *The Journal of Bone & Joint Surgery*. 88: 1374-1384.
- Grandolfo M, Vecchia P. 1987. Fundamentals of acoustic wave theory. In: *Ultrasound Medical Applications, Biological Effects, and Hazard Potential*. Ed: Repacholi MH, Grandolfo M, Rindi A. Plenum Press, New York. 13-28.
- Gray ML, Pizzanelli AM, Grodzinsky AJ, Lee RC. 1988. Mechanical and physiochemical determinants of the chondrocyte biosynthetic response. *Journal of Orthopaedic Research*. 6(6): 777-92.
- Gruber HE, Hanley EN Jr. 2000. Human disc cells in monolayer vs 3D culture: cell shape, division and matrix formation. *BMC Musculoskeletal Disorders*. 1: 1.
- Guilak F, Meyer BC, Ratcliffe A. 1994. The effects of matrix compression on proteoglycan metabolism in articular cartilage explants. *Osteoarthritis and Cartilage*. 2: 91-101.
- Guilak F, Ratcliffe A, Mow VC. 1995. Chondrocyte deformation and local tissue strain in articular cartilage: a confocal microscopy study. *Journal of Orthopaedic Research*. 3(3): 410-21.
- Guilak F, Sah R, Setton LA. 1997. Physical regulation of cartilage metabolism. In: *Basic Orthopaedic Biomechanics*. 2nd Edition. Ed: Mow VC, Hayes WC. Lippincott-Raven Publishers, Philadelphia. 179-207.
- Guilak F, Zell RA, Erickson GR, Grande DA, Rubin C, McLeod KJ, Donahue HJ. 1999. Mechanically induced calcium waves in articular chondrocytes are inhibited by gadolinium and amiloride. *Journal of Orthopaedic Research*. 17: 421-429.
- Hall AC, Starks I, Shoults CL, Rashidbigi S. 1996. Pathways for K⁺ transport across the bovine articular chondrocyte membrane and their sensitivity to cell volume. *The American Journal of Physiology: Cell Physiology*. 270(5): C1300-10.

- Hall AC. 1998. Physiology of cartilage. In: *Sciences Basic to Orthopaedics*. Ed: Hughes S, McCarthy I. WB Saunders Cambridge Limited. 45-69.
- Hall AC. 1999. Differential effects of hydrostatic pressure on cation transport pathways of isolated articular chondrocytes. *Journal of Cellular Physiology*. 178(2): 197-204.
- Hardingham T, Bayliss M. 1990. Proteoglycans of articular cartilage: changes in aging and in joint disease. *Seminars in Arthritis and Rheumatism*. 20(3): 12-33.
- Hardingham TE. 1979. The role of link-protein in the structure of cartilage proteoglycan aggregates. *Biochemical Journal*. 177: 237-247.
- Hardingham, TE, Fosang AJ, Dudhia J. 1992. Aggrecan, the chondroitin sulfate/keratan sulfate proteoglycan from cartilage. In: *Articular Cartilage and Osteoarthritis*. Ed: Kuettner KE, Schleyerback R, Peyron JG, Hascall VC. Raven Press Ltd., New York. 5-20.
- Harle J, Salih V, Knowles JC, Mayia F, Olsen I. 2001. Effects of therapeutic ultrasound on osteoblast gene expression. *Journal of Materials Science. Materials in Medicine*. 12(10-12): 1001-4.
- Harle J, Salih V, Knowles JC, Mayia F, Olsen I. 2005. Effects of ultrasound on transforming growth factor- β genes in bone cells. *European Cells & Materials*. 10: 70-6.
- Hauselman HJ, Aydelotte MB, Schumacher BL, Kneutter K, Gitelis SH, Thonar JMA. 1992. Synthesis and turnover of proteoglycans by human and bovine adult articular cartilage cultured in alginate beads. *Matrix*. 12: 116-129.
- Heckman JD, Ryaby JP, McCabe J, Frey JJ, Kilcoyne RF. 1994. Acceleration of tibial fracture-healing by non-invasive, low-intensity pulsed ultrasound. *Journal of Bone and Joint Surgery*. 76(1): 26-34.
- Heckman JD, Sarasohn-Kahn J. 1997. The economics of treating tibia fractures. The cost of delayed unions. *Bulletin of the NYU Hospital for Joint Diseases*. 56(1): 63-72.
- Heinegård DK and Pimentel ER. 1992. Cartilage matrix proteins. In: *Articular Cartilage and Osteoarthritis*. Ed: Kuettner KE, Schleyerback R, Peyron JG, Hascall VC. Raven Press Ltd., New York. 95-111.

- Helmlinger G, Berk BC, Nerem RM. 1996. Pulsatile and steady flow-induced calcium oscillations in single cultured endothelial cells. *Journal of Vascular Research*. 33(5): 360-9.
- Heywood HK, Sembi PK, Lee DA, Bader DL. 2004. Cellular utilization determines viability and matrix distribution profiles in chondrocyte-seeded alginate constructs. *Tissue Engineering*. 10(9-10): 1467-79.
- Heywood HK, Bader DL, Lee DA. 2006. Glucose concentration and medium volume influence cell viability and glycosaminoglycan synthesis in chondrocyte-seeded alginate constructs. *Tissue Engineering*. 12: 3487-96.
- Horton WA. 1993. Morphology of connective tissue: Cartilage. In: *Connective Tissues and Its Heritable Disorders*. Ed: Royce PM, Steinmann B. Wiley-Liss, Inc. 73-84.
- Hsu SH, Kuo CC, Whu SW, Lin CH, Tsai CL. 2006. The effect of ultrasound stimulation versus bioreactors on neocartilage formation in tissue engineering scaffolds seeded with human chondrocytes in vitro. *Biomolecular Engineering*. 23(5): 259-64.
- Hsu HC, Fong YC, Chang CS, Hsu CJ, Hsu SF, Lin JG, Fu WM, Yang RS, Tang CH. 2007. Ultrasound induces cyclooxygenase-2 expression through integrin, integrin-linked kinase, Akt, NF-kappaB and p300 pathway in human chondrocytes. *Cellular Signalling*. 19(11): 2317-28.
- Huber M, Trattnig S, Lintner F. 2000. Anatomy, biochemistry, and physiology of articular cartilage. *Investigative Radiology*. 35(10): 573-580.
- Hung CT, Allen FD, Pollack SR, Brighton CT. 1996a. What is the role of the convective current density in the real-time calcium response of cultured bone cells to fluid flow? *Journal of Biomechanics*. 29(11): 1403-9.
- Hung CT, Allen FD, Pollack SR, Brighton CT. 1996b. Intracellular Ca^{2+} stores and extracellular Ca^{2+} are required in the real-time Ca^{2+} response of bone cells experiencing fluid flow. *Journal of Biomechanics*. 29(11): 1411-7.
- Hung CT, Henshaw DR, Wang CC, Mauck RL, Raia F, Palmer G, Chao PH, Mow VC, Ratcliffe A, Valhmu WB. 2000. Mitogen-activated protein kinase signaling in bovine articular chondrocytes in response to fluid flow does not require calcium mobilization. *Journal of Biomechanics*. 33(1): 73-80.

- Hung CT, LeRoux MA, Palmer GD, Chao PH, Lo S, Valhmu WB. 2003. Disparate aggrecan gene expression in chondrocytes subjected to hypotonic and hypertonic loading in 2D and 3D culture. *Biorheology*. 40(1-3): 61-72.
- Hunziker EB. 1992. Articular cartilage structure in humans and experimental animals. In: *Articular Cartilage and Osteoarthritis*. Ed: Kuettner KE, Schleyerback R, Peyron JG, Hascall VC. Raven Press Ltd., New York. 183-199.
- Hunziker EB. 1999. Articular cartilage repair: are intrinsic biological constraints undermining this process insuperable? *Osteoarthritis and Cartilage*. 7: 15-28.
- Hunziker EB. 2001. Articular cartilage repair: basic science and clinical progress. A review of the current status and prospects. *Osteoarthritis and Cartilage*. 10: 432-463.
- Huo MH, Gilbert NF, Parvizi J. 2007. What's new in total hip arthroplasty. *American Journal of Bone and Joint Surgery*. 89(8): 1874-85.
- Idowu BD, Knight MM, Bader DL, Lee DA. 2000. Confocal analysis of cytoskeletal organisation within isolated chondrocyte sub-populations cultured in agarose. *Histochemical Journal*. 32: 165-174.
- Ikeda K, Takayama T, Suzuki N, Shimada K, Otsuka K, Ito K. 2006. Effects of low-intensity pulsed ultrasound on the differentiation of C2C12 cells. *Life Sciences*. 79(20): 1936-43.
- Ikenoue T, Trindade MC, Lee MS, Lin EY, Schurman DJ, Goodman SB, Smith RL. 2003. Mechanoregulation of human articular chondrocyte aggrecan and type II collagen expression by intermittent hydrostatic pressure in vitro. *Journal of Orthopaedic Research*. 21(1): 110-6.
- Ishida T, Takahashi M, Corson MA, Berk BC. 1997. Fluid shear stress-mediated signal transduction: how do endothelial cells transduce mechanical force into biological responses? *Annals of the New York Academy of Sciences*. 811: 12-23.
- Isogai N, Kusuhara H, Ikada Y, Ohtani H, Jacquet R, Hillyer J, Lowder E, Landis WJ. 2006. Comparison of different chondrocytes for use in tissue engineering of cartilage model structures. *Tissue Engineering*. 12(4): 691-703.

- Ito M, Azuma Y, Ohta T, Komoriya K. 2000. Effects of ultrasound and 1,25-dihydroxyvitamin D3 on growth factor secretion in co-cultures of osteoblasts and endothelial cells. *Ultrasound in Medicine and Biology*. 26(1): 161-6.
- Iwashina T, Mochida J, Miyazaki T, Watanabe T, Iwabuchi S, Ando K, Hotta T, Sakai D. 2006. Low-intensity pulsed ultrasound stimulates cell proliferation and proteoglycan production in rabbit intervertebral disc cells cultured in alginate. *Biomaterials*. 27(3): 354-61.
- Jacobs CR, Yellowley CE, Davis BR, Zhou Z, Cimbala JM, Donahue HJ. 1998. Differential effect of steady versus oscillating flow on bone cells. *Journal of Biomechanics*. 31(11): 969-76.
- Jadin KD, Wong BL, Bae WC, Li KW, Williamson AK, Schumacher BL, Price JH, Sah RL. Depth-varying density and organization of chondrocytes in immature and mature bovine articular cartilage assessed by 3d imaging and analysis. *The Journal of Histochemistry and Cytochemistry*. 53(9): 1109-19.
- James, JA. 1963. New developments in the ultrasonic therapy of Meniere's disease. *Annals of the Royal College of Surgeons of England*. 33: 226-44.
- Janmey PA. 1998. The cytoskeleton and cell signaling: component localization and mechanical coupling. *Physiological Reviews*. 78(3): 763-81.
- Jingushi S, Azuma V, Ito M, Harada Y, Takagi H, Ohta T, Komoriya K. 1998. Effects of non-invasive pulsed low-intensity ultrasound on rat femoral fracture. *Proceedings of the Third World Congress of Biomechanics*. 175b.
- Jiřík R, Taxt T, Jan J. 2004. Ultrasound Attenuation Imaging. *Journal of Electrical Engineering*. 55(7-8): 180-87.
- Jones ARC, Glegorn JP, Hughes CE, Fitz LJ, Zollner R, Wainwright SD, Caterson B, Morris EA, Bonassar LJ, Flannery CR. 2007. Binding and localization of recombinant lubricin to articular artilage surfaces. *Journal of Orthopaedic Research*. 25(3): 283-292.
- Jortikka MO, Inkinen RI, Tammi M, Parkkinen JJ, Haapala J, Kiviranta I, Helminen HJ, Lammi M. 1997. Immobilisation causes longlasting matrix changes both in the immobilised and contralateral joint cartilage. *Annals of the Rheumatic Diseases*. 56: 255-261.

- Junqueira LC, Carneiro J, O'Kelley R. 1998. *Basic Histology. 9th Edition. Appleton Lange.* 127-133.
- Kaufman JJ, Einhorn TA. 1993. Ultrasound assessment of bone. *Journal of Bone and Mineral Research.* 8(5): 517-25.
- Kelly TA, Wang CC, Mauck RL, Ateshian GA, Hung CT. 2004. Role of cell-associated matrix in the development of free-swelling and dynamically loaded chondrocyte-seeded agarose gels. *Biorheology.* 41(3-4): 223-37.
- Kelman, CD. 1967. Phaco-emulsification and aspiration. A new technique of cataract removal. *American Journal of Ophthalmology.* 64: 23–35.
- Kempson G. 1979. Mechanical properties of articular cartilage. In: *Adult Articular Cartilage. 2nd Edition. Ed: Freeman MAR. Pitman Medical, Tunbridge Wells, United Kingdom.* 333-414.
- Kempson GE. 1982. Relationship between the tensile properties of articular cartilage from the human knee and age. *Annals of the Rheumatic Diseases.* 41: 508-511.
- Kempson GE. 1991. Age-related changes in the tensile properties of human articular cartilage: a comparative study between the femoral head of the hip joint and the talus of the ankle joint. *Biochimica et Biophysica Acta.* 1075: 223-230.
- Kerin AJ, Wisnom MR, Adams MA. 1998. The compressive strength of articular cartilage. *Proceedings of the Institution of Mechanical Engineers: Part H, Journal of Engineering in Medicine.* 212(4): 273-80.
- Kerrigan MJ, Hook CS, Qusous A, Hall AC. 2006. Regulatory volume increase (RVI) by in situ and isolated bovine articular chondrocytes. *Journal of Cellular Physiology.* 209(2): 481-92.
- Kessel RG. 1998. *Basic Medical Histology: The Biology of Cells, Tissues and Organs. Oxford University Press.* 128-137.
- Kim YJ, Sah RL, Doong JY, Grodzinsky AJ. 1988. Fluorometric assay of DNA in cartilage explants using Hoechst 33258. *Analytical Biochemistry.* 174(1): 168-76.

- Kiviranta I, Tammi M, Jurvelin J, Saamanen A-M, Helminen HJ. 1988. Moderate running exercise augments glycosaminoglycans and thickness of articular cartilage in the knee joint of young beagle dogs. *Journal of Orthopaedic Research*. 6: 188-195.
- Kiviranta I, Tammi M, Jurvelin J, Arokoski JPA, Saamanen A-M, Helminen HJ. 1994. Articular cartilage thickness and glycosaminoglycan distribution in the young canine knee joint after remobilization of the immobilized limb. *Journal of Orthopaedic Research*. 12: 161-167.
- Knight MM, Lee DA, Bader DL. 1996. Distribution of chondrocyte deformation in compressed agarose gel using confocal microscopy. *Journal of Cell Engineering*. 1: 97-102.
- Knight MM, Ghori SA, Lee DA, Bader DL. 1998a. Measurement of the deformation of isolated chondrocytes in agarose subjected to cyclic compression. *Medical Engineering & Physics*. 20(9): 684-8.
- Knight MM, Lee DA, Bader DL. 1998b. The influence of elaborated pericellular matrix on the deformation of isolated articular chondrocytes cultured in agarose. *Biochimica et Biophysica Acta*. 1405(1-3): 67-77.
- Knight MM, Ross JM, Sherwin AF, Lee DA, Bader DL, Poole CA. 2001. Chondrocyte deformation within mechanically and enzymatically extracted chondrons compressed in agarose. *Biochimica et Biophysica Acta*. 1526: 141-146.
- Knight MM, van de Breevaart Bravenboer J, Lee DA, van Osch GJVM, Weinans H, Bader DL. 2002. Cell and nucleus deformation in compressed chondrocyte-alginate constructs: temporal changes and calculation of cell modulus. *Biochimica et Biophysica Acta*. 1570: 1-8.
- Knight MM, Bomzon Z, Kimmel E, Sharma AM, Lee DA, Bader DL. 2006a. Chondrocyte deformation induces mitochondrial distortion and heterogeneous intracellular strain fields. *Biomechanics and Modeling in Mechanobiology*. 5(2-3): 180-91.
- Knight MM, Toyoda T, Lee DA, Bader DL. 2006b. Mechanical compression and hydrostatic pressure induce reversible changes in actin cytoskeletal organisation in chondrocytes in agarose. *Journal of Biomechanics*. 39(8): 1547-51.

- Knudson CB. 1993. Hyaluronan Receptor-directed Assembly of Chondrocyte Pericellular Matrix. *The Journal of Cell Biology*. 120(3): 825-834.
- Kokubu T, Matsui N, Fujioka H, Tsunoda M, Mizuno K. 1999. Low intensity pulsed ultrasound exposure increases prostaglandin E2 production via the induction of cyclooxygenase-2 mRNA in mouse osteoblasts. *Biochemical and Biophysical Research Communications*. 256(2): 284-7.
- Kono T, Nishikori T, Kataoka H, Uchio Y, Ochi M, Enomoto K. 2006. Spontaneous oscillation and mechanically induced calcium waves in chondrocytes. *Cell Biochemistry and Function*. 24(2): 103-11.
- Kopakkala-Tani M, Leskinen JJ, Karjalainen HM, Karjalainen T, Hynynen K, Töyräs J, Jurvelin JS, Lammi MJ. 2006. Ultrasound stimulates proteoglycan synthesis in bovine primary chondrocytes. *Biorheology*. 43(3-4): 271-82.
- Kremkau FW. 1985. Physical considerations. In: *Clinics in Diagnostic Ultrasound Volume 16. Biological Effects of Ultrasound*. Ed: Nyborg WL, Ziskin MC. Churchill Livingstone. 9-21.
- Kristiansen TK, Ryaby JP, McCabe J, Frey JJ, Roe LR. 1997. Accelerated healing of distal radial fractures with the use of specific, low-intensity ultrasound. *Journal of Bone & Joint Surgery*. 79A(7): 961-973.
- Kuettner KE, Pauli BU, Gall G, Memoli VA, Schenk RK. 1982. Synthesis of cartilage matrix by mammalian chondrocytes in vitro. I. Isolation, culture characteristics, and morphology. *Journal of Cell Biology*. 93(3): 743-50.
- Lagneaux L, de Meulenaer EC, Delforge A, Dejeneffe M, Massy M, Moerman C, Hannecart B, Canivet Y, Lepeltier MF, Bron D. 2002. Ultrasonic low-energy treatment: a novel approach to induce apoptosis in human leukemic cells. *Experimental Hematology*. 30(11):1293-301
- Langelier E, Suetterlin R, Hoemann CD, Aebi U, Buschmann MD. 2000. The chondrocyte cytoskeleton in mature articular cartilage: structure and distribution of actin, tubulin, and vimentin filaments. *Journal of Histochemistry & Cytochemistry*. 48(10): 1307-1320.

Langelier E, Buschmann MD. 2003. Increasing strain and strain rate strengthen transient stiffness but weaken the response to subsequent compression for articular cartilage in unconfined compression. *Journal of Biomechanics*. 36(6): 853-9.

Leddy HA, Guilak F. 2003. Site-specific molecular diffusion in articular cartilage measured using fluorescence recovery after photobleaching. *Annals of Biomedical Engineering*. 31(7): 753-60.

Lee DA, Bader DL. 1995. The development and characterization of an in vitro system to study strain-induced cell deformation in isolated chondrocytes. *In Vitro Cellular & Developmental Biology - Animal*. 31(11): 828-35.

Lee DA, Bader DL. 1997. Compressive strains at physiological frequencies influence the metabolism of chondrocytes seeded in agarose. *Journal of Orthopaedic Research*. 15: 181-188.

Lee DA, Bentley G, Archer CW. 1994. Proteoglycan depletion alone is not sufficient to stimulate proteoglycan synthesis in cultured bovine cartilage explants. *Osteoarthritis and Cartilage*. 2(3): 175-85.

Lee DA, Knight MM, Bolton JF, Idowu BD, Kayser MV, Bader DL. 2000a. Chondrocyte deformation within compressed agarose constructs at the cellular and sub-cellular levels. *Journal of Biomechanics*. 33(1): 81-95.

Lee DA, Noguchi T, Frean SP, Lees P, Bader DL. 2000b. The influence of mechanical loading on isolated chondrocytes seeded in agarose constructs. *Biorheology*. 37(1-2): 149-61.

Lee DA, Reisler T, Bader DL. 2003. Expansion of chondrocytes for tissue engineering in alginate beads enhances chondrocytic phenotype compared to conventional monolayer techniques. *Acta Orthopaedica Scandinavica*. 74(1): 6-15.

Lee HJ, Choi BH, Min BH, Son YS, Park SR. 2006. Low-intensity ultrasound stimulation enhances chondrogenic differentiation in alginate culture of mesenchymal stem cells. *Artificial Organs*. 30(9): 707-15.

Légaré A, Garon M, Guardo R, Savard P, Poole AR, Buschmann MD. 2002. Detection and analysis of cartilage degeneration by spatially resolved streaming potentials. *Journal of Orthopaedic Research*. 20(4): 819-26.

LeRoux MA, Guilak F, Setton LA. 1999. Compressive and shear properties of alginate gel: effects of sodium ions and alginate concentration. *Journal of Biomedical Materials Research*. 47(1): 46-53.

LeRoux MA, Cheung HS, Bau JL, Wang JY, Howell DS, Setton LA. 2001. Altered mechanics and histomorphometry of canine tibial cartilage following joint immobilization. *Osteoarthritis and Cartilage*. 9: 633-640.

Leskinen J, Kopakkala-Tani M, Karjalainen T, Hynynen K, Lammi MJ. 2005. Effect of ultrasound stimulation on chondrocytes. *4th International Symposium on Mechanobiology of Cartilage and Chondrocyte*. Budapest. 17.

Li JK, Chang WH, Lin JC, Ruaan RC, Liu HC, Sun JS. 2003. Cytokine release from osteoblasts in response to ultrasound stimulation. *Biomaterials*. 24: 2379-2385.

Li KW, Williamson AK, Wang AS, Sah RL. 2001. Growth responses of cartilage to static and dynamic compression. *Clinical Orthopaedics and Related Research*. 391S: S34-S48.

Mankin HJ. 1964. Mitosis in articular cartilage of immature rabbits. A histologic, stathmokinetic (colchicine) and autoradiographic study. *Clinical Orthopaedics and Related Research*. 34: 170-83.

Maroudas A. 1979. Physicochemical properties of articular cartilage. In: *Adult Articular Cartilage*. 2nd Edition. Ed: Freeman MAR. Pitman Medical, Tunbridge Wells, United Kingdom. 215-290.

Martins GG, Kolega J. 2006. Endothelial cell protrusion and migration in three-dimensional collagen matrices. *Cell Motility and the Cytoskeleton*. 63(2): 101-15.

Masuda K, Shirota H, Thonar EJ. 1994. Quantification of ³⁵S-labeled proteoglycans complexed to alcian blue by rapid filtration in multiwell plates. *Analytical Biochemistry*. 217(2): 167-75.

Mauck RL, Soltz MA, Wang CC, Wong DD, Chao PH, Valhmu WB, Hung CT, Ateshian GA. 2000. Functional tissue engineering of articular cartilage through dynamic loading of chondrocyte-seeded agarose gels. *Journal of Biomechanical Engineering*. 122(3): 252-60.

- Mauck RL, Wang CC, Oswald ES, Ateshian GA, Hung CT. 2003. The role of cell seeding density and nutrient supply for articular cartilage tissue engineering with deformational loading. *Osteoarthritis and Cartilage*. 11(12): 879-90.
- McGlashan SR, Jensen CG, Poole CA. 2006. Localization of extracellular matrix receptors on the chondrocyte primary cilium. *The Journal of Histochemistry and Cytochemistry: Official Journal of the Histochemistry Society*. 54(9): 1005-14.
- Meachim G and Stockwell RA. 1979. The matrix. In: *Adult Articular Cartilage*. 2nd Edition. Ed: Freeman MAR. Pitman Medical, Tunbridge Wells, United Kingdom. 1-67.
- Millward-Sadler SJ, Salter DM. 2004. Integrin-dependent signal cascades in chondrocyte mechanotransduction. *Annals of Biomedical Engineering*. 32(3): 435-46.
- Mizuno S, Tateishi T, Ushida T, Glowacki J. 2002. Hydrostatic fluid pressure enhances matrix synthesis and accumulation by bovine chondrocytes in three-dimensional culture. *Journal of Cellular Physiology*. 193(3): 319-27.
- Mizuno S. 2005. A novel method for assessing effects of hydrostatic fluid pressure on intracellular calcium: a study with bovine articular chondrocytes. *American Journal of Physiology: Cell Physiology*. 288(2): C329-37.
- Mobasher A, Carter SD, Martín-Vasallo P, Shakibaei M. 2002. Integrins and stretch activated ion channels; putative components of functional cell surface mechanoreceptors in articular chondrocytes. *Cell Biology International*. 26(1): 1-18.
- Moed BR, Subramanian S, van Holsbeeck M, Watson JT, Cramer KE, Karges DE, Craig JG, Bouffard JA. 1998. Ultrasound for the early diagnosis of tibial fracture healing after static interlocked nailing without reaming: clinical results. *Journal of Orthopaedic Trauma*. 12(3): 206-13.
- Morrison, JB. 1970. The mechanics of the knee joint in relation to normal walking. *Journal of Biomechanics*. 3: 51-61.
- Mow VC and Ratcliffe A. 1997. Structure and function of articular cartilage and meniscus. In: *Basic Orthopaedic Biomechanics*. 2nd Edition. Ed: Mow VC, Hayes WC. Lippincott-Raven Publishers, Philadelphia. 113-177.

- Muir H, Carney SL. 1987. Pathological and biochemical changes in cartilage and other tissues of the canine knee resulting from induced joint instability. In: *Joint Loading: Biology and Health of Articular Structures*. Ed: H. Helminen, I. Kiviranta, M. Tammi, A.-M. Saamanen, K. Paukkonen, J. Jurvelin. Wright, Bristol. 47-63.
- Muir H. 1995. The chondrocyte, architect of cartilage: Biomechanics, structure, function and molecular biology of cartilage matrix macromolecules. *BioEssays*. 17(12): 1039-1048.
- Muir IHM. 1979. Biochemistry. In: *Adult Articular Cartilage. 2nd Edition*. Ed: Freeman MAR. Pitman Medical, Tunbridge Wells, United Kingdom. 145-214.
- Mukai S, Ito H, Nakagawa Y, Akiyama H, Miyamoto M, Nakamura T. 2005. Transforming growth factor- β 1 mediates the effects of low-intensity pulsed ultrasound in chondrocytes. *Ultrasound in Medicine & Biology*. 31(12): 1713-21.
- Murata T, Ushida T, Mizuno S, Tateisha T. 1998. Proteoglycan synthesis by chondrocytes cultured under hydrostatic pressure and perfusion. *Materials Science and Engineering*. 6: 297-300.
- Myers KA, Rattner JB, Shrive NG, Hart DA. 2007. Hydrostatic pressure sensation in cells: integration into the tensegrity model. *Biochemistry and Cell Biology*. 85(5): 543-51.
- Naruse K, Miyauchi A, Itoman M, Mikuni-Takagaki Y. 2003. Distinct anabolic response of osteoblast to low-intensity pulsed ultrasound. *Journal of Bone and Mineral Research*. 18(2): 360-9.
- Nelson FR, Brighton CT, Ryaby J, Simon BJ, Nielson JH, Lorch DG, Bolander M, Seelig J. 2003. Use of physical forces in bone healing. *Journal of the American Academy of Orthopaedic Surgeons*. 11(5): 344-54.
- Ng KW, Mauck RL, Statman LY, Lin EY, Ateshian GA, Hung CT. 2006. Dynamic deformational loading results in selective application of mechanical stimulation in a layered, tissue-engineered cartilage construct. *Biorheology*. 43(3-4): 497-507.
- Nieminen HJ, Saarakkala S, Laasanen MS, Hirvonen J, Jurvelin JS, Töyräs J. 2004. Ultrasound attenuation in normal and spontaneously degenerated articular cartilage. *Ultrasound in Medicine and Biology*. 30(4): 493-500.

Nishikori T, Ochi M, Uchio Y, Maniwa S, Kataoka H, Kawasaki K, Katsube K, Kuriwaka M. 2002. Effects of low-intensity pulsed ultrasound on proliferation and chondroitin sulfate synthesis of cultured chondrocytes embedded in Atelocollagen gel. *Journal of Biomedical Materials Research*. 59: 201-206.

Nolte PA, Klein-Nulend J, Albers GH, Marti RK, Semeins CM, Goei SW, Burger EH. 2001. Low-intensity ultrasound stimulates endochondral ossification in vitro. *Journal of Orthopaedic Research*. 19(2): 301-7.

Noriega S, Mamedov T, Turner JA, Subramanian A. 2007. Intermittent applications of continuous ultrasound on the viability, proliferation, morphology, and matrix production of chondrocytes in 3D matrices. *Tissue Engineering*. 13(3): 611-8.

Nyborg WL. 1985. Mechanisms. In: *Clinics in Diagnostic Ultrasound Volume 16. Biological Effects of Ultrasound*. Ed: Nyborg WL, Ziskin MC. Churchill Livingstone. 23-33.

O'Brien, WD. 2007. Ultrasound–biophysics mechanisms. *Progress in Biophysics and Molecular Biology*. 93: 212–255.

Ohashi T, Hagiwara M, Bader DL, Knight MM. 2006. Intracellular mechanics and mechanotransduction associated with chondrocyte deformation during pipette aspiration. *Biorheology*. 43(3-4): 201-14.

Palmoski MJ, Colyer RA, Brandt KD. 1980. Joint motion in the absence of normal loading does not maintain normal articular cartilage. *Arthritis and Rheumatism*. 23(3): 325-34.

Park K, Hoffmeister B, Han DK, Hasty K. 2007. Therapeutic ultrasound effects on interleukin-1 α stimulated cartilage construct in vitro. *Ultrasound in Medicine and Biology*. 33(2): 286-95.

Parkkinen JJ, Lammi M, Pelttari A, Helminen HJ, Tammi M, Virtanen I. 1993. Altered golgi apparatus in hydrostatically loaded articular cartilage chondrocytes. *Annals of the Rheumatic Diseases*. 52: 192-198.

Parkkinen JJ, Lammi MJ, Inkinen R, Jortikka M, Tammi M, Virtanen I, Helminen HJ. 1995. Influence of short-term hydrostatic pressure on organization of stress fibers in cultured chondrocytes. *Journal of Orthopaedic Research*. 13(4): 495-502.

Parvizi J, Wu C-C, Lewallen DG, Greenleaf JF, Bolander M. 1999. Low-intensity ultrasound stimulates proteoglycan synthesis in rat chondrocytes by increasing aggrecan gene expression. *Journal of Orthopaedic Research*. 17: 488-494.

Parvizi J, Parpura V, Greenleaf JF, Bolander ME. 2002. Calcium signaling is required for ultrasound-stimulated aggrecan synthesis by rat chondrocytes. *Journal of Orthopaedic Research*. 20(1): 51-7.

Paukkonen K, Selkäinen K, Jurvelin J, Kiviranta I, Helminen HJ. 1985. Cells and nuclei of articular cartilage chondrocytes in young rabbits enlarged after non-strenuous physical exercise. *Journal of Anatomy*. 142: 13-20.

Pavalko FM, Norvell SM, Burr DB, Turner CH, Duncan RL, Bidwell JP. 2003. A model for mechanotransduction in bone cells: the load-bearing mechanosomes. *Journal of Cellular Biochemistry*. 88(1): 104-12.

Pederson JA, Swartz MA, 2005. Mechanobiology in the third dimension. *Annals of Biomedical Engineering*. 33(11): 1469-1490.

Petit B, Freyria AM, and van der Rest M. 1992. Cartilage collagens. In: *Biological Regulation of the Chondrocyte*. Ed: Adolphe M. CRC Press. 33-84.

Pilla AA, Mont MA, Nasser PR, Khan SA, Figueiredo M, Kaufman JJ, Siffert RS. 1990. Non-invasive low-intensity pulsed ultrasound accelerates bone healing in the rabbit. *Journal of Orthopaedic Trauma*. 4(3): 246-253.

Pingguan-Murphy B, Lee DA, Bader DL, Knight MM. 2005. Activation of chondrocytes calcium signalling by dynamic compression is independent of number of cycles. *Archives of Biochemistry and Biophysics*. 444(1): 45-51.

Pingguan-Murphy B, El-Azzeh M, Bader DL, Knight MM. 2006. Cyclic compression of chondrocytes modulates a purinergic calcium signalling pathway in a strain rate- and frequency-dependent manner. *Journal of Cellular Physiology*. 209(2): 389-97.

Poole AR, Pidoux I, Reiner A, Rosenberg L. 1982. An immunoelectron microscope study of the organization of proteoglycan monomer, link protein, and collagen in the matrix of articular cartilage. *The Journal of Cell Biology*. 93: 921-937.

Poole CA, Flint MA, Beaumont BW. 1987. Chondrons in cartilage: Ultrastructural analysis of the pericellular microenvironment in adult human articular cartilages. *Journal of Orthopaedic Research*. 5: 509-522.

Poole CA. 1997. Articular cartilage chondrons: form, function and failure. *Journal of Anatomy*. 191: 1-13.

Poole CA, Zhang Z-J, Ross JM. 2002. The differential distribution of acetylated and detyrosinated α -tubulin in the microtubular cytoskeleton and primary cilia of hyaline cartilage chondrocytes. *Journal of Anatomy*. 199(4): 393-405.

Poole RA, Kojima T, Yasuda T, Mwale F, Kobayashi M, Lavery S. 2001. Composition and structure of articular cartilage. *Clinical Orthopaedics and Related Research*. 391S: S26-S33.

Pullig O, Weseloh G, Swoboda B. 1999. Expression of type VI collagen in normal and osteoarthritic human cartilage. *Osteoarthritis and Cartilage*. 7(2): 191-202.

Quinn TM, Grodzinsky AJ, Buschmann MD, Kim Y-J, Hunziker EB. 1998. Mechanical compression alters proteoglycan deposition and matrix deformation around individual cells in cartilage explants. *Journal of Cell Science*. 111: 573-583.

Quinn TM, Schmid P, Hunziker EB, Grodzinsky AJ. 2002. Proteoglycan deposition around chondrocytes in agarose culture: Construction of a physical and biological interface for mechanotransduction in cartilage. *Biorheology*. 39: 27-37.

Raghunath J, Salacinski HJ, Sales KM, Butler PE, Seifalian AM. 2005. Advancing cartilage tissue engineering: the application of stem cell technology. *Current Opinion in Biotechnology*. 16: 503-509.

Rees SG, Davies JR, Tudor D, Flannery CR, Hughes CE, Dent CM, Caterson B. 2002. Immunolocalisation and expression of proteoglycan 4 (cartilage superficial zone proteoglycan) in tendon. *Matrix Biology*. 21: 593-602.

Repacholi MH. 1987. Standards and recommendations on ultrasound exposure. In: *Ultrasound: Medical Applications, Biological Effects, and Hazard Potential*. Ed: Repacholi MH, Grandolfo M, Rindi A. Plenum Press, New York. 233-239.

- Richardson DW, Clark CC. 1993. Effects of short-term cast immobilization on equine articular cartilage. *American Journal of Veterinary Research*. 3: 449-453.
- Ritchlin CT. 2004. Mechanisms of erosion in rheumatoid arthritis. *Journal of Rheumatology*. 31(7): 1229-1237.
- Roberts SR, Knight MM, Lee DA, Bader DL. 2001. Mechanical compression influences intracellular Ca^{2+} signaling in chondrocytes seeded in agarose constructs. *Journal of Applied Physiology*. 90(4): 1385-91.
- Rowley JA, Madlambayan G, Mooney DJ. 1999. Alginate hydrogels as synthetic extracellular matrix materials. *Biomaterials*. 20: 45-53.
- Rubin C, Bolander M, Ryaby JP, Hadjiargyrou M. 2001. Current concepts review: The use of low-intensity ultrasound to accelerate the healing of fractures. *Journal of Bone & Joint Surgery*. 83A(2): 259-270.
- Ruggiero F, Petit B, Ronziere MC, Farjanel J, Hartmann DJ, Herbage D. 1993. Composition and organization of the collagen network produced by fetal bovine chondrocytes cultured at high density. *The Journal of Histochemistry and Cytochemistry*. 41(6): 867-75.
- Ryaby JT, Bachner EJ, Bendo JA, Dalton PF, Tannenbaum S, Pilla AA. 1989. Low intensity ultrasound increases calcium incorporation in both differentiating cartilage and bone cell cultures. *Transactions of the Orthopaedic Research Society*. 14: 15.
- Sachs F. 1991. Mechanical transduction by membrane ion channels: a mini review. *Molecular Cellular Biochemistry*. 104: 57-60.
- Sah RL, Kim Y-J, Doong J, Grodzinsky AJ, Plaas AHK, Sandy JD. 1989. Biosynthetic response of cartilage explants to dynamic compression. *Journal of Orthopaedic Research*. 7: 619-636.
- Sah RL-Y, Grodzinsky AJ, Plaas AHK, Sandy JD. 1992. Effects of static and dynamic compression on matrix metabolism in cartilage explants. In: *Articular Cartilage and Osteoarthritis*. Ed: Kneutter K. New York, Raven Press Ltd. 373-392.

Saito M, Soshi S, Tanaka T, Fujii K. 2004. Intensity-related differences in collagen post-translational modification in MC3T3-E1 osteoblasts after exposure to low- and high-intensity pulsed ultrasound. *Bone*. 35(3): 644-55.

Sander EA, Nauman EA. 2003. Permeability of musculoskeletal tissues and scaffolding materials: experimental results and theoretical predictions. *Critical Reviews™ in Biomedical Engineering*. 31(1-2): 1-26.

Sano H, Saijo Y, Kokubun S. 2006. Non-mineralized fibrocartilage shows the lowest elastic modulus in the rabbit supraspinatus tendon insertion: measurement with scanning acoustic microscopy. *Journal of Shoulder and Elbow Surgery*. 15: 743-749.

Schinagl RM, Gurskis D, Chen AC, Sah RL. 1997. Depth-dependent confined compression modulus of full-thickness bovine articular cartilage. *Journal of Orthopaedic Research*. 15(4): 499-506.

Schneiderman R, Keret D, Maroudas A. 1986. Effects of mechanical and osmotic pressure on the rate of glycosaminoglycan synthesis in the human adult femoral head cartilage: an in vitro study. *Journal of Orthopaedic Research*. 4(4): 393-408.

Schumann D, Kujat R, Zellner J, Angele MK, Nerlich M, Mayr E, Angele P. 2006. Treatment of human mesenchymal stem cells with pulsed low intensity ultrasound enhances the chondrogenic phenotype in vitro. *Biorheology*. 43(3-4): 431-43.

Schwab W, Hempel U, Funk RH, Kasper M. 1999. Ultrastructural identification of caveolae and immunocytochemical as well as biochemical detection of caveolin in chondrocytes. *Histochemistry Journal*. 31(5): 315-20.

Shelton JC, Bader DL, Lee DA. 2003. Mechanical conditioning influences the metabolic response of cell-seeded constructs. *Cells, Tissues, Organs*. 175(3):140-50.

Shier D, Butler JL, Lewis R. 1999. *Hole's Human Anatomy & Physiology*. 8th Edition. McGraw-Hill.

Slowman SD, Brandt KD. 1986. Composition and glycosaminoglycan metabolism of articular cartilage from habitually loaded and habitually unloaded sites. *Arthritis and Rheumatism*. 29(1): 88-94.

Smith RL, Donlon BS, Gupta MK, Mohtai M, Das P, Carter DR, Cooke J, Gibbons G, Hutchinson N, Shurman DJ. 1995. Effects of fluid-induced shear on articular chondrocyte morphology and metabolism. *Journal of Orthopaedic Research*. 13: 824-831.

Smith RL, Rusk SF, Ellison BE, Wessels P, Tsuchiya K, Carter DR, Caler WE, Sandell LJ, Schurman DJ. 1996. In vitro stimulation of articular chondrocytes mRNA and extracellular matrix synthesis by hydrostatic pressure. *Journal of Orthopaedic Research*. 14: 53-60.

Smith RL, Trindade MC, Ikenoue T, Mohtai M, Das P, Carter DR, Goodman SB, Schurman DJ. 2000. Effects of shear stress on articular chondrocyte metabolism. *Biorheology*. 37: 95-107.

Söderhäll C, Marenholz I, Kersch T, Rüschenhoff F, Esparza-Gordillo J, Worm M, Gruber C, Mayr G, Albrecht M, Rohde K, Schulz H, Wahn U, Hubner N, Lee YA. 2007. Variants in a novel epidermal collagen gene (COL29A1) are associated with atopic dermatitis. *PLoS Biology*. 5(9): 1952-1961.

Stefanovic-Racic M, Stadler J, Ceorgescu HI, Evans CH. 1994. Nitric oxide and energy production in articular chondrocytes. *Journal of Cellular Physiology*. 159: 274-280.

Stockwell RA. 1978. Chondrocytes. *Journal of Clinical Pathology*. 31: 7-13.

Stockwell RA and Meachim G. 1979. The chondrocytes. In: *Adult Articular Cartilage*. 2nd Edition. Ed: Freeman MAR. Pitman Medical, Tunbridge Wells, United Kingdom. 69-144.

Sugimoto T, Yoshino M, Nagao M, Ishii S, Yabu H. 1996. Voltage-gated ionic channels in cultured rabbit articular chondrocytes. *Comparative Biochemistry and Physiology: Part C, Pharmacology, Toxicology & Endocrinology*. 115(3): 223-32.

Szafranski JD, Grodzinsky AJ, Burger E, Gaschen V, Hung HH, Hunziker EB. 2004. Chondrocyte mechanotransduction: effects of compression on deformation of intracellular organelles and relevance to cellular biosynthesis. *Osteoarthritis and Cartilage*. 12(12): 937-46.

Tabuchi Y, Ando H, Takasaki I, Feril LB Jr, Zhao QL, Ogawa R, Kudo N, Tachibana K, Kondo T. 2007. Identification of genes responsive to low intensity pulsed ultrasound in a human leukemia cell line Molt-4. *Cancer Letters*. 246(1-2): 149-56.

Tammi M, Paukkonen K, Kiviranta I, Jurvelin J, Säämänen A-M, Helminen HJ. 1987. Joint Loading-induced alterations in articular cartilage. In: *Joint Loading: Biology and Health of Articular Structures*. Ed: H. Helminen, I. Kiviranta, M. Tammi, A.-M. Saamanen, K. Paukkonen, J. Jurvelin. Wright, Bristol. 64-88.

Taylor KR, Gallo RL. 2006. Glycosaminoglycans and their proteoglycans: host-associated molecular patterns for initiation and modulation of inflammation. *The FASEB Journal*. 20: 9–22.

Temenoff JS, Mikos AG. 2001. Review: tissue engineering for regeneration of articular cartilage. *Biomaterials*. 21: 431-440.

ter Harr, G. 2007. Therapeutic applications of ultrasound. *Progress in Biophysics and Molecular Biology*. 93: 111–129.

Terkeltaub R, Johnson K, Murphy A, Ghosh S. 2002. Invited review: the mitochondrion in osteoarthritis. *Mitochondrion*. 1: 301-319.

Thomas JT, Ayad S, Grant ME. 1994. Cartilage collagens: strategies for the study of their organisation and expression in the extracellular matrix. *Annals of the Rheumatic Diseases*. 53: 488-496.

Tien YC, Lin SD, Chen CH, Lu CC, Su SJ, Chih TT. 2008. Effects of pulsed low-intensity ultrasound on human child chondrocytes. *Ultrasound in Medicine and Biology*. 34(7): 1174-81.

Toyoda T, Seedhom BB, Yao JQ, Kirkham J, Brookes S, Bonass WA. 2003. Hydrostatic pressure modulates proteoglycan metabolism in chondrocytes seeded in agarose. *Arthritis and Rheumatism*. 48(10): 2865-72.

Tyler JA, Bolis S, Dingle JT, Middleton FS. Mediators of matrix catabolism. 1992. In: *Articular Cartilage and Osteoarthritis*. Ed: Kuettner KE, Schleyerback R, Peyron JG, Hascall VC. Raven Press Ltd., New York. 251-264.

Uglow MG, Peat RA, Hile MS, Bilston LE, Smith EJ, Little DG. 2003. Low-intensity ultrasound stimulation in distraction osteogenesis in rabbits. *Clinical Orthopaedics and Related Research*. 417: 303-312.

Urban JP. 2000. Present perspectives on cartilage and chondrocyte mechanobiology. *Biorheology*. 37(1-2): 185-90.

Urban JPG, Hall AC. 1992. Physical modifiers of cartilage metabolism. In: *Articular Cartilage and Osteoarthritis*. Ed: Kneutner K, Schleyerbach R, Peyron JG, Hascall VC. New York, Raven Press. 393-407.

Urban JPG. 1994. The chondrocyte: A cell under pressure. *British Journal of Rheumatology*. 33: 901-908.

Van der Rest M, Garrone R. 1991. Collagen family of proteins. *FASEB Journal*. 5: 2814-2823.

van Osch GJ, van der Veen SW, Buma P, Verwoerd-Verhoef HL. 1998. Effect of transforming growth factor- β on proteoglycan synthesis by chondrocytes in relation to differentiation stage and the presence of pericellular matrix. *Matrix Biology*. 17(6): 413-24.

Van Wynsberghe DM, Noback C, Carola R. 1995. *Human Anatomy and Physiology*. 3rd Edition. McGraw-Hill, Inc.

Veit G, Kobbe B, Keene DR, Paulsson M, Koch M, Wagener R. 2006. Collagen XXVIII, a novel von Willebrand factor A domain-containing protein with many imperfections in the collagenous domain. *The Journal of Biological Chemistry*. 281(6): 3494-3504.

Vunjak-Novakovic G, Martin I, Obradovic B, Treppo S, Grodzinsky AJ, Langer R, Freed LE. 1999. Bioreactor cultivation conditions modulate the composition and mechanical properties of tissue-engineered cartilage. *Journal of Orthopaedic Research*. 17(1): 130-8.

Wang N, Butler JP, Ingber DE. 1993. Mechanotransduction across the cell surface and through the cytoskeleton. *Science*. 260(5111): 1124-7.

- Wang N, Naruse K, Stamenović D, Fredberg JJ, Mijailovich SM, Tolić-Nørrelykke IM, Polte T, Mannix R, Ingber DE. 2001. Mechanical behavior in living cells consistent with the tensegrity model. *Proceedings of the National Academy of Sciences of the United States of America*. 98(14): 7765-70.
- Wang S-J, Lewallen DG, Bolander ME, Chao EYS, Ilstrup DM, Greenleaf JF. 1994. Low intensity ultrasound treatment increases strength in a rat femoral fracture model. *Journal of Orthopaedic Research*. 12(1): 40-47.
- Warden SJ. 2003. A new direction for ultrasound therapy in sports medicine. *Sports Medicine*. 33(2): 95-107.
- Weightman B, Kempson G. 1979. Load carriage. In: *Adult Articular Cartilage*. Ed: Freeman MAR. London, Pitman Medical. 293-341.
- Weisser J, Rahfoth B, Timmermann A, Aigner T, Bräuer R, von der Mark K. 2001. Role of growth factors in rabbit articular cartilage repair by chondrocytes in agarose. *Osteoarthritis and Cartilage*. 9(Supp A): S48-S54.
- Werb Z. The biologic role of metalloproteinases and their inhibitors. 1992. In: *Articular Cartilage and Osteoarthritis*. Ed: Kuettner KE, Schleyerback R, Peyron JG, Hascall VC. Raven Press Ltd., New York. 295-304.
- Whitfield JF. 2008. The solitary (primary) cilium - a mechanosensory toggle switch in bone and cartilage cells. *Cellular Signalling*. 20(6): 1019-24.
- Wilkins RJ, Hall AC. 1995. Control of matrix synthesis in isolated bovine chondrocytes by extracellular and intracellular pH. *Journal of Cellular Physiology*. 164(3): 474-81.
- Williams MR, Garrido M, Oz MC, Argenziano M. 2004. Alternative energy sources for surgical atrial ablation. *Journal of Cardiac Surgery*. 19(3): 201 – 206.
- Wilson JR, Duncan NA, Giles WR, Clark RB. 2004. A voltage-dependent K⁺ current contributes to membrane potential of acutely isolated canine articular chondrocytes. *The Journal of Physiology*. 557(1): 93-104.
- Wright MO, Stockwell RA, Nuki G. 1992. Response of plasma membrane to applied hydrostatic pressure in chondrocytes and fibroblasts. *Connective Tissue Research*. 28(1-2): 49-70.

Wright MO, Nishida K, Bavington C, Godolphin JL, Dunne E, Walmsley S, Jobanputra P, Nuki G, Salter DM. 1997. Hyperpolarisation of cultured human chondrocytes following cyclical pressure-induced strain: evidence of a role for $\alpha 5 \beta 1$ integrin as a chondrocyte mechanoreceptor. *Journal of Orthopaedic Research*. 15(5): 742-7.

Wu C-C, Lewallen DG, Bolander M, Bronk J, Kinnick R, Greenleaf JF. 1996. Exposure to low intensity ultrasound stimulates aggrecan gene expression by cultured chondrocytes. *Transactions of the Orthopaedic Research Society*. 21: 622.

Wu F, Wang ZB, Lu P, Xu ZL, Chen WZ, Zhu H, Jin CB. 2004. Activated anti-tumor immunity in cancer patients after high intensity focused ultrasound ablation. *Ultrasound in Medicine and Biology*. 30(9): 1217-22.

Xia SL, Ferrier J. 1995. Calcium signal induced by mechanical perturbation of osteoclasts. *Journal of Cellular Physiology*. 163(3): 493-501.

Yang K-H, Parvizi J, Wang S-J, Lewallen DG, Kinnick R, Greenleaf JF, Bolander M. 1996. Exposure to low-intensity ultrasound increases aggrecan gene expression in a rat femur fracture model. *Journal of Orthopaedic Research*. 14: 802-809.

Yang RS, Lin WL, Chen YZ, Tang CH, Huang TH, Lu BY, Fu WM. 2005. Regulation by ultrasound treatment on the integrin expression and differentiation of osteoblasts. *Bone*. 36(2): 276-83.

Yellowley CE, Jacobs CR, Donahue HJ. 1999. Mechanisms contributing to fluid-flow-induced Ca^{2+} mobilization in articular chondrocytes. *Journal of Cellular Physiology*. 180(3): 402-8.

Zhang Z, Huckle J, Francomano CA, Spencer RGS. 2002. The influence of pulsed low-intensity ultrasound on matrix production of chondrocytes at different stages of differentiation: an explant study. *Ultrasound in Medicine & Biology*. 28(11-12): 1547-1553.

Zhang Z, Huckle J, Francomano CA, and Spencer RGS. 2003. The effects of pulsed low-intensity ultrasound on chondrocyte viability, proliferation, gene expression and matrix production. *Ultrasound in Medicine & Biology*. 29(11): 1645-1651.

Zhou S, Schmelz A, Seufferlein T, Li Y, Zhao J, Bachem MG. 2004. Molecular mechanisms of low intensity pulsed ultrasound in human skin fibroblasts. *The Journal of Biological Chemistry*. 279(52): 54463-9.

Zhou S, Bachem MG, Seufferlein T, Li Y, Gross HJ, Schmelz A. 2008. Low intensity pulsed ultrasound accelerates macrophage phagocytosis by a pathway that requires actin polymerization, Rho, and Src/MAPKs activity. *Cellular Signalling*. 20(4): 695-704.

PRESENTATIONS AND CONFERENCES

1. Vaughan NM; Bader DL; Knight, MM. 2003. Low intensity ultrasound stimulates proteoglycan synthesis by isolated articular chondrocytes cultured in agarose. In: Smith and Nephew, York, England.
2. Vaughan NM; Sivapitchai AR; Bader DL; Knight, MM. 2005. Low intensity pulsed ultrasound stimulates GAG synthesis in chondrocytes in agarose. In: 51st Annual Meeting of the Orthopaedic Research Society, Washington DC, USA. 904.
3. Vaughan NM; Knight, MM; Bader DL. 2006. Low intensity pulsed ultrasound does not stimulate cartilage matrix synthesis in 3D agarose constructs. In: 5th World Congress of Biomechanics, Munich, Germany.
4. Bader DL, Vaughan NM, Akanji O-O, Knight MM. 2007. Role of engineering strategies in tissue engineering. In: 13th IPEM Annual Scientific Meeting, Cardiff, Wales.

LOW INTENSITY PULSED ULTRASOUND STIMULATES GAG SYNTHESIS IN CHONDROCYTES IN AGAROSE

Vaughan, N M; Sivapitchai, A R; Bader, D L; Knight, M M

Medical Engineering Division and IRC in Biomedical Materials, Queen Mary University of London, Mile End Rd., London, E1 4NS, UK
m.m.knight@qmul.ac.uk

Introduction

Pulsed low intensity ultrasound (PLIUS) has been widely documented to promote bone fracture healing and callus formation both in animal models [1] and clinical trials [2]. More recent studies have shown that PLIUS stimulates chondrocyte synthesis of glycosaminoglycan by up-regulating gene expression [3,4]. Consequently, there is an increasing interest in the application of PLIUS for the treatment of cartilage injury and disease, either directly or in conjunction with tissue engineering strategies involving cells in 3D constructs. The present study utilizes a well-established 3D chondrocyte model system to test the hypothesis that pulsed low intensity ultrasound stimulates the synthesis and elaboration of glycosaminoglycan and that this response is influenced by the intensity of the ultrasound.

Method

Specimen Preparation. Articular chondrocytes were isolated from bovine metacarpal-phalangeal joints by digestion in pronase and collagenase and seeded at 4×10^6 cells/ml in 3% agarose (Sigma) [5]. Each well of a 6 well plate was filled to a height of 3 mm with 4 ml of cell-agarose suspension and gelled at 4°C. The cell-agarose gels were covered with 6 ml of DMEM+20%FCS (Sigma) and maintained at 37°C / 5% CO₂.

Ultrasound Stimulation. Ultrasound transducers (supplied by Smith & Nephew Inc.) [3,4], were used to apply a 20 min period of pulsed low intensity ultrasound to each well of the 6 well plate at a spatial and temporal averaged intensity of 30 mW/cm². The frequency was set at 1.5 MHz with a pulse burst of 200 μ s repeating at 1 kHz. Controls remained unstimulated in separate 6 well plates. Medium was changed every 2 to 3 days and the aspirated medium was frozen for biochemical analysis.

Temporal changes in sulphated GAG content. At days 1, 2, 5, 9, 12, and 16, samples of 6 cylindrical constructs, 6 mm in diameter, were excised from the central region of a well, weighed and frozen for subsequent biochemical analysis. At the end of the experiment, individual constructs and their associated culture media, were assayed for total sulphated GAG (sGAG) content using the DMB method [6].

Effect of ultrasound intensity. Separate cell-agarose gels were subjected to ultrasound intensities of 13, 30, 70, 110, 209 or 300 mW/cm² applied for 20 mins every 24 hrs. At day 9, constructs were assayed for total sGAG content as previously. In addition, a separate group of constructs were subjected to intensities of 13, 30, 110, or 209 mW/cm². On day 8 of culture, medium was supplemented with 10 μ Ci/ml ³⁵SO₄ for a 24 hr period after which incorporation of ³⁵SO₄ into newly synthesized sGAG was calculated using Alcian blue precipitation and normalized to DNA content determined using the Hoescht 33258 method [3,5].

Cell Viability. At all time points and ultrasound intensities, separate specimens were stained with calcein AM and ethidium homodimer (Molecular Probes) and visualized using confocal microscopy to determine cell viability throughout the thickness of the construct.

Results

Cell viability was maintained at greater than 95% in all constructs except those subjected to 300 mW/cm², where there was significant loss of cell viability towards the base of the construct in contact with the bottom of the plate. This was attributed to rapid heating caused by attenuation of the ultrasound in the plastic. There was an increase in total sGAG content over a 16 day period (Fig. 1). From day 5 to day 12, the two groups diverged with pulsed low intensity ultrasound treated constructs showing a slightly greater sGAG content. However, there were no statistically significant differences in total sGAG content between ultrasound treated constructs and controls at any time points. There were also no statistically significant differences in total sGAG content at day 9 between controls and constructs treated with ultrasound at intensities from 13 to 209 mW/cm² (data not shown). At 300 mW/cm² there was a reduction in sGAG content which was attributed to the loss of viability at this intensity. In apparent contrast, ³⁵SO₄ incorporation measured between days 8 and 9 indicated that ultrasound significantly stimulated the synthesis of sGAG at intensities up to 209 mW/cm². Maximal stimulation occurred at 13 mW/cm² with a reduction in synthesis at 110 and 209 mW/cm² (Fig. 2). The amount of sGAG released into the medium was unaffected by ultrasound treatment.

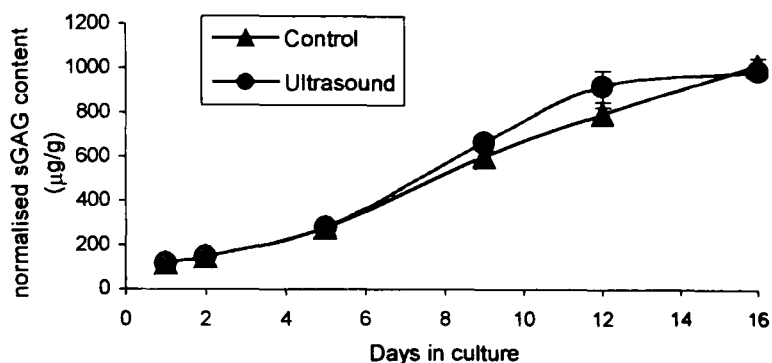


Fig. 1. Effect of PLIUS on sGAG content normalized to wet weight for constructs exposed to 30mW/cm² every 24hrs. Error bars indicate SEM.

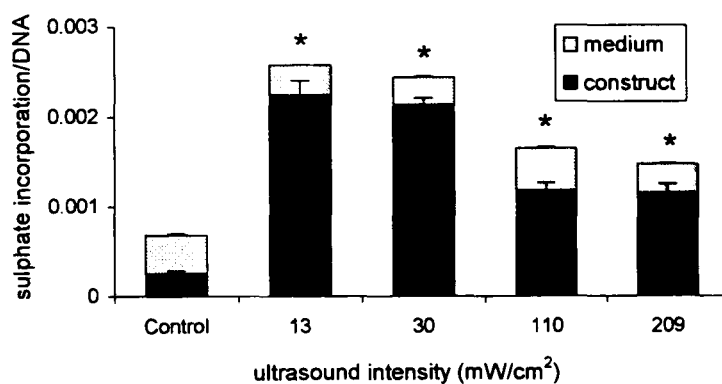


Fig. 2. Effect of PLIUS intensity, applied every 24 hrs, on sGAG synthesis from day 8 to 9. Incorporation of ³⁵SO₄ normalized to DNA levels in μ M³⁵SO₄/hr/ μ gDNA. Error bars indicate SEM n=7. (* p<0.001)

Discussion

The present study has utilized a well-characterized agarose model which maintains chondrocytic phenotype and reduces potential artifacts associated with ultrasound-induced heating of the culture plates and fluid flow caused by standing waves. Results indicate that PLIUS stimulates chondrocyte synthesis of sGAG as indicated by ³⁵SO₄ incorporation (Fig. 2). However this was not translated into an increase in total sGAG content (Fig. 1). This suggests that there is a limited period at which PLIUS may have a stimulatory effect on chondrocytes in agarose, specifically days 8 and 9. This may be associated with the presence of sufficient pericellular matrix to provide a mechanical interface enabling perturbation of cellular mechanoreceptors. This hypothesis is supported by previous studies in which PLIUS has increased GAG content for chondrocytes in monolayer [3] or in 3D collagen gels [4]. In both these model systems the cells are attached to their pericellular environment in contrast to the situation in early agarose cultures. Thus the pericellular environment and presence of matrix may significantly influence the metabolic response to ultrasound as is the case with mechanical strain [7]. Clearly if pulsed low intensity ultrasound is to be optimized for cartilage repair and tissue engineering, it will be necessary to elucidate the associated mechanisms so as to translate the increases in sGAG synthesis to increases in matrix content and tissue mechanical properties.

References

- [1] Azuma Y, et al. (2002) *J Bone Min Res.* 16:671-80.
- [2] Heckman JD, et al. (1994) *J Bone Joint Surg.* 76:26-34.
- [3] Parvizi J, et al. (1999) *J Orthop Res.* 17:488-94.
- [4] Nishikori T, et al. (2002) *J Biomed Mat Res.* 59:201-6.
- [5] Lee DA, et al. (1998) *Biochem Biophys Res Comm.* 251:580-5.
- [6] Farndale RW, et al. (1982) *Connect Tiss Res.* 9:247-8
- [7] Hunter CJ, et al. (2004) *Osteoarthritis Cartilage.* 12:117-30

Acknowledgements

The authors gratefully acknowledge EPSRC and Smith & Nephew, UK who support N Vaughan on an EPSRC CASE PhD studentship MM Knight is funded by an EPSRC Advanced Research Fellowship

